

Short- and medium-chain length methyl ketones are important commodity chemicals that are currently produced from petrochemical resources. To date, there is only limited research regarding the biotechnological production and purification of those methyl ketones in the scope of a circular bioeconomy.

This work elucidates integrated bioprocesses to produce methyl ketones using genetically modified microorganisms.

Methyl ketones with a chain length of  $C_{11}$  to  $C_{17}$  are produced by genetically modified *Pseudomonas taiwanensis* VLB120 with addition of an organic solvent to the cultivation medium for *in situ* liquid-liquid product extraction. The applied organic solvent decisively influences important process parameters. However, the type of solvent for *in situ* extraction of methyl ketones was not investigated so far, and one of the major challenges of *in situ* liquid-liquid extraction, the formation of stable emulsions, was unsolved. We describe an in-depth investigation of the organic solvent for *in situ* product extraction of methyl ketones and the subsequent recovery of the organic phase. 2-Undecanone was found as a solvent that is biocompatible, non-biodegradable, and safe, and in an advanced bioreactor setup, the multiphase loop reactor, formation of stable emulsions was circumvented. Subsequent examinations highlighted the methyl ketone blend's potential as a drop-in diesel fuel replacement.

Next, the carbon sources that are converted to the  $C_{11}$  to  $C_{17}$  methyl ketones and the associated feeding strategies were investigated. By an *in silico* screening approach using a genome-scale metabolic model, ethanol was found as a co-feed carbon source that enabled superior product yields. Additionally, sustainable methyl ketone production was shown to be possible by utilizing lignocellulosic hydrolysates.

A bioprocess cascade was also developed for the production of  $C_4$  methyl ketones acetoin and 2-butanone. Acetoin was produced by resting cells of *Lactococcus lactis* at product yields close to the theoretical maximum. The resting cell buffer was tailored to meet the requirements of an ensuing electrocatalytic reduction, transforming biotechnologically produced acetoin into 2-butanone.

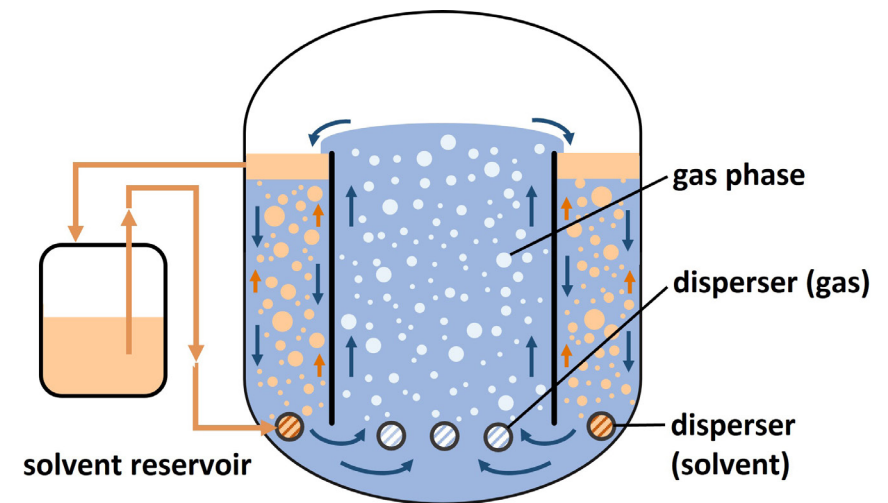
Concluding, the bioprocesses for the biotechnological production of methyl ketones were developed and improved in a holistic manner. Biotechnological methods were integrated into the preceding and consecutive process steps and optimized beyond their isolated figures of merit.

Carolin Grütering

## Producing methyl ketones in integrated bioprocesses

Producing methyl ketones in integrated bioprocesses

Carolin Grütering



# **Producing methyl ketones in integrated bioprocesses**

Von der Fakultät für Mathematik, Informatik und Naturwissenschaften der  
RWTH Aachen University zur Erlangung des akademischen Grades einer  
Doktorin der Ingenieurwissenschaften genehmigte Dissertation

vorgelegt von

**Carolin Grütering**  
Master of Science

aus

Marl, Deutschland

Berichter:

Univ.-Prof. Dr.-Ing. Lars M. Blank

Univ.-Prof. Dr.-Ing. Andreas Jupke

Tag der mündlichen Prüfung: 30.04.2024

Diese Dissertation ist auf den Internetseiten der Universitätsbibliothek  
verfügbar.

**Bibliografische Information der Deutschen Nationalbibliothek**

Die Deutsche Nationalbibliothek verzeichnet diese Publikation in der Deutschen Nationalbibliografie; detaillierte bibliografische Daten sind im Internet über <https://portal.dnb.de> abrufbar.

Carolin Grütering:

Producing methyl ketones in integrated bioprocesses

1. Auflage, 2024

Gedruckt auf holz- und säurefreiem Papier, 100% chlorfrei gebleicht.

Copyright Apprimus Verlag, Aachen, 2024

Wissenschaftsverlag des Instituts für Industriekommunikation und Fachmedien  
an der RWTH Aachen

Steinbachstr. 25, 52074 Aachen

Internet: [www.apprimus-verlag.de](http://www.apprimus-verlag.de), E-Mail: [info@apprimus-verlag.de](mailto:info@apprimus-verlag.de)

Alle Rechte, auch das des auszugsweisen Nachdruckes, der auszugsweisen oder vollständigen Wiedergabe, der Speicherung in Datenverarbeitungsanlagen und der Übersetzung, vorbehalten.

Printed in Germany

ISBN 978-3-98555-221-4

---

Man sieht nur, was man weiß

---





---

## Danksagung

Mein erster und herzlichster Dank gilt meinem Doktorvater, Prof. Dr. Ing. Lars M. Blank. Danke, dass du mir alle Freiheiten auf der Spielwiese der Wissenschaften gegeben hast und du dir trotzdem immer Zeit für Diskussionen nimmst. Danke, dass du das iAMB zu so einem tollen, internationalen, beeindruckenden Ort machst.

Ein großes Dankeschön geht außerdem an Prof. Dr. Ing. Andreas Jupke, der in vielen Projekttreffen von Fuel Science Center und BioSC spannende Aspekte angestoßen hat und die Zweitbetreuung dieser Arbeit übernimmt.

Diese Arbeit wäre nicht möglich gewesen ohne die Kooperationspartner innerhalb und außerhalb des Fuel Science Centers, nämlich Matti Froning, Anita Ziegler, Christian Honecker, Marcel Neumann, Bastian Lehrheuer, Marius Hofmeister, Miaomiao Du, Max von Campenhausen und Tobias Harhues. Danke für euer Vertrauen in Mikroorganismen und Methylketone. Zudem danke ich Till Tiso für seine Unterstützung und Philipp Demling für die kompetenteste Bioprozessberatung, die man sich wünschen kann.

Ein großer Dank geht auch an die Studierenden, die ich während dieser Arbeit, zum Teil sogar in mehreren Projekten, betreuen durfte. Danke Franziska, Leon, Fabian und Rebecca für eure Ideen, eure Zeit und eure Begeisterung. Mit euch zu arbeiten war ein großes Highlight der letzten Jahre.

The iAMB lives through its fantastic people and researchers. I would like to thank all current and former members for making the institute such a great place. Big thanks go to my dear friends and colleagues Alessandra, Alex, Denise, Fred, Itzel, Katrin, Lorenzo, Pedro, Upasana, and Valentina. You have made these years one of the most interesting times in my life. It is an honor to work with such lovely, fascinating, and great people. I will miss all the fabulous morning hugs (at least 8 a day!), lunches, and evening activities. Besitos! At this point, I would like to express my special thanks to my secret sister Jana Fees, who kept me sane more than once.

I am also very grateful for my time in the BCBT research group at DTU Copenhagen, where Solange I. Mussatto and Celina shared their immense knowledge and experience with me.

Außerdem möchte ich den Heldinnen und Helden des iAMB, Manja, Julia, Gisela, Isabel und Martin danken, dass sie jederzeit bei vielen kleinen und großen Fragen weiterhelfen.

Lena und Alex, ihr wart so wichtig.

Großer Dank gilt meiner Familie, Birgit, Hans-Dieter, Juli, Andre, Doris, Günther, und Ruth dafür, dass ihr Begeisterung, Neugierde und Zusammenhalt immer gefördert habt, und mich bis hier hin unterstützt. *Jeder Mensch hat hundert Punkte!*

Jonas, dir möchte ich danken, dass wir das alles zusammen durchziehen. Wenn mir jemand im Jahr 2004 gesagt hätte, dass wir mal eine WissenschaftlerInnen-WG haben, ich hätte ihn für verrückt erklärt. Ich bin unglaublich dankbar für deine Geduld, deine Ruhe, deine Beratung zu sämtlichen Strukturformeln, und deinen Rückhalt.

---



---

# Eidesstattliche Erklärung

Ich, Carolin Grütering, erkläre hiermit, dass diese Dissertation und die darin dargelegten Inhalte die eigenen sind und selbstständig, als Ergebnis der eigenen originären Forschung, generiert wurden. Hiermit erkläre ich an Eides statt:

1. Diese Arbeit wurde vollständig oder größtenteils in der Phase als Doktorandin dieser Fakultät und Universität angefertigt;
2. Sofern irgendein Bestandteil dieser Dissertation zuvor für einen akademischen Abschluss oder eine andere Qualifikation an dieser oder einer anderen Institution verwendet wurde, wurde dies klar angezeigt;
3. Wenn immer andere eigene- oder Veröffentlichungen Dritter herangezogen wurden, wurden diese klar benannt;
4. Wenn aus anderen eigenen- oder Veröffentlichungen Dritter zitiert wurde, wurde stets die Quelle hierfür angegeben. Diese Dissertation ist vollständig meine eigene Arbeit, mit der Ausnahme solcher Zitate;
5. Alle wesentlichen Quellen von Unterstützung wurden benannt;
6. Wenn immer ein Teil dieser Dissertation auf der Zusammenarbeit mit anderen basiert, wurde von mir klar gekennzeichnet, was von anderen und was von mir selbst erarbeitet wurde;
7. Teile dieser Arbeit wurden zuvor veröffentlicht und zwar in:

C. Grütering, C. Honecker, M. Hofmeister, M. Neumann, L. Raßpe-Lange, M. Du, B. Lehrheuer, M. von Campenhausen, F. Schuster, M. Surger, B. E. Ebert, A. Jupke, T. Tiso, K. Leonhard, K. Schmitz, S. Pischinger, L. M. Blank. Methyl ketones: a comprehensive study of a novel biofuel. Sustainable Energy & Fuels. 2024, 8(9), 2059-2072.

A. L. Ziegler, C. Grütering, L. Poduschnick, A. Mitsos, L. M. Blank. Co-feeding enhances the yield of methyl ketones. Journal of Industrial Microbiology and Biotechnology, 2023, 50(1).

C. Grütering, T. Harhues, F. Speen, R. Keller, M. Zimmermann, P. R. Jensen, M. Wessling, L. M. Blank. Acetoin production by resting cells of *Lactococcus lactis* for direct electrochemical synthesis of 2-butanone. Green Chemistry, 2023, 25(22), 9218-9225.

Aachen, 20.05.2024



Carolin Grütering

---



---

## Funding

This work was part of the Cluster of Excellence 2186 “The Fuel Science Center”, Deutsche Forschungsgemeinschaft (DFG, German Research Foundation) under Germany’s Excellence Strategy ID: 390 919 832 and by the Ministry of Culture and Research of the German federal state of North Rhine Westphalia within the framework of the NRW-Strategieprojekt BioSC (No. 313/323-400-002 13).



The foundation of this thesis is the long-term acquired knowledge and expertise gained at the Institute of Applied Microbiology at RWTH Aachen, which is gratefully appreciated.

---



---

## Contributions

This was a highly interdisciplinary work that was only possible thanks to many cooperation partners and students. The detailed contributions are included in each chapter. An overview of all contributors is given below.

Name	Contribution	Project/Institution
Matti Froning	Determination of double bond position	Institute of Inorganic and Analytical Chemistry, University of Münster
Maximilian von Campenhausen	Planning of the solvent screening	AVT.FVT, RWTH Aachen
David Wollborn	Cultivations with temperature gradients	AVT.BioVT, RWTH Aachen
Franziska Schuster	Solvent screening cultivations	Bachelor Thesis, iAMB, RWTH Aachen
Hendrik Mengers	Setup of the <i>in situ</i> gas stripping bioreactor	Fuel Science Center, iAMB, RWTH Aachen
Marcel Neumann	Determination of derived cetane number	Fuel Science Center, TME, RWTH Aachen
Bastian Lehrheuer	Planning experiments in the single-cylinder research engine	Fuel Science Center, TME, RWTH Aachen
Christian Honecker	Experiments in the single-cylinder research engine	Fuel Science Center, TME, RWTH Aachen
Marius Hofmeister	Material compatibility of methyl ketones	Fuel Science Center, IFAS, RWTH Aachen
Lukas Raßpe-Lange	Physical property predictions for methyl ketones	Fuel Science Center, LTT, RWTH Aachen
Miaomiao Du	Ecotoxicology of methyl ketones	Fuel Science Center, Bio5, RWTH Aachen
Maximilian Surger	Storability of methyl ketones	Fuel Science Center, iAMB, RWTH Aachen
Philipp Demling	Setup of the multiphase loop reactor	iAMB, RWTH Aachen
Diana Wall	Setup of the multiphase loop reactor	BioSC, AVT.FVT, RWTH Aachen
Solange I. Mussatto	Planning of wheat straw hydrolysis	BCBT, DTU Copenhagen
Celina K. Yamakawa	Generation of wheat straw hydrolysates	BCBT, DTU Copenhagen
Tobias Alter	Generation of the genome-scale model of <i>Pseudomonas taiwanensis</i> Δ6 pProd	iAMB, RWTH Aachen
Anita L. Ziegler	<i>In silico</i> assisted screening of co-feeding substances	Fuel Science Center, AVT.SVT, RWTH Aachen
Leon Poduschnick	<i>In silico</i> assisted screening of co-feeding substances	Master Thesis, iAMB, RWTH Aachen

---



---

Name	Contribution	Project/Institution
Tobias Harhues	Electrochemical reduction of acetoin to 2-butanone	Fuel Science Center, AVT.SVT, RWTH Aachen
Fabian Speen	Acetoin production with <i>Lactococcus lactis</i>	Master Thesis, iAMB, RWTH Aachen
Rebecca Breit	Genetic engineering of thioesterases and investigation of different carbon sources	Research Internship and Master Thesis, iAMB, RWTH Aachen
Eva Miriam Buhl	Transmission electron microscopy	Uniklinik RWTH Aachen

---

# Table of Contents

Summary .....	V
Zusammenfassung .....	VII
Nomenclature .....	IX
List of Figures .....	XV
List of Tables .....	XVII
<b>1 General Introduction .....</b>	<b>3</b>
1.1 Bioeconomy .....	3
1.1.1 Biotechnology within a sustainable bioeconomy .....	5
1.1.2 Biorefineries for biofuels and bulk chemicals .....	6
1.2 Biofuels .....	8
1.2.1 Production of medium-chain length methyl ketones .....	8
1.2.2 Production of acetoin and 2-butanone .....	10
1.3 Integrated bioprocesses .....	11
1.3.1 <i>In situ</i> extraction .....	12
1.3.2 Solvent selection strategies .....	14
1.4 Scope of this thesis .....	16
<b>2 Material and Methods .....</b>	<b>21</b>
2.1 Chemicals .....	21
2.2 Strains .....	21
2.3 Biotechnological production of medium-chain length methyl ketones .....	22
2.3.1 <i>Pseudomonas taiwanensis</i> VLB120 strains and growth media .....	22
2.3.2 Plasmid and strain construction .....	22
2.3.3 <i>Pseudomonas taiwanensis</i> VLB120 pre-cultures and shaken cultures .....	24
2.3.4 <i>Pseudomonas taiwanensis</i> VLB120 cultivations in bioreactors .....	26
2.4 Solvent screening for <i>in situ</i> extraction of methyl ketones .....	27
2.4.1 Physicochemical parameters .....	27
2.4.2 Assessment of solvent toxicity to <i>Pseudomonas taiwanensis</i> VLB120 .....	27
2.4.3 Partition coefficient and interphase formation .....	27
2.5 Suitability of the methyl ketone blend as a drop-in fuel .....	28
2.5.1 Determination of kinematic viscosity and density .....	28
2.5.2 Material compatibility and lubricity .....	29
2.5.3 Prediction of flash point and boiling point .....	29
2.5.4 Determination of the derived cetane number and combustion properties in a single-cylinder research engine .....	30
2.5.5 Storability test of 2-undecanone .....	31

2.5.6	Ecotoxicology assessments .....	32
2.6	Preparation of hydrolysates and growth assay .....	32
2.6.1	Pre-treatment .....	32
2.6.2	Generation of (washed) cellulosic hydrolysate .....	33
2.6.3	Generation of (decolorized) hemicellulosic hydrolysate .....	33
2.6.4	Cultivations with hydrolysates .....	33
2.7	Biotechnological production of acetoin and 2-butanone .....	34
2.7.1	Batch cultivations of <i>Lactococcus lactis</i> .....	34
2.7.2	Resting cell assay .....	34
2.7.3	Electrochemical conversion of acetoin to 2-butanone .....	35
2.8	Analytical methods.....	35
2.8.1	Sample preparation.....	35
2.8.2	Metabolite quantification using high-performance liquid chromatography .....	35
2.8.3	Methyl ketone identification and quantification using gas chromatography .....	36
2.9	<i>In silico</i> model of <i>Pseudomonas taiwanensis</i> VLB120.....	36
2.9.1	Genome-scale model.....	36
2.9.2	Flux balance analysis.....	38
<b>3</b>	<b>Results.....</b>	<b>43</b>
3.1	Bioprocess intensification for efficient methyl ketone production and extensive evaluation of methyl ketones as a drop-in biofuel.....	43
3.1.1	Abstract.....	43
3.1.2	Introduction .....	43
3.1.3	Results and Discussion.....	45
3.1.4	Conclusions.....	57
3.2	In-depth evaluation of different feeding strategies and carbon sources for methyl ketone production.....	61
3.2.1	Abstract.....	61
3.2.2	Introduction .....	61
3.2.3	Results and Discussion.....	63
3.2.4	Conclusion .....	72
3.3	Acetoin production by resting cells of <i>Lactococcus lactis</i> for direct electrochemical synthesis of 2-butanone.....	77
3.3.1	Abstract.....	77
3.3.2	Introduction .....	77
3.3.3	Results and Discussion.....	79
3.3.4	Conclusion .....	86
3.4	Foundations of biotechnological methyl ketone production .....	89
3.4.1	Abstract.....	89
3.4.2	Introduction .....	89

---

3.4.3	Results and Discussion .....	91
3.4.4	Conclusion .....	96
<b>4</b>	<b>General Discussion and Outlook .....</b>	<b>101</b>
4.1	Fuel and bulk chemical production in integrated bioreactors .....	101
4.2	Co-feeding and application of hydrolysates .....	103
4.3	Bio-based production of C <sub>4</sub> molecules .....	104
4.4	Concluding remarks .....	105
	<b>Appendix .....</b>	<b>109</b>
	<b>References .....</b>	<b>127</b>
	<b>Curriculum Vitae .....</b>	<b>147</b>



## Summary

Short- and medium-chain length methyl ketones such as 2-butanone and 2-undecanone are important commodity chemicals that are currently produced from petrochemical resources. To date, there is only limited research regarding the biotechnological production and purification of those methyl ketones in the scope of a circular bioeconomy.

This work elucidates integrated bioprocesses for the production of methyl ketones using genetically modified microorganisms.

Methyl ketones with a chain length of C<sub>11</sub> to C<sub>17</sub> are produced by genetically modified *Pseudomonas taiwanensis* VLB120 in a bioprocess with addition of an organic solvent to the cultivation medium for *in situ* liquid-liquid product extraction. The applied organic solvent can decisively influence important process parameters. However, the type of solvent for *in situ* extraction of methyl ketones was not investigated so far, and one of the major challenges of *in situ* liquid-liquid extraction, the formation of stable emulsions, is still unsolved. This work describes an in-depth investigation of the organic solvent for *in situ* product extraction of methyl ketones and the subsequent recovery of the organic phase. By performing a hierarchical solvent screening, we found 2-undecanone as a solvent that is biocompatible, non-biodegradable, and safe. With 2-undecanone as a solvent in an advanced bioreactor setup, the multiphase loop reactor, formation of stable emulsions was successfully circumvented. Here, countercurrent liquid-liquid extraction occurred in a downcomer compartment, and the organic phase could be recovered by decantation in a coalescing unit. Subsequent examinations highlighted the methyl ketone blend's potential as a drop-in diesel fuel replacement. Investigations in, e.g., a single-cylinder research engine demonstrated efficient and clean combustion with little NO<sub>x</sub> and soot emissions.

As a next step, the carbon sources that are converted to the C<sub>11</sub> to C<sub>17</sub> methyl ketones and the associated feeding strategies were investigated. By an *in silico* screening approach using a genome-scale metabolic model of the production host, ethanol was found as a co-feed carbon source that enabled superior product yields. Additionally, methyl ketone production was shown to be possible by utilizing lignocellulosic hydrolysates. Notably, also the hemicellulosic fraction that contains xylose as a carbon source and inhibitors such as furfural and vanillin was converted to methyl ketones.

A bioprocess cascade was also developed for the production of C<sub>4</sub> methyl ketones acetoin and 2-butanone. Acetoin was produced by resting cells of *Lactococcus lactis* at product yields close to the theoretical maximum. The resting cell buffer was tailored to meet the requirements of an ensuing electrocatalytic reduction, transforming biotechnologically produced acetoin into 2-butanone.

Concluding, the bioprocesses for the biotechnological production of methyl ketones were developed and improved in a holistic manner. Biotechnological methods were integrated into the preceding and consecutive process steps and optimized beyond their isolated figures of merit.



## Zusammenfassung

Kurz- und mittelkettige Methylketone wie 2-Butanon und 2-Undecanon sind wichtige Grundchemikalien, die derzeit aus petrochemischen Ressourcen hergestellt werden. Bislang gibt es nur limitierte Kenntnisse zur Herstellung dieser Methylketone in nachhaltigen Bioprozessen im Rahmen einer nachhaltigen Kreislaufwirtschaft.

In dieser Arbeit werden integrierte Bioprozesse für die Produktion von Methylketonen unter Verwendung gentechnisch veränderter Mikroorganismen aufgezeigt.

Methylketone mit einer Kettenlänge von C<sub>11</sub> bis C<sub>17</sub> wurden von gentechnisch veränderten *Pseudomonas taiwanensis* VLB120 mit *in situ* Produktextraktion unter Zugabe eines organischen Lösungsmittels zum Kultivierungsmedium hergestellt. Das gewählte Lösungsmittel kann wichtige Prozessparameter entscheidend beeinflussen. Das Lösungsmittel für die *in situ* Extraktion von Methylketonen wurde jedoch bisher nicht untersucht, und eine der größten Herausforderungen der *in situ* Flüssig-Flüssig-Extraktion, die Bildung stabiler Emulsionen, ist noch ungelöst. Im ersten Teil dieser Arbeit wurde eine umfassende Untersuchung des organischen Lösungsmittels für die *in situ* Extraktion von Methylketonen und die anschließende Rückgewinnung der organischen Phase beschrieben. In einem hierarchischen Lösungsmittelscreening fanden wir 2-Undecanon als Lösungsmittel, das biokompatibel, nicht biologisch abbaubar, und sicher ist. In einem neuartigen Bioreaktor, dem *multiphase loop reactor*, wurde außerdem die Bildung stabiler Emulsionen erfolgreich umgangen. Die organische Phase konnte durch Dekantieren in einer Koaleszenzeinheit zurückgewonnen werden. Anschließende Experimente, zum Beispiel in einem Einzylinderforschungsmotor, zeigten die Eignung des Methylketongemischs als nachhaltiger *drop-in* Biokraftstoff.

In einem nächsten Schritt wurde die Kohlenstoffquelle, die in die C<sub>11</sub>- bis C<sub>17</sub>-Methylketone umgewandelt wird, und die damit verbundenen Fütterungsstrategien untersucht. Durch ein *in silico screening* unter Verwendung eines genomskaligen Modells des Produktionsstamms wurde Ethanol als Kohlenstoffquelle gefunden, die durch *co-feeding* eine höhere Produktausbeute ermöglicht. Darüber hinaus konnte gezeigt werden, dass die Methylketonproduktion mit Lignocellulosehydrolysaten möglich ist. Insbesondere war auch der Einsatz der Hemicellulosefraktion mit Xylose als Kohlenstoffquelle und Inhibitoren wie Furfural und Vanillin möglich.

Auch für die Herstellung der C<sub>4</sub> Methylketone Acetoin und 2-Butanon wurde ein integrierter Bioprozess entwickelt. Acetoin wurde von ruhenden *Lactococcus lactis* mit Produktausbeuten nahe dem theoretischen Maximum produziert. Der Puffer der ruhenden Zellen wurde auf die Anforderungen einer anschließenden elektrokatalytischen Reduktion zugeschnitten, bei der das biotechnologisch hergestellte Acetoin in 2-Butanon umgewandelt wird.

In dieser Arbeit wurden die Bioprozesse ganzheitlich entwickelt und verbessert. Die biotechnologischen Methoden wurden in die vor- und nachgelagerten Prozessschritte integriert und über ihre isolierten Leistungskennzahlen hinaus optimiert.





# Nomenclature

## Abbreviations

Abbreviation	Description
2,4,6-TriHBP	2,4,6-trihydroxybenzophenone
a. u.	arbitrary units
ABE	acetone-butanol-ethanol
ACP	acyl carrier protein
aq	aqueous
ATP	adenosine triphosphate
ATPM	adenosine triphosphate maintenance
BCBT	Biomass Conversion and Bioprocess Technology
CA50	center of combustion
CDM	chemically defined medium
CDMPC	chemically defined medium for prolonged cultivation
CDW	cell dry weight
CH	cellulosic hydrolysate
COSMO-RS	conductor-like screening model for real solvents
CTR	carbon dioxide transfer rate
DFT	density function theory
DHH	decolorized hemicellulosic hydrolysate
DNA	deoxyribonucleic acid
DO	dissolved oxygen
DOI	duration of injection
DSMZ	German Collection of Microorganisms and Cell Cultures GmbH
DTU	Danmarks Tekniske Universitet
<i>e.g.</i>	<i>exempli gratia</i>
EC <sub>50</sub>	median effective concentration
EDTA	ethylenediaminetetraacetic acid
EGR	exhaust gas recirculation
EPDM	ethylene propylene diene monomer rubber
EU	European Union

Abbreviation	Description
FBA	flux balance analysis
FE	Faraday efficiency
FID	flame ionization detector
FKM	fluorine kautschuk material
FPU	filter paper units
FSN	filter smoke number
GC	gas chromatography
GEM	genome-scale metabolic model
HAA	3-(3-hydroxy-alkanoyloxy)alkanoate
HC	unburned hydrocarbons
HER	hydrogen evolution reaction
HH	hemicellulosic hydrolysate
HPLC	high-pressure liquid chromatography
HS	Hestrin Schramm medium
iAMB	Institute of Applied Microbiology
IMEP	indicated mean effective pressure
IPTG	isopropyl $\beta$ -D-1-thiogalactopyranoside
IRHD	international rubber hardness degree
ISPR	<i>in situ</i> product removal
KPI	key performance indicator
LB	lysogeny broth
LC <sub>50</sub>	50% lethal concentration
LCA	life cycle analysis
LCC	life cycle costing
LOEC	lowest observed effect concentration
Log <i>P</i>	water-octanol partition coefficient
ME	malt extract
MK	methyl ketones
MPRL	multiphase loop reactor
MS	mass spectrometer

---

Abbreviation	Description
MSM	mineral salt medium
MTP	microtiter plate
NBR	nitrile butadiene rubber
NGAM	non-growth associated ATP maintenance
nm	nanometer
NOEC	no observed effect concentration
OD <sub>600</sub>	optical density at a wavelength of 600 nm
org	organic
OTR	oxygen transfer rate
PCR	polymerase chain reaction
PEGB	potato extract glucose bouillon
PRR	pressure rise rate
PTFE	polytetrafluoroethylene
RCB	resting cell buffer
RI	refractive index
RME	rapeseed oil methyl ester
RNA	ribonucleic acid
rpm	rotations per minute
SOI	start of injection
spp	subspecies
STR	stirred tank reactor
TEA	techno-economic assessment
TEM	transmission electron microscopy
UV	ultraviolet
VMQ	vinyl methyl silicone
vvm	volume air per volume liquid per minute
WCH	washed cellulosic hydrolysate
wsd	wear scar diameter
WT	wild type
YEP	yeast extract peptone

---

## Symbols

Symbol	Description	Unit
$\mu$	dynamic viscosity	$\text{kg} \cdot \text{m}^{-1} \cdot \text{s}^{-1}$
$c$	concentration	$\text{g} \cdot \text{L}^{-1}$
$D$	dilution rate	$\text{h}^{-1}$
$d_d$	droplet diameter	m
$d_0$	shaking diameter	mm
$F$	flow rate	$\text{m}^3 \cdot \text{h}^{-1}$
$F_{\text{Faraday}}$	Faraday constant	-
$F_{\text{in}}$	flow rate of the cultivation broth in the bioreactor	$\text{m}^3 \cdot \text{h}^{-1}$
$F_{\text{out}}$	flow rate of the cultivation broth out of the bioreactor	$\text{m}^3 \cdot \text{h}^{-1}$
$g$	acceleration constant	$\text{m} \cdot \text{s}^{-2}$
$I$	applied current	A
$n$	stirrer speed	$\text{min}^{-1}$
$N$	engine speed	$\text{min}^{-1}$
$P$	partition coefficient	-
$p_{\text{ex}}$	exhaust pressure	bar
$p_{\text{in}}$	boost pressure	bar
$p_{\text{rail}}$	rail pressure	bar
$\text{STY}$	space-time yield	$\text{g} \cdot \text{L}^{-1} \cdot \text{h}^{-1}$
$T$	temperature	$^{\circ}\text{C}$
$T_{\text{in}}$	charge air temperature	$^{\circ}\text{C}$
$T_{\text{pi}}$	time offset for a pilot injection	min
$V$	volume	mL
$V_{\text{L}}$	liquid volume	mL
$Y_{\text{P/S}}$	product yield	$\text{g}_{\text{product}} \cdot \text{g}_{\text{substrate}}^{-1}$
$Y_{\text{X/S}}$	biomass yield	$\text{g}_{\text{biomass}} \cdot \text{g}_{\text{substrate}}^{-1}$
$z$	number of electrons	-
$\eta$	indicated efficiency of combustion	-
$\lambda$	relative air fuel ratio	-
$\mu_x$	growth rate	$\text{h}^{-1}$

Symbol	Description	Unit
$\Phi$	phase ratio	$\text{mL}_{\text{org}} \cdot \text{mL}_{\text{aq}}^{-1}$
$V_{\text{buoyancy}}$	volume of the bouyancy body	$\text{m}^3$
$m_{\text{buoyancy}}$	mass of a buoyancy body	kg
$m_{\text{measured}}$	measured mass	kg
$v_c$	settling velocity	$\text{m} \cdot \text{s}^{-1}$
$\rho$	density	$\text{kg} \cdot \text{m}^{-3}$

## Metabolites and proteins

Abbreviation	Description
2KDPG	2-keto-3-desoxyphosphogluconate
2PG	2-phosphoglycerate
6PG	6-phosphogluconate
ACAH	acetaldehyde
AcCoA	acetyl-CoA
ACP	acyl carrier protein
adhE	alcohol dehydrogenase E
Ald	$\alpha$ -acetolactate decarboxylase
Als	$\alpha$ -acetolactate synthase
ara	arabinose
ButBA	butanediol dehydrogenases A and B
CIT	citrate
co_aco	codon optimized version of the acyl-CoA oxidase from <i>Micrococcus luteus</i>
CoA	coenzyme A
CpFatB1	<i>Cuphea palustris</i> thioesterase FatB1
DHAP	dihydroxyacetone phosphate
E4P	erythrose 4-phosphate
F6P	fructose 6-phosphate
FadA	3-ketoacyl-CoA thiolase
fadB	subunit of the fatty acid oxidation complex with hydratase activity
FadD	acyl-CoA synthetase

Abbreviation	Description
FadE	acyl-CoA dehydrogenase
FADH <sub>2</sub>	(reduced) dihydroflavin adenine dinucleotide
FadM	type III thioesterase
FatB	type I thioesterase
FBP	fructose 1,6-bisphosphate
G3P	glyceraldehyde 3-phosphate
G6P	glucose 6-phosphate
gcd	glucose dehydrogenase
GLX	glyoxylate
ICIT	isocitrate
ldh	lactate dehydrogenase
MAL	malate
MalCoA	malonyl-CoA
NADH	(reduced) nicotinamide adenine dinucleotide
NoxE	NADH oxidase E
OAA	oxalacetate
P5P	5-phosphate pentose
PEP	phosphoenolpyruvate
PHA	polyhydroxyalkanoate
phaC	polyhydroxyalkanoate synthases
phaZ	polyhydroxyalkanoate depolymerase
PsFadM	<i>Providencia sneebia</i> thioesterase
pSTY	native megaplasmid of <i>Pseudomonas taiwanensis</i> VLB120
PTA	phosphotransacetylase
PYR	pyruvate
S7P	seduheptolose 7-phosphate
SUC	succinate
tesA	type I thioesterase
tesB	type II thioesterase
TtgGHI	solvent efflux pump of <i>Pseudomonas</i> spp.

## List of Figures

<b>Figure 1</b> Visualization of the circular economy.....	3
<b>Figure 2</b> Replacing the oil barrel. ....	4
<b>Figure 3</b> The bow-tie structure of microbial metabolism .....	5
<b>Figure 4</b> Scheme of a lignocellulosic biorefinery.....	7
<b>Figure 5</b> Scheme of the metabolic pathway of methyl ketone production with genetically modified <i>P. taiwanensis</i> VLB120 $\Delta 6$ pProd .....	9
<b>Figure 6</b> Scheme of the metabolic pathway of enantiopure (3 <i>R</i> )-acetoin production with genetically modified <i>L. lactis</i> VJ017 .....	11
<b>Figure 7</b> Steps during the destabilization of emulsions.....	13
<b>Figure 8</b> Scheme of the multiphase loop reactor (MPLR) .....	14
<b>Figure 9</b> Overview of the chemical structures of the methyl ketones relevant to this study.....	16
<b>Figure 10</b> Measurement setup for determining the fluid density .....	28
<b>Figure 11</b> Partition coefficients of the methyl ketones after extraction from cultivation broth .....	47
<b>Figure 12</b> Biocompatibility and biodegradability assessment of the solvents.....	49
<b>Figure 13</b> Methyl ketone production with 2-undecanone as the organic phase for <i>in situ</i> extraction .....	50
<b>Figure 14</b> Images of bioreactors with <i>P. taiwanensis</i> VLB120 $\Delta 6$ pProd and 2-undecanone as the organic solvent for <i>in situ</i> methyl ketone extraction.....	51
<b>Figure 15</b> Efficiency and emission results for a selected lower part load operating point, comparing the methyl ketone blend with diesel .....	54
<b>Figure 16</b> Investigating fuel storage in the presence of microbial contaminations ...	55
<b>Figure 17</b> The methyl ketone exchange flux as a result of varying the glucose and co-substrate uptake rates during the FBA .....	63
<b>Figure 18</b> Scheme of the central carbon metabolism of <i>P. taiwanensis</i> VLB120 including the metabolization of different substrates .....	64
<b>Figure 19</b> Cultivation of <i>P. taiwanensis</i> $\Delta 6$ pProd with glucose and ethanol.....	66
<b>Figure 20</b> Methyl ketone yield of (co-fed) shake flask cultivation after 24 hours and corresponding concentration of the carbon source .....	67
<b>Figure 21</b> Flow-chart showing the preparation of cellulosic hydrolysate (CH), washed cellulosic hydrolysate (WCH), hemicellulosic hydrolysate (HH), and decolourized hemicellulosic hydrolysate (DHH).....	68
<b>Figure 22</b> Wheat straw hydrolysates as cultivation media in bioreactors with <i>P. taiwanensis</i> VLB120 $\Delta 6$ pProd .....	70
<b>Figure 23</b> Schematic representation of the substrates and products that are involved in our suggested cascade from glucose to 2-butanone .....	78
<b>Figure 24</b> CO <sub>2</sub> accumulation during growth of <i>L. lactis</i> VJ017 in the presence of various initial acetoin concentrations .....	79
<b>Figure 25</b> Growth of <i>L. lactis</i> VJ017 and acetoin formation with different media.....	81



<b>Figure 26</b> Influence of the resting cell buffer composition on acetoin production by <i>L. lactis</i> VJ017 .....	83
<b>Figure 27</b> Electrochemical conversion yields of the assessed supernatants .....	84
<b>Figure 28</b> Thioesterases involved in the metabolic pathway for methyl ketone production .....	90
<b>Figure 29</b> Growth, methyl ketone production, and congener distribution of a bioreactor cultivation with <i>in situ</i> gas stripping .....	92
<b>Figure 30</b> Methyl ketone congener distribution that resulted from different thioesterase combinations .....	94
<b>Figure 31</b> Growth rate of <i>P. taiwanensis</i> VLB120 Δ6 pProd over a temperature range from 22.6 °C to 44.0 °C .....	95
Figure A 1 Methyl ketone production by <i>P. taiwanensis</i> Δ6 pProd in shake flasks with different induction time points .....	110
Figure A 2 Details of the pre-screening .....	111
Figure A 3 Images of the cultivation broth of the growth assay .....	112
Figure A 4 Images of interphases after <i>in situ</i> extraction of methyl ketones .....	112
Figure A 5 Change of volume and hardness for different bio-hybrid fuels and reference elastomer sealing materials .....	122
Figure A 6 Biomass growth of <i>P. taiwanensis</i> VLB120 Δ6 pProd in microtiter plates with glucose and the five different co-fed substrates ethylene glycol, glycerol, ethanol, acetate, and formate in BioLector cultivations .....	123
Figure A 7 Transmission electron microscopy of <i>P. taiwanensis</i> VLB120 wild type (A) and <i>P. taiwanensis</i> VLB120 Δ6 pProd (B) in stationary phase 30 hours after inoculation .....	124

## List of Tables

<b>Table 1</b> Desirable solvent properties for <i>in situ</i> product extraction in bioprocesses .	15
<b>Table 2</b> Bacterial strains used in this study .....	21
<b>Table 3</b> Plasmids used in this study .....	22
<b>Table 4</b> Oligonucleotides used in this study .....	23
<b>Table 5</b> DNA sequences introduced in this study.....	24
<b>Table 6</b> Physical parameters and respective limits for the pre-screening of solvent candidates .....	45
<b>Table 7</b> Selected properties of fossil diesel, measured and simulated properties of the methyl ketone blend, and the specifications according to the EN590 norm.....	52
<b>Table 8</b> Aquatic toxicity on fish for methyl ketones, gasoline, and diesel .....	56
<b>Table 9</b> Growth of <i>P. taiwanensis</i> VLB120 Δ6 pProd using the different hydrolysates and the respective concentration of different carbon sources and inhibitors .....	69
<b>Table 10</b> Comparison of methyl ketone product yields with different substrates .....	73
<b>Table 11</b> Toxicity of acetoin towards <i>L. lactis</i> VJ017.....	80
<b>Table 12</b> Acetoin and microbial biomass yield by <i>L. lactis</i> VJ017 in different media from 40 g·L <sup>-1</sup> of glucose .....	82
<b>Table 13</b> Composition of the complex media for acetoin production with <i>L. lactis</i> VJ017 .....	85
<b>Table 14</b> Thioesterases and respective substrate specificities and origins used in this study.....	93
 Table A 1 Composition of the stock solutions that were used for preparation of the MSM .....	 109
Table A 2 Strains used in this study for the defined inoculum of the fuel tank simulation. ....	113
Table A 3 Composition of the chemically defined medium (CDM) according to Otto <i>et al</i> and Poolman and Konings.....	114
Table A 4 Composition of the CDMPC medium.....	117
Table A 5 Composition of the resting cell buffer .....	119
Table A 6 Acetoin concentrations and current densities in supernatants .....	119
Table A 7 Deleted genes in the mutant strain <i>P. taiwanensis</i> VLB120 Δ6 pProd for the genome-scale model. ....	120
Table A 8 Score explanation for establishing the weighted decision matrix .....	120
Table A 9 Results of the weighted decision matrix .....	121
Table A 10 Influence of the oxygen transfer rate (OTR) on acetoin formation.....	122



---

# Chapter 1

## General Introduction

### Contributions

This chapter was written by Carolin Grütering and reviewed by Lars M. Blank.

---



# 1 General Introduction

## 1.1 Bioeconomy

Unlimited growth is incompatible with the fundamental laws of nature.<sup>1</sup>

The current linear economy strictly depends on coal, oil, and natural gas for the production of goods, the generation of energy, and transportation. The exploitation of these reserves has led to great improvements in the quality of life for billions of individuals since the industrial revolution. Behind the current form of resource utilization, there is an “take, make, use, dispose” mindset, where disposal is the end of life of every product.<sup>2</sup> However, the usage of fossil resources causes massive emission of CO<sub>2</sub> and other greenhouse gases (GHGs). This has given rise to the climate crisis, with all its disastrous consequences on the environment and human health, including extreme weather events, insecurities in food supply, and land shortage.<sup>3-7</sup> Additionally to greenhouse gas emissions and the resulting climate crisis, the linear economy massively endangers the biosphere, referred to as the “biosphere crisis”. The ongoing destruction of key ecosystems, for example by deforestation, and the resulting loss in biodiversity, also endangers human survival.<sup>8, 9</sup>

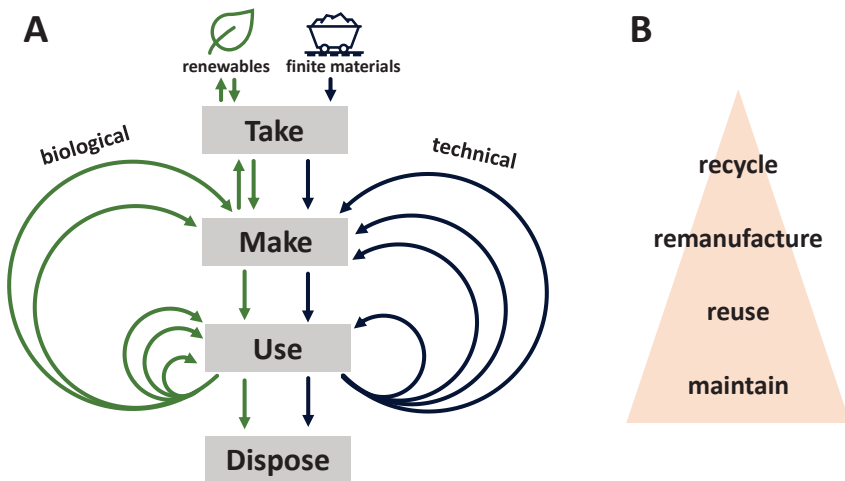


**Figure 1** Visualization of the circular economy. (A) Technical and biological utilization of renewables and finite materials in the circular economy and the linear economy. In the linear economy, materials undergo the “take, make, use, dispose” lifeline, while in a circular economy, materials fluctuate between “make” and “use” by maintaining, reusing, remanufacturing, and recycling. This scheme is an adapted version of the iconic “Butterfly Diagram” of the Ellen MacArthur Foundation.<sup>10</sup> (B) Hierarchy of the options to incorporate materials and goods in a circular economy. Maintaining a material usually requires the least energy, thus, it is the preferred option. If maintenance is not possible, the material should be reused, then remanufactured. Recycling of a material should only be done if it is unavoidable.<sup>11</sup>

To limit the effects of the climate crisis and the biodiversity crisis, it is evident that humanity must transition from the current linear economy to a circular economy. Accordingly, we have to phase out fossil fuels, and treat waste as a valuable resource. The basis of the circular economy is closed material loops, which implies the minimization of waste generation and the preservation of the value of products, materials, and resources (**Figure 1A**). Notably, recycling a material usually requires more energy than maintaining or reusing it. Thus, recycling is not the preferred option for the preservation of materials in a circular economy (**Figure 1B**). Still, recycling is often necessary and a valid method in this context.<sup>12, 13</sup>

One key player in the circular economy is the so called bioeconomy, where lithospheric inputs such as fossils are substituted with biogenic inputs such as biomass in economic activities.<sup>14, 15</sup> In the envisaged bioeconomy, renewable carbon reserves such as agricultural biomass, organic waste, and industrial side streams (e.g. CO<sub>2</sub>, plastics), are used to generate material, chemicals, fuels, and energy (**Figure 2**).<sup>16, 17</sup>

Circular (bio)economies are not a new concept; in fact, circular practices are deeply rooted in human history. A mindset of reusing, remanufacturing, and recycling of materials was found to be the foundation of, e.g., ancient Indian cultures, making the circularity concept one of the oldest one known to humanity.<sup>18, 19</sup>

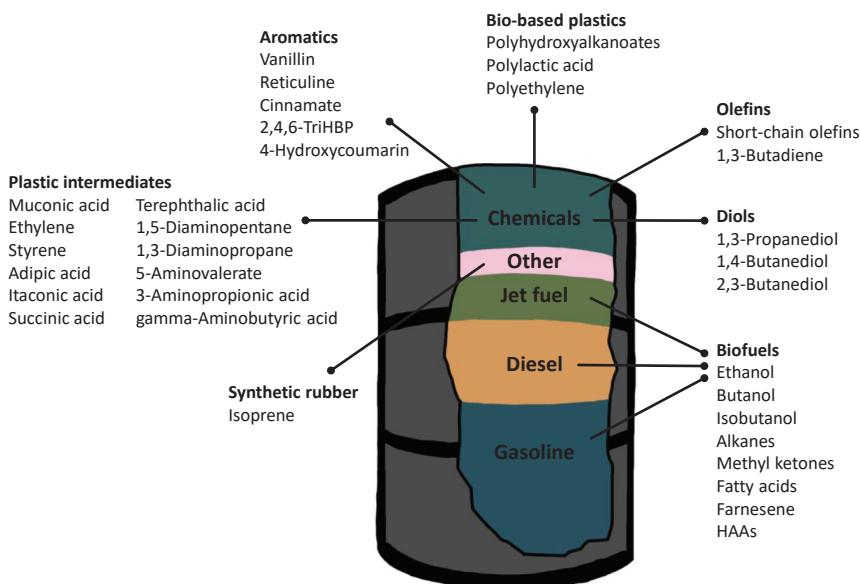


**Figure 2** Replacing the oil barrel. Possibilities of a more sustainable production for various chemicals, with different degrees of commercialization.<sup>20</sup> 2,4,6-TriHBP = 2,4,6-trihydroxybenzophenone; HAAs = 3-(3-hydroxy-alkanoyloxy)alkanoates.<sup>21, 22</sup>

It should also be noted that a bioeconomy is not inherently sustainable or “circular”. The bio-based production of goods does not necessarily imply its re-use or recycling and the general avoidance of over-consumption.<sup>23, 24</sup> Also an increased pressure on water supply and natural ecosystems for the generation of biomass are part of the risks of a bioeconomy.<sup>14, 25</sup>

However, with the techniques of the life sciences and biotechnology, modern or “knowledge based” bioeconomy can be transformed into one of the most advanced and sustainable economic concepts, securing the prosperity of humanity.<sup>26</sup>

### 1.1.1 Biotechnology within a sustainable bioeconomy

The 21<sup>st</sup> century was claimed to be the “Century of Biology”.<sup>27</sup> The application of biological methods in the production of goods is referred to as industrial biotechnology, and it plays a key role in the bioeconomy. In industrial biotechnology, biological systems such as microorganisms or enzymes are used as catalysts for the generation of value-added goods, preferably from renewable carbon sources. The application of living microorganisms in fermentation processes plays a key role in industrial biotechnology.<sup>28, 29</sup> One remarkable feature of microorganisms is their capability to transform a broad variety of carbon sources, including those obtained from industrial side streams, biomass, and CO<sub>2</sub>, into various products (Figure 3).<sup>30</sup>

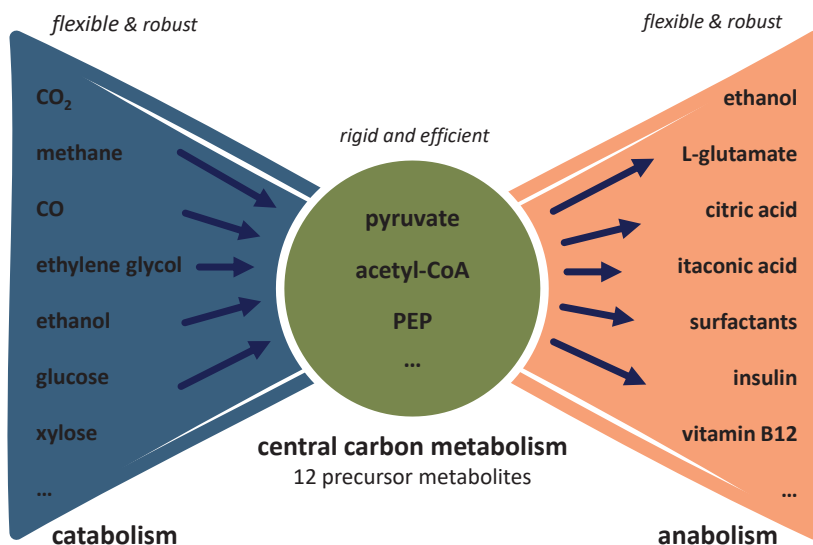


**Figure 3** The bow-tie structure of microbial metabolism. Various substrates can be utilized in catabolic enzymatic reactions (left) to form the building blocks of the central carbon metabolism (center). Those central precursor metabolites can be converted to value-added goods in anabolic reactions (right), partly enabled by genetic engineering. The products are shown in declining order of their market size. Both catabolism and anabolism have a high variation and flexibility within species, while the central carbon metabolism is mostly conserved for efficiency. PEP = phosphoenolpyruvate.<sup>31-34</sup>



The utilization of the metabolic networks in living cells has the benefit of highly stereoselective product formation and a high product purity. Additional advantages of industrial biotechnology include a lowered energy consumption, the use of non-toxic aqueous solvents, and decreased generation of waste, compared to purely chemical production.<sup>35, 36</sup>

In ancient times, the fermentation of *e.g.* food products with non-adapted microbes was practiced as an inherently biotechnological process. Since the 70s, pioneering DNA-based technologies such as polymerase chain reaction (PCR), DNA sequencing, and, more recently, CRISPR Cas9, have been developed that turn microorganisms into “programmable biocatalysts”.<sup>37</sup> Currently, mRNA technologies and the utilization of artificial intelligence are being researched and open up new possibilities in the production of advanced chemicals and pharmaceuticals.<sup>38-41</sup> The possibility to tailor a cell’s genetic repertoire to specific applications transformed the entire field of industrial biotechnology and generally accelerated bioprocess development.<sup>42, 43</sup> Using those optimized microorganisms as biocatalysts can benefit both the sustainability and the efficiency of existing processes, *e.g.* by allowing for higher product yields, and facilitate the development of new, revolutionary products, such as mRNA vaccines.<sup>20, 44</sup>

Further examples of successful industrial implementation of biotechnological processes for fine and bulk chemicals include the production of citric acid, glycerol, lysine, xanthan, and insulin, to name a few.<sup>28, 45-47</sup> Common microbial workhorses in these processes include well-known model organisms such as *Escherichia coli* and *Saccharomyces cerevisiae* as well as novel microorganisms such as *Ogataea polymorpha* or *Paracoccus pantotrophus* that can be exploited for their advanced properties.<sup>48, 49</sup> Some features, *e.g.* a high robustness towards fluctuating conditions and a high genomic stability are critical for the application of microorganisms as cell factories in industrial processes and biorefineries.<sup>50, 51</sup>

### 1.1.2 Biorefineries for biofuels and bulk chemicals

Refineries are facilities where different unit operations are combined to convert a raw material into fuels, electricity, heat, and chemicals. Traditionally, petrochemical refineries split crude oil into different fractions that are further processed into an immense variety of products that are the foundation of our society, fueling the linear economy.<sup>52</sup> The unit operations of petrochemical refineries have been optimized for decades, so that most processes operate at the upper limit of capacity and efficiency.<sup>53-55</sup> The product range of a petrochemical refinery includes platform chemicals and fuels, which form the basis of chemical and pharmaceutical industries.<sup>56, 57</sup>

Just as a petrochemical refinery is the foundation of the linear economy, biorefineries are their counterpart in a circular bioeconomy. Biomass serves as the primary carbon source for biorefineries and results from the fixation of CO<sub>2</sub> from the atmosphere during photosynthesis, which creates a circular approach by nature.<sup>58</sup> First generation biorefineries are based on the edible parts of crops rich in starch, sugars, or oils (wheat, sugar cane, oil palm etc.). While these have the potential to reduce GHG emissions,

first generation biorefineries compete with food production.<sup>59</sup> Second generation biorefineries work with non-edible feedstocks such as lignocellulosic plant material or industrial side streams. By using these feedstocks, products can be produced sustainably, while waste accumulation can be reduced.

Lignocellulose in particular is an abundant resource that has the potential to replace fossils. It has a high carbohydrate content and is, unlike fossil resources, available fairly consistently throughout the world.<sup>60</sup> Additionally, the cultivation of dedicated energy crops with high biomass yields on marginal soils holds great potential.<sup>61</sup>

In a lignocellulosic refinery, biomass first undergoes pre-treatment to obtain the major components cellulose, hemicellulose, and lignin in an accessible form (**Figure 4**). These are subjected to different bio- and chemocatalytic conversion steps for the generation of a broad variety of products.<sup>62</sup> While this concept holds great potential for a more sustainable future and some sites are already operating, the large-scale economic feasibility has to be improved.<sup>63</sup> The technologies for processing crude oil were developed since the 1860s, while bio-refineries still lack standardized methods and a uniform processing approach.<sup>64</sup> For example, it is unclear which pre-treatment method is best during the processing of different forms of lignocellulosic material.<sup>65-67</sup> It is widely recognized that industrial biotechnology will play a key role in the conversion of lignocellulosic building blocks to fine and bulk products.<sup>20, 68</sup> However, bioprocessing is currently often not as effective as chemical processing and often has low product titers, resulting in higher costs for products of renewable origin.<sup>69, 70</sup>

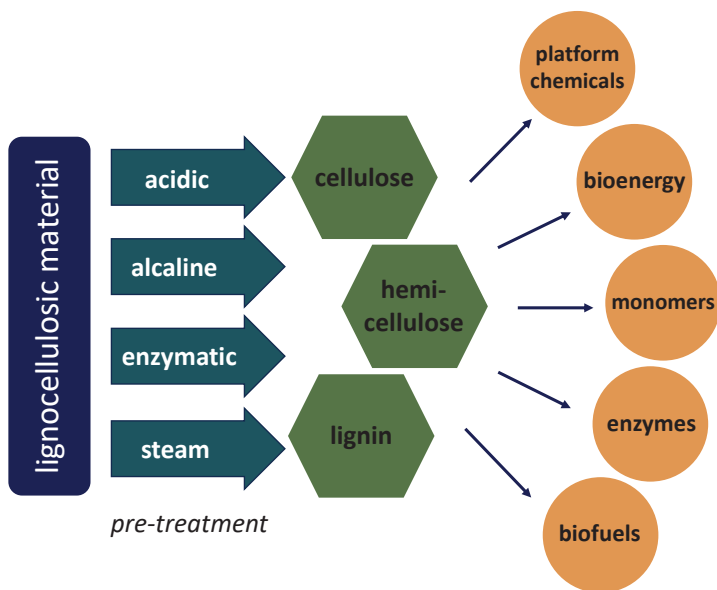


**Figure 4** Scheme of a lignocellulosic biorefinery.<sup>62</sup>

## 1.2 Biofuels

A main product of refineries are fuels. The global transportation sector mainly depends on the combustion of these liquid transportation fuels derived from fossil resources and contributes to around 25% of the total CO<sub>2</sub> emissions.<sup>71</sup> Electric vehicles are considered to be the future of transportation, however, the existing global fleet is still predominantly using fossil fuels. In fact, by 2030, around 80% of the global vehicles are supposed to be powered by internal combustion engines and are therefore relying on fuels.<sup>72</sup> In the upcoming decades, liquid transportation fuels are also essential for long-distance and heavy-duty transportation.<sup>73, 74</sup> To render the transportation sector more sustainable under these conditions, the usage of more environmentally friendly fuels is inevitable. Those can be e-fuels or biofuels that have a high volumetric energy content and simultaneously profit from the infrastructure of their fossil equivalents.<sup>75, 76</sup> Petroleum-derived fossil fuels directly elevate atmospheric CO<sub>2</sub> levels by their combustion. In contrast, biofuels produced from renewable resources have the potential to simultaneously reduce the emitted CO<sub>2</sub> and the accumulation of waste.<sup>77</sup> Two biofuels are widely commercialized: bio-ethanol from yeast fermentation and biodiesel from esterified plant oils. However, these are mostly derived from first generation feedstocks that are in direct competition with food production and have drawbacks, e.g. in their compatibility with the fuel infrastructure. Consequently, the objective of many efforts is to find a high energy drop-in biofuel that is compatible with the existing fleet and fuel infrastructure and can be synthesized from non-edible, second generation feedstocks. Promising alternative biofuel candidates such as isoprenoids, fatty acids, alcohols, and methyl ketones are produced by utilizing genetically modified microorganisms as the biocatalyst.<sup>78-81</sup> Those potential fuels are often hydrocarbons that originate from the fatty acid metabolism, and several challenges have to be considered during their production. Fatty acid metabolism is a process that is absolutely essential for the viability of a cell. It is tightly regulated and aims for homeostasis, making genetic engineering of the fatty acid metabolism demanding. Intermediates of the fatty acid metabolism are also associated with the assembly of cellular membranes, and small changes in the membrane composition have immense effects on the cell.<sup>82</sup> An additional challenge during the synthesis is the high demand for redox and energy cofactors such as NADPH and ATP.<sup>71, 83</sup> Accordingly, product synthesis from fatty acid metabolism competes with other cellular processes that depend on these cofactors. Also, product toxicity can be an obstacle to both biocatalyst and bioprocess design.<sup>84, 85</sup> Many biofuels are known to interact with the cell membrane and impede fundamental cellular functions, so that the production of high product titers in conventional bioreactor setups is usually challenging.<sup>86</sup>

### 1.2.1 Production of medium-chain length methyl ketones

Methyl ketones are hydrocarbons with a carbonyl group at the C<sub>2</sub> position. In industry, methyl ketones are commonly produced chemically by oxidation of terminal olefins.<sup>87</sup> Depending on the number of carbon atoms and the branching, different methyl ketones

have different properties and applications, ranging from bulk chemicals to insect repellents and flavor compounds.<sup>78, 88, 89</sup> The shortest methyl ketone, acetone, is widely used as an industrial solvent and as a platform chemical.<sup>90</sup> Aliphatic methyl ketones with a chain length of C<sub>11</sub> to C<sub>17</sub> were recently described as potential diesel fuel replacements. The cetane number, a value for the suitability as a diesel fuel, of a mixture of saturated and monounsaturated methyl ketone was determined to be 54, which is in the so-called “diesel range”.<sup>78, 91</sup>

In biology, aliphatic medium-chain length methyl ketones usually originate from intermediates of the fatty acid metabolism. For example, in wild tomato (*Solanum habrochaites*),  $\beta$ -ketoacyl-acyl carrier protein (ACP) thioesters are hydrolyzed to generate  $\beta$ -keto acids, which are then decarboxylated to methyl ketones.<sup>92, 93</sup> By means of genetic engineering, biotechnological production of methyl ketones was implemented using various microorganisms such as *Escherichia coli*, *Yarrowia lipolytica*, *Saccharomyces cerevisiae*, and *Pseudomonas putida* from renewable resources.<sup>78, 94-96</sup> The best reported methyl ketone yield of 0.17 g<sub>methyl ketones</sub>·g<sub>glucose</sub><sup>-1</sup> was achieved by using genetically modified *Pseudomonas taiwanensis* VLB120  $\Delta$ 6 pProd in fed-batch mode. This strategy for the production of methyl ketones included the overproduction of enzymes that are involved in the fatty acid metabolism adjacent to the  $\beta$ -keto acids, a completely disrupted  $\beta$ -oxidation at the *fadA* reaction, and the overexpression of a *FadM* thioesterase (**Figure 5**).<sup>97</sup>

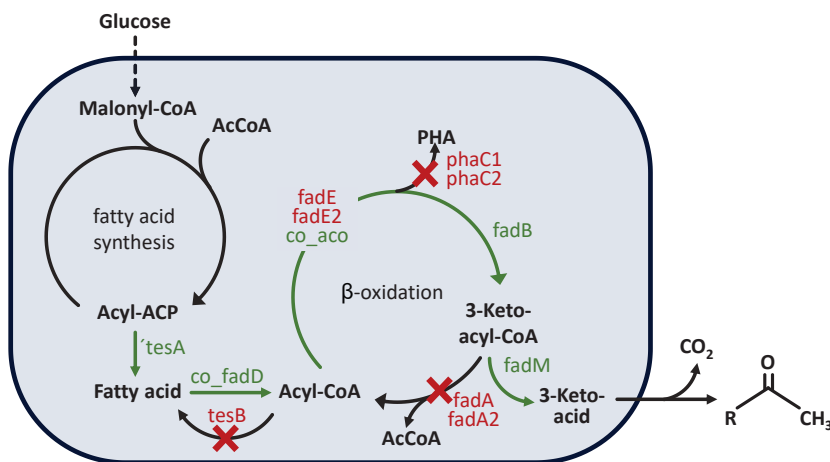


**Figure 5** Scheme of the metabolic pathway of methyl ketone production with genetically modified *P. taiwanensis* VLB120  $\Delta$ 6 pProd. Green arrows signify plasmid-based overproduction of the gene, while red crosses signify deletion of a certain gene. R = (CH<sub>2</sub>)<sub>8-14</sub>CH<sub>3</sub>; PHA = polyhydroxyalkanoate; AcCoA = acetyl-CoA; 'tesA = truncated variant of TesA, type I thioesterase; co\_fadD = acyl-CoA synthetase; fadA = 3-ketoacyl-CoA thiolase; fadE = acyl-CoA dehydrogenase; co\_aco = codon optimized version of the acyl-CoA oxidase from *Micrococcus luteus*; phaC1 and phaC2 = polyhydroxyalkanoate synthases; fadB = subunit of the fatty acid oxidation complex with hydratase activity; tesB = type II thioesterase; fadM = type III thioesterase.<sup>97</sup>

Notably, the substrate specificity of the applied thioesterase was described to determine the chain length of the methyl ketones and thus their application.<sup>98, 99</sup>

The exhaustion of reducing equivalents such as NADH is one of the main limiting factors in the production of biofuels with a high energy content, which also applies to the production of methyl ketones.<sup>100</sup> *P. taiwanensis* VLB120, however, is a microorganism that is particularly beneficial for the production of reduced products such as the medium-chain length methyl ketones, because it has an exceptionally high redox cofactor regeneration rate, that can be adapted to the metabolic demand.<sup>101</sup> These microorganisms express a pyridine nucleotide transhydrogenase, which catalyzes the reversible conversion of NADH to NADPH, making the cell generally more flexible with regard to redox metabolism.<sup>102</sup> Additionally, *Pseudomonas* spp have a high potential for industrial processes due to their fast growth, high solvent tolerance, and versatile metabolism.<sup>103, 104</sup> Recently, *P. putida* KT2440, a close relative of *P. taiwanensis* VLB120, was described to endure oscillating oxygen limiting conditions of 2 minutes without a major decrease in product yield, highlighting the robustness of *Pseudomonas* spp. also in large-scale bioreactors.<sup>105</sup>

### 1.2.2 Production of acetoin and 2-butanone

The second most important ketone after acetone is 2-butanone, the C<sub>4</sub> methyl ketone. It is applied as a low-boiling solvent and activating agent for oxidative reactions in the chemical industry.<sup>106</sup> Furthermore, 2-butanone is discussed as a more sustainable fuel for spark-ignition engines.<sup>107</sup> As opposed to the high demand for the sustainable biotechnological production from non-petrochemical, renewable resources, there was only limited success in developing a microbial host for 2-butanone production. Attempts using microbial cell factories such as *E. coli* resulted in low product titers, not exceeding 0.5 g·L<sup>-1</sup>, while biotechnological production of the precursor butanediol was shown to be feasible in the range of 100 g·L<sup>-1</sup>.<sup>108-111</sup> The availability of coenzyme B<sub>12</sub>, an essential cofactor of the diol dehydratase, was identified as the bottleneck in 2-butanone production.<sup>109</sup> A more promising approach that was recently described is the electrochemical reduction of acetoin of sustainable origin to 2-butanone.<sup>112</sup>

Acetoin, a methyl ketone and hydroxyketone, is a value added C<sub>4</sub> compound that serves as a precursor for various chemical syntheses and as a flavor and fragrant ingredient in the food industry.<sup>113, 114</sup> Unlike 2-butanone, acetoin can be produced at high titers and yields with microorganisms as the biocatalyst. For example, using *S. cerevisiae*, 100 g·L<sup>-1</sup> of acetoin were produced from glucose by disruption of the butanediol dehydrogenase.<sup>115</sup> Efficient production of enantiopure (3*R*)-acetoin without any side product formation was possible using *Lactococcus lactis* as a production host (**Figure 6**). By blocking of all competing pathways, this attempt resulted in a product yield of 0.42 g<sub>acetoin</sub>·g<sub>glucose</sub><sup>-1</sup>. Since all NAD<sup>+</sup> producing reactions were removed, growth and product formation was feasible under strict aerobic conditions, which enabled NAD<sup>+</sup> regeneration by a water forming NADH oxidase (NoxE).<sup>116</sup>

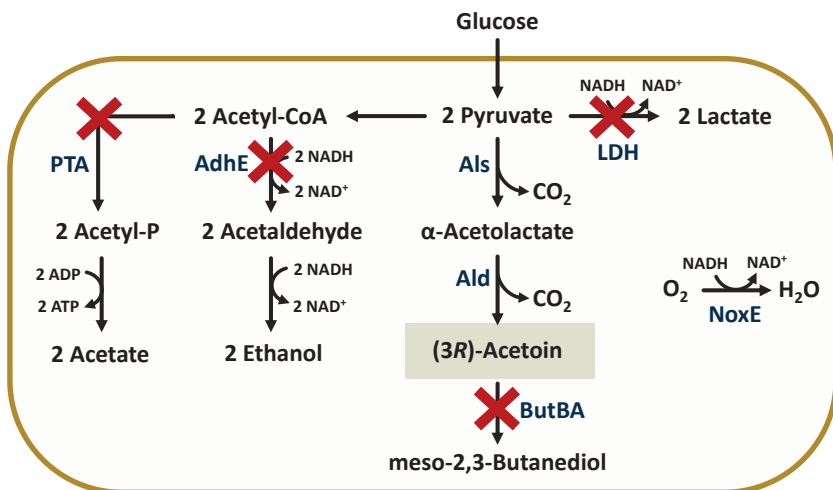


**Figure 6** Scheme of the metabolic pathway of enantiopure (3R)-acetoin production with genetically modified *L. lactis* VJ017. The production host is a *L. lactis* MG1363 variant with deletions of three homologues of the lactate dehydrogenase, the phosphotransacetylase, two homologues of the butanediol dehydrogenase, and the alcohol dehydrogenase (*L. lactis* MG1363  $\Delta 3dh$   $\Delta pta$   $\Delta adhE$   $\Delta butBA$ ). Red crosses signify deletion of a certain gene. Aerobic growth and regeneration of NAD<sup>+</sup> is possible by water forming NoxE, an NADH oxidase. Als =  $\alpha$ -acetolactate synthase; Ald =  $\alpha$ -acetolactate decarboxylase; PTA = phosphotransacetylase; AdhE = alcohol dehydrogenase E; LDH = lactate dehydrogenase; ButBA = butanediol dehydrogenases A and B; NoxE = NADH oxidase.<sup>116, 117</sup>

Recently, a process cascade for the direct electrochemical reduction of acetoin to 2-butanone in cultivation broth without any intermediate purification steps was shown to be feasible in a flow cell.<sup>112</sup> This process presents a possibility for sustainable production of 2-butanone. However, the conversion yield was shown to be limited by the formation of side products and detrimental hydrogen evolution.<sup>118</sup>

### 1.3 Integrated bioprocesses

The prerequisite for the biotechnological production of fuels and other bulk chemicals that can compete with the petrochemical synthesis is the achievement of high product titers, yields, and productivities.<sup>71</sup> The integration and intensification of bioprocesses can play a major role in achieving these goals. Integration is achieved by performing multiple unit operations in one reaction vessel. This leads to a reduced number of necessary apparatuses, while high product recovery rates can be maintained.<sup>119</sup> A promising approach for bioprocess intensification is *in situ* recovery of the product, which is defined as the immediate separation of a product from its producing cell.<sup>86, 120, 121</sup> Different *in situ* product recovery (ISPR) approaches were described to enhance the productivity and cost-effectiveness of different bioprocesses. ISPR can be

performed by adsorption, extraction, gas stripping, ion exchange, electrodialysis, or crystallization, among other methods.<sup>122, 123</sup> The ISPR strategy should be tailored to the targeted product, including its physical (molecular weight, volatility, hydrophobicity) and chemical (charge, functional groups) properties.<sup>124</sup> For example, for volatile compounds such as lower alcohols, *in situ* gas stripping can be an excellent choice for a cost-efficient and highly selective ISPR approach.<sup>125, 126</sup> A combination of *in situ* ultrafiltration combined with ion exchange was shown to be feasible for the purification of lactic acid, while more hydrophobic products such as long-chain fatty acids can be purified by *in situ* adsorption.<sup>127, 128</sup> For acetone-butanol-ethanol (ABE) fermentations, ISPR by pervaporation lead to a 67% increase in n-butanol yield and a 126% increase in productivity.<sup>129</sup>

It should be noted that every ISPR method comes with its limitations. For a systematic bioprocess design, each parameter needs to be adapted to fit both the requirements of the microorganism's cultivation and the respective recovery method. Accordingly, the operational window of a bioprocess with integrated ISPR is more narrow than the operational windows of the separate cultivation and purification.<sup>130, 131</sup> For example, the integration of advanced membrane modules for ISPR of ethanol was feasible, however, membrane fouling posed a new challenge during the process.<sup>132</sup> A well described ISPR approach is *in situ* product extraction, which will be depicted in the following.

### 1.3.1 *In situ* extraction

*In situ* extraction particularly emerged due to its versatility, applicability to a broad range of products, and the potential for extractant phase recycling.<sup>133</sup> The addition of a second liquid phase that exhibits a miscibility gap with the aqueous fermentation broth enables simultaneous product extraction and fermentation, thereby lowering the concentration of the product in the broth. Most commonly, organic solvents are used for *in situ* product extraction, however, this ISPR method was also shown to be possible with ionic liquids, deep eutectic solvents, or a surfactant-based micelle solvent as the second liquid phase.<sup>119, 124, 134</sup> One possibility for *in situ* product extraction is to connect a separate extraction unit to the bioreactor. The spatially separated operation of cultivation and extraction allows both units to operate at their respective optimum conditions. However, this approach necessitates additional technical refinements and partly causes detrimental conditions for the production host while it resides in the extraction unit. By performing the extraction in the same vessel as the cultivation (extractive fermentation), these drawbacks can be circumvented.<sup>135, 136</sup>

*In situ* product extraction is described to be especially advantageous in cases where the product is inhibitory to the biocatalyst. Additionally, *in situ* extraction can be applied to shift unfavorable reaction equilibria, reduce the number of downstream processing steps, and prevent product losses due to degradation or volatility.<sup>137</sup> However, since the second liquid phase is in direct contact with the cultivation broth during the fermentation and thus with the microorganisms, the solvent should be well

investigated. Decisive factors for the solvent are its biocompatibility and biodegradability, the hydrophobicity, product partition, selectivity, safety, and toxicology.<sup>45, 138</sup> Additionally, an intrinsic challenge during extractive fermentations is the formation of stable emulsions. While emulsification is desirable during upstream processing for a larger surface area of the droplets and higher mass transfer rates, it decisively hinders the further recovery of a coherent organic phase layer. A broad variety of surface-active components, for example biosurfactants or complex media components, are described to stabilize those emulsions.<sup>139</sup> Notably, also cells and colloidal particles can lead to emulsification by mechanical interface stabilization, that hinders coalescence of the droplets.<sup>140, 141</sup> The emulsion-stabilizing effects of the microorganisms themselves make extractive fermentations particularly challenging. Three steps are generally required for the recovery of two separate liquid phases from emulsions. (**Figure 7**). The first step is droplet growth, followed by creaming, and finally the formation of a continuous second liquid phase. If the dispersed phase has a lower density than the continuous phase, the creaming velocity  $v_c$  can be described by Stoke's law (eqn (1)). Here,  $\rho_{org}$  and  $\rho_{aq}$  are the densities of the dispersed (here: organic) and the continuous (here: aqueous) phase,  $\mu$  is the dynamic viscosity of the continuous phase,  $d_d$  is the droplet diameter, and  $g$  the acceleration constant, which can be increased e.g. by centrifugation.

$$v_c = \frac{1}{18} \frac{(\rho_{org} - \rho_{aq})}{\mu} g \cdot d_d^2 \quad (1)$$

Stoke's law emphasizes the importance of the droplet diameter, where larger droplets of the dispersed phase lead to faster creaming and accordingly to an easier breakup of the emulsion.<sup>142</sup> In stirred tank bioreactors (STRs) that are commonly used for bioprocesses with *in situ* product extraction, the stirrer can cause peaks in shear stress that lead to small, finely dispersed droplets of the organic phase. This effect can adversely influence the formation of stable emulsions.<sup>143, 144</sup>

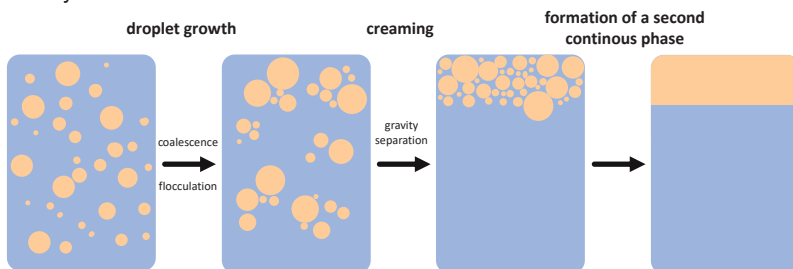


**Figure 7** Steps during the destabilization of emulsions. For an emulsion of two non-miscible liquid phases, e.g., of an aqueous fermentation broth (blue) and dispersed droplets of an organic solvent (orange), the destabilization of the emulsions occurs in several steps. The first step is the growth of the droplets caused by coalescence or flocculation. Coalescence is the merging of droplets, while during flocculation, droplets form aggregates. This is followed by creaming, and formation of a second continuous liquid phase.<sup>142</sup>



Recently, it was shown that the application of an advanced bioreactor concept, namely a multiphase loop reactor (MPLR, **Figure 8**), can work efficiently against the formation of stable emulsions while maintaining sufficient oxygen supply and mixing. In this non-stirred internal loop airlift reactor, air bubbles in the inner riser compartment induce a loop flow, and countercurrent liquid-liquid extraction occurs in the downcomer. The solvent settles in a coalescing compartment, from where the coherent organic phase can be recirculated. Due to the homogeneous, low shear stress, cultivations with *in situ* product extraction are less prone to detrimental emulsification.<sup>145</sup>

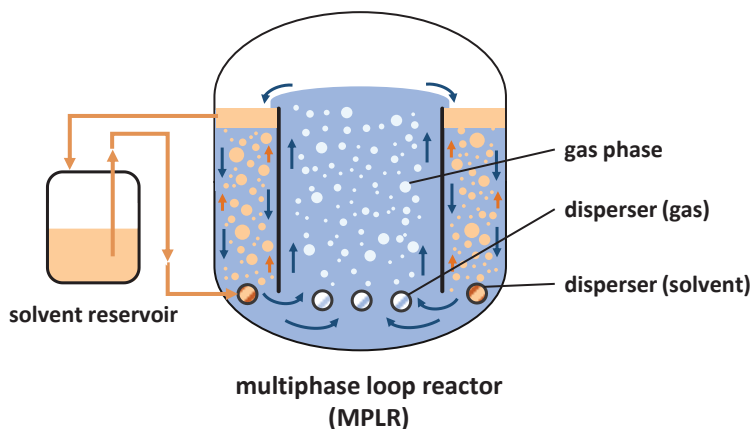


**Figure 8** Schematic representation of the multiphase loop reactor (MPLR). In the inner compartment (riser), gas spargers induce a loop flow of the aqueous phase. In the outer (downcomer) compartment, solvent dispersers are located. The solvent droplets rise and lead to continuous countercurrent liquid-liquid product extraction. In the upper part of the downcomer, a coalescing unit leads to accumulation of the solvent droplets. The organic solvent can be pumped into a solvent reservoir, from where it is continuously reintroduced into the MPLR.<sup>145-147</sup> MPLR = multiphase loop reactor. The figure was previously published<sup>148</sup> and is reprinted with permission of Sustainable Energy & Fuels.

### 1.3.2 Solvent selection strategies

Like shown above, the extractant phase of bioprocesses with *in situ* product extraction distinctly influences both up- and downstream processing. The solvent should meet the requirements of both the liquid-liquid extraction and the fermentation, including the impact on the biocatalyst. There is a wide range of desirable properties of a solvent (**Table 1**), and there are numerous solvent candidates that potentially fulfill these criteria. In order to find the best solvent for a specific application, solvent screenings of various extents were described. Hierarchical solvent screenings were found to be particularly useful to systematically reduce the solution space for the extractant phase.<sup>135, 138, 149-151</sup>

**Table 1** Desirable solvent properties for *in situ* product extraction in bioprocesses.<sup>151, 152</sup>

Favorable distribution coefficient for the product
Biocompatibility
Non-biodegradability
Non-toxicity
High selectivity for the product
Low emulsion forming tendency
Low cross solubility with the aqueous phase/high hydrophobicity
Low viscosity
High density difference with the aqueous phase
Chemical and thermal stability
Favorable for product recovery
Favorable for solvent recycling
Sustainable origin
Affordability
Large-scale availability

For an initial reduction of the number of solvent candidates, a selection of solvents with desirable physical properties that can be derived from model-based predictions or databases is possible. However, for bioprocesses, the solvent's biocompatibility and biodegradability is an indispensable factor that cannot be derived from databases or *in silico* modelling approaches.<sup>152-154</sup>

The hydrophobicity of a solvent can be expressed by the log *P* value, the water-octanol partition coefficient. The log *P* value can also serve as a first hint for a solvents' toxicity. Substances with a log *P* between 1 and 5 were generally shown to be toxic to cells, because they can partition into the lipid bilayer of the cell membrane, thus disturbing the integrity of the membrane and cause *e.g.* permeabilization.<sup>155, 156</sup> For example, the addition of toluene with a log *P* of 2.7 to *E. coli* cells was shown to lead to a leakage of proteins and RNA.<sup>157</sup> However, the damaging effects of solvents and the respective tolerance mechanisms of cells are highly individual and do not only depend on the log *P* value. Certain structural features of molecules such as nitro functional groups generally cause a high toxicity.<sup>158</sup> Consequently, growth and product formation with the respective microorganisms has to be tested for each solvent-biocatalyst pair.<sup>159</sup> Additionally, the feasibility of further downstream processing methods such as back-extraction or distillation of the product should be included in solvent selection strategies

to generate a holistic approach. Especially for bulk products such as biofuels, techno-economic assessments showed that solvents that are compatible with the final product formulation are particularly useful, because they do not have to be separated from the product.<sup>160</sup> Another factor that attracting increasing attention is the potential for recycling of the solvent, and the sustainability of the solvent production itself.<sup>161</sup>

## 1.4 Scope of this thesis

This thesis aims to generate integrated approaches for sustainable and efficient biotechnological production of aliphatic methyl ketones with a chain length from C<sub>4</sub> to C<sub>17</sub> (**Figure 9**). Both *P. taiwanensis* VLB120 and *L. lactis* are investigated for their ability to serve as advanced genetically modified microbial cell factories in different cultivation setups. The utilization of various methods, ranging from strain engineering and bioprocess engineering to the generation of lignocellulosic hydrolysates and application of computational models, aimed for the generation of bioprocesses that allow for an improved sustainable production for aliphatic methyl ketones.

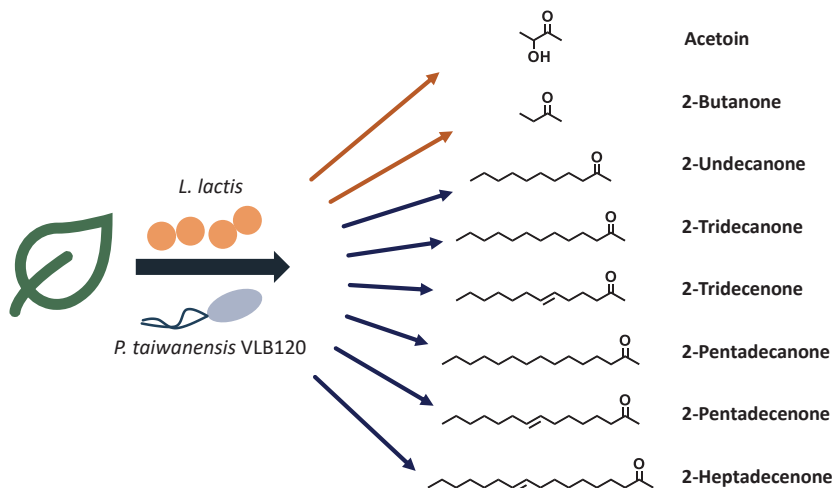


**Figure 9** Overview of the chemical structures of the methyl ketones relevant to this study. *L. lactis* VJ017 is utilized to produce acetoin and 2-butanone, while *P. taiwanensis* VLB120 Δ6 pProd is used to produce the saturated and monounsaturated medium-chain length methyl ketones 2-undecanone to 2-heptadecenone. The position of the double bond of 2-tridecenone, 2-pentadecenone, and 2-heptadecenone was determined to be at the ω-7 position, counting from the aliphatic end.<sup>162</sup>

In Chapter 3.1, we investigate a bioprocess for efficient production and purification of methyl ketones with *in situ* product purification. *In situ* extraction of the methyl ketones was chosen as the ISPR method. The evaluation included a comprehensive, reductive screening of 97 solvents. 2-Undecanone, the best solvent candidate of the screening, is compatible with the product mixture. Since in STRs, emulsion formation hindered

efficient recovery of the organic phase, an advanced multiphase loop bioreactor was successfully applied for methyl ketone production. In this bioreactor setup, the methyl ketone was recovered by straight-forward decantation. The resulting blend of methyl ketones was also extensively tested for its applicability in diesel engines, showing a high suitability as a fuel that is backwards-compatible with the existing fuel infrastructure.

In Chapter 3.2, we examine the utilization of alternative carbon sources for the production of methyl ketones. Single-fed glucose is often not the best substrate in terms of efficiency and sustainability, despite its common usage in research and development. By using a genome-scale metabolic model, ethanol was found as a co-feeding substance that enables the highest measured methyl ketone yields with *P. taiwanensis* VLB120 in batch cultures. Additionally, the feasibility of lignocellulosic hydrolysates generated from wheat straw as a carbon source generated from agricultural waste streams was tested. Both, co-feeding with ethanol and the application of more sustainable hydrolysates have a high potential for more efficient and sustainable production of methyl ketones.

In Chapter 3.3, we explore an integrated bioprocess that fulfills both the requirements of the biocatalysis and the electrocatalysis to efficiently produce 2-butanone out of glucose. Resting cells of *L. lactis* were applied to transform glucose to acetoin at high product yields close to the theoretical maximum. By systematically reducing the amount of dissolved components in the resting cell buffer, the acetoin-containing broth could be tailored to the subsequent reduction to 2-butanone, notably without intermediate purification steps. This closes a gap in current research, namely the efficient bio-based production of 2-butanone.

In Chapter 3.4, we dive deeper into the fundamentals of microbial production of methyl ketones. This chapter includes the investigation of gas stripping as an alternative technology for *in situ* removal of methyl ketones. In addition, different thioesterases were applied to adapt the ratio of the methyl ketone congeners in the product mixture. Finally, the growth of the production host at different temperatures was evaluated in order to cater the process for a better decarboxylation of the  $\beta$ -keto acid to the corresponding methyl ketone.

Chapter 4 concludes the findings of this thesis, places the results into a broader context, and discusses further work to be performed for the bioproduction of methyl ketones.



---

# Chapter 2

## Material and Methods

### Partially published as

C. Grütering, C. Honecker, M. Hofmeister, M. Neumann, L. Raßpe-Lange, M. Du, B. Lehrheuer, M. von Campenhausen, F. Schuster, M. Surger, B. E. Ebert, A. Jupke, T. Tiso, K. Leonhard, K. Schmitz, S. Pischinger, L. M. Blank. Methyl ketones: a comprehensive study of a novel biofuel. *Sustainable Energy & Fuels*. 2024, 8(9), 2059-2072.

Reprinted (adapted) with permission of *Sustainable Energy & Fuels*. Copyright The Royal Society of Chemistry.

A. L. Ziegler<sup>§</sup>, C. Grütering<sup>§</sup>, L. Poduschnick, A. Mitsos, L. M. Blank. Co-feeding enhances the yield of methyl ketones. *Journal of Industrial Microbiology and Biotechnology*, 2023, 50(1).

Reprinted (adapted) with permission of *Journal of Industrial Microbiology and Biotechnology*. Copyright Oxford University Press. <sup>§</sup>equally contributing authors

C. Grütering, T. Harhues, F. Speen, R. Keller, M. Zimmermann, P. R. Jensen, M. Wessling, L. M. Blank. Acetoin production by resting cells of *Lactococcus lactis* for direct electrochemical synthesis of 2-butanone. *Green Chemistry*, 2023, 25(22), 9218-9225.

Reprinted (adapted) with permission of *Green Chemistry*. Copyright The Royal Society of Chemistry.

### Contributions

Marius Hofmeister is the original author of the section “Determination of kinematic viscosity and density” and “Material compatibility and lubricity” that was adapted for this thesis.. Lukas Raßpe-Lange is the original author of the section “Prediction of flash point and boiling point”. Christian Honecker is the original author of the section “Determination of the derived cetane number and combustion properties in a single-cylinder research engine” that was adapted for this thesis. Miaomiao Du is the original author of the section “Ecotoxicology assessments”. Tobias Harhues is the original author of the section “Electrochemical conversion of acetoin to 2-butanone”. Anita L. Ziegler is the original author of the section “*In silico* model of *Pseudomonas taiwanensis* VLB120” that was adapted for this thesis. All other parts were written by Carolin Grütering and reviewed by Lars M. Blank.

---



## 2 Material and Methods

### 2.1 Chemicals

The chemicals used in this study were obtained from Carl Roth (Carl Roth GmbH + Co. KG, Karlsruhe, Germany), Sigma-Aldrich (Merck KGaA, Burlington, USA), or TCI (Tokyo Chemical Industry Co., Ltd., Tokyo, Japan), unless stated otherwise.

### 2.2 Strains

All bacterial strains used in this study, including Gram-negative *Pseudomonas taiwanensis* VLB120 and *Escherichia coli* and Gram-positive *Lactococcus lactis*, are listed in **Table 2**.

**Table 2** Bacterial strains used in this study.

Strain	Genotype	Reference
<i>P. taiwanensis</i> VLB120	Wild type, isolated from forest soil near Stuttgart, Germany, carrying the megaplasmid pSTY	Prof. Andreas Schmid, UFZ Leipzig, DE
<i>P. taiwanensis</i> VLB120 Δ6 pProd	VLB120 Δ <i>fadA</i> (PVLB_07895), Δ <i>fadE</i> (PVLB_07065), Δ <i>fadE2</i> (PVLB_10075), Δ <i>fadA2</i> (PVLB_12575), Δ <i>pha</i> (PVLB_02155-02165), Δ <i>tesB</i> (PVLB_03305), carrying pSN1 and pSN2, pSTY	Nies <i>et al.</i> <sup>97</sup>
<i>P. taiwanensis</i> VLB120 Δ6	VLB120 Δ <i>fadA</i> (PVLB_07895), Δ <i>fadE</i> (PVLB_07065), Δ <i>fadE2</i> (PVLB_10075), Δ <i>fadA2</i> (PVLB_12575), Δ <i>pha</i> (PVLB_02155-02165), Δ <i>tesB</i> (PVLB_03305), pSTY	This study
<i>P. taiwanensis</i> VLB120 Δ6 pSN1 pCG2	VLB120 Δ <i>fadA</i> (PVLB_07895), Δ <i>fadE</i> (PVLB_07065), Δ <i>fadE2</i> (PVLB_10075), Δ <i>fadA2</i> (PVLB_12575), Δ <i>pha</i> (PVLB_02155-02165), Δ <i>tesB</i> (PVLB_03305), carrying pSN1 and pCG2, pSTY	This study
<i>P. taiwanensis</i> VLB120 Δ6 pCG1 pSN2	VLB120 Δ <i>fadA</i> (PVLB_07895), Δ <i>fadE</i> (PVLB_07065), Δ <i>fadE2</i> (PVLB_10075), Δ <i>fadA2</i> (PVLB_12575), Δ <i>pha</i> (PVLB_02155-02165), Δ <i>tesB</i> (PVLB_03305), carrying pCG1 and pSN2, pSTY	This study
<i>P. taiwanensis</i> VLB120 Δ6 pCG1 pCG2	VLB120 Δ <i>fadA</i> (PVLB_07895), Δ <i>fadE</i> (PVLB_07065), Δ <i>fadE2</i> (PVLB_10075), Δ <i>fadA2</i> (PVLB_12575), Δ <i>pha</i> (PVLB_02155-02165), Δ <i>tesB</i> (PVLB_03305), carrying pCG1 and pCG2, pSTY	This study
<i>E. coli</i> DH5α	<i>fhuA2 lac</i> (del)U169 <i>phoA glnV44</i> Φ80' <i>lacZ</i> (del)M15 <i>gyrA96 recA1 relA1 endA1 thi-1 hsdR17</i>	Hanahan <sup>163</sup>
<i>L. lactis</i> VJ017	MG1363 Δ <sup>3</sup> <i>ldh</i> Δ <i>pta</i> Δ <i>adhE</i> Δ <i>butBA</i> , strictly aerobic by expression of NoxE	Kandasamy <i>et al.</i> <sup>116</sup>



## 2.3 Biotechnological production of medium-chain length methyl ketones

### 2.3.1 *Pseudomonas taiwanensis* VLB120 strains and growth media

In this work, the Gram-negative *P. taiwanensis* VLB120 wild type, isolated from forest soil in Stuttgart, Germany, and the methyl ketone producing *P. taiwanensis* VLB120 Δ6 pProd variant, devoid of the pSTY megaplasmid, were applied in cultivations, unless stated otherwise. Further variants of *P. taiwanensis* VLB120 Δ6 pProd were generated to test different thioesterases (**Table 2**, Chapter 3.4).

For pre-cultures and strain construction, *P. taiwanensis* VLB120 variants were propagated in lysogeny broth (LB) medium containing 10 g·L<sup>-1</sup> peptone, 5 g·L<sup>-1</sup> sodium chloride, and 5 g·L<sup>-1</sup> yeast extract. Solid LB was prepared by adding 1.5% (wt/vol) agar to the liquid medium. Mineral salt media (MSM, adapted from Hartmans *et al.*<sup>164</sup>) contained 2.0 g·L<sup>-1</sup> (NH<sub>4</sub>)<sub>2</sub>SO<sub>4</sub>, 0.1 g·L<sup>-1</sup> MgCl<sub>2</sub>·6H<sub>2</sub>O, 10.0 mg·L<sup>-1</sup> EDTA, 2.0 mg·L<sup>-1</sup> ZnSO<sub>4</sub>·7H<sub>2</sub>O, 1.0 mg·L<sup>-1</sup> CaCl<sub>2</sub>·2H<sub>2</sub>O, 5.0 mg·L<sup>-1</sup> FeSO<sub>4</sub>·7H<sub>2</sub>O, 0.2 mg·L<sup>-1</sup> Na<sub>2</sub>MoO<sub>4</sub>·2H<sub>2</sub>O, 0.2 mg·L<sup>-1</sup> CuSO<sub>4</sub>·5H<sub>2</sub>O, 0.4 mg·L<sup>-1</sup> CoCl<sub>2</sub>·6H<sub>2</sub>O, 1.0 mg·L<sup>-1</sup> MnCl<sub>2</sub>·2H<sub>2</sub>O, and the respective carbon source. In bioreactor cultivations with continuous pH regulation, 3.88 g·L<sup>-1</sup> of K<sub>2</sub>HPO<sub>4</sub> and 1.63 g·L<sup>-1</sup> of NaH<sub>2</sub>PO<sub>4</sub> were added, while shaken cultures in shake flasks, microtiter plates (MTPs), glass bioreactors, and test tubes without pH regulation had a doubled concentration of 7.76 g·L<sup>-1</sup> K<sub>2</sub>HPO<sub>4</sub> and 3.26 g·L<sup>-1</sup> NaH<sub>2</sub>PO<sub>4</sub> to ensure sufficient pH buffering. An overview of the stock solutions that were used for preparation of the MSM is given in Appendix Table A 1. If necessary, gentamycin and kanamycin were added at concentrations of 25 mg·L<sup>-1</sup> and 50 mg·L<sup>-1</sup>, respectively, for plasmid maintenance. For storage, cells were kept at -80 °C with 25 vol% glycerol in cryopreserved stocks.

### 2.3.2 Plasmid and strain construction

**Table 3** Plasmids used in this study. Plasmids pCG1 and pCG2 were generated in Rebecca Breit's Master Thesis, supervised by Carolin Grütering.<sup>165</sup>

Plasmid	Characteristics	Reference
pSN1	production plasmid, PCR fragment of <i>araC</i> -P <sub>BAD</sub> - <i>fadR</i> -co. <i>fadD</i> -P <sub>trc</sub> - <i>fadM</i> from pSN2 cloned into pTn-1 backbone without <i>nagR</i> /pNagAa, Amp <sup>R</sup> , Gm <sup>R</sup>	Nies <i>et al.</i> <sup>97</sup>
pSN2	production plasmid, PCR fragment P <sub>lacUV5</sub> - <i>tesA</i> - <i>fadB</i> -co. <i>aco</i> from pEG1675 cloned into pBNTmcs backbone without <i>nagR</i> /pNagAa promoter, Km <sup>R</sup>	Nies <i>et al.</i> <sup>97</sup>
pCG1	production plasmid, PCR fragment of <i>psFadM</i> in pSN1, resulting in <i>araC</i> -P <sub>BAD</sub> - <i>fadR</i> -co. <i>fadD</i> -P <sub>trc</sub> - <i>psFadM</i> in the pTn-1 backbone without <i>nagR</i> /pNagAa, Amp <sup>R</sup> , Gm <sup>R</sup>	This study
pCG2	production plasmid, PCR fragment of <i>cpFatB1</i> in pSN2, resulting in P <sub>lacUV5</sub> - <i>cpFatB1</i> - <i>fadB</i> -co. <i>aco</i> in the pBNTmcs backbone without <i>nagR</i> /pNagAa promoter, Km <sup>R</sup>	This study

**Table 4** Oligonucleotides used in this study. The oligonucleotides were ordered as unmodified DNA oligonucleotides, Eurofins Genomics GmbH (Ebersberg, Germany). The sequences are given in the 5' to 3' direction. The oligonucleotides were generated in Rebecca Breit's Master Thesis, supervised by Carolin Grütering.<sup>165</sup>

Name	Sequence (overlap/ANNEAL)	Application
cpFatB1_fwd	aggccatcctATGTTTGACCGTAAATCCAAGC	CpFatB1 overhang fragment
cpFatB1_rev	taccgagctcTTACGTCTTGCCGGTCGAAATTG	
pSN2_fwd	caagacgtaaGAGCTCGGTACGACCAGATC	pSN2 overhang fragment
pSN2_rev	ggtaaacaatAGGATGGCCTCCTTTGAATTC	
psFadM_fwd	ttattgcgctATGGCGACGCAAATTAAG	PsFadM overhang fragment
psFadM_rev	cacaaaacgtTTAGTTCACCTCGATAAACTG	
pSN1_fwd	ggtgaaactaaACGTTTTGTGGTGCCGGATG	pSN1 overhang fragment
pSN1_rev	gcgtgcctatAGCGCAATAACCTTACGTTGTG	
cpFatB1_in_pSN2_fwd	TATCATCGATAAGCTTCCGATGGC	validation pCG2
cpFatB1_in_pSN2_rev	ATCATACCAACCAGGCGTCAACCC	
psFadM_in_pSN1_fwd	TAATGTGAGTTAGCGGAATTG	validation pCG1
psFadM_in_pSN1_rev	GTCACGTCCGAAATCAGGGTCTTC	

In this work, the FadM thioesterase was exchanged for the PsFadM thioesterase (plasmid pCG1), and the 'tesA thioesterase was exchanged for the CpFatB1 thioesterase (plasmid pCG2). The template plasmids pSN1 and pSN2 were isolated from *E. coli* DH5 $\alpha$  using the Monarch Plasmid MiniprepKit (New England Biolabs GmbH, Ipswich, USA). The construction of the new plasmids (**Table 3**) was planned using the NEBuilder Assembly tool (New England Biolabs GmbH, Ipswich, USA). For the assembly of the plasmids, the DNA fragments of plasmid backbones and inserts were amplified with the primers listed in **Table 4** using the Q5 High-Fidelity DNA Polymerase (New England Biolabs GmbH, Ipswich, USA). The PCR products were controlled via gel electrophoresis with a 1% TAE-agarose gel at 100 V for 30 minutes and the GeneRuler 1kb DNA ladder (Thermo Fisher Scientific Inc., Waltham, USA) as a reference. The nucleotide sequences are given in

**Table 5.** The PCR products were purified using the Monarch PCR & DNA Cleanup Kit (New England Biolabs GmbH, Ipswich, USA). The template DNA was removed by DpnI digestion. Then, Gibson Assembly was performed according to the instructions of the supplier (New England Biolabs GmbH, Ipswich, USA). The products were transformed to chemically competent *E. coli* DH5 $\alpha$ 163 and the transformants were screened by colony PCR with the OneTaq2x Master Mix (New England Biolabs GmbH, Ipswich, USA).

**Table 5** DNA sequences introduced in this study. The DNA fragments were ordered from IDT (Integrated DNA Technologies, Inc., Coralville, USA).

Protein	DNA sequence	Reference
PsFadM	ATG GCG ACG CAA ATT AAA GTG TAT GGC CAT CAT ATT GAT GTC TTT AAT CAT GTG AAT AAT GCT CGC TAT TTG GAG TTC TAC GAG GAA GCA CGC TGG GCG TGG TTG GAA AAT CAT AAT CTC CTG AAC TTC CTC CTC AAG AAT AAT CTG GGG ATG GTG GCG GTG AAC ATC AAT ATC AAT TAC TGC CAA GGG GCG GTC CTC TTC GAC CAA CTC ACC GTC ATC TCC CGT TTG GAA CGG ATT GGC ACG AAA AGC GCT TCC TGC TAT CAA CAG ATT ATC CGT GAG AAG AAT GGT AAG AAG ACC CTG ATT TCG GAC GTG ACC GTG ACG TTC GTC TTT GTC GAA TTG GCA ACG AAC AAG AGC GTG GTC ATC TCG GGG GAA CTC CTC GAA CAC CTG GAG CCG CTC CTC CAA GGC GAG TCC GAC CAG TTT ATC GAG GTG AAC TAA	Yan <i>et al.</i> <sup>99</sup>
CpFatB1	ATG TTT GAC CGT AAA TCC AAG CGT CCG AGC ATG TTG ATG GAT TCC TTT GGG CTC GAG CGT GTG GTG CAA GAT GGC CTC GTG TTT CGG CAG TCG TTC TCG ATC CGT AGC TAT GAA ATC TGC GCC GAC CGC ACC GCG TCG ATG GAA ACG GTG ATG AAT CAT GTC CAG GAA ACG TCG CTG AAC CAA TGC AAA AGC ATT GGC CTC TTG GAC GAT GGG TTC GGT CGC AGC CCT GAG ATG TGC AAA CGC GAC CTG ATT TGG GTC GTG ACG CGC ATG AAG ATC ATG GTG AAT CGG TAT CCG ACC TGG GGT GAC ACG ATC GAG GTC TCG ACG TGG TTG TCC CAA AGC GGT AAA ATC GGC ATG GGG CGG GAT TGG TTG ATT TCC GAT TGT AAT ACC GGC GAG ATT TTG GTC CGC GCC ACG AGC GTG TAT GCG ATG ATG AAT CAA AAG ACC CGC CGT TTT TCC AAA TTG CCC CAC GAG GTC CGG CAG GAA TTT GCG CCT CAC TTT CTC GAC TCG CCG CCT GCG ATT GAA GAC AAT GAT GGT AAA CTC CAA AAA TTC GAC GTG AAG ACG GGT GAC TCG ATC CGT AAA GGG TTG ACG CCT GGT TGG TAT GAT CTC GAT GTG AAT CAG CAT GTG AGC AAT GTC AAA TAT ATC GGT TGG ATT CTC GAG TCC ATG CCC ACG GAA GTC TTG GAA ACC CAA GAG CTC TGC TCC CTG ACG CTC GAA TAC CGG CGC GAG TGC GGC CGG GAT TCG GTC TTG GAG TCG GTG ACG AGC ATG GAC CCA TCC AAA GTG GGC GAT CGG TTC CAA TAT CGT CAT TTG TTG CGT TTG GAG GAC GGC GCA GAC ATT ATG AAA GGT CGT ACC GAA TGG CGC CCG AAG AAC GCT GGG ACC AAT GGC GCA ATT TCG ACC GGC AAG ACG TAA	Yan <i>et al.</i> <sup>99</sup> Hernandez Lozada <i>et al.</i> <sup>166</sup>

The successfully assembled plasmids pCG1 and pCG2 were analyzed by Sanger sequencing (Mix2Seq Kit NightXpress, Eurofins Genomics GmbH, Ebersberg, Germany) and transformed into the *P. taiwanensis* VLB120  $\Delta 6$  strain as described previously.<sup>167</sup> In brief, the transformation was done via electroporation GenePulser Xcell (Bio-Rad Laboratories, Inc., Hercules, USA) in a sterile cuvette with a 2 mm gap and the settings 2.5 kV, 200  $\Omega$ , and 25  $\mu$ F and a pulse of 6 ms. Cells were cultivated on solid LB medium with the respective antibiotics. Again, a colony PCR was performed to check for successful transformation as described above. *E. coli* DH4 $\alpha$  and *P. taiwanensis* VLB120 strains with the respective plasmids were stored with 25 vol% glycerol at -80 °C.

### 2.3.3 *Pseudomonas taiwanensis* VLB120 pre-cultures and shaken cultures

Unless stated otherwise, all cultivation steps with *P. taiwanensis* VLB120 variants were performed at 30 °C. For initial seed cultures, the respective strain was streaked from the cryopreserved stock on a LB plate. The next day, a single colony was used to

inoculate 5 mL of liquid LB media in a 15 mL glass tube that was cultivated at 200 rpm and a shaking diameter  $d_0$  of 50 mm. The second pre-culture was performed in a 500 mL shake flask with 10 vol% MSM supplemented with 10 g·L<sup>-1</sup> glucose at 300 rpm and a  $d_0$  of 50 mm. It was inoculated to an optical density at a wavelength of 600 nm ( $OD_{600}$ ) of 0.1 and cultivated until the late exponential phase for inoculation of the main culture. In main cultures of the methyl ketone producing variants, 2 mM isopropyl  $\beta$ -D-1-thiogalactopyranoside (IPTG) and 1 mM arabinose were added to the media as inducers for product formation. The inducers were added from the beginning of the main culture, since this was shown to result in the best product formation (Figure A 1). The initial  $OD_{600}$  of main cultures was 0.1, unless stated otherwise.

In shake flasks, main cultures were performed in 500 mL non-baffled flasks with a filling volume of 10 vol% at 300 rpm and a  $d_0$  of 50 mm. For *in situ* extraction of methyl ketones in shake flasks, 12.5 mL of the respective organic solvent was added. In the case of simultaneous measurement of CDW and product concentration, six equal shake flasks were run under the same conditions. This was necessary since the overlay with the organic solvent hinders reproducible biomass quantification due to emulsion formation. Three shake flasks had an overlay of the organic solvent for methyl ketone measurement, while three shake flasks did not include an organic phase and were used for cell dry weight (CDW) quantification.

Main cultures of 200  $\mu$ L in 96 well MTPs (round well, Breathseal Sealer, Greiner Bio-One, Kremsmünster, Austria) were performed in the BioLector (Beckman Coulter Life Sciences, Brea, USA) for online measurement of scattered light during growth. The scattered light signal was measured with a gain of 30 and 50 at a wavelength of 620 nm. The measurement interval was set to 13 minutes. The temperature was set to 30 °C, and the humidity was kept at 85%. The culture was shaken at 900 rpm with a shaking diameter  $d_0$  of 3 mm. Each experimental condition had three additional blank wells without microorganisms to determine the baseline signal for light scattering. The MTP cultivation with a temperature gradient was performed as described previously.<sup>168</sup> For online CO<sub>2</sub> measurement in shake flasks, BlueSens BCP-CO<sub>2</sub> sensors connected to the BlueVis software (both BlueSens GmbH, Herten, Germany) were used. The sensors were installed on 1.3 L closed shake flasks filled with 0.05 L of MSM medium containing 3 g·L<sup>-1</sup> glucose and 2 mL of the respective organic solvent. The cultivations were performed at 150 rpm at a  $d_0$  of 51 mm with an initial  $OD_{600}$  of 0.1.

Biomass concentration of *P. taiwanensis*  $\Delta 6$  pProd was measured in aqueous phases and determined as CDW in pre-dried glass vials and  $OD_{600}$  values. Prior to the cultivations, the correlation of these two units was measured. In the case that only the  $OD_{600}$  value was measured using an Ultrospec TM 10 Cell Density Meter (Harvard Bioscience, Holliston, USA), CDW values were determined by eqn (2).

$$CDW [g \cdot L^{-1}] = 0.44 \cdot OD_{600} [-] \quad (2)$$

### 2.3.4 *Pseudomonas taiwanensis* VLB120 cultivations in bioreactors

Stirred tank bioreactor cultivations were performed in glass vessels with a total volume of 1.3 L and a working volume of 0.5 L of MSM with 2 mM IPTG and 1 mM arabinose, 10 g·L<sup>-1</sup> of glucose, and 100 mL of the respective organic solvent, unless stated otherwise. The inducers were added from the beginning of the main culture, since this was shown to result in the best product formation (Figure A 1). The cultivations were controlled by BioFlo120 units and DASware Control Software 5.3.1 (both Eppendorf SE, Hamburg, Germany). The pH was controlled at a value of 7.0 by addition of 4 M KOH and 4 M H<sub>2</sub>SO<sub>4</sub> and the temperature was kept at 30 °C. The dissolved oxygen (DO) level was kept above 30% using a stirring cascade from 400 rpm to 1,200 rpm. Exhaust gas analysis was performed using BlueInOne Ferm gas analyzers, and data was recorded with BlueVis (both BlueSens GmbH, Herten, Germany).

The multiphase loop reactor (MPLR) consisted of a 5.0 L glass vessel (Eppendorf SE, Hamburg, Germany) and an in-house manufactured head plate as a basis for the MPLR-specific internals. A stainless-steel cylinder separated the inner riser from the outer downcomer compartment. In the former, a 3D printed porous poly(dodecane-12-lactam) spiral sparger with a porosity of 15% and pore diameters ranging from 0.7 µm to 8.0 µm was used for aeration. Both riser and downcomer had probes for temperature, pH, and DO measurements. The probes in both compartments were connected to one BioFlo110 unit each (Eppendorf SE, Hamburg, Germany). The pH of the riser was kept constant at 7.0 by addition of 4 M KOH and 4 M H<sub>2</sub>SO<sub>4</sub>. The aeration was varied from 0.6 to 1.3 volume air per volume aqueous phase per minute (vvm) to guarantee sufficient supply of oxygen. The aqueous phase was 4.18 L of MSM with 10 g·L<sup>-1</sup> of glucose. As a solvent phase, 1.0 L of 2-undecanone was pumped from the coalescing compartment to a solvent reservoir and from the solvent reservoir back to the solvent disperser in the downcomer using external peristaltic pumps. The solvent cycle consisted solely out of polytetrafluoroethylene (PTFE), stainless steel, and boronsilicate glass. Exhaust gas analysis was performed using BlueVary gas analyzers (BlueSens GmbH, Herten, Germany). For the details of the MPLR setup, refer to Campenhausen *et al.*<sup>145</sup> and **Figure 14B**.

For methyl ketone formation with *in situ* gas stripping, the main culture was performed in one double-walled glass bioreactors with a total volume of 0.25 L. The temperature was kept at 30 °C with a thermostat. Methyl ketone production was performed in 0.2 L MSM (7.76 g·L<sup>-1</sup> K<sub>2</sub>HPO<sub>4</sub> and 3.26 g·L<sup>-1</sup> NaH<sub>2</sub>PO<sub>4</sub>) with 10 g·L<sup>-1</sup> glucose at a stirrer speed of 800 rpm. The aeration was performed via a needle with a diameter of 0.8 µm with humidified air at a rate of 0.5 L·min<sup>-1</sup>, resulting in an aeration rate of 2.5 vvm. The off gas was run through a solvent trap with 0.05 L of n-decane that was cooled on ice. After 27 hours, 2 mL of a 500 g·L<sup>-1</sup> glucose solution was added.

## 2.4 Solvent screening for *in situ* extraction of methyl ketones

### 2.4.1 Physicochemical parameters

An initial pre-screening of 97 potential solvent candidates was performed for the density, the water-octanol partition coefficient ( $\log P$ ), the melting point, and the flash point. The respective values were derived from the PubChem website, the GESTIS-Stoffdatenbank, or the website of the supplier.<sup>169, 170</sup> 1-Octanol was included in the later screening due to its common usage for extraction in bioprocesses, and nonanal was included as a negative control due to its low  $\log P$ .<sup>171</sup> The details of this screening step can be found in Appendix, Figure A 2.

### 2.4.2 Assessment of solvent toxicity to *Pseudomonas taiwanensis* VLB120

For an initial growth assay of methyl ketone producing *P. taiwanensis* VLB120  $\Delta 6$  pProd in the presence of the preselected solvent candidates, the main cultures were performed in closed 15 mL glass tubes using 1 mL of MSM with 2 g·L<sup>-1</sup> glucose and 0.5 mL of the corresponding solvent. The initial OD<sub>600</sub> was 0.1. After 48 hours of incubation at 30 °C and 200 rpm and a shaking diameter  $d_0$  of 50 mm, the turbidity of the aqueous phase was compared by taking pictures, since no spectrophotometric biomass measurement is possible as soon as organic solvents are present in the cultivation broth (Appendix, Figure A 3).

### 2.4.3 Partition coefficient and interphase formation

To test the partition coefficient and interphase formation using the pre-selected solvents, a main culture of methyl ketone producing *P. taiwanensis* VLB120  $\Delta 6$  pProd was performed in nine 500 mL shake flasks, each with 0.05 L (10 vol%) of MSM with 10 g·L<sup>-1</sup> glucose. The initial OD<sub>600</sub> was 0.1. After 52 hours at 30 °C and 300 rpm and a shaking diameter  $d_0$  of 50 mm, the cultivation was stopped. 1.6 mL of the cultivation broth was shaken with 0.4 mL of the corresponding organic solvent at 900 rpm and 30 °C in a horizontal shaker in triplicates. After centrifugation of the sample for 5 minutes at 13,300 rpm, aqueous and organic phases were separated and analyzed. For determination of the partition coefficient, the concentration of the remaining methyl ketones in the aqueous phase was measured. The methyl ketone partition coefficient  $P$  was calculated according to eqn (3) with  $c_0$  and  $c_1$  as the product concentration in the cultivation broth before (0) and after (1) the extraction, and  $\Theta$  as the phase ratio (in (vol/vol) organic to aqueous phase) from triplicate measurements.

$$P = \frac{c_0 - c_1}{c_1 \cdot \Theta} \quad (3)$$

Interphases often occur as a third, undefined layer after phase separation for cultivation broths with *in situ* product extraction and lead to a loss of product and the organic solvent. The formation of these process-hindering interphases was assessed by qualitatively analyzing images of the extraction vials after centrifugation (Appendix Figure A 4).<sup>138, 172</sup>

## 2.5 Suitability of the methyl ketone blend as a drop-in fuel

### 2.5.1 Determination of kinematic viscosity and density

All fluid mechanical measurements and fuel property measurements were performed with a surrogate mixture of the saturated methyl ketones (22.4 wt% 2-undecanone, 51.2 wt% 2-tridecanone, and 26.4 wt% 2-pentadecanone) representing the chain length distribution that was determined for the methyl ketone blend produced by *P. taiwanensis* VLB120.<sup>97</sup>

The kinematic viscosity of the sample liquid was determined by means of an Ubbelohde viscometer according to DIN 51562.<sup>173</sup> For the temperature control of the sample liquid and the viscometer, a temperature control unit with a manufacturer guaranteed accuracy of 0.01 K was used. To ensure a constant and uniform temperature distribution, the viscometer was placed in the temperature control unit for 30 minutes before each measurement series. The actual measurement series consisted of two preliminary measurements and five main measurements where only the main measurements were considered for the evaluation of the viscosity results. For the measurement of liquid density, the setup from **Figure 10** was used.

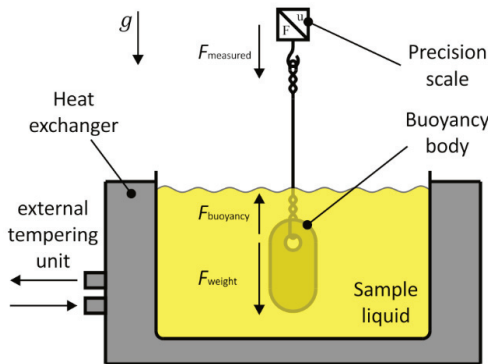


**Figure 10** Measurement setup for determining the fluid density.<sup>174</sup> The figure was originally created by Marius Hofmeister, Institute for Fluid Power Drives and Systems, was previously published,<sup>148</sup> and is reprinted with permission of Sustainable Energy & Fuels.

The setup consisted of a tension scale with a measurement resolution of 0.01 mg, a buoyancy body, and a vessel filled with the sample liquid. According to the Archimedes' principle, the liquid density  $\rho_L$  equals the difference between measured mass  $m_{\text{measured}}$  and the actual mass of the buoyancy body  $m_{\text{buoyancy}}$  divided by the volume  $V_{\text{buoyancy}}$  of the buoyancy body (eqn (4)).<sup>175</sup>

$$\rho_L = \frac{m_{\text{buoyancy}} - m_{\text{measured}}}{V_{\text{buoyancy}}} \quad (4)$$

The described measurement procedure was performed ten times for each measurement series. The temperature of the sample liquid was controlled by means of an external tempering unit and an internal heat exchanger. The temperature accuracy of the used tempering unit is 0.02 K.

### 2.5.2 Material compatibility and lubricity

To evaluate the material compatibility of the methyl ketone blend and different sealing materials, an immersion test according to DIN ISO 1817 was conducted.<sup>176</sup> During the test, reference sealing specimens according to ISO 13226 were immersed into the sample liquid for a total duration of 672 hours.<sup>177</sup> At defined times, the specimens were removed from the sample liquid and measured regarding the change of volume, mass, and hardness. The International Rubber Hardness Degree (IRHD) hardness is determined according to DIN ISO 48. For each elastomer specimen, six measurements were conducted, with a duration of each measurement of 30 seconds.<sup>178</sup>

For the volume measurement, the same setup as shown in **Figure 10** was used. In contrast to the density measurement, the density of the liquid  $\rho_L$  is known, so that the volume of the specimen  $V_{\text{specimen}}$  can be calculated using eqn (5).

$$V_{\text{specimen}} = \frac{m_{\text{buoyancy}} - m_{\text{measured}}}{\rho_L} \quad (5)$$

The mass of the elastomer specimen was measured by means of a precision scale with a resolution of 0.01 mg and a device-specific standard deviation of 0.02 mg. Volume and mass measurement were repeated three times for each specimen and the corresponding mean value was calculated. Three test specimens were tested for each combination of sealing material and sample liquid. The geometric dimensions of the sealing specimens were  $25 \cdot 25 \cdot 2 \text{ mm}^3$  and the volume of the sample liquid was 40 mL. During the entire test period, the specimens and liquid samples were kept inside a climatic chamber with a temporal and local temperature accuracy of 0.5 K at 23 °C.

The high frequency reciprocating rig (HFRR) test according to ISO 12156 evaluates whether a fuel has good lubricating properties.<sup>179</sup> For this purpose, a steel ball was pressed onto a steel surface and moved back and forth. Subsequently, the resulting wear area was measured by means of a digital microscope, with a translational resolution in the x and y axis of 350 nm. The average value of the width and length of the wear area is defined as the wear scar diameter (wsd). Small wsd values are associated with good lubricating properties. The described measurement process was repeated five times for each sample liquid. The test duration was 75 minutes and the liquid temperature 60 °C.

### 2.5.3 Prediction of flash point and boiling point

To complement experimental data, flash points and boiling points were predicted with computer-aided methods. Predictions for both properties were performed using the Conductor-like Screening Model for Real Solvents (COSMO-RS).<sup>180, 181</sup> The COSMO-



RS model in combination with density functional theory (DFT) calculations allows the prediction of multiple thermodynamic properties based on the molecules' 3D structure. The molecular geometries were optimized in an implicit solvation model assuming an ideal conductor. The screening charge densities of the molecules in a self-consistent state (COSMO-state) were obtained, which, when transformed into a histogram, yielded the sigma profiles that were the basis for all mixture and pure component properties calculated with the COSMO-RS model.<sup>180</sup> The DFT calculations are performed using the BP-86 functional and a def2-TZVPD basis set.<sup>182-184</sup> Geometry optimization and conformer search were executed in the COSMOconf Software while property data was predicted using the COSMOthermX19 Software package (both Dassault Systèmes, Vélizy-Villacoublay, France).

#### **2.5.4 Determination of the derived cetane number and combustion properties in a single-cylinder research engine**

The derived cetane number (DCN) of the methyl ketone blend (22.4 wt% 2-undecanone, 51.2 wt% 2-tridecanone, and 26.4 wt% 2-pentadecanone) was determined in an AFIDA 2085 advanced fuel ignition delay analyzer (ASG Analytik-Service AG, Neusäß, Germany). This device uses a heated and pressurized constant volume combustion chamber of 0.39 L to measure ignition delay times.<sup>185</sup> For injection, the fuel candidate was pressurized up to 1,200 bar, and the constant-volume combustion chamber reached 50 bar and 730 °C using compressed air. Ignition was detected by a defined relative pressure rise, measured through a dynamic pressure transmitter. From these ignition delay times, the DCN was calculated based on a calibration curve of reference fuels in accordance with ASTM D8183.<sup>186</sup>

Engine experiments were conducted using a single-cylinder research engine designed to mimic the characteristics of contemporary light-duty compression ignition engines. The engine has a bore of 75 mm and 0.39 L of displacement. The engine setup was described earlier in detail.<sup>187-189</sup> To achieve realistic but challenging conditions, a compression ratio of 19:1 was chosen for this test.

Boost pressure ( $p_{in}$ ), exhaust pressure ( $p_{ex}$ ), and charge air temperature ( $T_{in}$ ) were externally conditioned to the desired value. Exhaust gas recirculation (EGR) was performed by cooled high-pressure EGR. Oil and coolant were externally conditioned to 90 °C. The engine speed ( $n$ ) was controlled using an eddy current dynamometer and an external electric motor to enable operation also at very low load. An automatic controller adjusted the centre of combustion (CA50) and the indicated mean effective pressure (IMEP) to the desired target value by adapting the duration and phasing of the main injection with a specific duration of injection (DOI) and start of injection (SOI). Indication data was obtained via a Kistler 6041A water-cooled piezoelectric pressure transducer (Kistler Instrumente AG, Winterthur, Switzerland) and analyzed using the FEVIS combustion analysis software (FEV Software and Testing Solutions GmbH, Aachen, Germany) in real-time.

Relevant engine operating points were chosen based on New European Driving Cycle and Worldwide Harmonized Light Vehicles Test Cycle reference points calculated for a 1,590 kg passenger car with a 1.6 L diesel engine.<sup>187, 188</sup> Additionally, a comparison point for alternative combustion systems was added to the test matrix.<sup>190</sup> All tested operating points were optimized for diesel operation, yielding standard values for CA50 rail pressure ( $p_{\text{rail}}$ ), boost pressure ( $p_{\text{in}}$ ), exhaust backpressure ( $p_{\text{ex}}$ ), and, where applicable, duration of injection (DOI), and offset ( $t_{\text{pi}}$ ) for a pilot injection.<sup>188, 190</sup> These parameters were kept constant between fuels. All measurements were conducted under stationary operation. Indication data was cycle-averaged over 50 consecutive cycles, while the remaining data was sampled in 10 Hz intervals and averaged for 30 seconds. The tests were carried out as EGR variations with constant  $p_{\text{in}}$ , beginning with fresh air. To determine the suitability of the methyl ketone blend from an emission perspective, a FEVER exhaust analysis system (FEV Software and Testing Solutions GmbH, Aachen, Germany) was used to measure unburned hydrocarbons (HC), CO, CO<sub>2</sub>, residual O<sub>2</sub>, NO<sub>x</sub>, and NO. Soot was measured with the filter paper method using an AVL415 SmokeMeter (AVL List GmbH, Graz, Austria). The intake CO<sub>2</sub> concentration was used to determine EGR rates.

### 2.5.5 Storability test of 2-undecanone

As a representative of the methyl ketones, 2-undecanone was compared to summer diesel and winter diesel. Each fuel was supplemented with 4 vol% rapeseed oil methyl ester (RME) in triplicates. To mimic the biological origin of the methyl ketone, 2-undecanone was mixed with media supernatant. This supernatant was generated from a main culture of *P. taiwanensis* VLB120 Δ6 prod in 500 mL shake flasks with 50 mL of MSM with 10 g·L<sup>-1</sup> of glucose and arabinose and IPTG for methyl ketone formation like described above. After 48 hours of cultivation, the broth was centrifuged for 20 minutes at 12,000 rpm and stored at -20 °C until further usage. After 30 seconds of mixing this supernatant with 2-undecanone, the methyl ketone was separated from the cultivation broth by settling for 24 hours. The storability experiments were performed in a closed 500 mL flask with 50 mL of aqueous phase (0.1% NaCl) and 250 mL of the corresponding organic phase, resulting in 200 mL headspace. The bottle was not shaken and kept in the dark to mimic a storage tank. Valves between the opening of the bottle and the BCP-CO<sub>2</sub> sensor (BlueSens GmbH, Herten, Germany) enabled relocation of the sensors between the flasks. The water phase was inoculated with a mixture of 20 microbes as specified by Leuchtle *et al.*<sup>191</sup> Pre-cultures of these microorganisms were prepared at 30 °C and 200 rpm in LB medium, yeast extract peptone (YEP) medium, potato extract glucose bouillon (PEGB, 26.5 g·L<sup>-1</sup>), and malt extract (ME) medium for bacteria, yeasts, *Rhodotorula mucilaginosa*, and molds, respectively. The method was adapted according to Ackermann *et al.* for methyl ketones.<sup>192</sup> Appendix, Table A 2 shows the defined inoculum used for the assessment of storability.

### 2.5.6 Ecotoxicology assessments

The acute toxicity of methyl ketone blends A and B was tested by performing zebrafish (*Danio rerio*) fish embryo toxicity tests. Blend A was a mixture of the saturated methyl ketones with 22.4 wt% 2-undecanone, 51.2 wt% 2-tridecanone, and 26.4 wt% 2-pentadecanone. Blend B was derived from cultivation broth with the unsaturated methyl ketones, namely 2-undecanone, 2-tridecanone, 2-tridecenone, 2-pentadecanone, 2-pentadecenone, and 2-heptadecenone. The detailed method of the toxicity test has been described previously.<sup>193</sup> Briefly, zebrafish embryos were exposed to two different mixtures of methyl ketones for 96 hours. Fertilized zebrafish eggs were examined under the microscope, then those developed normally were transferred into glass vials filled with exposure solutions (one egg per vial with 11 mL exposure solution). Each exposure concentration and control group consisted of ten glass vials with eggs. The testing concentration ranged for mixture A and mixture B were 0.10 to 2.00 mg·L<sup>-1</sup> and 1.00 mg·L<sup>-1</sup> to 3.00 mg·L<sup>-1</sup>, respectively. Ethanol (concentration: 800 µL·L<sup>-1</sup>) was added as a co-solvent in both exposure group and negative control group, to enhance the solubility of methyl ketones in water. All zebrafish embryos were incubated at 26 °C and a 14:10 hour light:dark cycle. All the embryos were examined under the microscope every 24 hours, and abnormal development, lethality as well as the number of hatched embryos were recorded. The median effective concentration (EC<sub>50</sub>), 50% lethal concentration (LC<sub>50</sub>), lowest observed effect concentration (LOEC), and no observed effect concentration (NOEC) were calculated by using the software ToxRat Professional (ToxRat Solutions GmbH, Alsdorf, Germany).

## 2.6 Preparation of hydrolysates and growth assay

From straw, cellulosic hydrolysate, mainly containing glucose, and hemicellulosic hydrolysate, mainly containing xylose, were generated. An overview of the generation of the cellulosic hydrolysate (CH), the washed cellulosic hydrolysate (WCH), the hemicellulosic hydrolysate (HH), and the decolourized hemicellulosic hydrolysate (DHH) can be found in **Figure 21**.

### 2.6.1 Pre-treatment

The pre-treatment of wheat straw was performed according to Vollmer *et al.*<sup>194</sup> First, the moisture content of the wheat straw was determined with an automated moisture analyzer in triplicates (VWR International GmbH, Darmstadt, Germany). Subsequently, 30 g of dry wheat straw were mixed with 0.3 L of 1.25 wt% H<sub>2</sub>SO<sub>4</sub>. Diluted acid pre-treatment was performed in sealed 0.6 L non-stirred pressure vessels (Parr Instrument Company, Moline, USA) for 18 minutes at 195 °C in a silicone bath. After the residence time at 195 °C, the reactors were cooled on ice to interrupt further degradation of the material. The content of the reactors was filtered through a metal sieve to separate the solid and the liquid fraction.

### 2.6.2 Generation of (washed) cellulosic hydrolysate

For the cellulosic hydrolysate, enzymatic hydrolysis was performed according to Liu *et al.* with the solid fraction of the pre-treatment.<sup>195</sup> To generate washed cellulosic hydrolysate (WCH), the solid fraction was washed with distilled H<sub>2</sub>O until the liquid had a pH of 7.0. To generate cellulosic hydrolysate (CH), this washing step was omitted. For the hydrolysis, the moisture content of the solid fraction was measured like described above. Then, the pre-treated wheat straw was mixed with 10% (wt/vol of the dry matter) with 0.05 M sodium citric buffer at pH 5.8 and 12.25 FPU·g<sub>dry matter</sub><sup>-1</sup> (FPU = filter paper units, Cellic C-Tec2, Novozymes A/S, Bagsvaerd, Denmark). The hydrolysis was conducted at 50 °C and 50 rpm on a bottle roller for 72 hours. The remaining solids were removed by centrifugation at 10,000 rpm for 20 minutes and the pH was adjusted to 7.0 with NaOH. Then, the liquid was filtered with a 0.2 µm bottle top filter for sterility.

### 2.6.3 Generation of (decolorized) hemicellulosic hydrolysate

The hemicellulosic hydrolysate was obtained from the liquid fraction of the pre-treatment. For the decolorized hemicellulosic hydrolysate (DHH), the liquid fraction was mixed with 10% (wt/vol) activated charcoal in a beaker with a magnetic stirrer at 500 rpm at room temperature for 30 minutes. Then, the activated charcoal was separated by centrifugation at 10,000 rpm for 20 minutes. In case of the hemicellulosic hydrolysate (HH), this step was omitted. The concentration of the total phenolic compounds was measured according to Ballesteros *et al.*<sup>196</sup> Next, the pH was adjusted to 7.0 with NaOH, and the liquid was filtered with a 0.2 µm bottle top filter for sterility.

### 2.6.4 Cultivations with hydrolysates

The HH, DHH, CH, and WCH fractions of the lignocellulosic hydrolysates with and without addition of the 2x phosphate buffer, 1x nitrogen source, and 1x trace element solution (see Chapter 2.3.1, concentration of the stock solutions given in Appendix, Table A 1) were tested in 96 well MTPs (round well) in a Spectramax iD3-3428 microplate reader (Molecular Devices, LLC., San Jose, USA). Main cultures of 200 µL with *P. taiwanensis* VLB120 wild type and variant *P. taiwanensis* VLB120 Δ6 pProd were inoculated to an initial OD<sub>600</sub> of 0.1 and cultivated at 30 °C and an orbital shaking setting "high". Biomass formation was measured at 600 nm with measurement intervals of 20 minutes. As a positive control, the strains were cultivated in MSM with 10 g·L<sup>-1</sup> of glucose, and the increase of the absorbance at 600 nm was compared qualitatively for the minimal media and the hydrolysates. Each experimental condition had three additional blank wells without microorganisms to determine the baseline signal for light scattering.

The cultivations with the hydrolysates in bioreactors were performed as described in Chapter 2.3.4 with 0.4 L of the respective hydrolysate and 0.1 L of n-decane for *in situ* extraction of methyl ketones.

## 2.7 Biotechnological production of acetoin and 2-butanone

### 2.7.1 Batch cultivations of *Lactococcus lactis*

The acetoin producing *L. lactis* MG1363 VJ017 was kindly provided by the authors of Kandasamy *et al.*<sup>116</sup> The strain is a plasmid-free variant of Gram-positive *L. lactis* subsp. *cremoris* MG1363 with deletions of three homologues of the lactate dehydrogenase, the phosphotransacetylase, two homologues of the butanediol dehydrogenase, and the alcohol dehydrogenase ( $\Delta^3dh \Delta pta \Delta adhE \Delta butBA$ ). Cells were stored with 25 vol% glycerol at  $-80^\circ\text{C}$  and cultivated at  $30^\circ\text{C}$ . M17 medium, containing  $0.5\text{ g}\cdot\text{L}^{-1}$  ascorbic acid,  $5\text{ g}\cdot\text{L}^{-1}$  lactose,  $5\text{ g}\cdot\text{L}^{-1}$  meat extract,  $2.5\text{ g}\cdot\text{L}^{-1}$  meat peptone,  $19\text{ g}\cdot\text{L}^{-1}$  sodium glycerophosphate,  $5\text{ g}\cdot\text{L}^{-1}$  soya peptone,  $2.5\text{ g}\cdot\text{L}^{-1}$  tryptone,  $2.5\text{ g}\cdot\text{L}^{-1}$  yeast extract, and the respective carbon source, was used for strain maintenance and pre-cultures. For cultivations, the glycerol stocks were streaked on M17 plates with  $20\text{ g}\cdot\text{L}^{-1}$  agar and  $5\text{ g}\cdot\text{L}^{-1}$  glucose. As a pre-culture, liquid cultures with M17 media were inoculated from single colonies from an agar plate and grown in 100 mL shake flasks with 10 vol% M17 media and  $10\text{ g}\cdot\text{L}^{-1}$  glucose at 200 rpm and a shaking diameter  $d_0$  of 50 mm. Main cultures were performed in 500 mL shake flasks at 300 rpm and a shaking diameter  $d_0$  of 50 mm with 5 vol% of the respective media and a glucose concentration of  $40\text{ g}\cdot\text{L}^{-1}$  if not stated otherwise. For inoculation of the main cultures, mid-exponential cells of the pre-culture were transferred for an initial  $\text{OD}_{600}$  of 0.1. The compositions of the different media that were used for the main cultures are given in Table A 3 and Table A 4 in the Appendix. For online monitoring of  $\text{CO}_2$  evolution, BCP- $\text{CO}_2$  sensors (Bluesens Gas Sensor GmbH, Herten, Germany) were used. The sensors were installed on 1.3 L closed shake flasks filled with 0.05 L of M17 medium containing  $3\text{ g}\cdot\text{L}^{-1}$  glucose. The cultivations were performed at 150 rpm and a shaking diameter  $d_0$  of 51 mm. The  $\text{OD}_{600}$  values for growth monitoring were determined with a spectrophotometer (Ultrospec 10, Thermo Fisher Scientific Inc., Waltham, USA). The correlation of  $\text{OD}_{600}$  and CDW values was determined as described in Chapter 2.3.3 (eqn (6)).

$$\text{CDW} [\text{g} \cdot \text{L}^{-1}] = \text{OD}_{600}[-] \cdot 0.34 \quad (6)$$

### 2.7.2 Resting cell assay

Resting cell experiments consisted of a growth phase and a resting cell phase. The growth phase was performed in 500 mL shake flasks at 300 rpm and a shaking diameter  $d_0$  of 50 mm with 5 vol% of M17 media and  $40\text{ g}\cdot\text{L}^{-1}$  glucose. After reaching an  $\text{OD}_{600}$  of 13–16, the culture broth was centrifuged for 10 minutes at 5,000 rpm. The cell pellet was washed using a washing buffer and finally resuspended in resting cell buffer (for the composition of the respective solutions, see Chapter 3.3.3, Appendix Table A 5). The resting cell phase was conducted at  $30^\circ\text{C}$  and 300 rpm and a shaking diameter  $d_0$  of 50 mm in 500 mL shake flasks and 5 vol% of the respective buffer.

### 2.7.3 Electrochemical conversion of acetoin to 2-butanone

Supernatants from cultivation in different media were employed as the electrolyte for the electrochemical conversion of acetoin to 2-butanone. For biomass removal and to ensure that no undissolved particles were present, the supernatants were centrifuged (8,000 rpm, 15 minutes) to avoid damage to pumps and sensors during the experiments. Independent of the ion concentration in the fermentation broth, 0.1 M potassium phosphate buffer was added to ensure sufficient conductivity of the electrolyte. Experiments were conducted according to previous studies in a flex-E-cell (flex-X-cell GbR, Aachen, Germany) with 25 cm<sup>2</sup> electrode area to ensure comparability. Due to lower titers, the current density was adjusted to 10 mA·cm<sup>-2</sup> when the acetoin concentration was below 10 g·L<sup>-1</sup> and 25 mA·cm<sup>-2</sup> when it was above 10 g·L<sup>-1</sup>. This was done to avoid mass transport limitations. All experiments were evaluated after sufficient charge for the full conversion of acetoin to 2-butanone was supplied, according to eqn (7), where  $z$  is the number of electrons in the reaction (2 for 2-butanone),  $n_{\text{acetoin}}$  is the initial amount of acetoin,  $F_{\text{Faraday}}$  is the Faraday constant, and  $I$  is the applied current.

$$t_{\text{FC}} = z \cdot n_{\text{acetoin}} \cdot F_{\text{Faraday}} \cdot I^{-1} \quad (7)$$

Thus, the duration of the experiment was governed by the acetoin concentration and the current density. The individual acetoin concentrations and current densities are given in Appendix Table A 6.

## 2.8 Analytical methods

### 2.8.1 Sample preparation

All samples from cultivations were centrifuged for 2 minutes at 13,300 rpm. Aqueous phases were filtered (0.2 µm pore size, 4 mm diameter, Phenomenex Inc., Torrance, USA) and analyzed using high-pressure liquid chromatography (HPLC, Chapter 2.8.2). In case of aqueous-organic two-phase cultivations, the upper, organic phase was used for methyl ketone identification and quantification using a gas chromatography (GC) with a flame ionization detector (FID) or a mass spectrometer (MS) as described in Chapter 2.8.3. The lower, aqueous phase was obtained with a syringe from the lower part of the sample tube and processed as described above. All samples were stored at -20 °C until further analysis.

### 2.8.2 Metabolite quantification using high-performance liquid chromatography

The aqueous phases of cultivations were analyzed via high-performance liquid chromatography equipped with a refractive index and a UV detector (HPLC-UV-RI). All metabolites in aqueous phases were quantified using a DIONEX UltiMate 3000 HPLC System (Thermo Fisher Scientific Inc., Waltham, USA) with a Metab-AAC column (300 × 7.8 mm column, ISERA GmbH, Düren, Germany). Elution for aqueous samples from cultivations with *P. taiwanensis* VLB120 variants was performed with 5 mM H<sub>2</sub>SO<sub>4</sub>

at a flow rate of  $0.6 \text{ mL} \cdot \text{min}^{-1}$  and a column temperature of  $40 \text{ }^{\circ}\text{C}$ . For cultivations with *L. lactis*, elution was performed at a flow rate of  $0.5 \text{ mL} \cdot \text{min}^{-1}$  of  $5 \text{ mM H}_2\text{SO}_4$  and a column temperature of  $60 \text{ }^{\circ}\text{C}$ , while pyruvate from these cultivations was eluted at a flow rate of  $0.6 \text{ mL} \cdot \text{min}^{-1}$  of  $5 \text{ mM H}_2\text{SO}_4$  and a column temperature of  $30 \text{ }^{\circ}\text{C}$ . For detection, a SHODEX RI-101 detector (Showa Denko Europe GmbH, Munich, Germany) and a DIONEX UltiMate 3000 Variable Wavelength Detector set to  $210 \text{ nm}$  were used. The substrates were identified and quantified via retention time and the UV/RI quotient was compared to the corresponding external standards.

### 2.8.3 Methyl ketone identification and quantification using gas chromatography

Quantification of methyl ketones in the respective organic solvent was performed using a Trace GC Ultra (Thermo Fisher Scientific Inc., Waltham, USA) equipped with a FID and a polar ZB-WAX column (30 m length,  $0.25 \text{ mm}$  inner diameter, and  $0.25 \text{ }\mu\text{m}$  film thickness, Zebron, Phenomenex Inc., Torrance, USA). The injector temperature was set to  $250 \text{ }^{\circ}\text{C}$  and the injection volume was  $1 \text{ }\mu\text{L}$ . The measurements were performed at a constant helium flow rate of  $2 \text{ mL} \cdot \text{min}^{-1}$  and the split ratio was adapted to the analyte concentration. The initial oven temperature of  $80 \text{ }^{\circ}\text{C}$  was held for 2.5 minutes, increased to  $250 \text{ }^{\circ}\text{C}$  at  $20 \text{ }^{\circ}\text{C} \cdot \text{min}^{-1}$ , and then held constant at  $250 \text{ }^{\circ}\text{C}$  for 10 minutes, and the temperature of the FID was  $290 \text{ }^{\circ}\text{C}$ . Methyl ketones were quantified using external standards of 2-undecanone, 2-tridecanone, 2-pentadecanone, and 2-heptadecanone (Tokyo Chemical Industry Co., Tokyo, Japan). Since no standards for the monounsaturated methyl ketones 2-tridecenone, 2-pentadecenone and 2-heptadecenone were available, their concentration was derived from their peak area using the same calibration curve as their saturated counterparts. The presence of the monounsaturated methyl ketones was confirmed using GC-MS methods as described earlier.<sup>78, 97</sup>

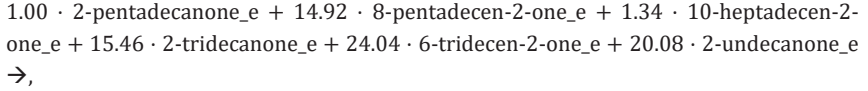
## 2.9 In silico model of *Pseudomonas taiwanensis* VLB120

### 2.9.1 Genome-scale model

For the reconstruction of the metabolic network of *P. taiwanensis* VLB120  $\Delta 6 \text{ pProd}$ , the most current and complete network of the closely related organism *Pseudomonas putida* KT2440 was used, i.e., *i*JN1463.<sup>197</sup> The network *i*JN1463 contains 2,153 metabolites, 2,927 reactions, and 1,463 genes. Herein, the network *i*JN1463 was adjusted according to the modifications introduced by Nies *et al.* (Appendix Table A 7).<sup>97</sup> In their genome-scale metabolic model (GEM) of *P. taiwanensis* VLB120, named *i*JN1411\_MK, they took the metabolic network reconstruction *i*JN1411 for *P. putida* KT2440 as a basis.<sup>198</sup> They adapted *i*JN1411 by removing and adding reactions and metabolites to switch from *P. putida* to *P. taiwanensis* VLB120. The GEM *i*JN1463 was modified according to *i*JN1411\_MK, with the following differences: The reactions DABAAT2 and AHSERL2 were not relevant for biomass production in *i*JN1411 but are relevant for biomass production in *i*JN1463 and were therefore not

deleted. Moreover, the reaction SHSL2r instead of SHSL2 was deleted, due to SHSL2 does not exist in *iJN1463*.

In the model *iJN1411\_MK*, Nies *et al.* added a methyl ketone pooling reaction.<sup>97</sup> Different to their suggestion, in this work, we accounted the pooling reaction for the C<sub>17</sub> congener 2-heptadecanone. The new pooling reaction reads:



where e indicates that the metabolites are extracellular and where the stoichiometry corresponds to the molar ratio of the methyl ketone congeners that was determined experimentally by Nies *et al.*<sup>97</sup> Note that, as the reaction is a so-called exchange reaction, only reactants and no products are assigned to this reaction. Additionally, two reactions, *i.e.*, one producing 2-undecanone and one transporting 2-undecanone to the extracellular space, were added, in alignment with the other congener reactions. With the aforementioned adaptations implemented, the adapted GEM was named *iJN1463\_MK*.

The genetically modified strain  $\Delta 6$  pProd was implemented in the model by constraining the corresponding reactions in the GEM *iJN1463\_MK* to zero. An overview of the genes can be found in the Appendix Table A 7. Knocking out the genes *fadE* and *fadE2*, however, made the production of methyl ketones computationally impossible, because certain metabolites that are important for the production of methyl ketones could not be synthesized anymore. The reason for this is that the gene *co\_aco* is not implemented in *iJN1463\_MK* but present in the mutant strain. The gene *co\_aco* originates from *Micrococcus luteus* and encodes the enzyme acyl-CoA dehydrogenase that catalyzes the synthesis of the needed metabolite, just as *fadE* and *fadE2*, however with different reaction partners. Eqn (8) shows the reaction originating from the genes *fadE* and *fadE2*, while eqn (9) shows the heterologous equivalent from *M. luteus* with the gene *co\_aco*.



All 35 reactions catalyzed by acyl-CoA dehydrogenase were adjusted in the metabolic network such that FAD and FADH<sub>2</sub> were replaced with O<sub>2</sub> and H<sub>2</sub>O<sub>2</sub>, respectively. With the knockouts implemented, we refer to the modulated network as *iJN1463\_MK*  $\Delta 6$  pProd in the following. All adaptations in this section were conducted in Python™ version 3.9.12. (Python Software Foundation, Beaverton, USA). The model *iJN1463\_MK*  $\Delta 6$  pProd is openly available at Ziegler *et al.*<sup>199</sup>



### 2.9.2 Flux balance analysis

The maximization of the methyl ketone exchange reaction or the biomass exchange reaction BIOMASS\_KT2440\_WT3 was chosen as cellular objective for the flux balance analysis (FBA). The lower bound on the adenosine triphosphate maintenance (ATPM) reaction, which corresponds to non-growth associated ATP maintenance requirement (NGAM), was set to  $0.52 \text{ mmol} \cdot \text{g}_{\text{CDW}}^{-1} \cdot \text{h}^{-1}$  according to experimental data from Ebert *et al.*<sup>200</sup> The computations were performed using the software COBRApy and the optimization software Gurobi 9.5.1 (Gurobi Optimization, LLC, Beaverton, USA).<sup>201</sup> For comparison of experimental results with computational results, time-resolved concentrations from HPLC-UV-RI measurements in the exponential growth phase were used to calculate flux rates.<sup>202, 203</sup> The code for the FBA computations is openly available at Ziegler *et al.*<sup>199</sup>

---

# Chapter 3

## Results

---



---

# Chapter 3.1

## Bioprocess intensification for efficient methyl ketone production and extensive evaluation of methyl ketones as a drop-in biofuel

### Partially published as

C. Grütering, C. Honecker, M. Hofmeister, M. Neumann, L. Raßpe-Lange, M. Du, B. Lehrheuer, M. von Campenhausen, F. Schuster, M. Surger, B. E. Ebert, A. Jupke, T. Tiso, K. Leonhard, K. Schmitz, S. Pischinger, L. M. Blank. Methyl ketones: a comprehensive study of a novel biofuel. *Sustainable Energy & Fuels*. 2024, 8(9), 2059-2072.

Reprinted (adapted) with permission of *Sustainable Energy & Fuels*. Copyright The Royal Society of Chemistry.

### Contributions

Carolin Grütering designed all biotechnological experiments, partly in cooperation with others. The experiment shown in Figure 12 was partly performed by Franziska Schuster under the supervision of Carolin Grütering. All other experiments with *P. taiwanensis* VLB120 were performed by Carolin Grütering. Marcel Neumann and Christian Honecker performed the experiments with the AFIDA and the research internal combustion engine. Marius Hofmeister evaluated the density, the  $\eta_{sp}$ , the viscosity, and the material compatibility. Lukas Raßpe-Lange determined the flash point and the boiling point. Miaomiao Du investigated the ecotoxicology. Maximilian Surger performed the storability tests. Philipp Demling assisted with the setup of the multiphase loop reactor.

Marius Hofmeister is the original author of the section “Fuel properties of the methyl ketone blend” that was adapted for this thesis. Christian Honecker is the original author of the section “Combustion behavior in a single-cylinder research engine” that was adapted for this thesis. Miaomiao Du is the original author of the section “Ecotoxicological assessment of the methyl ketone blend” that was adapted for this thesis.

All other parts were written by Carolin Grütering and reviewed by Lars M. Blank.

---



## 3 Results

### 3.1 Bioprocess intensification for efficient methyl ketone production and extensive evaluation of methyl ketones as a drop-in biofuel

#### 3.1.1 Abstract

For several burning reasons, humanity must rapidly reduce greenhouse gas emissions in the transportation sector. While the vision is to rely on electric vehicles in the future, the existing fleet will depend predominantly on liquid transportation fuels for the decades to come. Here, we suggest a blend of saturated and monounsaturated medium-chain length methyl ketones as a sustainable biofuel that is fully compatible with the existing diesel fleet. These methyl ketones can be produced by genetically modified *Pseudomonas taiwanensis* VLB120 at high yields from glucose. By performing a comprehensive, reductive solvent screening for *in situ* extraction of methyl ketones, we developed a bioprocess for methyl ketone production that facilitates simple product purification by decantation. The use of an advanced multiphase loop bioreactor with countercurrent liquid-liquid extraction averted stable emulsion formation in a setup that can run in continuous mode in the future. We extensively tested the methyl ketones for their applicability in combustion engines. Here, parameters such as the derived cetane number, the flash point, and the kinematic viscosity match the diesel fuel specifications. Experiments in a research internal combustion engine showed that methyl ketones as a biofuel combine the efficient combustion of diesel fuel with the clean combustion of other oxygenates. Also, good storability and reduced ecotoxicology compared to common diesel fuel were demonstrated. Accordingly, we conclude that the presented blend of methyl ketones can serve as an advanced drop-in fuel in the scope of the envisaged sustainable bioeconomy.

#### 3.1.2 Introduction

The climate crisis demands quick and large-impact solutions. Fossil-based transportation fuels contribute largely to the global greenhouse gas emissions and accounted for about 20% in 2021.<sup>204, 205</sup> The future seems bright for electric vehicles by using renewable electricity, overcoming the challenge of fossil-based transportation. However, by 2030, approximately 80% of the global vehicle fleet will still be powered by internal combustion engines.<sup>72</sup> Without a reduction of greenhouse gas emissions by this fleet, carbon neutrality, *e.g.*, in 2050 in the EU and 2060 in China according to the Paris Climate Agreement, seems out of reach.<sup>206</sup> In a foreseeable timeframe, liquid fuels are also necessary for long-distance and heavy-duty transportation.<sup>73, 74</sup> Sustainably produced fuels, *i.e.*, e-fuels, biofuels, or biohybrid fuels, can profit from the current fuel infrastructure and fleet, while maintaining the beneficial high energy content of the fossil counterparts.<sup>75, 76, 207, 208</sup> Industrial biotechnology has the potential

to enable the transformation of traditional petroleum-based value chains to a sustainable bioeconomy relying on biomass, CO<sub>2</sub>, green H<sub>2</sub>, and industrial side streams as carbon sources.<sup>209-212</sup> Catalysts such as microorganisms can utilize these renewable, non-edible feedstocks to synthesize value-added substances such as biofuels, bioplastics, organic solvents, and biosurfactants in the declining order of the market size.<sup>213-216</sup>

Due to their favorable cetane numbers, medium-chain length methyl ketones gained attention as possible fuel alternatives.<sup>91</sup> Since the implementation of heterologous methyl ketone production in *Escherichia coli*,<sup>78</sup> methyl ketones have been produced in various microorganisms, including *Saccharomyces cerevisiae*, *Yarrowia lipolytica*, and *Pseudomonas putida*.<sup>94-96</sup> *P. taiwanensis* VLB120 was demonstrated to be a suitable production host for methyl ketones since this strain has an exceptionally high redox cofactor regeneration rate, a trait that is beneficial for the production of such reduced products.<sup>217</sup> Genetic modifications for producing methyl ketones included a complete disruption of the  $\beta$ -oxidation cycle and the obviation of the flux from acyl-CoA esters to free fatty acids. By these means, methyl ketones were produced from glucose at 53% of the theoretical maximum yield in a fed-batch process with n-decane as a solvent for *in situ* product extraction, representing the highest reported methyl ketone yield so far.<sup>97</sup>

The addition of organic solvents to the fermentation broth for *in situ* product extraction brings a wide range of benefits to bioprocesses. These include the prevention of product degradation and evaporation, the reduction of downstream processing steps, and a favorable shift of reaction equilibria.<sup>119, 137</sup> Many applications also benefit from a reduced concentration of a toxic product in the aqueous phase and thus a better performance of the biocatalyst.<sup>218</sup> While a wide variety of solvents can potentially be suitable for a specific application, the applied type of organic solvent should be thoroughly investigated since the solvent is in direct contact with the fermentation broth. Inappropriate solvent choices can lead to poor phase separation or reduced biocatalyst performance, among other things.<sup>150, 219</sup> In order to systematically reduce the solution space, comprehensive solvent evaluation procedures were developed that match the requirements of biological systems. Several studies have shown that such approaches can improve the performance of bioprocesses.<sup>149, 220</sup> For example, an extensive solvent screening was indispensable for the efficient recovery of biosurfactants by *in situ* extraction.<sup>138</sup> The suggested reductive, multi-step approach can serve as a blueprint for solvent selection for other applications including methyl ketone production. However, *in situ* product extraction often goes hand in hand with the formation of stable emulsions due to surface-active compounds, such as proteins and phospholipids synthesized by the whole cell catalyst. A range of technologies were suggested to break these emulsions, including centrifugation, supercritical CO<sub>2</sub>, and catastrophic phase inversion, besides others, however, all requiring an additional step and hence complicate purification.<sup>221-225</sup> Recently, a new bioreactor type, namely a multiphase loop reactor (MPLR, **Figure 8**), was designed for the circumvention of

cumbersome emulsion formation, reducing the energy entry enormously, while compromising only little on extraction efficiency.<sup>145, 146</sup>

In this study, the previously engineered *P. taiwanensis* VLB120 Δ6 pProd<sup>97</sup> that efficiently converts glucose to methyl ketones was exploited, and the product mixture was evaluated as a fuel that is backward-compatible with the existing vehicle fleet. As the fermentation relies on *in situ* extraction, a hierarchical organic solvent screening was carried out, taking such different parameters as physicochemical properties, green solvent categorization, partition coefficient, biocompatibility, and suitability for extracting methyl ketones into account. 2-Undecanone was identified as a solvent with superior properties that considerably simplifies downstream processing. In an ideal scenario, here realized by using the novel multiphase loop reactor, only decanting is required.<sup>145, 226</sup> The resulting methyl ketone mixture was extensively evaluated for its suitability as a fuel in combustion engines based on a range of performance parameters, including flash point, viscosity, and lubrication behavior. Using this information, a surrogate mixture was assessed in terms of the combustion performance in a single-cylinder engine. The results revealed full compatibility with existing internal combustion engines and importantly superior combustion properties when compared to standard diesel fuel under the tested conditions. These positive results motivated us to investigate the ecotoxicology and the susceptibility to microbial degradation during storage. The results are discussed in the context of methyl ketones as an advanced, potentially sustainable fuel blend in existing diesel engines.

### 3.1.3 Results and Discussion

#### Solvent screening

##### Physicochemical parameters

A high number of organic solvents is potentially suitable for efficient, sustainable, and safe *in situ* extraction of methyl ketones. In order to systematically reduce the initial number of candidates, 97 organic solvents were evaluated regarding density, log *P*, melting point, and flash point (Table 6, Appendix Figure A 2).

**Table 6** Physical parameters and respective limits for the pre-screening of solvent candidates. The table was previously published<sup>148</sup> and is reprinted with permission of Sustainable Energy & Fuels.

Factor	Limit	Unit
Density	< 880	kg·m <sup>-3</sup>
Log <i>P</i>	≥ 3.4	-
Melting point	< 18	°C
Flash point	> 40	°C



The density of a solvent is of relevance because of the suitability for gravity-based separation techniques (see  $\rho_{\text{org}}$  in Stoke's Law, eqn (1)). The threshold was set to  $880 \text{ kg}\cdot\text{m}^{-3}$  to ensure a sufficient density difference to the aqueous fermentation that has a density of approximately  $1,000 \text{ kg}\cdot\text{m}^{-3}$ .

The log  $P$  as a measure of the hydrophobicity of a liquid describes the miscibility with the fermentation broth and can also serve as a first hint for estimating the compatibility of the solvent with the microbial production host. Solvents with a log  $P$  lower than 4.0 are described to be toxic towards most microorganisms, however, *Pseudomonas* spp. are generally known to have a high tolerance towards solvents that inhibit the growth of other microorganisms, also below a log  $P$  of 4.0.<sup>159</sup> With a restriction to solvents with a log  $P$  higher than 3.4, the respective solvent candidate is hydrophobic enough to avoid adverse cross solubility with the cultivation broth as well as interaction with the cell membrane of the production host.<sup>155, 227</sup> A melting point lower than  $18^\circ\text{C}$  ensures the liquid state of the candidate at cultivation conditions. The threshold for the flash point was set to values higher than  $40^\circ\text{C}$  to exclude solvents that are unsafe due to flammability. The described approach reduced the initial 97 solvents to a set of 20 solvents. In addition, nonanal was included in this set of solvents as a negative control due to its low log  $P$  value and 1-octanol due to its common usage as a sustainable solvent in extractions.<sup>171</sup>

### Weighted decision matrix

The next factors that were considered for the solvent selection were the toxicity on the production host, the green solvent score, the partition coefficient of the methyl ketones, and the formation of interphases.

As a first measure of solvent toxicity on the production host, the microbe was grown in the presence of 33 vol% of the respective solvent in a growth assay. After 48 hours of incubation time, cell growth was compared by estimating the turbidity of the aqueous phase (Appendix Figure A 3). *P. taiwanensis*  $\Delta 6$  pProd was able to grow with 20 out of the 22 solvent candidates. No growth was observed for 1-octanol and nonanal, that have a log  $P$  of 3.0 and 3.3., respectively. When octyl acetate, a solvent with a log  $P$  of 3.4 was added, growth was possible. Accordingly, the threshold for the minimal log  $P$  value for this variant seems to be 3.4. Notably, the production host has a deletion of the pSTY megaplasmid and thus does not express the TtgGHI solvent efflux pump, that is a main contributor to the high solvent tolerance of the *P. taiwanensis* VLB120 wild type.<sup>228, 229</sup> However, the strain still has a higher solvent tolerance than other microbial cell factories, since most require a minimum log  $P$  of 4.0.<sup>230</sup> For example, apart from the TtgGHI efflux pump, a cis/trans isomerase was found as a contributor to the high solvent tolerance of *P. taiwanensis* VLB120, making the cell membrane more robust towards solvents.<sup>228, 231</sup> These results again emphasize the high solvent tolerance of this strain and its general suitability for applications that involve potentially toxic organic compounds.

At this stage of the solvent screening, the candidates were also examined regarding health and safety scores. The health score is a measure to estimate the solvents toxic effects on humans, while the safety score describes whether the solvent is safe to work with. Here, *e.g.* butylbenzene had an undesirably high score as it causes serious eye irritations.<sup>232, 233</sup>

The partition of the methyl ketones in the organic phase after the extraction from the aqueous cultivation broth is one of the major requirements for *in situ* extraction. All solvent candidates show high partition coefficients of at least 24 for ethyl oleate and up to 135 for ethyl laurate (**Figure 11**). These high product partition coefficients can be explained with the hydrophobicity of the methyl ketones themselves. The product congeners have log *P* values of 4.1 to 6.3, which implies that they have a low solubility in the aqueous fermentation broth and thus easily accumulate in the organic solvent.<sup>234</sup> Accordingly, concerning the extraction of the methyl ketones regardless of the other tested factors, all 22 solvents show beneficial properties.

Lastly, interphase formation was compared as a measure of efficient and reproducible separation of the aqueous and organic phase after the extraction of the methyl ketones from cultivation broth (Appendix Figure A 4). Those interphases have a gel-like structure and consist mainly out of proteins. Interphase formation in bioprocess with *in situ* product extraction was shown to be detrimental as it leads to product and solvent loss.<sup>172</sup> For *in situ* extraction of methyl ketones, interphase formation highly depended on the respective solvent candidate. No correlation between the interphase formation and the properties of the respective solvent, *e.g.* the solvents hydrophobicity, could be observed.

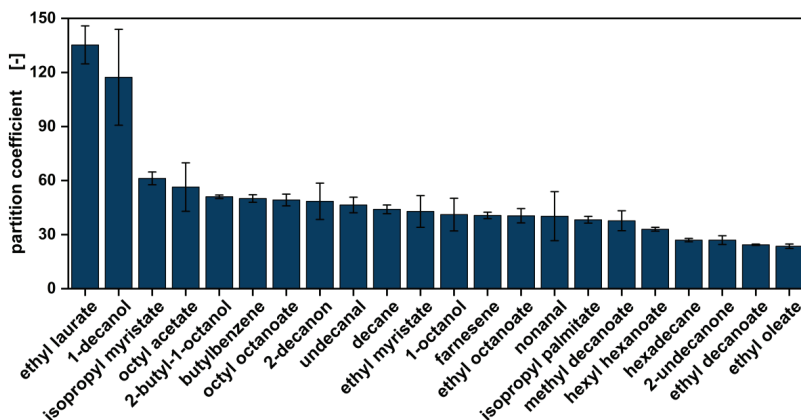


**Figure 11** Partition coefficients of the methyl ketones after extraction from cultivation broth. The coefficients represent methyl ketone partition between the aqueous cultivation broth and the 22 pre-selected solvents. The obtained values were included as a score in the ranking for the weighted decision matrix. The figure was previously published<sup>148</sup> and is reprinted with permission of Sustainable Energy & Fuels.

Highly hydrophobic solvents such as isopropyl myristate had a strong interphase, while hexadecane with a similar hydrophobicity had almost no interphase. This can probably result from the highly individual metabolic reaction of the production host to the corresponding solvent and the resulting individual formation of interphase-stabilizing proteins. Also the chemical structure of the solvent with functional groups such as the ester group of isopropyl myristate might influence interphase formation.

In order to systematically compare and rank 22 solvent candidates regarding the mentioned properties, a weighted decision matrix was created. For this, each property was given a weight regarding its importance for the biotechnological synthesis setup. Since the growth of the production host in the presence of the solvent is fundamental, this factor was given the highest weight of 40%. The green solvent score had a weight of 30%, the interphase formation and partition coefficient accounted for 20% and 10%, respectively. Then, all solvents were rated considering all properties with grades from one (worst performance) to five (best performance). The detailed explanation for the ranking including all results is given Appendix Table A 8. To generate a solvent score by which the candidates could be ranked, the sum of the weighting times the score was calculated.<sup>235</sup> This gave each solvent a specific value for direct comparison. Using the solvent score, all tested candidates could be ranked according to their performance, with octyl octanoate as the highest scoring solvent and nonanal with the lowest score (Appendix Table A 9). Octyl octanoate, farnesene, methyl decanoate, 2-undecanone, hexadecane, and ethyl decanoate had a score equal to or higher than 92% of the theoretical maximum score, so these were considered in the subsequent step of the solvent screening.

### **Biocompatibility**

For a suitable solvent candidate, the time-resolved growth behavior of the cells in the presence of the organic phase is an essential information. Therefore, biocompatibility and biodegradation of the mentioned candidates was assessed in shake flask cultivation by online monitoring of the CO<sub>2</sub> accumulation in the headspace (**Figure 12**) in the presence of the corresponding solvent.

The production host was able to grow with addition of all pre-selected solvents. The highest growth rates were measured with 2-undecanone and ethyl decanoate. Especially in the first hours, the production host grew best with 2-undecanone. Interestingly, the biocompatibility of a solvent does not strictly correlate with its log *P* value under these conditions, as growth was faster with methyl decanoate (log *P* 4.7) than with hexadecane (log *P* 8.8). The damaging effects of solvents were described to be highly individual and cannot only be derived from the log *P* value, since this value only gives an estimate of the degree of membrane interaction and thus toxicity. Regarding e.g. *Pseudomonas oleovorans*, it is described that it metabolizes generally non-toxic solvents such as octane (log *P* 4.9) intracellularly to more toxic 1-octanol (log *P* 3.0), which can cause toxicity also from solvents with a high log *P*. Also aromatic solvents are commonly more toxic than aliphatic ones with the same log *P*.<sup>159, 236</sup>

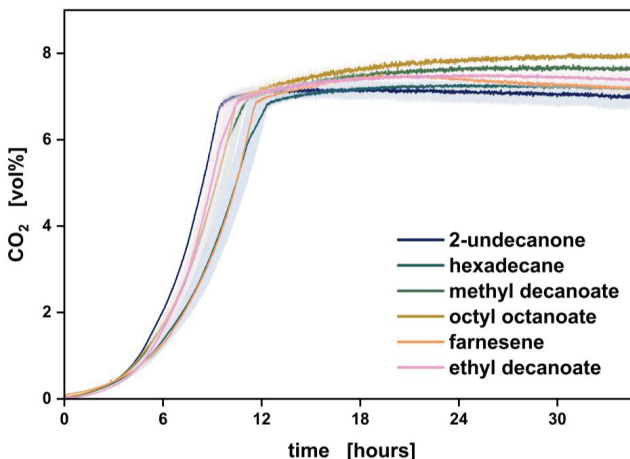


**Figure 12** Biocompatibility and biodegradability assessment of the solvents. CO<sub>2</sub> accumulation in the headspace of closed shake flasks in the presence of pre-selected solvent candidates was measured to quantify biomass formation. To ensure comparability of the course of the graphs, the data was standardized for the same vol% CO<sub>2</sub> at the point of reaching the stationary phase. Log *P* values: 2-undecanone 4.1; hexadecane 8.8; methyl decanoate 4.7; octyl octanoate 6.5; farnesene 6.1; ethyl decanoate 4.6. The data associated with this figure was partly obtained from Franziska Schuster's Bachelor Thesis under supervision by Carolin Grütering.<sup>237</sup> The figure was previously published<sup>148</sup> and is reprinted with permission of Sustainable Energy & Fuels.

Additionally, with octyl octanoate and methyl decanoate, a second increase in the CO<sub>2</sub> signal was observed, indicating biodegradation of the solvent. The production host used these solvents as a carbon source, which impairs the envisaged recycling of the solvent. Notably, those two solvents have in common that they are esters. Presumably, the production host's chromosomal carboxylesterases can hydrolyze these, which can make the corresponding alcohol and carboxylate accessible for anabolic reactions.<sup>103</sup> Both delayed and decelerated growth on glucose and usage of the solvent as a carbon source is unfavorable for the pursued methyl ketone production process. 2-Undecanone proved to be a candidate that neither caused a delay of the primary growth phase nor was degraded by the microorganism.

### 2-Undecanone as a solvent for *in situ* extraction of methyl ketones in bioreactors

With the described solvent screening procedure, 2-undecanone was found as a suitable solvent candidate regarding physicochemical parameters, growth assays, health score, safety score, partition coefficient, interphase formation, biocompatibility, and biodegradability. Furthermore, this C<sub>11</sub> methyl ketone is one of the product congeners itself. Accordingly, 2-undecanone also holds the big advantage of decisively

simplified product purification. For recovery of the methyl ketone mixture, no costly or energy demanding techniques for solvent removal such as distillation must be applied. The organic phase from the bioprocess can be used directly as the final product, for example as a biofuel blend. It was shown for other bioprocesses with *in situ* product extraction that a solvent that is compatible with the final product formulation can significantly lower production costs and minimize environmental impacts. This is especially true for bulk products like biofuels.<sup>160, 238</sup> Additionally, 2-undecanone has a log *P* of 4.1. This is in the lower range of the log *P* values that most microorganisms can tolerate for growth.<sup>155</sup> For example, different lactic acid bacteria were shown to not tolerate solvents with a log *P* lower than 4.2 and *S. cerevisiae* only had normal growth with solvents with a log *P* higher than 5.0.<sup>239, 240</sup> Since the production host has a high tolerance to this solvent, 2-undecanone can contribute to autosterile conditions in the envisaged bioprocess. Moreover, the comparatively low density of 2-undecanone of 820 kg·m<sup>-3</sup> is beneficial for phase separation, since there is a large density difference compared to the aqueous fermentation broth. This can increase the settling velocity (see Stoke's law, eqn (1)).

Accordingly, the performance of 2-undecanone as a second liquid phase was tested in stirred tank bioreactors (STRs, **Figure 13A**). The cultivation revealed superior suitability of 2-undecanone for continuous *in situ* extraction of methyl ketones. During the batch phase, there was no foam formation as previously observed during *in situ* extraction of methyl ketones with n-decane.<sup>78, 89, 241</sup> However, the detrimental emulsion formation still occurred in the STRs and the organic and the aqueous phase had to be separated by centrifugation (**Figure 14A**). This is highly undesirable regarding the scale-up of the bioprocess.

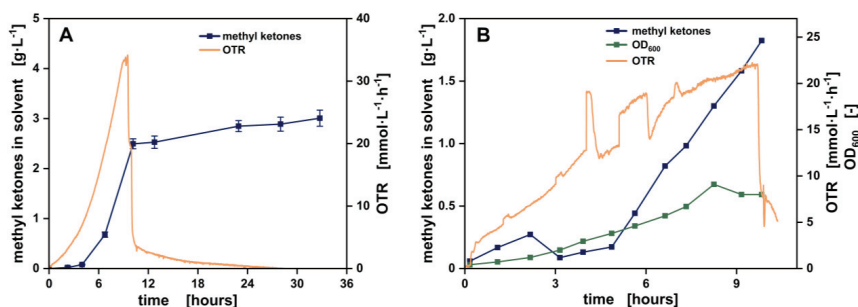


**Figure 13** Methyl ketone production with 2-undecanone as the organic phase for *in situ* extraction. Results are shown for both a stirred tank bioreactor (STR, A) and a novel multiphase loop reactor for improved phase separation (MPLR, B). Images of the cultivation broth of both (A) and (B) can be found in Figure 14. The OD<sub>600</sub> value as a measure for biomass concentration could only be measured for the cultivation in the MPLR, since here no emulsification occurred that usually hinders measurement of the OD<sub>600</sub>. The methyl ketone concentration of A is shown as the average of three biological replicates, while one representative set of OTR data is shown. OTR = oxygen transfer rate. The figure was previously published<sup>148</sup> and is reprinted with permission of Sustainable Energy & Fuels.

To circumvent the formation of stable emulsions, the STR-based bioprocess was transferred to the multiphase loop reactor (MPLR, **Figure 13B**), where aeration happened in the inner compartment (riser), and the methyl ketones were extracted by countercurrent liquid-liquid extraction in the outer compartment (downcomer). Because there were no peaks in shear stress due to stirring, emulsification was highly reduced compared to the STRs.<sup>145</sup> Using the MPLR, stable phase separation was achieved in the coalescing unit. From here, a coherent layer of the organic phase formed, which was then continuously recirculated. Images of the cultivation in the MPRL and the solvent reservoir are shown in **Figure 14B** and **Figure 14C**.

Notably, the product yield of both STR and MPLR was the same, while detrimental formation of stable emulsions was circumvented in the latter. Using the MPLR, oxygen supply is especially challenging in the non-aerated downcomer compartment. However, no oxygen limitation occurred, and oxygen supply was sufficient for growth and product formation. This proof-of-concept cultivation showed that by using 2-undecanone for *in situ* extraction in the MPLR, phase separation can be achieved by settling. Settling or decantation are far less costly and energy demanding as alternative recovery methods such as centrifugation. Here, the vision is to run the MPLR in continuous mode, where the production host would continuously produce the organic phase for product extraction. Accordingly, 2-undecanone also fits into the envisaged solvent recycling in this bioprocess. The obtained organic phase can serve as a proxy biofuel for further evaluation of the fuel properties.

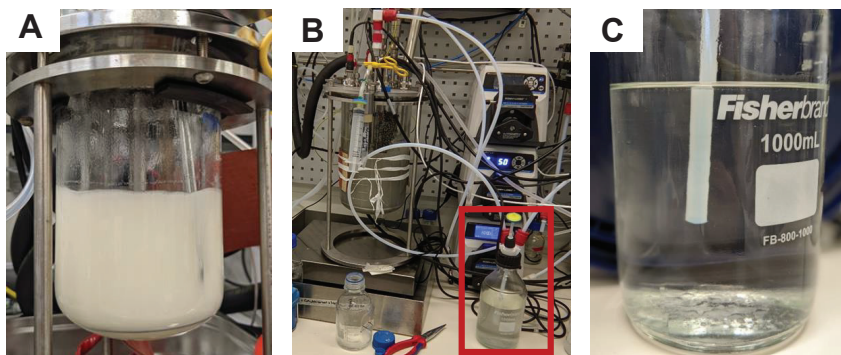


**Figure 14** Images of bioreactors with *P. taiwanensis* VLB120 Δ6 pProd and 2-undecanone as the organic solvent for *in situ* methyl ketone extraction. (A) Cultivation broth in a stirred tank bioreactor (STR) with emulsion formation. (B) Cultivation in the novel multiphase loop reactor with countercurrent liquid-liquid extraction in the outer compartment. (C) Solvent reservoir of the MPLR. From the solvent reservoir (red box in B, C), the organic phase is pumped in a cycle. Notably, there is no emulsification in (B) and (C). The figure was previously published<sup>148</sup> and is reprinted with permission of Sustainable Energy & Fuels.

### Fuel properties of the methyl ketone blend

Next, the fuel properties and the material compatibility of the methyl ketone blend were determined and compared to the values for fossil diesel (**Table 7**). The derived cetane number (DCN) was determined to be 64. This is substantially higher than the DCN required by EN590 and higher than the DCN of the currently used diesel. The flash point, the kinematic viscosity, and the lubricity fulfill the requirements of EN590. The wsd values for lubricity are low compared to other fuels, which is favorable in terms of friction and wear. The density at 15 °C could not be determined since the mixture forms crystals at 17 °C. However, at 20 °C, the density fits into the requirements of the norm. Consequently, the density criterion can only be fulfilled by adding additives such as 1-octanol for lowering the freezing point.<sup>242</sup>

**Table 7** Selected properties of fossil diesel, measured and simulated properties of the methyl ketone blend, and the specifications according to the EN590 norm. The measured values were obtained from a methyl ketone blend with 22.4 wt% 2-undecanone, 51.2 wt% 2-tridecanone, and 26.4 wt% 2-pentadecanone. <sup>a</sup> = derived cetane number determined in the AFIDA; <sup>b</sup> = flash point, vapor pressure, and boiling point determined by simulations in COSMO RS; <sup>c</sup> = kinematic viscosity and wsd measured according to DIN 51562 and ISO12156; \* = density of the methyl ketone blend measured at 20 °C; wsd = wear scar diameter; AFIDA = advanced fuel ignition delay analyzer. The derived cetane number was measured by Marcel Neumann. The kinematic viscosity, density, and material compatibility were measured by Marius Hofmeister. The flash point and the boiling point were determined by Lukas Raßpe-Lange. The table was previously published<sup>148</sup> and is reprinted with permission of Sustainable Energy & Fuels.

	Unit	EN 590 norm	Fossil diesel <sup>21</sup>	Methyl ketones
Molecular weight	g·mol <sup>-1</sup>	-	~200	210
Derived cetane number	-	> 51	55	64 <sup>a</sup>
Flash point	°C	> 55	67	115.6 <sup>b</sup>
Boiling point	°C	-	180 - 360	268 <sup>b</sup>
Kinematic viscosity at 40 °C	mm <sup>2</sup> ·s <sup>-1</sup>	2.0 - 4.5	~2.6	2.4
Density at 15 °C	kg·m <sup>-3</sup>	820 - 845	835	833.1*
Lubricity, wsd	µm	< 460	301 - 544 <sup>243</sup>	300 <sup>c</sup>
Oxygen mass fraction	-	-	-	8.1
Hydrogen mass fraction	-	-	-	13.1
Carbon mass fraction	-	-	-	78.8
Lower heating value	MJ·kg <sup>-1</sup>	-	35.7	39.1

The immersion test for material compatibility was performed according to DIN ISO 1817 (Appendix Figure A 5). Only for diesel and DnBE (di-n-butyl ether) results within the tolerance area for static or dynamic seals can be achieved. For most of the investigated bio-hybrid fuels, the change of hardness as well as volume change exceed the tolerance range. This also applies for the methyl ketone blend indicated by the blue marker. The pure methyl ketone blend would not perform well in real-life applications regarding compatibility with the materials present in the fuel segment of vehicles. The materials were co-evolved to be compatible with the historically present fuels, namely diesel and gasoline. Accordingly, the methyl ketone blend is only compatible with sealings made from PTFE.<sup>174</sup> Apart from that, the investigated methyl ketone blend fits into the standards defined by EN590 with some minor adaptations. The high DCN of the methyl ketone blend, exceeding the DCN of currently used fossil diesel, is especially beneficial for the envisaged application in combustion engines. These results emphasize that methyl ketones have similar or even advanced properties compared to conventional diesel fuel.

### Combustion behavior in a single-cylinder research engine

To assess the suitability of the methyl ketone blend under realistic conditions, engine testing in a single-cylinder research engine was performed on an operating range covering six representative speed-load points ranging from low load to medium part-load. **Figure 15** shows an overview of the typical load point in the urban driving range. The combustion behavior of the methyl ketone blend is characterized by a short ignition delay and low pressure rise rates (PRR), which are essential for smooth engine operation. At high, usually challenging EGR rates, combustion showed a high share of mixing controlled combustion. This can be attributed to the high reactivity of the methyl ketones, as evidenced by the high DCN of 64. The resulting relatively short ignition delay times are decisive for maintaining low noise and good combustion efficiency. Simultaneously, the use of methyl ketones brought about a significant reduction in soot emissions due to the presence of molecular oxygen in the fuel. Notably, this reduction did not compromise engine noise or efficiency characteristics by virtue of avoiding the shift towards a more premixed combustion as commonly observed for alternative diesel fuels such as 1-octanol.<sup>188, 189, 244, 245</sup> Additionally, the low soot emission would, in a real-life use case, translate to a reduced need for diesel particulate filter regeneration, thus lowering fuel consumption and wear on engine, oil, and aftertreatment system along with effectively further reduced tailpipe emissions. Maintaining a high share of diffusive combustion also averted the formation of overly lean areas in the fuel spray, thus allowing for low HC and CO emissions. Those were slightly better than for diesel combustion. Thus, applied to an unmodified diesel engine, it is likely that no control adaptations would be required to maintain emission compliance, thereby enabling the use of this methyl ketone blend as a drop-in fuel with no need for modifications from a combustion point of view.



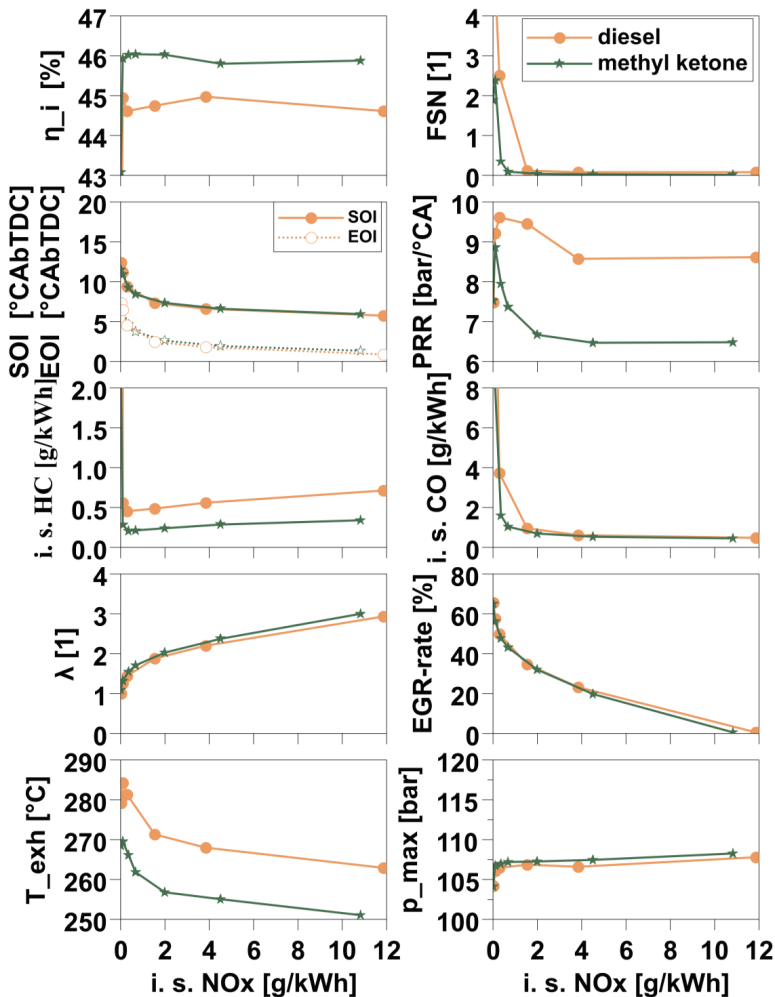


**Figure 15** Efficiency and emission results for a selected lower part load operating point, comparing the methyl ketone blend with diesel.  $N = 1500 \text{ min}^{-1}$ ; IMEP = 6.8 bar;  $p_{\text{rail}} = 900 \text{ bar}$ ; CA50 = 5.8 °CAaTDC;  $p_{\text{in}} = 1.5 \text{ bar}$ ;  $p_{\text{exh}} = 1.6 \text{ bar}$ .  $\eta$  = indicated efficiency; FSN = filter smoke number; SOI = start of injection; DOI = duration of injection; PRR = pressure rise rate; HC = unburned hydrocarbon;  $\lambda$  = relative air fuel ratio; EGR = exhaust gas recirculation; IMEP = indicated mean effective pressure; CA50 = centre of combustion; °CAaTDC = degree crank angle after top dead center. All measurements were performed under stationary conditions. Soot was measured in triplicates and averaged, indication data was cycle-averaged over 50 consecutive cycles, and the remaining data was sampled in 10 Hz intervals and averaged for 30 seconds to ensure statistical validity. The figure was originally created by Christian Honecker with the data obtained in cooperation with Christian Honecker, was previously published,<sup>148</sup> and is reprinted with permission of Sustainable Energy & Fuels.

In addition, their improved EGR compatibility grants this methyl ketone blend the potential to further lower emissions by increasing EGR rates of either adapted or dedicated engines or as pilot-ignition fuel.

In the single-cylinder research engine, we found that using the methyl ketone blend, we can combine the efficient combustion of diesel fuel with the clean combustion of oxygenate fuels.

### Microbial storage stability

With these favorable results in hand, we decided to assess the storage ability and ecotoxicology of the methyl ketones. To test the storability of methyl ketones as a diesel fuel substitute, CO<sub>2</sub> formation in the presence of 2-undecanone as a representative of the methyl ketones was measured in simulated oil tanks and compared to summer and winter diesel (**Figure 16**). CO<sub>2</sub> as the endpoint of metabolic activity serves as a marker for microbial activity.<sup>246</sup> Detailed information about the used microorganisms and storage conditions can be found in Appendix, Table A 2.

Until day eight, the simulated storage tank with methyl ketones showed a comparable CO<sub>2</sub> formation to winter diesel and a lower CO<sub>2</sub> formation than summer diesel. During the 14-day evaluation period, around 30% more CO<sub>2</sub> was formed in presence of methyl ketones compared to the diesel variants. After the assessed 14 days, the CO<sub>2</sub> level of the diesel variants stabilized, while the curve with the methyl ketones was still increasing. Hence, in short storage, methyl ketones have a similar storability to winter diesel, which is more stable against microbial degradation than summer diesel due to additives for decreasing the melting point.<sup>247, 248</sup>

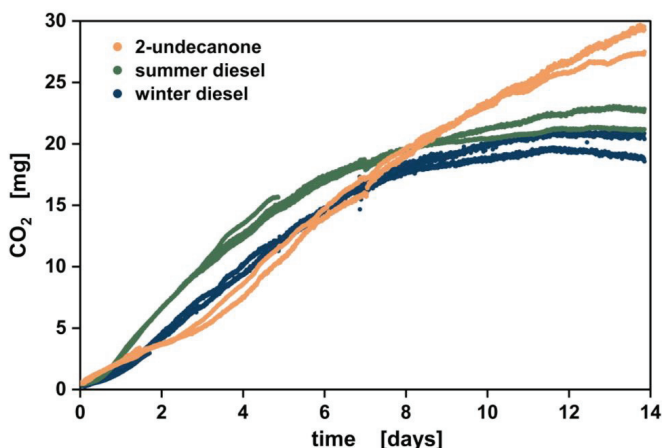


**Figure 16** Investigating fuel storage in the presence of microbial contaminations. CO<sub>2</sub> formation was used as a sign for microbial activity in the presence of 2-undecanone, a representative of the methyl ketones, summer diesel, and winter diesel in simulated storage tanks in triplicates. The data associated with this figure was obtained in cooperation with Maximilian Surger. The figure was previously published<sup>148</sup> and is reprinted with permission of Sustainable Energy & Fuels.

In longer storage experiments, methyl ketones have a reduced storability compared to diesel. This is probably due to the keto group at the C<sub>2</sub> position of the methyl ketones, which can serve as a starting point for enzymatic degradation.

In contrast, diesel consists mostly of saturated hydrocarbons.<sup>249-252</sup> Also, the methyl ketone blend was mixed with cultivation broth of *P. taiwanensis* VLB120 Δ6 pProd prior to this storability test to simulate its biological origin. This way, potential nitrogen and phosphorus sources can be present in the methyl ketones, that help to promote growth of microorganisms.<sup>253</sup> Fermentation broth carry over can be strongly reduced in an industrial production plant.

### Ecotoxicological assessment of the methyl ketone blend

The acute toxicity of two blends of medium-chain length methyl ketones was assessed by performing a fish embryo toxicity test with zebrafish embryos (*Danio rerio*). Blend A contained the saturated methyl ketones with a chain length of C<sub>11</sub> to C<sub>15</sub>, while blend B also contained monounsaturated methyl ketones.<sup>162</sup> The EC<sub>50</sub> and LOEC values for blend A were 2.12 mg·L<sup>-1</sup> and 1.50 mg·L<sup>-1</sup>, respectively. The EC<sub>50</sub> and LOEC values for blend B were 1.65 mg·L<sup>-1</sup> and 1.20 mg·L<sup>-1</sup>, respectively (**Table 8**).

The aquatic toxicity of methyl ketones on fish was similar to that of gasoline and lower than that of diesel. Regarding all examined factors that describe ecotoxicology, the methyl ketones were around ten times less toxic than diesel. Accordingly, methyl ketones can be considered a less toxic fuel regarding the toxic effects on ecosystems. Presumably, this reduced toxicity of the methyl ketones also contributes to their reduced storability as shown in **Figure 16**.

**Table 8** Aquatic toxicity on fish for methyl ketones, gasoline, and diesel. Methyl ketones A is a mixture of the saturated methyl ketones with 22.4 wt% 2-undecanone, 51.2 wt% 2-tridecanone, and 26.4 wt% 2-pentadecanone. Methyl ketones B is derived from cultivation broth and also contains the monounsaturated methyl ketones, namely 2-undecanone, 2-tridecanone, 2-tridecenone, 2-pentadecanone, 2-pentadecenone, and 2-heptadecenone. LC<sub>50</sub> = 50% lethal concentration; EC<sub>50</sub> = median effective concentration; LOEC = lowest observed adverse effect concentration; NOEC = highest concentration with no observed adverse effects; n.c.: not calculatable. The data associated with this table was obtained in cooperation with Miaomiao Du. The table was previously published<sup>148</sup> and is reprinted with permission of Sustainable Energy & Fuels.

Values [mg·L <sup>-1</sup> ]	Methyl ketones A	Methyl ketones B	Diesel <sup>254</sup>
LC <sub>50</sub>	n. c	2.01	0.23
EC <sub>50</sub>	2.12	1.65	n. c
LOEC	1.50	1.20	0.22
NOEC	n. c	1.00	0.15

### 3.1.4 Conclusions

There are molecules that can be produced sustainably by using microorganisms, and other molecules that are described to have favorable cetane numbers for application in diesel engines. In this study, it was shown that with the methyl ketones, the two aspects of sustainable production and potential for real-life applications can be combined. It was demonstrated that a solvent screening and the usage of the advanced MPLR enable a bioprocess for superior production of methyl ketones from renewable sugars. An extensive investigation of the properties of the methyl ketones revealed that regarding most tested criteria, this blend is already backward-compatible with the existing vehicle fleet at the current status. The examination in a research engine showed that the methyl ketone blend enables beneficial, efficient, and clean combustion already with diesel calibration and hardware, while the benefits were especially pronounced at low loads. The blend also has a reduced ecotoxicological impact compared to currently used diesel, presumably resulting in the demonstrated shorter recommended storage times. This issue can easily be solved by using additives that can improve storability. Additionally, additives are necessary for lowering the freezing point, and some adaptations regarding sealing materials will be required. Future investigations will focus on techno-economic and environmental analyses. The applicability of alternative, potentially CO<sub>2</sub> or plastic-derived carbon sources for the biotechnological production of the methyl ketones will be tested.<sup>90 255</sup> Blending the methyl ketones with existing diesel might lower the entrance barrier and contribute thereby directly to CO<sub>2</sub> reduction, a strategy that should be investigated. Concluding, a multi-discipline approach was shown to produce, test, and evaluate a diesel fuel blend that can directly contribute to lowering the greenhouse gas emissions of the existing diesel engines.



---

# Chapter 3.2

## In-depth evaluation of different feeding strategies and carbon sources for methyl ketone production

### Partially published as

A. L. Ziegler<sup>§</sup>, C. Grütering<sup>§</sup>, L. Poduschnick, A. Mitsos, L. M. Blank. Co-feeding enhances the yield of methyl ketones. *Journal of Industrial Microbiology and Biotechnology*, 2023, 50(1).

Reprinted (adapted) with permission of *Journal of Industrial Microbiology and Biotechnology*. Copyright Oxford University Press. <sup>§</sup>equally contributing authors.

### Contributions

In the Chapters “Flux balance analysis to simulate and optimize co-feeding” and “Ethanol achieves the highest reported yield in shake flask cultivation”, Carolin Grütering designed the laboratory experiments. Anita Ziegler designed the computations and the network adaptations. Leon Poduschnick performed the network adaptations, the computational work, and the experimental laboratory work under the supervision of Carolin Grütering and Anita Ziegler. Carolin Grütering, Anita Ziegler, and Leon Poduschnick visualized, analyzed, and discussed the data. Alexander Mitsos and Lars M. Blank conceptualized the project associated to these chapters.

In the Chapters “Utilization of wheat straw hydrolysates for methyl ketone production” and “Production of methyl ketones from wheat straw hydrolysates in bioreactors”, Carolin Grütering performed the laboratory experiments with support of Celina K. Yamakawa. Solange I. Mussatto conceptualized and supervised the associated work.

This chapter was written by Carolin Grütering and reviewed by Lars M. Blank and Solange I. Mussatto.

---



## 3.2 In-depth evaluation of different feeding strategies and carbon sources for methyl ketone production

### 3.2.1 Abstract

Glucose is a preferred carbon source of many microbial production hosts and usually allows for satisfactory growth and product formation. However, for many applications, utilization of glucose as the sole carbon source is not the best choice in terms of achieving high product yields and a sustainable bioprocess. Using flux balance analysis on a genome-scale metabolic model of methyl ketone producing *Pseudomonas taiwanensis* VLB120  $\Delta 6$  pProd for the screening of different co-fed carbon sources, we found that a combination of glucose and ethanol has the potential for obtaining high product yields. In shake flask cultivations, we confirmed that ethanol as a substrate result in the highest reported yield in batch production of methyl ketones with *P. taiwanensis* VLB120 to date, namely,  $0.154 \text{ g}_{\text{methyl ketones}} \cdot \text{g}_{\text{substrate}}^{-1}$ , which translates to 25.0% of the theoretical maximum yield. A combination of glucose and ethanol allowed for both higher methyl ketone titers and yields. Additionally, we tested the application of lignocellulosic hydrolysates as a carbon source that do not compete directly with food production. Notably, we can show here that methyl ketone production is feasible from both the cellulosic and hemicellulosic fractions. In bioreactor cultivations, the product yield with the cellulosic hydrolysate exceeded the yield obtained from glucose minimal media by more than 10%. These results indicate that the use of alternative carbon sources for methyl ketone production might be promising to establish an economic and ecologic bioprocess.

### 3.2.2 Introduction

In order to advance to a truly sustainable and economically competitive bioprocess, the in-depth investigation of the carbon source is compulsory.<sup>256, 257</sup> In many bioprocesses being researched, glucose is used as the sole carbon substrate. As glucose originates from starch (e.g. corn, wheat), sugar beet or sugar cane, biotechnology has a discussion to compete with food production for decades.<sup>258</sup> Although the main use of starch is feeding animals and not microbes, alternative carbon sources are key for a sustainable bioeconomy. These days, with the war in Ukraine, a major wheat exporter, the glucose price is skyrocketing, emphasizing the need for alternative substrates.<sup>259, 260</sup>

Different substrates are catabolized by different metabolic pathways, with different yields of metabolites from which the products of interest are synthesized. The theoretical yields can be computed, indicating which substrate-to-metabolite ratios are favorable. Consequently, a substrate might be beneficial for the production of one product, while not being suitable for another product, and single substrates can result in suboptimal product formation. Co-feeding of carbon and energy substrates apart from sugars can re-direct the metabolic fluxes for an optimized product formation.<sup>261-</sup>

<sup>263</sup> This was shown to benefit various applications such as the fungal production of



itaconate and recombinant proteins.<sup>264, 265</sup> Especially for the production of highly reduced compounds, such as medium-chain length methyl ketones, co-feeding was shown to be beneficial.<sup>266</sup> Also from an ecological perspective, bioprocesses can benefit from co-substrate use. Some substrates occur as industrial side streams, such as glycerol that accrues in biodiesel production.<sup>267</sup> Others, such as ethanol or acetate, can be produced from syngas fermentation or in case of formate, by electrochemical reduction of CO<sub>2</sub>.<sup>268, 269</sup>

Another promising source for carbon sources from potential side streams is the valorization of lignocellulosic biomass. Lignocellulose is the most abundant natural compound on earth.<sup>270</sup> It is industrially generated in agriculture, forestry, and sectors such as paper and whisky manufacturing.<sup>271, 272</sup> Additionally, the cultivation of robust non-food crops with high carbon yields and high suitability to poor soils as dedicated energy crops (e.g. switchgrass, *Miscanthus*) holds great potential.<sup>273-276</sup> Despite the economic and ecologic advantages, the usage of lignocellulose as a carbon source for microorganisms is challenging due to its chemical structure. It consists of the three polymers cellulose (~30% to 55%), hemicellulose (15 to 35%), and lignin (10 to 35%), all interconnected by complex cross-linkages. For full availability of the carbon stored in lignocellulose, the material has to go through different processing steps. During the so-called pre-treatment, the polymers break up into monomers, e.g. sugars such as glucose, xylose, arabinose, and galactose.<sup>277, 278</sup> Additionally, various potentially toxic and growth-inhibiting compounds such as furfural, formic acid, acetic acid, and phenols are also being produced in the pre-treatment, making the utilization of microbes as biocatalysts for value-added products from lignocellulosic hydrolysates challenging.<sup>279</sup> *Pseudomonas* spp. are known for their highly adaptable metabolism and their ability to metabolize a broad variety of carbon sources.<sup>32, 280</sup> Among this genus, especially *P. taiwanensis* VLB120 stands out with its natural capability to utilize not only hexose sugars such as glucose but also pentose sugars such as xylose. It utilizes the Weimberg pathway via a promiscuous glucose dehydrogenase and the intermediate metabolite 2-oxoglutarate for catabolization of xylose.<sup>281, 282</sup> For other microbial cell factories, extensive metabolic engineering has to be performed to enable the application of xylose as a carbon source.<sup>282</sup> Additionally, *P. taiwanensis* VLB120 is characterized by its high natural tolerance to the aforementioned biomass hydrolysate-derived inhibitors such as furfural and phenols.<sup>283</sup> These traits make it a promising microbial host for the production of value-added products from lignocellulose.

In this chapter, we investigate strategies to produce methyl ketones from alternative carbon sources. We examine different co-feeding strategies and the usage of lignocellulosic hydrolysates for the biotechnological production of methyl ketones. First, we used flux balance analysis (FBA) on a genome-scale model of the production host as a computational tool to screen the pre-selected co-substrates glycerol, ethylene glycol, ethanol, acetate, and formate for their ability to enable high yields of methyl ketones. With ethanol identified as the most promising candidate from the *in silico* analysis, we performed shake flask cultivations, examining the influence of

different glucose-to-ethanol ratios. Additionally, after producing lignocellulosic hydrolysates from wheat straw, the different fractions of the hydrolysate were tested for their ability to serve as the carbon source for methyl ketone production in bioreactors with *in situ* product extraction.

### 3.2.3 Results and Discussion

#### Flux balance analysis to simulate and optimize co-feeding

Five potential carbon sources, namely ethanol, glycerol, acetate, ethylene glycol, and formate, were pre-selected as potential co-feeding substrates. To simulate their co-feeding in the metabolic model, different uptake fluxes were used as the input for 20 times 20 FBA simulations (**Figure 17**). Using ethanol, the highest methyl ketone flux of  $0.026 \text{ mmol} \cdot \text{g}_{\text{CDW}}^{-1} \cdot \text{h}^{-1}$  was reached when both the glucose and the co-substrate uptake was maximized. The second-best co-substrate was glycerol, followed by acetate, ethylene glycol, and formate. With formate as the co-substrate, the maximum methyl ketone flux is  $0.015 \text{ mmol} \cdot \text{g}_{\text{CDW}}^{-1} \cdot \text{h}^{-1}$ .

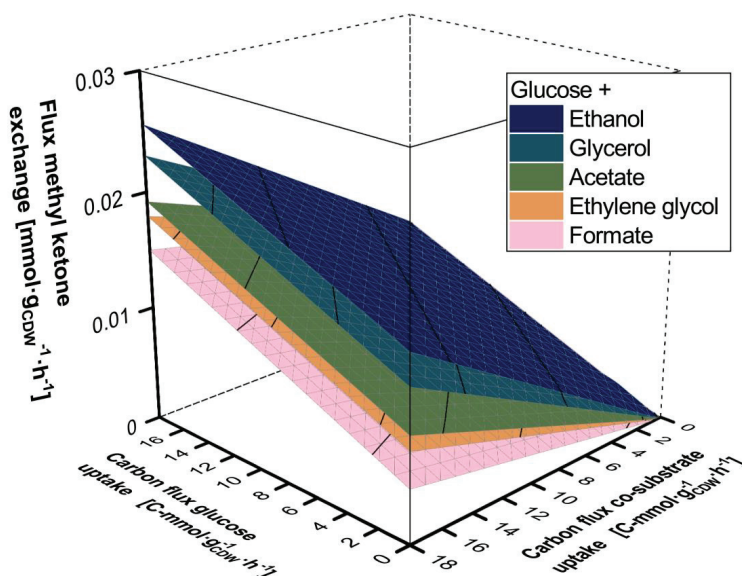


**Figure 17** The methyl ketone exchange flux as a result of varying the glucose and co-substrate uptake rates during the FBA. Different combinations of glucose and ethanol, glycerol, acetate, ethylene glycol, and formate were assessed in 20 times 20 FBA simulations. The exchange reaction is normalized for 2-pentadecanone. The biomass growth was set to 10% of the maximum theoretical growth rate. FBA = flux balance analysis. The figure, originally created by Leon Poduschnick under supervision by Carolin Grütering and Anita Ziegler, was previously published,<sup>284</sup> and is reprinted with permission of the Journal of Industrial Microbiology and Biotechnology.

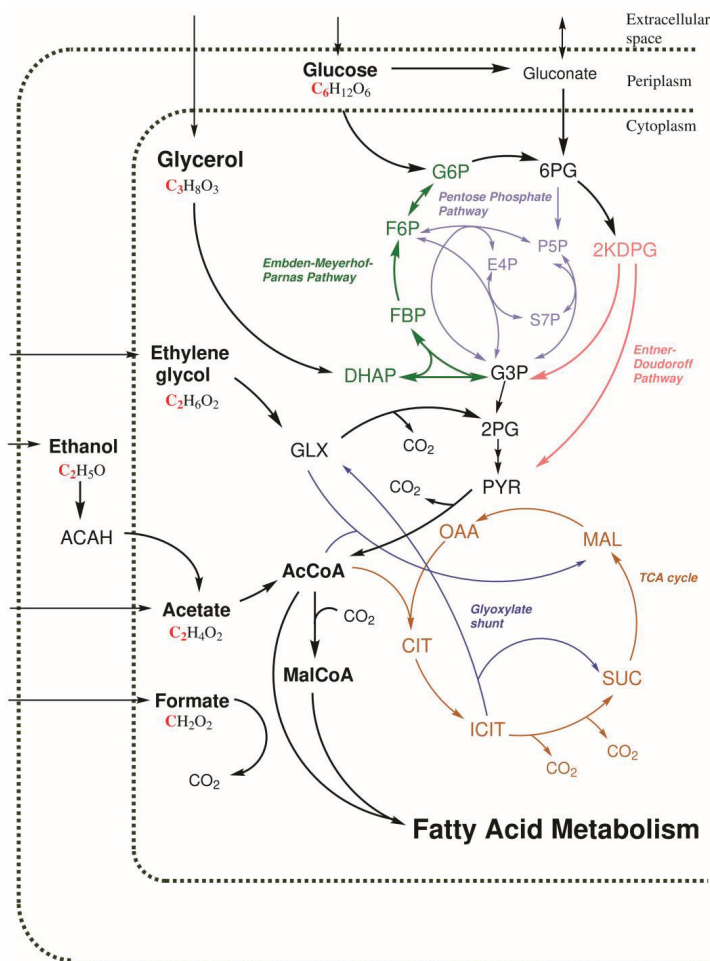


**Figure 18** Scheme of the central carbon metabolism of *P. taiwanensis* VLB120 including the metabolization of different substrates. The metabolic reactions of glucose, glycerol, ethylene glycol, ethanol, acetate, and formate, are shown as suggested by Li *et al.*, Tiso *et al.*, Yang *et al.*, Poblete-Castro *et al.*, and Zobel *et al.*<sup>285-289</sup> The scheme was created using ChemDraw 21.0.0. Abbreviations: G6P = glucose 6-phosphate; 6PG = 6-phosphogluconate; 2KDPG = 2-keto-3-deoxyphosphogluconate; F6P = fructose 6-phosphate; FBP = fructose 1,6-bisphosphate; G3P = glyceraldehyde 3-phosphate; DHAP = dihydroxyacetone phosphate; E4P = erythrose 4-phosphate; P5P = 5-phosphate pentose; S7P = seduheptolose 7-phosphate; 2PG = 2-phosphoglycerate; PYR = pyruvate; GLX = glyoxylate; AcCoA = acetyl-CoA; ACAH = acetaldehyde; MalCoA = malonyl-CoA; OAA = oxalacetate; CIT = citrate; ICIT = isocitrate; SUC = succinate; MAL = malate. The figure, originally created by Leon Poduschnick under supervision by Carolin Grütering and Anita Ziegler, was previously published,<sup>284</sup> and is reprinted with permission of the Journal of Industrial Microbiology and Biotechnology.

In **Figure 18**, the connection of each co-substrate to the central carbon metabolism of *P. taiwanensis* VLB120 is shown. Methyl ketones originate from intermediates of fatty acid *de novo* synthesis, where arguably the most important initial metabolite is acetyl-CoA. Ethanol as a carbon source is converted to acetate, which further reacts to acetyl-CoA with ATP as a cofactor. Thus, ethanol and acetate are both directly connected to the methyl ketone metabolism, notably without carbon losses, *i.e.*, CO<sub>2</sub> production.<sup>78, 290</sup> Glycerol is metabolized in the Embden-Meyerhof Parnas Pathway via dihydroxyacetone phosphate (DHAP), that is connected to the methyl ketone metabolism by its reaction to glyceraldehyde 3-phosphate. Glyceraldehyde 3-phosphate is first converted to pyruvate and then to acetyl-CoA by several enzymatic reactions.<sup>288</sup> Ethylene glycol can be used as an energy carrier to produce CO<sub>2</sub> and redox cofactors via the glyoxylate shunt, or as a carbon source by the conversion to pyruvate via tartronate semialdehyde with a loss of one CO<sub>2</sub>.<sup>285, 286</sup> Formate serves solely as an energy carrier, as it is converted NADH and CO<sub>2</sub> by formate dehydrogenase.<sup>289</sup>

The results of the FBA are coherent with the underlying metabolic pathways of the corresponding co-fed carbon sources. Accordingly, ethanol was chosen as the most promising carbon source for further investigation.

### Ethanol achieves the highest reported yield in shake flask cultivation

Prior to more detailed shake flask cultivations with the insights of the FBA, the growth behavior of *P. taiwanensis* Δ6 pProd with the five different co-fed carbon sources was investigated *in vivo* by online measurement of biomass formation in microtiter plates. This cultivation showed substrate inhibition in case of formate and acetate as a co-substrate (Appendix Figure A 6).

According to the FBA-based assessment of the co-substrates, ethanol was considered to be the most promising candidate for further evaluation in shake flask cultivations (**Figure 19**). The applied MSM media was developed to support cultivations with 10 g·L<sup>-1</sup> of glucose as a carbon source in shake flasks. To have the co-fed cultivations comparable to the glucose conditions, the same total molar amount of carbon was applied. A carbon ratio of two C-mol ethanol (2.4 g·L<sup>-1</sup>) to one C-mol glucose (8 g·L<sup>-1</sup>) was tested and biomass growth, carbon source uptake, and methyl ketone formation was measured (**Figure 19A**). Note that *P. taiwanensis* VLB120 produces minor amounts of gluconate as the only by-product, which is also metabolized after glucose depletion. Accordingly, there are no side products to be considered for the overall assessment of these cultivations.

Glucose and ethanol were taken up simultaneously, while the rate of glucose uptake rate of 1.44 mmol·g<sub>CDW</sub><sup>-1</sup>·h<sup>-1</sup> was higher than the rate of ethanol uptake of 1.05 mmol·g<sub>CDW</sub><sup>-1</sup>·h<sup>-1</sup>. After complete carbon source depletion after 24 hours, 0.84 g·L<sub>aq</sub><sup>-1</sup> of methyl ketones were produced, corresponding to a yield of 0.084 g<sub>methyl ketones</sub>·g<sub>substrate</sub><sup>-1</sup>. Cultivations under the same conditions with only glucose as a carbon source had an average yield of 0.058 g<sub>methyl ketones</sub>·g<sub>substrate</sub><sup>-1</sup>. This indicates

that regarding biomass growth, glucose is the preferred substrate of the production host. However, by applying ethanol as a co-substrate, increased product concentrations and yields compared to glucose as a single substrate can be achieved. Biomass concentration increases exponentially and appears to stop after around 10 hours, which might, however, be due to non-optimal sampling time points.

Presumably, the strain was still in the exponential phase after ten hours and grew around one or two hours more. According to our experimental experience, after reaching the stationary phase, the biomass decreases slightly. It is likely that the biomass concentration was higher than  $3.6 \text{ g} \cdot \text{L}^{-1}$  in the time when no sample was taken from the shake flask. The majority of product formation happened in the second half of the cultivation, presumably after substrate depletion. This was also observed earlier in cultivations with *P. taiwanensis*  $\Delta 6$  pProd for methyl ketone production. This can occur due to the rate-limiting spontaneous decarboxylation observed before.<sup>89, 97</sup> Potentially, the product concentration could have increased further after the 24 hours that were investigated.

The shake flask cultivation on ethanol (**Figure 19B**) revealed that ethanol can also serve as a sole carbon source for methyl ketone production. However, no high ethanol concentration can be applied due to the toxicity of this substance.<sup>227</sup>

After confirming the simultaneous consumption of ethanol and glucose using *P. taiwanensis*  $\Delta 6$  pProd as a production host, different combinations of glucose and ethanol were tested in shake flasks and compared regarding the methyl ketone yield (**Figure 20**). All samples were taken 24.0 or 25.5 hours after inoculation, presumably not corresponding to the highest product yield since product concentrations were still increasing at that time point. The highest yield within 24 hours was obtained by using pure ethanol as a substrate.

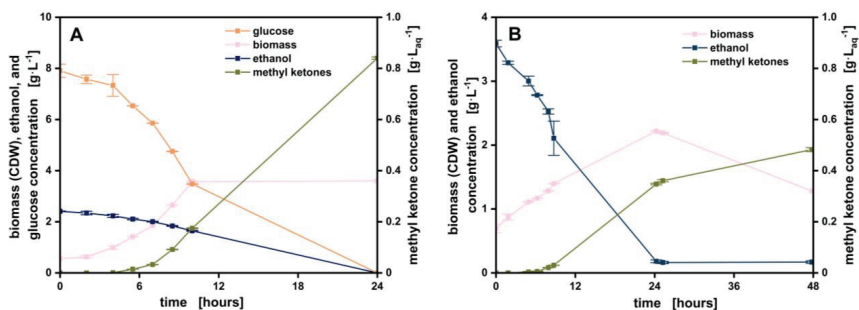


**Figure 19** Cultivation of *P. taiwanensis*  $\Delta 6$  pProd with glucose and ethanol. Concentration of biomass, ethanol, glucose, and methyl ketones are shown for a co-fed shake flask cultivation (A) and for a cultivation with ethanol as the sole carbon source (B). The C-molar ratios for (A) were one part glucose to two parts ethanol. The results are shown as the average of three experiments and the error bar represents the standard deviation from these biological replicates. The data associated with this figure was obtained from Leon Poduschnick's Master Thesis under supervision by Carolin Grütering and Anita Ziegler.<sup>291</sup> The figure was previously published<sup>284</sup> and is reprinted with permission of the Journal of Industrial Microbiology and Biotechnology.

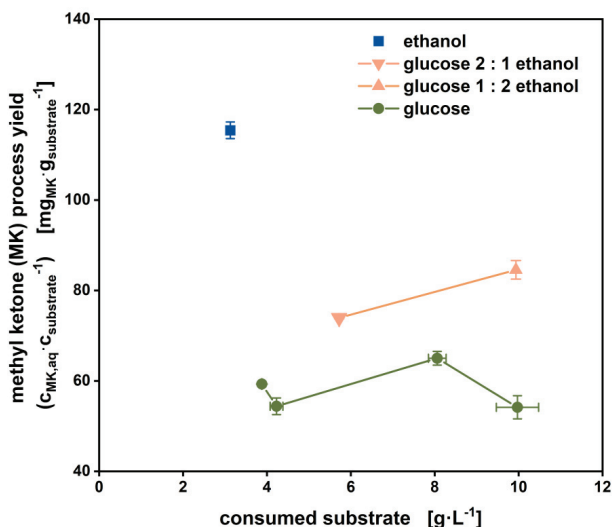


**Figure 20** Methyl ketone yield of (co-fed) shake flask cultivation after 24 hours and corresponding concentration of the carbon source. Glucose and ethanol were added in C-molar ratios of two parts glucose with one part ethanol (downward facing triangle) and one part glucose to two parts ethanol (upward facing triangle). Data is shown as average and standard deviation of three biological replicates. MK = methyl ketones. The data associated with this figure was obtained from Leon Poduschnick's Master Thesis under supervision by Carolin Grütering and Anita Ziegler.<sup>291</sup> The figure was previously published<sup>269</sup> and is reprinted with permission of the Journal of Industrial Microbiology and Biotechnology.

In the cultivation with ethanol as the only substrate, 2.82 g·L<sup>-1</sup> of ethanol were converted to methyl ketones with a product yield of 0.115 g<sub>methyl ketones</sub>·g<sub>substrate</sub><sup>-1</sup>. By applying ethanol and glucose in C-molar ratios of 2:1 and 1:2, yields of 0.085 g<sub>methyl ketones</sub>·g<sub>substrate</sub><sup>-1</sup> and 0.074 g<sub>methyl ketones</sub>·g<sub>substrate</sub><sup>-1</sup> were observed, respectively. When only glucose was used, the yield varied between 0.054 g<sub>methyl ketones</sub>·g<sub>substrate</sub><sup>-1</sup> and 0.066 g<sub>methyl ketones</sub>·g<sub>substrate</sub><sup>-1</sup>. Presumably, these variations derive from slightly different sampling time points. The higher the supplied amount of ethanol, the higher was the yield of methyl ketones. This suits the findings of the FBA study. Notably, after 48 hours of cultivation, a methyl ketone yield of 0.154 g<sub>methyl ketones</sub>·g<sub>substrate</sub><sup>-1</sup> (18.3 mmol<sub>methyl ketones</sub>·C-mol<sub>substrate</sub><sup>-1</sup>) was observed in a shake flask cultivation with single-fed ethanol (see **Figure 19B**). This translates to 25.0% of the theoretical maximum yield of methyl ketones on ethanol as a substrate. To our knowledge, this is the highest reported yield of methyl ketones in batch cultivations with *P. taiwanensis* VLB120 to date. Using genetically engineered *P. putida* KT2440, a methyl ketone yield of 0.169 g<sub>methyl ketones</sub>·g<sub>substrate</sub><sup>-1</sup> was observed in batch cultivations with glucose and high-value amino acids as co-substrates.<sup>96</sup> On glucose

as a single carbon source, application of *P. taiwanensis* VLB120  $\Delta 6$  pProd was shown to result in  $0.101 \text{ g}_{\text{methyl ketones}} \cdot \text{g}_{\text{substrate}}^{-1}$  in batch cultivations.<sup>97</sup> Approaches to produce methyl ketones from carbon sources other than glucose and glycerol are, to the best of our knowledge, not published.<sup>99</sup> However, ethanol conversion takes place at a reduced rate compared to glucose, and no high ethanol concentrations can be applied due to product toxicity. Thus, the final product concentration of  $0.48 \text{ g} \cdot \text{L}_{\text{aq}}^{-1}$  in the cultivation with ethanol is also lower than the  $0.84 \text{ g} \cdot \text{L}_{\text{aq}}^{-1}$  that were achieved with glucose and ethanol.

### Utilization of wheat straw hydrolysates for methyl ketone production

In Europe and in Germany in particular, wheat straw is the main side product of agriculture.<sup>292, 293</sup> To potentially exploit these resources, different hydrolysates were produced from wheat straw (**Figure 21**) and the growth of *P. taiwanensis* VLB120  $\Delta 6$  pProd was tested in preliminary growth assays (**Table 9**).

*P. taiwanensis* VLB120  $\Delta 6$  pProd did not grow in the presence of the hemicellulosic hydrolysate (HH) before decolorization, probably due to high concentrations of inhibitory phenols and furfural, exceeding  $500 \text{ mg} \cdot \text{L}^{-1}$  and  $7.2 \text{ g} \cdot \text{L}^{-1}$ , respectively. Phenols such as vanillin and furfural have been described to inhibit growth of the *P. taiwanensis* VLB120 wild type in case that the concentration is higher than  $1 \text{ g} \cdot \text{L}^{-1}$ .<sup>283</sup>

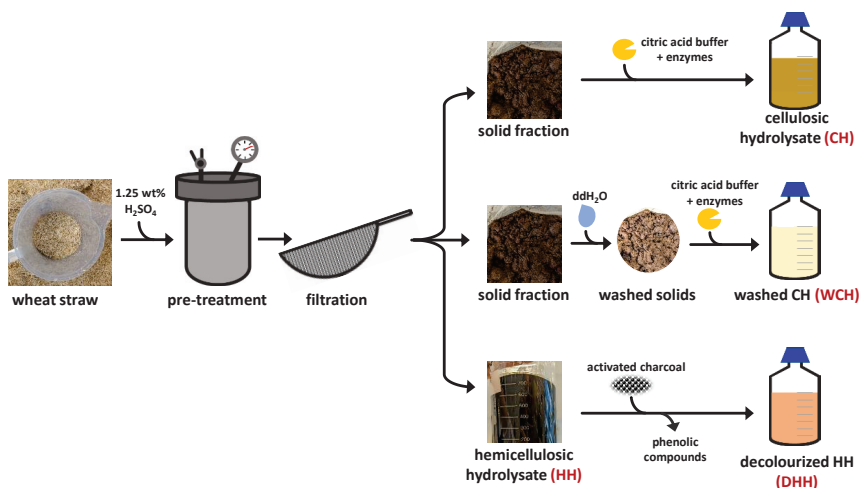


**Figure 21** Flow-chart showing the preparation of cellululosic hydrolysate (CH), washed cellululosic hydrolysate (WCH), hemicellulosic hydrolysate (HH), and decolourized hemicellulosic hydrolysate (DHH). The pre-treatment was performed according to Vollmer *et al.*<sup>194</sup> and the enzymatic hydrolysis according to Liu *et al.*<sup>195</sup> with Novozymes Cellic® CTec2 enzymes. The total concentration of phenolic compounds was measured using the protocol established by Ballesteros *et al.*<sup>196</sup> The hydrolysis was performed at Solange I. Mussatto's research group BCBT which is part of DTU Bioengineering at the Technical University of Denmark. The work was supervised by Solange I. Mussatto and performed with the help of Celina K. Yamakawa.

**Table 9** Growth of *P. taiwanensis* VLB120 Δ6 pProd using the different hydrolysates and the respective concentration of different carbon sources and inhibitors. The concentration of the carbon sources glucose, xylose, and acetic acid, formic acid, 5-HMF, furfural, and the total concentration of phenolic compounds in the four different hydrolysates HH, DHH, CH, and WCH was measured. The growth of *P. taiwanensis* VLB120 Δ6 pProd was assessed in microtiter plates (MTPs). Biomass formation was measured as the optical density at a wavelength of 600 nm in a plate reader. MSM components included the 2x phosphate buffer, the 1x nitrogen source, and 1x trace element solution (respective concentrations in Appendix Table A 1). The concentration of acetic acid, formic acid, 5-HMF, and furfural was not measured for WCH, and the concentration of the total phenolic compounds was not measured for CH and WCH. Analytics of HH and DHH were performed from two different batches, where HH had approximately 21 minutes instead of 19 minutes for the DHH at 95 °C during the pre-treatment. One checkmark signifies growth at a reduced rate with or without a lag phase, and two checkmarks signify growth at a rate comparable to the control on MSM with 10 g·L<sup>-1</sup> of glucose without a lag phase. MSM = mineral salt medium; 5-HMF = 5-hydroxymethylfurfural; Phenolics = phenolic compounds according to Ballesteros *et al.*<sup>196</sup> The data associated with this table was obtained at Solange I. Mussatto's research group BCBT which is part of DTU Bioengineering at the Technical University of Denmark. The work was supervised by Solange I. Mussatto and performed with the help of Celina K. Yamakawa.

	Growth	Growth with MSM	Glucose [g·L <sup>-1</sup> ]	Xylose [g·L <sup>-1</sup> ]	Acetic acid [g·L <sup>-1</sup> ]	Formic acid [g·L <sup>-1</sup> ]	5-HMF [g·L <sup>-1</sup> ]	Furfural [g·L <sup>-1</sup> ]	Phenolics [mg·L <sup>-1</sup> ]
HH	X	X	5.4	18.8	4.1	1.2	0.22	7.2	546
DHH	✓	✓✓	9.3	26.0	1.4	0.9	0.03	0.2	3
CH	✓	✓	6.2	5.2	1.1	0.0	0.02	0.1	-
WCH	✓	✓✓	42.1	1.2	-	-	-	-	-

After decolorization, the concentrations of phenolic compounds and furfural were reduced to 3 mg·L<sup>-1</sup> and 0.2 g·L<sup>-1</sup> in the decolorized hemicellulosic hydrolysate (DHH). Decolorization by adsorption to activated charcoal is described as an efficient and economic method for the removal of pre-treatment derived inhibitors.<sup>294</sup> The decolorization step made biomass growth on the hemicellulosic fraction that mainly contains xylose as a carbon source possible, particularly after supplementation with MSM components. In contrast to that, growth of the production host was possible on cellulosic hydrolysate (CH) before washing. The washing step reduces the residual amount of inhibitory compound originating from the preceding pre-treatment.<sup>195</sup> While the washing improved the enzymatic hydrolysis, as it can be seen by the higher concentration of glucose in the washed cellulosic hydrolysate (WCH) as opposed to the CH, it did not have an impact on the growth of the microorganism. However, after adding the MSM components, growth on WCH improved, likely due to improved buffering of the pH and a better supplementation with trace elements. Subsequent cultivations were performed using DHH and WCH with supplementation of MSM components.



## Production of methyl ketones from wheat straw hydrolysates in bioreactors

Bioreactor cultivations with *in situ* extraction of methyl ketones using both fractions of the wheat straw hydrolysate as the growth media were performed under the predetermined conditions (**Figure 22**). Using WCH (**Figure 22A**) for the cultivation,  $5.9 \text{ g}\cdot\text{L}^{-1}$  of methyl ketones accumulated in the organic phase after 48 hours of cultivation. The off-gas data revealed that there was no visible delay in the increase in both oxygen transfer rate (OTR) and carbon dioxide transfer rate (CTR) after inoculation. Both the OTR and CTR courses have two peaks. Until around five hours, the OTR increased to  $10 \text{ mmol}\cdot\text{L}^{-1}\cdot\text{h}^{-1}$ , followed by a second increase to  $30 \text{ mmol}\cdot\text{L}^{-1}\cdot\text{h}^{-1}$  after 14 hours. The samples of the aqueous phase show that there were  $0.8 \text{ g}\cdot\text{L}^{-1}$  of citrate in the WCH due to the application of a citrate buffer for the enzymatic reaction during hydrolysis. These results show that the production host grows without a lag phase, overcoming any inhibitory substance from the hydrolysis. Additionally, these findings hint at two distinct, sequential growth phases caused by catabolite repression.

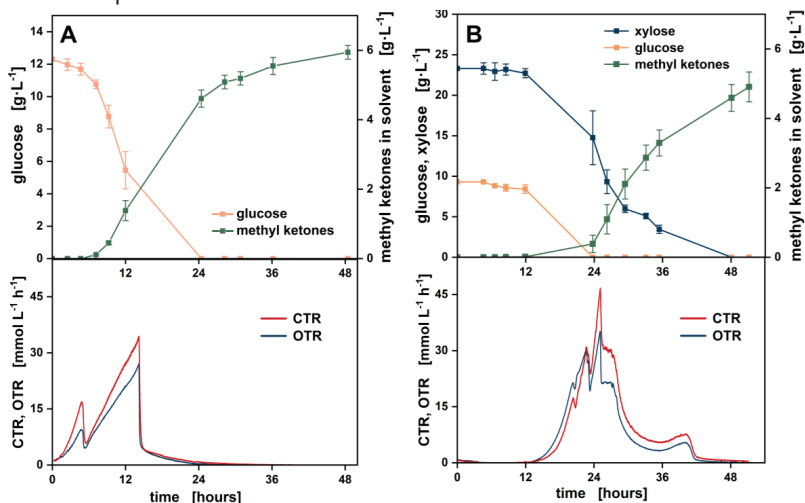


**Figure 22** Wheat straw hydrolysates as cultivation media in bioreactors with *P. taiwanensis* VLB120  $\Delta 6$  pProd. (A) Bioreactor cultivation using WCH as the aqueous phase. (B) Bioreactor cultivation using DHH as the aqueous phase. Cultivations were performed in 1.3 L glass vessels with 0.4 L of the respective hydrolysate and 0.1 L of *n*-decane for *in situ* extraction of methyl ketones. The DO was set to a minimum value of 30% by regulating the stirring rate from 400 to 1,200 rpm. The pH was kept constant at 7.0. The aqueous phase contained the MSM components (1x phosphate buffer, 1x nitrogen source, and 1x trace element solution, Appendix Table A 1). The data of the upper diagrams are shown as median values of two parallel bioreactor cultivations, while for the off-gas data, the values of one of the bioreactors are shown. The initial  $\text{OD}_{600}$  for A was 0.1, while the initial  $\text{OD}_{600}$  for B was 0.2. MSM = mineral salt media; CTR = carbon dioxide transfer rate; OTR = oxygen transfer rate. The hydrolysates were generated at Solange I. Mussatto's research group BCBT which is part of DTU Bioengineering at the Technical University of Denmark and applied in bioreactors with permission of Solange I. Mussatto.

The primary growth phase was on citrate, followed by a secondary growth phase from five to 14 hours on glucose. The preference of *Pseudomonas* spp. to catabolize organic acids prior to sugars was described previously. The presence of, e.g., citrate in the cultivation media suppresses the metabolism of glucose.<sup>295, 296</sup> No detrimental growth effects such as secondary substrate limitation or inhibition due to the usage of WCH were visible in the course of the OTR.<sup>297</sup> 0.8 g·L<sup>-1</sup> of citrate and 12.3 g·L<sup>-1</sup> of glucose were transformed to 5.9 g·L<sup>-1</sup> of methyl ketones in the organic phase, corresponding to a product yield of 0.112 g<sub>methyl ketones</sub>·g<sub>substrate</sub><sup>-1</sup>. Notably, this is a 10% increase in the product yield compared to the 0.101 g<sub>methyl ketones</sub>·g<sub>substrate</sub><sup>-1</sup> that were achieved using *P. taiwanensis* VLB120 Δ6 pProd in batch cultivation with minimal salt media.<sup>97</sup>

With DHH as a cultivation medium (**Figure 22B**), 4.9 g·L<sup>-1</sup> of methyl ketones were detected in the organic overlay after 50 hours. The off-gas data show a delay of the increase in the OTR and CTR signal of around 12 hours, even though this cultivation had the double initial amount of biomass for inoculation (initial OD<sub>600</sub> of 0.2 for the DHH instead of 0.1 for the WCH). Due to missing data points for the sugar content of the aqueous phase from 12 to 23 hours, it remains unclear whether glucose and xylose concentrations decreased simultaneously or consecutively. The OTR and CTR data show three peaks after 20 hours, 23 hours, and 25 hours with a maximum OTR of 35 mmol·L<sup>-1</sup>·h<sup>-1</sup>. These peaks likely originate from consecutive metabolism of glucose, xylose, gluconate, and xylonate. Regarding the *P. taiwanensis* VLB120 wild type, previous research has shown that it catabolizes these carbon sources consecutively. If both sugars are present, there is a first phase of glucose consumption, followed by the metabolism of xylose and glucose, a phase of xylose conversion, and a last phase with the consumption of xylonate.<sup>281</sup> Notably, the consumption of glucose was also delayed with DHH as the cultivation media. Presumably, this could have been caused by the presence of inhibitory compounds derived from the hydrolyzation process, or by the availability of xylose as a second carbon source.<sup>295, 298</sup> The 23.3 g·L<sup>-1</sup> of xylose and 9.3 g·L<sup>-1</sup> of glucose in the aqueous phase translate to a product yield of 0.037 g<sub>methyl ketones</sub>·g<sub>substrate</sub><sup>-1</sup>, which is only 37% of the product yield that Nies *et al.* obtained from the benchmark batch cultivations with this methyl ketones production host.<sup>97</sup>

The production of methyl ketones on both fractions of the wheat straw hydrolysate in bioreactor cultivations in batch mode was possible. With the WCH, no growth-hindering effects of the hydrolysate were observed. Presumably, small amounts of inhibitory compounds such as furans and phenols were still present in the medium, however, without a noticeable effect due to the inherent high tolerance of the production host.<sup>195, 283</sup> Notably, the methyl ketone yield exceeds the yield on minimal media with glucose. This may be due to complex media components in the hydrolysate that had a positive impact on growth and product formation, since complex media often lead to altered growth as opposed to minimal media.<sup>299</sup> It was also speculated that small amounts of inhibitory compounds can lead to reduced growth, and thus an increased carbon flux

for product formation. Using the DHH as the cultivation medium, growth and product formation were impeded. There was a lag phase of approximately 12 hours, and a significant decrease in product yield and titer, probably caused by the presence of inhibitors and xylose being a less preferred substrate. However, it is noteworthy to mention that the biotechnological production from the hemicellulosic fraction of wheat straw hydrolysate was possible at all. For many other microorganisms, extensive genetic engineering and adaptations are required for the conversion of xylose and the compatibility with inhibitors.<sup>300, 301</sup> *P. taiwanensis* VLB120, however, was shown to even consume hydrolysate-derived inhibitors such as furfural, 5-hydroxymethylfurfural, and vanillin.<sup>283</sup>

Additionally, the presence of an organic solvent for *in situ* extraction of the product could have been advantageous, as not only the product, but also other more hydrophobic molecules such as the inhibitory furans and phenols could have partly been extracted by the solvent. This effect was observed previously and can be used to detoxify hydrolysates.<sup>119, 302, 303</sup> The subsequent purification of the product, however, could be more challenging, as these side products of the hydrolysis likely have to be separated.

### 3.2.4 Conclusion

We showed that the utilization of FBA on an expanded genome-scale model of *P. taiwanensis* VLB120  $\Delta 6$  pProd can guide the development of co-feeding strategies for methyl ketone production. The *in silico* assisted screening of different co-substrates revealed ethanol as a superior (co-fed) carbon source to obtain high product yields. In subsequent shake flask cultivations, ethanol as the sole carbon source showed indeed superior product yields of  $0.154 \text{ g}_{\text{methyl ketones}} \cdot \text{g}_{\text{substrate}}^{-1}$ , while the toxicity of ethanol in higher concentrations caused reduced product concentrations. However, the combination of glucose and ethanol in shake flask cultivations lead to both high product yields and higher methyl ketone concentrations. Ethanol is also advantageous in terms of economic and ecologic aspects, as it is a low-cost and high-volume chemical (approximately 90 million tons per year) that can be obtained from industrial side streams or syngas fermentations, *e.g.*, in steel mills.<sup>272, 304, 305</sup> To improve ethanol conversion to methyl ketones even further, fed-batch strategies in bioreactors with a primary growth phase on glucose, followed by feeding of ethanol (and glucose) should be investigated to reduce the impact of substrate toxicity and improve product formation.

Furthermore, the production of methyl ketones from wheat straw hydrolysates was shown to be possible. Applying the cellulosic fraction after enzymatic hydrolysis as the cultivation medium, bioreactor cultivations resulted in the highest measured methyl ketone yield from glucose in batch mode,  $0.112 \text{ g}_{\text{methyl ketones}} \cdot \text{g}_{\text{substrate}}^{-1}$ . Likewise, the hemicellulosic hydrolysate that mainly contains xylose as a carbon source can serve as the cultivation medium for methyl ketone bioprocessing. Future investigation can aim for combined bioprocessing of both the hemicellulosic and the cellulosic fraction,

and an increased conversion of xylose to methyl ketones and biomass, *e.g.* molecular engineering of the host.<sup>282</sup> For example, the Dahms pathway was shown to result high product yields from xylose when it is enabled by expression of an 3-deoxy-D-pentulosonic acid aldolase.<sup>306</sup> Additionally, adaptive laboratory evolution was shown to be a tool to enhance the tolerance of a microbial cell factory towards hydrolysis-derived inhibitors, thus improving the robustness of the microorganism under these conditions.<sup>307</sup>

Comparing all approaches to optimize the substrate utilization for methyl ketone production in this chapter (**Table 10**), we can conclude that the application of ethanol as a (co-fed) carbon source and WCH as the cultivation medium outperformed the benchmark cultivations with glucose in MSM.<sup>97</sup>

**Table 10** Comparison of methyl ketone product yields with different substrates. All yields were obtained from batch cultivations with *P. taiwanensis* VLB120 Δ6 pProd. Note that the yield from ethanol + glucose was derived after 24 hours, presumably not corresponding to the highest product yield in this cultivation. WCH = washed cellulosic hydrolysate; DHH = decolorized hemicellulosic hydrolysate.

Substrate	Methyl ketone yield		Comment
	[g <sup>methyl ketones</sup> ·g <sup>substrate</sup> <sup>-1</sup> ]		
Glucose	0.101	shake flasks, Nies <i>et al.</i> <sup>97</sup>	
Ethanol	0.154	shake flasks, this work	
Ethanol + glucose	0.085	shake flasks, this work, measured after 24 hours	
WCH (glucose)	0.112	bioreactors, this work	
DHH (xylose)	0.037	bioreactors, this work	



---

# Chapter 3.3

## Acetoin production by resting cells of *Lactococcus lactis* for direct electrochemical synthesis of 2-butanone

### Partially published as

C. Grütering, T. Harhues, F. Speen, R. Keller, M. Zimmermann, P. R. Jensen, M. Wessling, L. M. Blank. Acetoin production by resting cells of *Lactococcus lactis* for direct electrochemical synthesis of 2-butanone. *Green Chemistry*, 2023, 25(22), 9218-9225.

Reprinted (adapted) with permission of Green Chemistry. Copyright The Royal Society of Chemistry.

### Contributions

Carolin Grütering and Tobias Harhues designed the experiments. Fabian Speen and Carolin Grütering performed the biological experiments including analytics. Tobias Harhues performed the electrochemical experiments including analytics. Carolin Grütering, Tobias Harhues, and Fabian Speen visualized, analyzed and discussed the data.

Tobias Harhues is the original author of the section “Electrochemical conversion of acetoin to 2-butanone”.

All other parts were written by Carolin Grütering and reviewed by Lars M. Blank.

---



### 3.3 Acetoin production by resting cells of *Lactococcus lactis* for direct electrochemical synthesis of 2-butanone

#### 3.3.1 Abstract

2-Butanone and acetoin are important commodity chemicals, while only the latter can be produced biotechnologically from renewable resources in high concentrations. Recently, electrochemical conversion of acetoin to 2-butanone was shown to be feasible directly from microbial cultivation broth supernatants. However, the electrocatalysis in cultivation broth suffered from parasitic reactions due to dissolved media components. Here, we propose enantiopure (3*R*)-acetoin production in dilute resting cell buffer using genetically modified *Lactococcus lactis* to cater for the subsequent electrochemical catalysis. In resting cell buffers with a minimal amount of ions and dissolved molecules, the strain achieved product yields as high as  $0.49 \text{ g}_{\text{acetoin}} \cdot \text{g}_{\text{glucose}}^{-1}$  and product titers of  $19.4 \text{ g} \cdot \text{L}^{-1}$ . The resting cell broth was directly applied as the electrolyte in an electrochemical flow cell, where the conversion of the produced acetoin to 2-butanone was assessed. The 2-butanone yield of more than 50% outperformed the synthesis from complex media fermentation supernatants and that of previous studies. This interdisciplinary study at the interface of bio- and electrocatalysis shows that resting cells have a high potential to move microbial synthesis towards a cascade of processes, instead of single isolated conversion steps for the valorization of biomass.

#### 3.3.2 Introduction

Acetoin is a C<sub>4</sub> methyl ketone with an additional hydroxy group that is commonly used in the fragrance and flavor industry for its pleasant buttery aroma.<sup>308</sup> Additionally, the U.S. Department of Energy classifies acetoin as one of the 30 most important sugar-derived platform chemicals.<sup>309</sup> To produce acetoin, microbial production hosts offer a non-petrochemical route, utilizing renewable resources, and industrial side streams. For example, *L. lactis* is a Gram-positive, facultative anaerobic, and GRAS-certified representative of such microorganisms.<sup>310, 311</sup> By means of genetic engineering, *L. lactis* is able to produce a wide variety of value-added chemicals, including recombinant proteins and vitamins.<sup>311, 312</sup> In 2017, Kandasamy *et al.* engineered *L. lactis* to produce (3*R*)-acetoin as the sole product by deleting the genes for all competing by-product pathways such as acetate and lactate. This resulted in the *L. lactis* strain VJ017, which was able to convert glucose to acetoin with a product yield of  $0.41 \text{ g}_{\text{acetoin}} \cdot \text{g}_{\text{glucose}}^{-1}$ , representing 82% of the theoretical yield, without any carbon flux to by-products.<sup>116</sup> While acetoin is an industrially relevant product itself, an emerging application of acetoin with great potential is its reduction to 2-butanone.<sup>113, 313, 314</sup> 2-Butanone is an important commodity chemical that is currently produced from the C<sub>4</sub> fraction of fossil oil. This C<sub>4</sub> methyl ketone is used as a low-toxicity solvent in various applications and has a potential use as a sustainable fuel for spark-ignition engines.<sup>315-317</sup> There is a high demand for the production of 2-butanone from



renewable resources in the context of a sustainable bioeconomy.<sup>318</sup> Although direct production using microorganisms is possible, previous attempts yielded product concentrations of less than  $0.5 \text{ g} \cdot \text{L}^{-1}$  of 2-butanone.<sup>108, 110, 319</sup> Especially the reduction step catalyzed by a diol dehydratase, a coenzyme B12-dependent enzyme, is slow and cumbersome.<sup>109</sup> Hence, replacing this enzymatic step with efficient electrocatalysis is attractive. Due to its high polarity and low vapor pressure, acetoin purification from aqueous cultivation broths for subsequent reduction is challenging and not cost-efficient. Thus, an integrated process with the direct utilization of acetoin from cultivation broths is a more promising approach. This is enabled by direct electrochemical conversion of biotechnologically derived acetoin to 2-butanone in an electro-flow cell.<sup>112</sup> Using a fermentation supernatant as the electrolyte, a 50% yield of 2-butanone and a product selectivity of 80% were achieved without intermediate purification. However, the overall yield and faraday efficiency (FE) were reduced by parasitic reactions, mainly hydrogen evolution reaction (HER), presumably caused by metal ions from the trace element solution that deposited on the cathode. This effect has been studied recently and was employed to boost HER when it was desired.<sup>118</sup> In addition to the parasitic HER, the conversion was inherently limited by the side product 2,3-butanediol that consists of two isomers, of which only one is converted to acetoin.<sup>112, 320</sup> Therefore, the use of an acetoin solution with a minimal amount of charged, reactive compounds and no other C<sub>4</sub> compounds than acetoin would improve the overall process. A reduced amount of dissolved components in the cultivation supernatant is for example possible by the application of resting cells.<sup>321</sup> Resting cells are cells that are metabolically active, but non-growing. The resting state can be achieved by cultivation in buffers with minimal nutrients except for the carbon substrate.<sup>322</sup> The application of the resting cell method offers the possibility of high product yields due to mitigated carbon flux to cell division and the potential for cell recycling. Resting cells are commonly used to investigate the maximal activity of a whole-cell catalyst in short assays of minutes or few hours, all detached from cell division.<sup>323-325</sup> Furthermore, resting cells of many different microorganisms were utilized for the formation of various value-added products at high yields.<sup>326-328</sup> Here, we suggest an integrated approach for a cascade from glucose to 2-butanone by bio- and electrocatalysis (**Figure 23**).

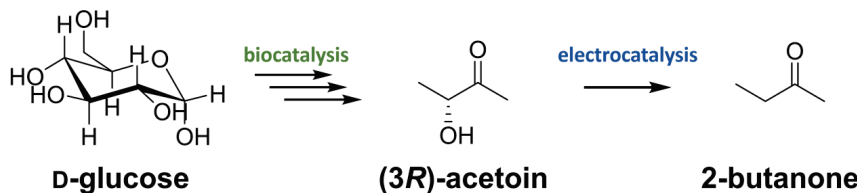


**Figure 23** Schematic representation of the substrates and products that are involved in our suggested cascade from glucose to 2-butanone. Ratios and co-products are omitted from this overview. The figure was previously published<sup>329</sup> and is reprinted with permission of Green Chemistry.

We improved the process introduced by Harhues *et al.* by using *L. lactis* VJ017 as a production host for enantiopure acetoin without any carbon flux to process-hindering side products. Additionally, we produced acetoin in a resting cell environment, where the supernatant has an increased compatibility with the electrochemical conversion 2-butanone. This enabled direct conversion of acetoin to 2-butanone with a yield of over 50%. The integrated process at the interface of bio- and electrocatalysis demonstrates the high potential of the production pathway from glucose to bio-based 2-butanone. The results are discussed in the context of exploiting the strengths of the different catalysis approaches to design ever more efficient synthesis pathways, a prerequisite for the establishment of a sustainable bioeconomy.

### 3.3.3 Results and Discussion

#### Acetoin toxicity for *L. lactis* VJ017

One of the main goals of this chapter was to produce a broth supernatant with high acetoin concentrations. Acetoin was shown to be toxic for *L. lactis* due to interactions of the keto group with proteins and DNA.<sup>330</sup> Accordingly, the effect of acetoin on the production host *L. lactis* VJ017 was tested. Growth in the presence of altering acetoin concentrations was monitored by CO<sub>2</sub> accumulation in the headspace (**Figure 24**).

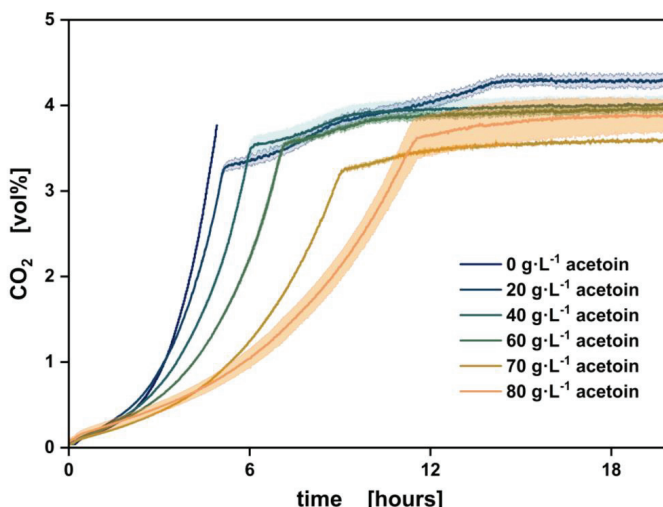


**Figure 24** CO<sub>2</sub> accumulation during growth of *L. lactis* VJ017 in the presence of various initial acetoin concentrations. BlueSens gas sensors were used to measure the vol% of CO<sub>2</sub> in the headspace of closed shake flasks with 3 g·L<sup>-1</sup> of glucose in M17 medium. The cultivation with 0 g·L<sup>-1</sup> acetoin had a higher amount of glucose, thus, only the exponential phase in the first 5 hours is shown. The data associated with this figure was obtained from Fabian Speen's Master Thesis under supervision by Carolin Grütering.<sup>331</sup> The figure was previously published<sup>329</sup> and is reprinted with permission of Green Chemistry.

The higher the initial acetoin concentration, the lower the rate of CO<sub>2</sub> formation and thus cell division (**Table 11**). Acetoin concentrations of 20 g·L<sup>-1</sup> lead to a rate reduction of 19%, while the highest tested concentration of 80 g·L<sup>-1</sup> caused a reduction of the CO<sub>2</sub> formation rate by 68%.

The rate of CO<sub>2</sub> accumulation was employed as a measure of bacterial growth earlier.<sup>138</sup> Accordingly, these values can be seen in the same context as the specific growth rates of the wild type *L. lactis* MG1363 that were determined by Kandasamy *et al.* before the strain was modified for acetoin production.<sup>116</sup> Without any initial acetoin, the CO<sub>2</sub> formation rate is 33% lower than the assessed values of the wild type of 1.17 h<sup>-1</sup>. This reduction can originate from the differing techniques for growth monitoring or from the rewiring of the central carbon metabolism that led to production of acetoin as a single product. Notably, the producer *L. lactis* VJ017 can tolerate higher acetoin concentrations than *L. lactis* MG1363. Even at high initial product concentrations of 80 g·L<sup>-1</sup>, exponential growth was still observed, while the wild type did not grow at all. Since acetoin is produced constitutively in every cultivation, *L. lactis* VJ017 may have acquired some mechanism to tolerate increased acetoin concentrations. *L. lactis* VJ017 is clearly suitable for the production of high acetoin titers.

**Table 11** Toxicity of acetoin towards *L. lactis* VJ017. The effect of different initial concentrations of acetoin on the CO<sub>2</sub> accumulation in closed shake flasks with *L. lactis* VJ017 and 3 g·L<sup>-1</sup> glucose was measured. The data associated with this table was obtained from Fabian Speen's Master Thesis under supervision by Carolin Grütering.<sup>331</sup> The table was previously published<sup>329</sup> and is reprinted with permission of Green Chemistry.

Acetoin concentration [g·L <sup>-1</sup> ]	CO <sub>2</sub> formation rate [h <sup>-1</sup> ]	Reduction in CO <sub>2</sub> formation rate [%]
0	0.80	-
20	0.65	19
40	0.58	28
60	0.45	44
70	0.36	55
80	0.26	68

### Tailored acetoin formation for optimal electrochemical conversion

To realize efficient conversion of acetoin to 2-butanone by electrochemistry, a high concentration of acetoin in a compatible medium is required. Three different media were tested for acetoin synthesis by *L. lactis* VJ017 (**Figure 25**). First, M17 medium is a complex medium that is mostly used for growth and maintenance of *L. lactis* strains.

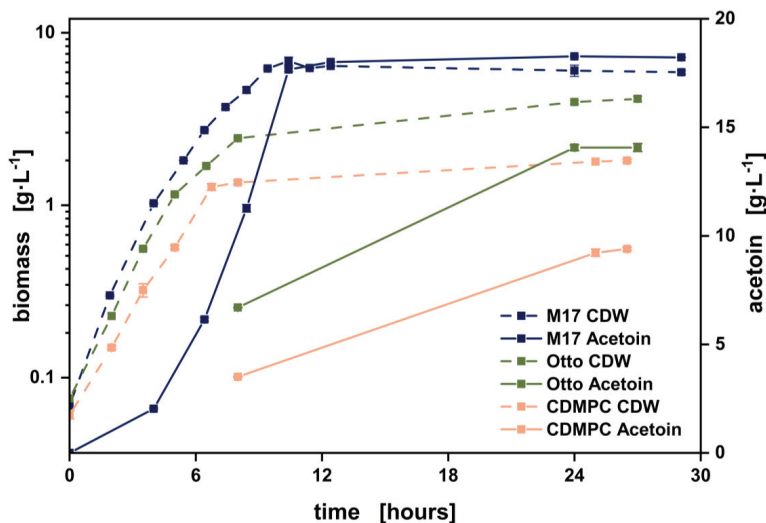


**Figure 25** Growth of *L. lactis* VJ017 and acetoin formation with different media. The applied media were the complex M17 medium, a chemically defined medium (CDM) by Otto *et al.*<sup>332</sup>, and a chemically defined medium for prolonged cultivation (CDMPC) by Price *et al.*<sup>333</sup> The different media for the cultivation of *L. lactis* VJ017 were tested in triplicates in shake flask with 40 g·L<sup>-1</sup> of glucose. The data associated with this figure was obtained from Fabian Speen's Master Thesis under supervision by Carolin Grütering.<sup>331</sup> The figure was previously published<sup>329</sup> and is reprinted with permission of Green Chemistry.

Second, a chemically defined medium (CDM) for *L. lactis* with additional amino acids was tested and is referred to as Otto medium.<sup>332</sup> The third medium is a CDM for prolonged cultivation, referred to as CDMPC.<sup>333</sup> The media compositions are shown in Appendix Table A 3 and Table A 4. The highest concentrations of acetoin and cells were achieved with the complex M17 medium (**Table 12**). Here, 18.3 g·L<sup>-1</sup> of acetoin was produced at 90% of the theoretical maximum yield. This is higher than the yield of 0.42 g<sub>acetoin</sub>·g<sub>glucose</sub><sup>-1</sup> that was obtained by Kandasamy *et al.* from the same amount of glucose, probably due to previously improved cultivation conditions regarding oxygen transfer (Appendix Table A 10). At higher oxygen transfer rates, the NADH oxidase NoxE can most likely regenerate NAD<sup>+</sup> more efficiently, which in turn can alleviate the bottleneck of limited NAD<sup>+</sup> availability.<sup>116, 334</sup> Using the CDMPC medium, cell division was almost in the range of the M17 media, however, the final product concentration was as low as 9.4 g·L<sup>-1</sup>, so only at 51% of the acetoin concentration that was achieved using the M17 medium. The Otto medium resulted in the lowest cell concentration of 4.1 g·L<sup>-1</sup>, while acetoin production was similar to the CDMPC medium. Notably, glucose was not consumed completely within the assessed 24 hours using the two CDM. Accordingly, acetoin and cell growth worked best in the complex M17 medium.

**Table 12** Acetoin and microbial biomass yield by *L. lactis* VJ017 in different media from 40 g·L<sup>-1</sup> of glucose. The bacteria were cultivated in shake flasks (500 mL, 25 mL filling volume, 30 °C, 300 rpm, 50 mm amplitude). The data associated with this table was obtained from Fabian Speen's Master Thesis under supervision by Carolin Grütering.<sup>331</sup> The table was previously published<sup>329</sup> and is reprinted with permission of Green Chemistry.

	Acetoin yield [g <sub>acetoin</sub> ·g <sub>glucose</sub> <sup>-1</sup> ]	Microbial biomass yield [g <sub>CDW</sub> ·g <sub>glucose</sub> <sup>-1</sup> ]
M17	0.46	0.17
Otto	0.35	0.10
CDMPC	0.24	0.05

These results emphasize that acetoin can be produced biotechnologically with good titers and yields. Since the CDMs tested did not support cell growth and acetoin formation to the extent the M17 medium did, the two CDMs were not considered for further evaluation. However, the complex M17 media is disadvantageous for the envisaged electrochemical conversion of acetoin to 2-butanone since it contains high amounts of complex, dissolved components such as meat extract and magnesium sulphate.

### Uncoupling growth and acetoin production by *L. lactis* VJ017

To produce acetoin in a medium with a reduced number of dissolved components, *L. lactis* VJ017 was incubated in a resting cell buffer with glucose as a carbon source (**Figure 26**). The biomass concentration remained constant, and acetoin was formed mainly in the first hours.

With 20 g·L<sup>-1</sup> of glucose, acetoin reached high yields of 0.48 g<sub>acetoin</sub>·g<sub>glucose</sub><sup>-1</sup> with 22 mM phosphate buffer and 0.49 g<sub>acetoin</sub>·g<sub>glucose</sub><sup>-1</sup> with 44 mM phosphate buffer, corresponding to 94% and 96% of the theoretical maximum, respectively. Higher glucose concentrations were not fully supported by the buffer systems, resulting in incomplete consumption of glucose. Notably, the final pH of all cultivations was below 6.0, far from the optimum pH of *L. lactis*. However, the same amount of acetoin was produced, indicating that another, probably acidic product accumulated. Since the genes that are necessary for the formation of all side products are removed from the genome of the production host, it is likely that an intermediate of the central carbon metabolism such as pyruvate accumulated. This can cause the ceased acetoin production at high glucose concentrations and the pH drop. Accumulated intra- and extracellular pyruvate was shown to be toxic to *L. lactis*.<sup>335-337</sup> Indeed, pyruvate concentrations ranging from 0.27 g·L<sup>-1</sup> to 3.50 g·L<sup>-1</sup> were detected in the final samples of the resting cell assays. Integration of a plasmid with an additional F<sub>1</sub>-ATPase was shown to lead to a threefold increased glycolytic flux of resting cells, which can be used for an ongoing acetoin formation under these conditions in future projects.<sup>338</sup>

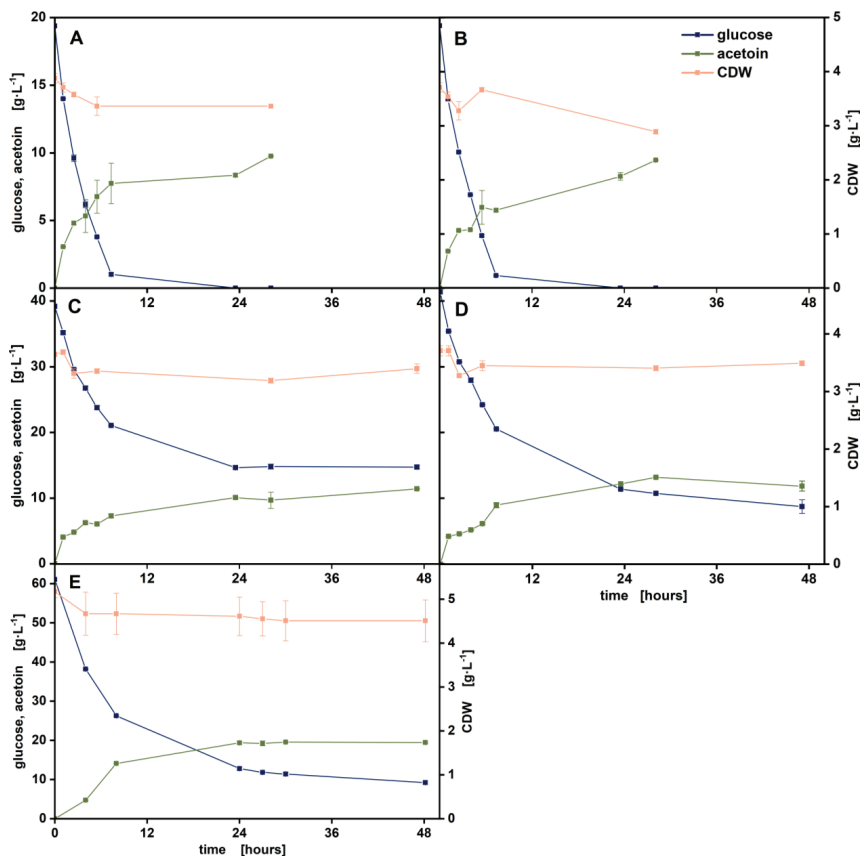


**Figure 26** Influence of the resting cell buffer composition on acetoin production by *L. lactis* VJ017. The resting cell buffer consisted of a phosphate buffer, a trace element solution, and glucose as a sole carbon source. The concentration of the trace elements was kept constant. (A) 22 mM phosphate buffer, 20  $\text{g}\cdot\text{L}^{-1}$  glucose; (B) 44 mM phosphate buffer, 20  $\text{g}\cdot\text{L}^{-1}$  glucose; (C) 22 mM phosphate buffer, 40  $\text{g}\cdot\text{L}^{-1}$  glucose; (D) 44 mM phosphate buffer, 40  $\text{g}\cdot\text{L}^{-1}$  glucose; (E) 66 mM phosphate buffer, 60  $\text{g}\cdot\text{L}^{-1}$  glucose. Final pH values C = 5.12; D = 5.45. Final pyruvate titers A = 0.27  $\text{g}\cdot\text{L}^{-1}$ ; B = 0.91  $\text{g}\cdot\text{L}^{-1}$ ; C = 1.24  $\text{g}\cdot\text{L}^{-1}$ ; D = 2.33  $\text{g}\cdot\text{L}^{-1}$ ; E = 3.50  $\text{g}\cdot\text{L}^{-1}$ . CDW = cell dry weight. The data associated with this figure was obtained from Fabian Speen's Master Thesis under supervision by Carolin Grütering.<sup>331</sup> The figure was previously published<sup>329</sup> and is reprinted with permission of Green Chemistry.

With a buffer concentration of 66 mM and an initial glucose concentration of 60  $\text{g}\cdot\text{L}^{-1}$ , 9.3  $\text{g}\cdot\text{L}^{-1}$  of glucose remained in the medium and 19.4  $\text{g}\cdot\text{L}^{-1}$  of acetoin was produced, corresponding to a yield on substrate of 0.38  $\text{g}_{\text{acetoin}}\cdot\text{g}_{\text{glucose}}^{-1}$ , a value that was lower than in previous attempts. Still, the high acetoin concentration was chosen for subsequent electrochemical conversion.

### Electrochemical conversion of acetoin to 2-butanone

Cell-free fermentation supernatants were used without any purification for the electrochemical conversion of acetoin to 2-butanone. As the different supernatants contained different amounts of acetoin, the applied current density and the duration of the experiments were adjusted (Appendix Table A 6). The resulting yields are displayed in **Figure 27** after the theoretical amount of charge necessary for a full conversion was passed through the electrode. The yield and Faraday Efficiency (FE) of the conversion in the different complex media (M17, HS, LB, and YEP) is comparable at 40 to 45% in most cases. Most likely, the hydrogen evolution reaction (HER) consumes most of the charge passed through the cathode, as shown in a previous study and also illustrated in a recent study that showed an increased HER with increased amount of trace metals.<sup>112, 118</sup> The yield of the conversion in M17 complex media at a low acetoin concentration is lower at 20%, likely due to the unfavorable ratio of acetoin and other medium components. The reproducible results in different complex media suggest that the overall amount of ions and organic substances hinder higher yields and facilitates HER (**Table 13**). This observation fits the results from the previous study.<sup>112</sup>

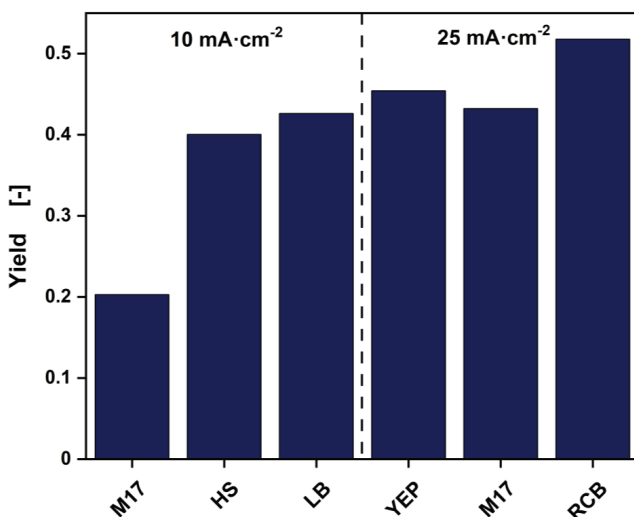


**Figure 27** Electrochemical conversion yields of the assessed supernatants. Four different complex media (M17, HS, LB, and YEP) were compared to the resting cell buffer (RCB). For the composition of the media, see **Table 13**. All media contained enantiopure acetoin produced from glucose produced by *L. lactis* VJ017. The data associated with this figure was obtained from Fabian Speen's Master Thesis.<sup>331</sup> The figure was originally created by Tobias Harhues with the data obtained in cooperation with Tobias Harhues and Fabian Speen, was previously published,<sup>329</sup> and is reprinted with permission of Green Chemistry.

**Table 13** Composition of the complex media for acetoin production with *L. lactis* VJ017. The table was previously published<sup>329</sup> and is reprinted with permission of Green Chemistry.

Medium	Component	Concentration [g·L <sup>-1</sup> ]
Hestrin Schramm (HS)	Peptone	5.0
	Yeast extract	5.0
	Sodium phosphate NaH <sub>2</sub> PO <sub>4</sub>	2.7
	Citric acid	1.2
	Glucose	20.0
Lysogeny broth (LB)	Yeast extract	5.0
	Tryptone	10.0
	Sodium chloride NaCl	10.0
	Glucose	20.0
Yeast extract peptone (YEP)	Peptone	5.0
	Yeast extract	10.0
	Sodium phosphate NaH <sub>2</sub> PO <sub>4</sub>	5.0
	Glucose	20.0
M17 broth	Ascorbic acid	0.5
	Lactose	5.0
	Magnesium sulphate	0.25
	Meat extract	5.0
	Meat peptone	2.5
	Sodium glycerophosphate	19.0
	Soya peptone	5.0
	Tryptone	2.5
	Yeast extract	2.5
	Glucose	60.0

In contrast, 2-butanone synthesis with the supernatant from the resting cells reaches a yield well above 50%, surpassing the yield from conversion in the different complex media. Additionally, the lower amount of dissolved components substantially reduced process-hindering foam formation during the electrolysis.

This increased yield is most likely due to two factors. Firstly, *L. lactis* VJ017 as a production host does not produce any process-hindering side products such as 2,3-butanediol, unlike the previously employed *Bacillus licheniformis*. Secondly, the resting cell buffer contained far less dissolved molecules compared to the Nakashimada medium that was used in the previous study. For example, the resting cell buffer did not contain any Na<sub>2</sub>SeO<sub>3</sub>, H<sub>3</sub>BO<sub>3</sub>, and AlK(SO<sub>4</sub>)<sub>2</sub>.<sup>112, 339</sup> The increasing yield indicates the adaptations benefit the subsequent electrochemical conversion. For the bio-based production of 2-butanone, a biocatalytic yield of 0.49 g<sub>acetoin</sub>·g<sub>glucose</sub><sup>-1</sup> and an electrochemical yield of 0.52 g<sub>2-butanone</sub>·g<sub>acetoin</sub><sup>-1</sup> result in an overall process yield



of  $0.25 \text{ g}_{2\text{-butanone}} \cdot \text{g}_{\text{glucose}}^{-1}$ . Regarding the evaluation of the economic competitiveness, we did not aim to translate achievable and achieved yields into prices due to highly volatile market prices.

However, an improved overall process yield and space-time yield might be obtained by applying a continuous reaction, like we recently discussed for model solutions.<sup>112</sup> Accordingly, continuous long-term reactions might benefit from a more robust and specific catalyst that could suppress the HER even in presence of low concentrations of metal ions in fermentation supernatants and thus favor the reduction of acetoin to 2-butanone. These investigations illustrate that experimental assessment of process chains under realistic conditions is necessary when determining the feasibility of integrated processes.<sup>340</sup>

### 3.3.4 Conclusion

Genetically modified *L. lactis* VJ017 is a suitable host for the production of acetoin since it can convert glucose with high efficiency and selectivity to the product. The product yield of  $0.46 \text{ g}_{\text{acetoin}} \cdot \text{g}_{\text{glucose}}^{-1}$  that was obtained in cultivations with an improved oxygen transfer is the highest acetoin yield from glucose so far.<sup>114</sup> Uncoupling growth and acetoin formation using a resting cell buffer for the latter allowed even higher yields of  $0.49 \text{ g}_{\text{acetoin}} \cdot \text{g}_{\text{glucose}}^{-1}$ , about 96% of the theoretical maximum. Using this dissolved components-reduced resting cell buffer for immediate electrochemical conversion of acetoin resulted in a 2-butanone yield well above 50%, higher than in previous attempts.<sup>112</sup> The suppression of the parasitic HER in the supernatant of the resting cell buffer compared to the different complex media leads to a higher FE and yield for 2-butanone and improves the electrochemical conversion.

Future investigations will aim for further improvement of the suggested cascade. For a continuous synthesis, a higher acetoin titer in the resting cell assay would be a prerequisite. This can be achieved by means of genetic engineering, e.g. by overexpression of an  $\alpha$ -acetolactate synthase and an  $\alpha$ -acetolactate decarboxylase. Subsequently, continuous purification of 2-butanone via stripping or extraction could increase 2-butanone yield. The additional process intensification of electrochemical reduction and product purification could counteract the overreduction observed in a previous study with higher acetoin titers and a longer duration of the reaction.<sup>112</sup>

In this work, we successfully developed an integrated process for the production of 2-butanone from sustainable carbon sources through interdisciplinary investigations, modifying the microbial process beyond its isolated figures of merit. Thereby, this strategy benefits the integrated process which can only be achieved by experimental work at the interface of the two disciplines, combining the advantages of bio- and electrocatalysis.

---

# Chapter 3.4

## Foundations of biotechnological methyl ketone production

### Contributions

Carolin Grütering designed all experiments. In the Chapter "Molecular engineering of thioesterases", Rebecca Breit performed the experiments under the supervision of Carolin Grütering. All other experiments were performed by Carolin Grütering.

This chapter was written by Carolin Grütering and reviewed by Lars M. Blank.

---



### 3.4 Foundations of biotechnological methyl ketone production

#### 3.4.1 Abstract

Methyl ketone production with tailored *Pseudomonas taiwanensis* VLB120 Δ6 pProd was shown to be feasible in high titers and yields. However, there are still several parameters that have to be investigated with greater detail for a comprehensive understanding of methyl ketone bioprocesses. In this chapter, we show that *in situ* gas stripping is feasible for the C<sub>11</sub> methyl ketone, of which 85% could be recovered. The longer chain length congeners could not be sufficiently enriched in the solvent trap using *in situ* gas stripping; accordingly, *in situ* extraction remains the recovery method of choice for the methyl ketone blend. In this context, the application of different thioesterases that can influence the hydrocarbon chain length was investigated. The applied changes in the metabolisms of methyl ketone formation led to a shift of the C<sub>11</sub> to C<sub>17</sub> production pattern towards the shorter congeners. The production of methyl ketones with a hydrocarbon chain length smaller than C<sub>11</sub> was not possible. Lastly, the growth temperature of the production host was evaluated, since this parameter can influence the last, non-enzymatic step of product formation, the decarboxylation of the β-keto acid to the corresponding methyl ketone. It was shown that 28 °C to 30 °C is the optimum temperature. These investigations show which parameters can still be adjusted to improve methyl ketone bioproduction.

#### 3.4.2 Introduction

To obtain a comprehensive, holistic understanding of biotechnological methyl ketone production and methyl ketone purification, more detailed investigations of certain aspects are necessary.

In terms of product purification, *in situ* product removal (ISPR) can benefit bioprocesses in various ways. Critical key performance indicators such as the product yield and the space-time yield can be improved, for example, by circumvention of product inhibition, a shift in the reaction equilibrium, or a generally reduced number of consecutive downstream processing steps.<sup>119, 120, 137</sup> For methyl ketones, *in situ* extraction by addition of a second, non-miscible organic solvent is often the ISPR method of choice.<sup>89, 97, 99, 241</sup> *In situ* extraction has the advantages mentioned above, however, the solvent can cause additional process costs. Moreover, recovery of the organic phase is often challenging due to detrimental emulsion formation.<sup>138</sup> An alternative ISPR method for volatile compounds is *in situ* gas stripping. Here, a gas stream in the bioreactor drags the volatile product out of the cultivation broth. In an ideal case, this is highly selective, simple, cheap, energy efficient, and does not harm the microorganism.<sup>341, 342</sup> However, gas stripping is only possible for volatile products that have a pronounced vapor pressure. Notably, the vapor pressure of the methyl ketones increases with a decrease in chain length, making gas stripping as an ISPR method especially attractive for the shorter chain length methyl ketones.<sup>343</sup>

In this context, thioesterases were found to be key enzymes that determine the hydrocarbon chain length of methyl ketones.<sup>78, 344</sup> Thioesterases catalyze, among

other reactions, the hydrolyzation of acyl-CoA or acyl-ACP thioesters in the fatty acid metabolism. The products of this reaction are free fatty acids and ACP or CoA coenzymes. Depending on their physiological role and the organism, thioesterases have different substrate spectra and thus produce fatty acids with different carbon chain lengths. For example, FadM is a cytosolic procaryote thioesterase with a wide substrate spectrum of C<sub>12</sub> to C<sub>18</sub>.<sup>345</sup> In contrast to that, eucaryotic *Cuphea palustris* thioesterase FatB1 (CpFatB1) is described to be highly specific for the production of shorter C<sub>8</sub> fatty acids.<sup>166, 346</sup> Due to its interconnection with the fatty acid metabolism, also methyl ketone production is affected by thioesterases (**Figure 28**). For example, when *Providencia sneebia* thioesterase FadM (PsFadM) and CpFatB1 are expressed in *E. coli*, methyl ketones with a chain length of C<sub>7</sub> to C<sub>11</sub> are produced.<sup>99</sup>

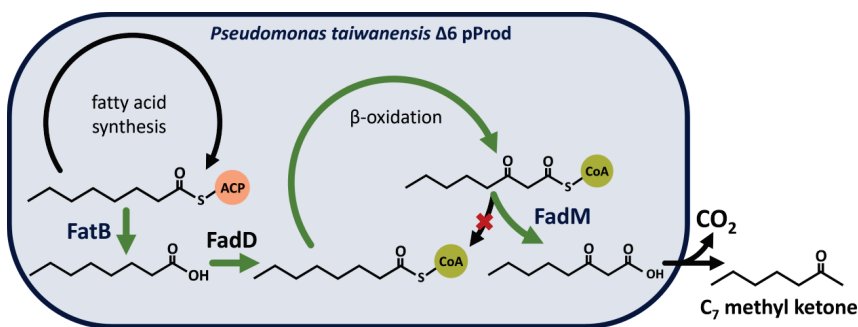


**Figure 28** Thioesterases involved in the metabolic pathway for methyl ketone production. The scheme shows the production of the C<sub>7</sub> methyl ketone 2-heptanone. FatB and FadM are shown as two exemplary thioesterases that can be the target of genetic engineering approaches. FadD = acyl-CoA synthetase, CoA = coenzyme A, ACP = acyl carrier protein.

Additionally, it was found that during methyl ketone production with genetically engineered *P. taiwanensis* VLB120 Δ6 pProd, there is a notable increase in the product concentration after depletion of the carbon source. For example, Nies *et al.* observed a 50% increase in methyl ketone concentration within approximately 6 hours after the total glucose was consumed in batch shake flask cultivations.<sup>97</sup> In contrast to that, this phenomenon was not observed when other strains such as *Escherichia coli* were applied as the genetically engineered microbial cell factory for methyl ketone production.<sup>89, 99</sup> There are two main theories that can explain this observation. First, the final reaction of methyl ketone production is the spontaneous decarboxylation of the corresponding β-keto acid. For example, the removal of one CO<sub>2</sub> from the C<sub>16</sub> β-keto acid leads to formation of the C<sub>15</sub> methyl ketone 2-pentadecanone. This step is not catalyzed by an enzyme.<sup>89</sup> If this reaction proceeds more slowly than the preceding enzymatic conversions, it becomes the rate limiting step that can still occur

after carbon source depletion. Accordingly, accumulation of the  $\beta$ -keto acid can cause the delayed formation of methyl ketones. Secondly, it is possible that some storage compounds such as the polyhydroxyalkanoates (PHAs) commonly found in *Pseudomonas* spp. serve as a carbon reservoir for methyl ketone production.<sup>347, 348</sup> Transmission electron microscopy is a method to evaluate the two options, since storage molecules such as PHAs get visible.

This being said, also the cultivation temperature can play a role in methyl ketone production. It was shown that the methyl ketone titer can be increased when the cultivation broth is heated to 70 °C after cultivation.<sup>97</sup> Therefore, increasing the temperature during the cultivation of *P. taiwanensis* VLB120  $\Delta 6$  pProd could be beneficial for methyl ketone production, provided that the viability of the cells does not decrease.

In this chapter, *in situ* gas stripping of methyl ketones was explored to evaluate alternative and potentially advantageous ISPR methods for the product recovery. In addition, the genes coding for alternative thioesterases were incorporated into the methyl ketone production plasmids to potentially increase the product spectrum of the methyl ketones in terms of chain length. The resulting hydrocarbon chain length distribution was investigated. Lastly, the optimum growth temperature of *P. taiwanensis* VLB120  $\Delta 6$  pProd was evaluated to assess the potential of an increased cultivation temperature for faster decarboxylation of  $\beta$ -keto acids to methyl ketone, and TEM images revealed the physiology of the production host.

### 3.4.3 Results and Discussion

#### Gas stripping for *in situ* product removal of methyl ketones

As an alternative to *in situ* extraction for methyl ketone purification, *in situ* gas stripping was implemented in bioreactors (**Figure 29A**). After 47 hours, 17 mg of methyl ketones were detected in the cultivation broth and 25 mg in the solvent trap through which the exhaust air was channeled. While the methyl ketone content in the solvent trap increased steadily, the maximum methyl ketone content in the cultivation broth of 26 mg was achieved after 29 hours. With a total amount of 3.0 g added glucose, this results in a product yield of  $0.014 \text{ g}_{\text{methyl ketones}} \cdot \text{g}_{\text{glucose}}^{-1}$ . Since no organic solvent was added to the bioreactor, biomass concentrations could be determined in this experiment. The maximum CDW of this cultivation was  $5.9 \text{ g} \cdot \text{L}^{-1}$ , resulting in a biomass yield of  $0.39 \text{ g}_{\text{CDW}} \cdot \text{g}_{\text{glucose}}^{-1}$ . This is a valuable insight, since methyl ketone formation with ISPR and biomass quantification cannot be performed simultaneously when *in situ* extraction is applied.

The congener distribution after 47 hours showed that in the cultivation broth, mainly 2-tridecanone and 2-tridecenone, the  $\text{C}_{13}$  congeners, were present (**Figure 29B**). In the solvent trap, the main detected congener was 2-undecanone, the  $\text{C}_{11}$  methyl ketone, which accounted for 76% of the total measured methyl ketones.

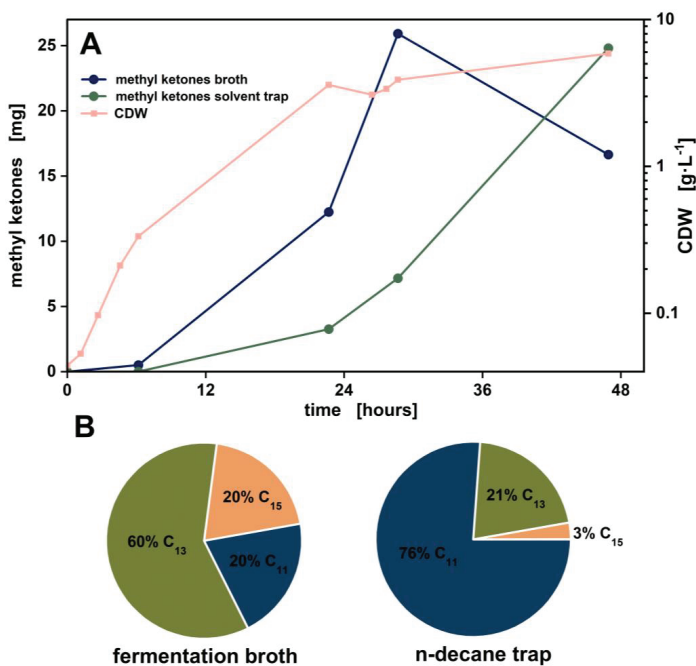


**Figure 29** Growth, methyl ketone production, and congener distribution of a bioreactor cultivation with *in situ* gas stripping. (A) Methyl ketone production was performed in 0.2 L MSM with 10 g·L<sup>-1</sup> glucose. The off gas was run through a solvent trap with 0.05 L of n-decane with a flow rate of 0.5 L·min<sup>-1</sup>, resulting in an aeration rate of 2.5 vvm. After 27 hours, 2 mL of a 500 g·L<sup>-1</sup> glucose solution was added. Methyl ketones broth refers to the absolute amount of product in the aqueous cultivation broth, while methyl ketones solvent trap refers to the absolute amount of product in the solvent trap. (B) Relative distribution of the C<sub>11</sub>, C<sub>13</sub>, and C<sub>15</sub> methyl ketones in the solvent trap after 47 hours. MSM = mineral salt media; vvm = volume air per volume aqueous phase per minute.

This translates to an 85% recovery of the C<sub>11</sub> methyl ketone in the solvent trap, while only 17% of the total C<sub>15</sub> methyl ketones could be captured in the solvent. The longer the hydrocarbon chain of the methyl ketone, the less it can be recovered by *in situ* gas stripping.

If applicable to the corresponding bioprocess, *in situ* gas stripping can be advantageous over *in situ* extraction as an ISPR method. For example, for acetone-butanol-ethanol (ABE) fermentation, gas stripping is the recovery method of choice.<sup>341, 342</sup> Also methyl ketones are in theory volatile organic compounds with a boiling point of 230 °C to 290 °C, so that gas stripping could be used as a recovery method.<sup>170</sup> In this attempt, for a mixture of C<sub>11</sub> to C<sub>17</sub> methyl ketones however, *in situ* gas stripping resulted in a 86% decreased product yield compared to *in situ* extraction. Still, it should be noted that gas stripping worked best for the C<sub>11</sub> methyl ketone, of which 85% could

be captured in the solvent trap. For an envisaged production of shorter chain length methyl ketone with hydrocarbon chain length equal to or shorter than  $C_{11}$ , *in situ* gas stripping can be a suitable product recovery method since the shorter chain methyl ketones have higher vapor pressures.

### Molecular engineering of thioesterases

Thioesterases were shown to be the key enzymes regarding the hydrocarbon chain length of methyl ketones. Two types of thioesterases are necessary for methyl ketone formation, namely an acyl-CoA thioesterase such as FadM or PsFadM, and an acyl-ACP thioesterase, such as 'tesA or CpFatB1. In *E. coli*, utilization of PsFadM and CpFatB1 as the thioesterases resulted in a methyl ketone congener distribution of  $C_7$  to  $C_{11}$ .<sup>99</sup> In this work, incorporation of the *PsFadM* gene into the methyl ketone production plasmid of *P. taiwanensis* VLB120 Δ6 pProd via Gibson assembly was validated by Sanger sequencing. Cultivations with the newly generated methyl ketone production host carrying the thioesterases PsFadM and 'tesA (Δ6 pCG1pSN2, **Table 14**) was possible.

**Table 14** Thioesterases and respective substrate specificities and origins used in this study. ACP = acyl carrier protein; CoA = coenzyme A.

Production host	Thioesterases	Substrate specificity	Origin
<i>P. taiwanensis</i> Δ6 pProd	'tesA	$C_{12}$ - $C_{16}$ acyl-ACPs <sup>345</sup>	<i>E. coli</i>
	FadM	$C_{12}$ - $C_{18}$ acyl-CoAs <sup>99</sup>	<i>E. coli</i>
<i>P. taiwanensis</i> Δ6 pCG1pSN2	'tesA	$C_{12}$ - $C_{16}$ acyl-ACPs <sup>345</sup>	<i>E. coli</i>
	PsFadM	$C_8$ - $C_{12}$ acyl-CoAs <sup>99</sup>	<i>C. palustris</i>

The standard methyl ketone production host Δ6 pProd (thioesterases 'tesA and FadM) produced  $0.20 \text{ g} \cdot \text{L}^{-1}$  of methyl ketones in the solvent phase from  $2 \text{ g} \cdot \text{L}^{-1}$  of glucose (**Figure 30A**). The newly generated production host Δ6 pCG1pSN2 (thioesterases 'tesA and PsFadM) produced  $0.14 \text{ g} \cdot \text{L}^{-1}$  methyl ketones under the same conditions. Regarding all methyl ketone congeners except for the saturated  $C_{11}$  and  $C_{15}$ , Δ6 pProd produced more than Δ6 pCG1pSN2. The relative distribution (**Figure 30B**) of the congeners showed that Δ6 pProd produced almost even percentages of  $C_{11}$ ,  $C_{13}$ ,  $C_{13:1}$ , and  $C_{15:1}$ , with  $C_{13}$  being the main congener. Δ6 pCG1pSN2 produced mainly the shorter chain length methyl ketones, namely 2-undecanone and 2-tridecanone ( $C_{11}$  and  $C_{13:1}$ ).

The standard methyl ketone production host Δ6 pProd harbours the two thioesterases FadM and 'tesA, which are characterized for a substrate specificity to  $C_{12}$  to  $C_{18}$ . Expression of these thioesterases results in methyl ketones ranging from  $C_{11}$  to  $C_{17}$ . The newly incorporated thioesterase PsFadM that was applied as a substitute to FadM is described to have a substrate specificity of  $C_8$  to  $C_{12}$ .<sup>99</sup>



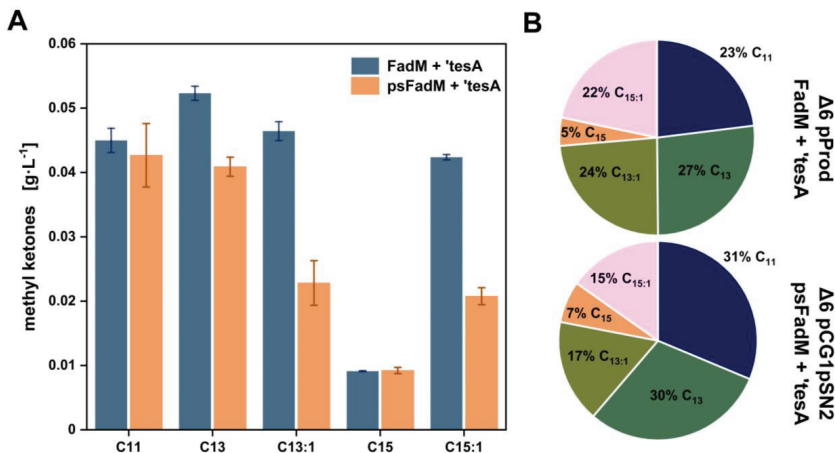


**Figure 30** Methyl ketone congener distribution that resulted from different thioesterase combinations. Absolute (A) and relative (B) results are shown after 48 hours. Two strains are being compared (1) *P. taiwanensis* VLB120 Δ6 pProd, harboring the genes of the two thioesterases FadM and 'tesA, and (2) *P. taiwanensis* VLB120 Δ6 pCG1pSN2. The methyl ketones were divided in saturated (C<sub>11</sub>, C<sub>13</sub>, and C<sub>15</sub>) and monounsaturated (C<sub>13:1</sub> and C<sub>15:1</sub>) methyl ketone congeners of different chain lengths. Cells were cultivated with 2 mM IPTG and 1 mM arabinose in 15 mL test tubes containing 1 mL MSM with 2 g·L<sup>-1</sup> glucose and 0.5 mL n-decane for methyl ketone extraction. MSM = mineral salt media; IPTG = isopropyl β-D-1-thiogalactopyranoside. The data associated with this figure was obtained from Rebecca Breit's Master Thesis under supervision by Carolin Grütering.<sup>165</sup>

The combination of PsFadM with 'tesA (strain Δ6 pCG1pSN2) resulted in methyl ketone production with the same chain length as Δ6 pProd, C<sub>11</sub> to C<sub>17</sub>. The concentration of methyl ketones was generally reduced as compared to the original production host, probably because PsFadM has a lower activity than FadM. However, a shift towards the production of C<sub>11</sub> was observed with Δ6 pCG1pSN2, suggesting that the thioesterase PsFadM favors the shorter chain lengths. Additionally, in decreased share of the monounsaturated methyl ketones with a double bond position at the ω-7 position was observed with PsFadM.<sup>162</sup>

Still, combining PsFadM with 'tesA in the newly generated variant Δ6 pCG1pSN2 did not result in production of C<sub>7</sub> and C<sub>9</sub> methyl ketones. Both Δ6 pProd and Δ6 pCG1pSN2 have a completely disrupted β-oxidation due to deletion of all FadA homologs. Consequently, the first thioesterase that is involved in the methyl ketone metabolism, namely the acyl-ACP thioesterase, e.g. CpFatB1 and 'tesA, determines the chain length of methyl ketones. An integration of CpFatB1 was not possible in this work, because all clones showed mutations in the nucleotide sequences that are necessary for the expression of a functional CpFatB1. There could be two possible reasons for this. First, intracellular short-chain fatty acids, mainly the C<sub>8</sub> and the C<sub>10</sub> congeners, are the products of the thioesterase CpFatB1.<sup>166</sup> These molecules are reported to be

toxic to microorganisms.<sup>349-351</sup> This toxicity can have generated a selection pressure against the expression of a functional CpFatB1. Second, CpFatB1 drains intermediates out of the fatty acid metabolism, instead of end products like 'tesA. Accordingly, the intermediates of fatty acid biosynthesis are not available for essential cellular functions such as the assembly of membrane lipids.<sup>352, 353</sup> For the formation of the C<sub>7</sub> and C<sub>9</sub> methyl ketones, expression of an acyl-ACP thioesterase with a substrate specificity towards the C<sub>8</sub> and C<sub>10</sub> acyl-ACPs is still necessary.

### Optimum growth temperature of *Pseudomonas taiwanensis* VLB120

An increased temperature of the cultivation broth with *P. taiwanensis* VLB120  $\Delta 6$  pProd was shown to result in an increased methyl ketone formation.<sup>97</sup> Accordingly, the growth rate of *P. taiwanensis* VLB120  $\Delta 6$  pProd was assessed at 46 individual temperatures within a range from 22.6 °C to 44.0 °C (**Figure 31**).

The course of the data points shows an increase of growth rates until a temperature of approximately 28 °C to 30 °C, followed by a rapid decrease in growth rates at temperatures exceeding 30 °C. The highest growth rate of 0.42 h<sup>-1</sup> was observed at a temperature of 28.0 °C. The lowest tested temperature of 22.6 °C resulted in a growth rate of 0.33 h<sup>-1</sup>. The highest temperature that still resulted in growth was 38.2 °C with a growth rate of 0.03 h<sup>-1</sup>. At temperatures higher than 38.2 °C, no growth was observed under these conditions. The overall curve shape resembles the course of an enzyme activity and thus microbial viability at different temperatures.

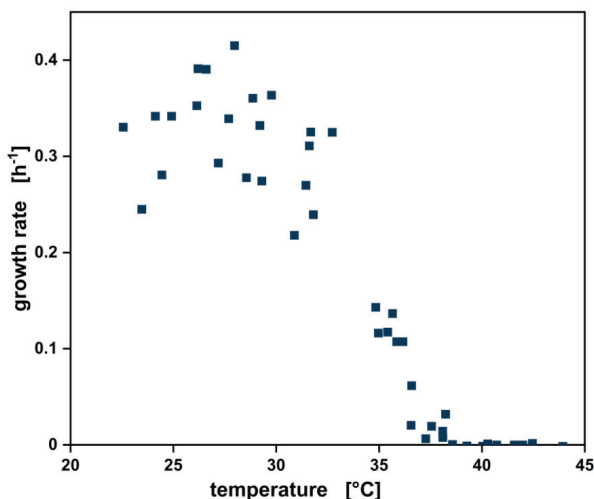


**Figure 31** Growth rate of *P. taiwanensis* VLB120  $\Delta 6$  pProd over a temperature range from 22.6 °C to 44.0 °C. The growth rate was calculated as the slope of the linear equation of the natural logarithm of the adsorption at 600 nm in the period from 5 hours to 10 hours after induction. 48 well flower plate, 620 nm, 800  $\mu$ L, MSM 10 g·L<sup>-1</sup> of glucose, 1,400 rpm, 3 mm shaking diameter. MSM = mineral salt media. The data associated with this figure was obtained in cooperation with David Wollborn.

Initially, there is an increased reaction rate with increasing temperatures, which causes an increase in enzyme or cell viability. After reaching the optimum temperature that is characteristic for a certain biocatalyst, there is a strong decline in activity due to protein denaturation.<sup>354</sup>

It was reported that many microorganisms of various phyla are cultivated at temperatures of 30 °C or 37 °C. However, this might not be the optimum growth temperature but rather a temperature that was chosen out of convenience, since those are the standard settings of shakers in laboratories.<sup>355</sup> Previously, for *P. taiwanensis* VLB120, an optimum growth temperature of 30 to 37 °C was described.<sup>280</sup> Here, this broader range was narrowed to a temperature optimum of 28 °C to 30 °C. Accordingly, for *P. taiwanensis* VLB120, the preferred cultivation temperature of 30 °C seems to be suitable to promote optimum growth. Therefore, at the current state of methyl ketone production, it is not recommended to use higher temperatures for a fastened decarboxylation of  $\beta$ -keto acids to the corresponding methyl ketones.

Lastly, transmission electron microscopy (TEM) images were generated to unravel the physiology of the methyl ketone production host. Micrographs during the stationary growth phase of the *P. taiwanensis* VLB120 wild type and the *P. taiwanensis* VLB120  $\Delta 6$  pProd methyl ketone production host were compared (Figure A 7). The stationary phase was chosen for this comparison since most of the methyl ketones are formed after glucose depletion. There was no difference in the cell membrane or the size of the periplasmic space, indicating that methyl ketone formation has no visible impact on the membrane, e.g. in terms of size, composition, or structure. However, the wild type had white granules with a size of approximately 60 nm. Presumably, those were PHA granules for carbon storage during the stationary phase, as they were observed for various *Pseudomonas* species.<sup>347, 356-358</sup> The *P. taiwanensis* VLB120  $\Delta 6$  pProd variant has a deletion of the *pha* operon with the polyhydroxyalkanoate synthase genes *phaC1* and *phaC1* and did not exhibit these granules. Therefore, it is unlikely that common carbon storage molecules as PHAs are responsible for the formation of methyl ketones during the stationary phase. Instead, it is more likely that one of the reactions of the beta oxidation is the bottleneck. As described earlier in this chapter, e.g. the decarboxylation of the  $\beta$ -keto acids to the methyl ketones can be the rate limiting step.

### 3.4.4 Conclusion

This investigation of the foundations of methyl ketone production with genetically engineered *P. taiwanensis* VLB120 showed that there are several opportunities to further improve and diversify this approach in terms of e.g. product recovery and product range. Regarding ISPR, gas stripping was shown to be possible for 2-undecanone, the C<sub>11</sub> congener of methyl ketones, of which 85% of the total amount could be captured in a solvent trap. The higher chain length methyl ketones have a lower vapor pressure and are thus less prone to gas stripping. In case that the production of methyl ketones with a hydrocarbon chain length equal or lower than C<sub>11</sub>

is aimed for, gas stripping can be a convenient ISPR method. It is likely that the C<sub>7</sub> and C<sub>9</sub> methyl ketone can be recovered at even higher shares by gas stripping due to their higher vapor pressure. *In situ* gas stripping does not require the addition of an organic solvent, as it is necessary for *in situ* extraction. Accordingly, there is no detrimental emulsion formation and no interference with the microorganisms, while still being a specific and easy ISPR method. In order to produce shorter chain length methyl ketones, functional expression of an active acyl-ACP thioesterase with a substrate specificity to shorter chain length such as CpFatB1 is still necessary. Here, e.g. the application of promoters with different expression strengths can balance the burden of expressing an enzyme that produces the potentially harmful medium-chain length free fatty acids.<sup>359, 360</sup> Additionally, FadD, the acyl-CoA synthetase, can be a target for future investigations. In *E. coli*, heterologous expression of a *Mycobacterium tuberculosis* FadD variant was shown to be necessary to direct the flux towards the shorter chain methyl ketones.<sup>166, 346</sup> In the future, a mix-and-match approach for the thioesterases is conceivable, with which the congener distribution and chain length of the methyl ketones can be adapted to a specific application.

The optimum growth temperature of the production host was revealed to be 30 °C. At higher temperatures, viability of the microorganisms rapidly decreases. If higher cultivation temperatures for an improved conversion of  $\beta$ -keto acids to methyl ketones are aimed for, adaptive laboratory evolution is an option to adapt the production host to these conditions. Adaptive laboratory evolution was shown to be a powerful tool to enhance the tolerance to harmful growth conditions for various applications.<sup>361, 362</sup> Under the current conditions however, methyl ketone production with *P. taiwanensis* VLB120  $\Delta$ 6 pProd should be performed at 30 °C. Still, the TEM images reveal that the production host does not form intracellular PHAs that could serve as a storage molecule. Therefore, it is likely that another intermediate of the fatty acid metabolism, such as the  $\beta$ -keto acids, is the reason why methyl ketone production proceeds after carbon source depletion. This is why an increased cultivation temperature could lead to improved performance indicators such as product yield and production rate.



---

# Chapter 4

## General Discussion and Outlook

### Contributions

This chapter was written by Carolin Grütering and reviewed by Lars M. Blank.

---



## 4 General Discussion and Outlook

### 4.1 Fuel and bulk chemical production in integrated bioreactors

It is inevitable that we need sustainable drop-in diesel fuel replacements, and it is inevitable that those need to be produced using straightforward, cost-efficient processes. Various molecules, including the methyl ketones, were shown to have suitable predicted cetane numbers. This work demonstrates that regarding methyl ketones, also all other important parameters, such as the lubricity, viscosity, and toxicology, are as good as or even better than the currently used diesel fuels. Additionally, as opposed to other molecules that are discussed as diesel fuel replacements, methyl ketones can be produced from renewables using microorganisms within the context of a circular bioeconomy.

*In situ* extraction itself is already a promising concept for such an endeavor. By performing *in situ* extraction in the multiphase loop reactor, the advantages of this recovery method were even more pronounced. For other extractive fermentations in conventional STRs, e.g. centrifugation is required to separate the organic solvent from the cultivation broth. While centrifugation seems undemanding in a laboratory scale, it gets costly and technically challenging during scale-up, especially for the envisaged application of the methyl ketones as bulk chemicals or fuels. Consequently, the *in situ* extraction with a solvent that is compatible with the final product mixture, 2-undecanone, and phase separation by settling, solves several challenges at once. Notably, comparing the methyl ketone production in the MPLR to STRs, the MPLR resulted in similar product yields and productivities until glucose depletion (MPLR:  $44 \text{ mg}_{\text{methyl ketones}} \cdot \text{g}_{\text{glucose}}^{-1}$ ,  $44 \text{ mg}_{\text{methyl ketones}} \cdot \text{L}_{\text{aq}}^{-1} \cdot \text{h}^{-1}$ ; STR:  $50 \text{ mg}_{\text{methyl ketones}} \cdot \text{g}_{\text{glucose}}^{-1}$ ,  $49 \text{ mg}_{\text{methyl ketones}} \cdot \text{L}_{\text{aq}}^{-1} \cdot \text{h}^{-1}$ ). There seem to be no negative effects of the MPLR, e.g. by the reduced oxygen concentration in the downcomer, on the product formation.

The overall attempt of producing methyl ketones in the MPLR has shown the potential of *in situ* product extraction and solvent screenings. However, key performance indicators (KPIs) such as the product yield, titer, and productivities were not in the range where biotechnological production can compete with petrochemical production. A fast conversion of the raw material to high concentrations of the product of interest without substantial carbon losses is essential to develop a successful bioprocess. Especially for the envisaged application of methyl ketones as a large-scale biofuel, those KPIs have to be further improved to allow for an economically feasible sustainable bioprocess.<sup>363, 364</sup> For example, the already commercialized biofuel bioethanol (global production of 140 billion liters in 2022) is being produced at product yields of approximately  $0.400 \text{ g}_{\text{ethanol}} \cdot \text{g}_{\text{substrate}}^{-1}$ , which is far from the maximum methyl ketone yield in this work, namely  $0.154 \text{ g}_{\text{methyl ketones}} \cdot \text{g}_{\text{substrate}}^{-1}$ .<sup>365, 366</sup> Several options to improve the bioprocess for methyl ketone production further are illustrated below.

Batch, fed-batch, and continuous mode are the three basic types of operation modes of bioreactors. The batch mode was successfully implemented in the MPLR,



showcasing the general high potential of this bioreactor setup. Performing a fed-batch cultivation in the MPLR would be a great challenge, since the filling volume is not constant in this mode. Consequently, the position of the coalescing unit and the solvent withdrawal would constantly have to be adapted to the liquid level, which is technically extremely challenging. When run in continuous mode however, the MPLR has the potential for an outstanding performance, combining the advantages of ISPR, phase separation by settling, and continuous fermentations.

In continuous mode in general, the flow rate of the aqueous phase in the reactor  $F_{in}$  equals the flow rate out of the reactor  $F_{out}$  (eqn (10)). For a constant volume  $V_{aq}$ , this leads to a steady state, with constant concentrations of biomass, substrate, and product, and a direct relation of the dilution rate  $D$  with the specific growth rate  $\mu_x$  (eqn (11)).

$$F_{in} = F_{out} = F \quad (10)$$

$$\frac{F}{V_{aq}} = D = \mu_x \quad (11)$$

Accordingly, the physiological parameter  $\mu_x$  can, within certain limits, directly be influenced by the operational parameter  $D$ , and the concentrations of the substrate and product can be adjusted to specific optimum values. This can in turn generally maximize the efficiency of the bioprocess, especially in cases of product toxicity or substrate inhibition.<sup>354</sup> For the MPLR, this translates to not only continuously feeding the aqueous phase to and harvesting the cultivation broth from the bioreactor, but also recirculating the organic phase continuously from the coalescer to the solvent disperser. A common drawback of continuous fermentations, the ease of contaminations, can be prevented by using a solvent that is at the lower range of the tolerated log  $P$  values, but is not hindering the production host, like shown for 2-undecanone with *Pseudomonas taiwanensis* VLB120  $\Delta 6$  pProd. This also holds the potential for the bioprocess to produce its own solvent. In continuous mode, the organic phase is enriched more and more with the methyl ketones, until the point when the organic phase has the same constitution as the product congener ratio produced by the microorganism.

For an improved product yield, further genetic engineering can be performed with the production host, that aims for a more efficient carbon flux towards the product. For example, an improved balancing of the promoters, or the knockout of further competing reactions, can be beneficial for this attempt.<sup>360</sup> In this context, also the extension of the methyl ketone product portfolio produced by *P. taiwanensis* VLB120 can be tackled. As shown in Chapter 3.4, expression of a *fadD* variant with a high specificity towards  $C_8$  to  $C_{12}$  fatty acids should, in combination with *PsFadM* and *CpFatB1*, lead also to formation of 2-heptanone and 2-nonanone.<sup>99</sup>

Also, the overall meaningfulness of biotechnological production of methyl ketones as a fuel has to be proven. Here, life cycle analysis (LCA), life cycle costing (LCC), and

techno-economic assessment (TEA) are tools to be applied. These can be used to identify the levers that have the greatest impact on the overall economic and ecologic feasibility, taking the physical limits of the bioprocess into account. Like described in Chapter 1.1, the bio-based production of a good does not necessarily imply its sustainability.

Regarding the analysis of the whole value chain for methyl ketones, product and solvent losses due to emulsification should be strictly avoided. Droplet coalescence is currently achieved in an unstructured stainless-steel mesh. This coalescing unit can be adapted and improved to aid stable, reproducible phase separation, also under more challenging conditions with e.g. higher biomass concentrations.<sup>367</sup> Additionally, the current bioreactor vessel has an absolute volume of 5 L. This was useful to generate a successful “proof-of-principle”, however, the fluid dynamics and emulsification behavior have to be tested in larger scales, from 100 L up to m<sup>3</sup>. In these scales that are closer to industrial applications, different challenges can be studied. For example, the residence time in the non-aerated downcomer compartment for liquid-liquid extraction is prolonged at a larger scale, and the flocculation and coalescence effects in the coalescing compartment can differ.

The general concept of the MPLR can also be a solution for other bioprocesses that struggle from e.g. product toxicity or emulsification. The production of biosurfactants, namely rhamnolipids, was shown to be possible in the MPLR with genetically modified *Pseudomonas putida* KT2440.<sup>145</sup> This strain is similarly robust towards stress conditions as *P. taiwanensis* VLB120.<sup>105</sup> However, the applicability of the MPLR with other microbial cell factories, e.g. eucaryotes, and other products, has yet to be proven. The MPLR can be a powerful tool to produce toxic chemicals and fuels, since the product is directly separated from its producing cell.<sup>153</sup> Also bioprocess with biocatalysts that are sensitive to peaks in shear stress can benefit from this setup. Due to the omission of a stirrer, shear stress is reduced and homogeneously distributed in the MPLR compared to STRs.<sup>145, 368, 369</sup>

## 4.2 Co-feeding and application of hydrolysates

It was shown that replacing fossil fuels with biofuels has the potential to reduce GHG emissions by around 85%.<sup>60</sup> However, it is obvious that fuel production from edible, first generation feedstocks, as it is currently practiced, is not desirable. Less than 10% of the terrestrial biomass can be used for food purposes, while more than 90% consists out of lignocellulose.<sup>52</sup> It is therefore highly inefficient to utilize only the edible parts of plants in general, which ultimately leads to land shortage, biodiversity loss, and competition with food supply. In contrast, making the enormous amounts of carbon that is stored in the global non-edible lignocellulose accessible holds great potential for the generation of more sustainable processes.

To address the issue of a sustainable supply of carbon, efficient bioprocesses that utilize more sustainable, renewable substrates such as lignocellulosic biomass, CO<sub>2</sub>, and waste plastic, have to be developed, not only for the generation of fuels. For methyl

ketone production, ethanol was shown to be an excellent co-fed carbon source that enhances high product yields and titers and can be produced in syngas fermentations or in second-generation biorefineries.<sup>370</sup> The results of Chapter 3.2 show that by applying ethanol in a batch culture, high product yields of 25% of the theoretical maximum can be achieved, while the methyl ketone yield on glucose in batch cultures is in the range of 10% of the theoretical maximum. However, ethanol is a chemical that is toxic to microorganisms when it is applied in higher concentrations, as highlighted by the fact that it is commonly used as a disinfecting agent.<sup>371</sup> Accordingly, applying ethanol as a carbon source in batch mode might not be the best option for developing a bioprocess for methyl ketones from ethanol. Alternatively, feeding ethanol in a fed-batch approach can make the positive effects of ethanol even more pronounced. A primary batch phase on *e.g.* glucose would allow for a robust development of higher cell densities. Consecutively, feeding ethanol could allow for a high flux of this secondary carbon source to the methyl ketones.

Regarding the utilization of wheat straw hydrolysates, *P. taiwanensis* VLB120 Δ6 pProd was again showcased to be an outstanding production host to turn lignocellulosic biomass to value-added products. It is inherently robust towards hydrolysis-derived inhibitors such as phenolics and furans and utilizes xylose as a carbon source. For many other microorganisms, tremendous adaptations have to be performed regarding robustness and C<sub>5</sub> sugar utilization to enable the application of lignocellulosic hydrolysates.<sup>282, 372</sup> Still, combined bioprocessing of cellulosic and hemicellulosic hydrolysates has to be tested, and the conversion of xylose to methyl ketones can be improved, *e.g.* by implementation of the Dahms pathway. Also, the hydrolysates should be applied in the MPLR, that was currently only tested with minimal media. The complex composition of the hydrolysates might pose an additional challenge to *e.g.* phase separation during bioprocessing of methyl ketones in the MPLR.

Concerning the application of hydrolysates in bioprocesses in general, large-scale feasibility can only be achieved by conducting more research and generating more knowledge of the hydrolysis process. Lignocellulose is an extremely complex structure. More standardized methods, also for the generation of hydrolysates from varying feedstocks, have to be developed to render biorefinery approaches economically feasible. Another key challenge is to reduce the enzyme load during the hydrolysis, since the enzymes are a main contributor to the total cost of the hydrolysis.<sup>60, 373</sup>

### 4.3 Bio-based production of C<sub>4</sub> molecules

The biotechnological production of enantiopure (3*R*)-acetoin by resting cells was shown to be feasible in yields close to the theoretical, physically possible maximum. The electrochemical conversion of acetoin to 2-butanone was improved by adapting the process parameters not only to the biocatalysis, but also to the electrocatalysis. This again demonstrates the importance of holistic, interdisciplinary research to achieve a common goal. Herein, the next step is to develop further downstream

processing approaches for both acetoin and 2-butanone, depending on which molecule is the product of interest.

Acetoin has a high boiling point and is highly hydrophilic, making it difficult to separate from the aqueous fermentation broth by e.g. distillation or extraction. However, membrane pervaporation was shown to be possible.<sup>374</sup> In contrast to this, 2-butanone is more volatile and hydrophobic, and recovery of 2-butanone from the electrolyte can be accomplished by e.g. solvent extraction or gas stripping.<sup>112</sup> Also in terms of applicable recovery methods, electrochemical conversion of acetoin to 2-butanone in the fermentation broth seems to be meaningful, since the purification of the latter from the aqueous media is more straightforward.

#### **4.4 Concluding remarks**

Industrial biotechnology is considered to be a key technology to tackle environmental and climate challenges and to promote economic growth.<sup>375</sup> There has been much progress in recent years, such as the construction of several plants to produce ethanol by fermenting CO, CO<sub>2</sub>, and H<sub>2</sub> gases from steel mills by LanzaTech.<sup>376</sup>

However, much remains to be done to unleash the full potential of industrial biotechnology. This work depicts some technical approaches to tackle those hurdles. All problem-solving attempts have one thing in common: a strong focus on communication and interdisciplinarity. It will be a joined effort to establish a circular bioeconomy, and no discipline alone can provide all the answers. In addition to the necessary technology, public communication around the bioeconomy narrative needs to be improved. It has been shown that the term "bioeconomy" has a generally positive connotation among the public, while there is still a lack of understanding of what a bioeconomy actually is.<sup>377</sup> Public perception and comprehension of biotechnology with its emotive terms such as "genetically modified organisms" needs to change. This is why we need a better science communication, with a comprehensive vocabulary that clarifies the intention behind the scientific efforts. The implementation of model regions can help to demonstrate the true potential of the bioeconomy. In Germany for instance, the Rheinische Revier, Europe's largest lignite mining area, is supposed to be transformed into such a bioeconomy model region.<sup>378</sup> This can shine a light on the economical and ecological potential of bioeconomic concepts.

Ultimately, policymakers are called upon to discontinue fossils and stop the "unlimited economic growth" mindset. In December 2023, at the very time this thesis was written, the COP28 climate summit pledged to "transition away from fossil fuels" which gives hope that we are moving in the right direction; a direction where it will become easier to generate an economic advantage out of pursuing ecological goals.<sup>379</sup>

In the end, unlimited growth is not possible in a limited world.<sup>380</sup>



---

# Appendix

---



## Appendix

Table A 1 Composition of the stock solutions that were used for preparation of MSM. The phosphate buffer was applied in as a 50x stock in case that no pH regulation was possible, e.g. in shake flasks, MTPs, and tubes.<sup>164</sup> MSM = mineral salt media.

Name	Stock [L <sup>-1</sup> ]
<b>100x phosphate buffer</b>	
K <sub>2</sub> HPO <sub>4</sub>	388 g
NaH <sub>2</sub> PO <sub>4</sub>	163 g
<b>100x (NH<sub>4</sub>)<sub>2</sub>SO<sub>4</sub></b>	
(NH <sub>4</sub> ) <sub>2</sub> SO <sub>4</sub>	200 g
<b>100x mineral salts</b>	
EDTA	1000 mg
MgCl <sub>2</sub> · 6H <sub>2</sub> O	10 g
ZnSO <sub>4</sub> · 7H <sub>2</sub> O	200 mg
CaCl <sub>2</sub> · 2H <sub>2</sub> O	100 mg
FeSO <sub>4</sub> · 7H <sub>2</sub> O	500 mg
Na <sub>2</sub> MoO <sub>4</sub> · 2H <sub>2</sub> O	20 mg
CuSO <sub>4</sub> · 5H <sub>2</sub> O	20 mg
CoCl <sub>2</sub> · 6H <sub>2</sub> O	40 mg
MnCl <sub>2</sub> · 2H <sub>2</sub> O	100 mg
<b>Glucose stock solution</b>	
Glucose monohydrate	550 g



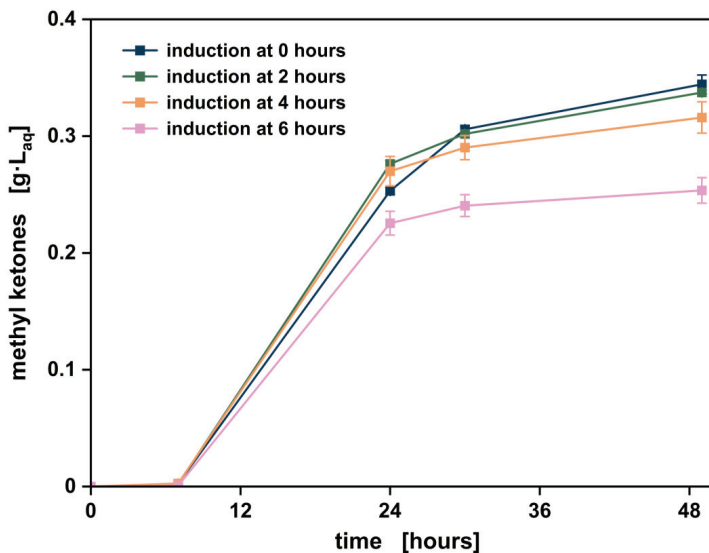


Figure A 1 Methyl ketone production by *P. taiwanensis* Δ6 pProd in shake flasks with different induction time points. 1 mM arabinose and 2 mM IPTG were added at inoculation (0 hours) and 2 hours, 4 hours, and 6 hours after inoculation. Cultivations were performed in 50 mL MSM with 10 g·L<sup>-1</sup> glucose and 12.5 mL n-decane for *in situ* extraction of methyl ketones. Values are shown as mean and deviation of biological duplicates. MSM = mineral salt media; IPTG = isopropyl β-D-1-thiogalactopyranoside.

Name	Density [g cm <sup>-3</sup> ]	Log P [-]	MP [°C]	Flash Point [°C]	CAS-No.	Formula	Molecular Weight [g mol <sup>-1</sup> ]
n-decane	0.73	5	-29.7	46	124-18-5	C10H22	142.3
Farnesol	0.88	4.8	25	155	4602-84-0	C15H26O	222.4
α-farnesene	0.84	6.1	25	103	502-61-4	C15H24	204.4
Limonene	0.85	3.4	-95	46	138-86-3	C10H16	136.2
Ethyl palmitate	0.86	7.8	24	110	628-97-7	C18H34O2	284.5
Ethyl myristate	0.86	6.7	12.3	113	124-06-1	C16H32O2	256.4
Ethyl octanoate	0.86	3.5	-43	79	106-32-1	C10H20O2	172.3
Ethyl hexanoate	0.87	2.4	-67	49	123-66-0	C8H16O2	144.2
Ethyl butyrate	0.88	1.3	-98	24	105-54-4	C6H12O2	116.2
Toluene	0.87	2.7	-94	4	108-88-3	C7H8	92.1
Ethyl benzene	0.87	3.1	-94	13	100-41-4	C8H10	106.2
1-phenylethanol	1.01	1.4	21	93	98-85-1	C8H10O	122.2
Butylbenzene	0.86	4.4	-87	71	104-51-8	C10H14	134.2
1,3 dioxolane	1.06	-0.4	-95	2	646-06-0	C3H6O2	74.1
2-Methyltetrahydrofuran	0.86	1	-136	-10	25265-68-3	C5H10O	86.1
Ethyl acetate	0.9	0.7	-83.6	7	141-78-6	C4H8O2	88.1
Hexyl acetate	0.88	2.4	-80.9	45	142-92-7	C8H16O2	144.2
Ethyl valerate	0.87	1.9	-91	39	539-82-2	C7H14O2	130.18
2-Octanone	0.82	2.4	-16	52	111-13-7	C8H16O	128.2
2-Nonanone	0.83	3.1	-15	64	821-55-6	C9H18O	142.2
2-Decanone	0.82	3.7	14	71	693-54-9	C10H20O	156.3
2-Undecanone	0.83	4.1	12	89	112-12-9	C11H22O	170.3
2-Dodecanone	0.83	4.6	21	110	6175-49-1	C12H24O	184.3
2-Tridecanone	0.82	5.2	30	107	593-98-8	C13H26O	198.3
2-Pentadecanone	0.81	6.3	39	113	2345-28-0	C15H30O	226.4
2-Heptadecanone	0.81	7.1	48	>110	2922-51-2	C17H34O	254.5
1-Heptadecanol	0.85	7.8	55	155	1464-85-9	C17H36O	256.5
Hexyl acetate	0.88	2.9	-50	68	112-96-1	C8H16O2	158.2
Octyl acetate	0.87	3.4	-38	86	112-14-1	C10H20O2	172.3
Dibutoxymethane	0.84	3.2	-58	43	2568-90-3	C9H20O2	160.3
Diethoxymethane	0.83	0.8	-66	-5	462-55-5	C5H12O2	104.2
4,5-oxadiazole	0.9	1.5	-	117	22507-10-9	C2H2N2O2	106.3
Dibutyl ether	0.77	3.2	-95	25	142-96-1	C8H18O	130.2
1-Decanol	0.83	4.6	7	108	112-30-1	C10H22O	158.3
Methyl decanoate	0.87	4.7	-18	110	110-42-9	C11H22O2	186.3
Methyl nonanoate	0.88	4.1	-35	86	731-84-6	C10H20O2	172.3
Methyl linoleate	0.89	6.9	-35	97	112-63-0	C19H34O2	294.5
Dibutyl sebacate	0.96	5.3	-10	178	109-43-3	C18H34O4	314.5
Tributyl citrate	1.04	2.7	-20	184	77-94-1	C18H32O7	360.4
Dibutyl phthalate	1.04	4.7	-35	157	84-74-2	C18H22O4	278.3
2-Butyl-1-octanol	0.83	4.8	-80	110	8913-02-8	C12H26O	186.3
2-Methyltetrahydrofuran	0.86	1	-136	-11	96-47-9	C5H10O	86.1
Chlorylene	0.81	7.6	21	154	112-80-3	C18H19N	267.5
1,4-Butanediol	1.02	-0.8	21	121	110-63-4	C4H10O2	90.1
Bis(2-ethylhexyl) phthalate	0.99	7.4	-55	215	117-81-7	C24H38O4	390.6
1,4-Diaminopentane	0.9	-0.5	9	57	591-77-5	C5H14N2	102.2
Methyl tert-butyl ether	0.74	0.9	-108	-33	1634-04-4	C5H12O	88.2
Undecanal	0.83	4.3	-2	105	112-44-7	C11H22O	170.3
Nonanal	0.83	3.3	-19	64	124-19-6	C9H18O	128.2
Octanal	0.82	2.7	12	56	124-13-0	C8H16O	142.2
Ethyl oleate	0.86	8	-32	113	111-42-6	C20H38O2	310.5
2-Ethylhexan-1-ol	0.83	3.1	-70	81	104-76-7	C8H18O	130.3
Tributyrin	1.03	2.4	-75	180	60-01-5	C15H26O6	302.4
Heptadecane	0.77	8.8	18	135	544-76-3	C16H34	226.4
n-octane	0.7	4.8	-56	13	111-55-9	C8H18	114.2
alpha pinene	0.86	2.8	-63	31	80-56-8	C10H16	136.2
3-Methoxy-3-methyl-1-butanol	0.93	0.4	-	71	56539-66-3	C6H14O2	118.2
Cetyl acetate	0.86	3.4	-88	86	112-14-1	C10H20O2	172.3
m-Xylene	0.86	3.2	-47	25	108-38-3	C8H10	106.16
2-Ethylhexyl acetate	0.87	3.2	-80	82	103-09-3	C10H20O2	172.3
2,5-Dimethylfuran	0.88	2.2	-63	1	625-96-5	C6H8O	96.1
Ethyl laurate	0.86	5.6	-10	145	106-33-2	C14H28O2	228.4
Cyclohexane	0.78	3.4	7	-18	110-82-7	C6H12	84.2
Cyclohexanol	0.95	1.2	25	63	108-93-0	C6H12O	100.2
Mesitylene	0.87	3.3	-44.7	50	108-47-8	C9H12	120.2
Di-n-butylether	0.77	3.2	-95	25	142-96-1	C8H18O	130.2
Di-n-pentylether	0.78	3.7	-69	57	693-65-2	C10H22O	158.3
Di-n-propylether	0.75	2	-122	-18	111-43-3	C6H14O	102.2
1-Dodecanol	0.83	5.1	24	127	112-53-8	C12H26O	186.3
1-Octene	0.72	4.6	102	10	111-46-0	C8H16	112.2
Nonane	0.72	5.7	-51	31	111-84-2	C9H20	128.3
Cyclooctane	0.83	4.5	15	28	292-84-8	C8H16	112.2
Cetyl octanoate	0.86	6.5	-18	110	2306-88-9	C18H34O2	256.4
Isopropyl myristate	0.85	7.2	3	164	110-27-0	C17H34O2	270.5
Isopropyl palmitate	0.85	8.2	13.5	110	142-91-6	C19H38O2	298.5
Hexyl hexanoate	0.86	4.9	-55	110	6378-65-0	C12H24O2	200.3
Hexyl octanoate	0.86	5.3	-51	110	11173-55-1	C14H28O2	228.4
Methyl octanoate	0.88	3.6	-37	82	111-11-5	C9H18O2	158.2
4-methyl anisole	0.92	2.7	-32	59	104-93-8	C8H10O	122.2
3-octanone	0.87	2.3	-23	59	106-88-3	C8H16O	128.2
Octanal	0.82	2.8	-23	52	124-13-0	C8H16O	128.2
Nerolidol	0.87	4.6	25	96	7212-44-4	C15H26O	222.37
delta-Decalactone	0.96	2.5	-27	110	705-86-2	C10H18O2	170.3
1-Octanol	0.83	1	-16	81	111-87-5	C8H18O	130.3
Ethyl formate	0.92	0.5	-80.5	-20	109-84-4	C3H6O2	74.1
Ethyl propionate	0.89	1.2	-73.9	12	105-37-3	C5H10O2	102.1
Ethyl lactate	1.03	0.2	-26	46	97-64-3	C5H10O3	118.13
Ethyl glycolate	1.1	-0.2	13	62	623-60-7	C4H8O3	108.2
Ethyl 2,4-dioxvalerate	1.13	0.2	17	110	615-79-2	C7H10O4	158.2
Farnesene isomeric mixture	0.84	6.1	4	110	125037-13-0	C15H24	204.4
Ethyl decanoate	0.86	4.6	-20	102	110-38-3	C12H24O2	200.3
1-Hexanol	0.86	2	-44	60	111-27-3	C6H14O	102.3
1-Heptanol	0.82	2.7	-34	77	111-70-6	C7H16O	116.2
Pentane	0.63	3.41	-130	-40	109-66-0	C5H12	72.2
Hexane	0.66	3.9	-95	-22	110-54-3	C6H14	86.2
Propyl acetate	0.87	1.2	-93	14	109-60-4	C5H10O2	102.1
Butyl acetate	0.88	1.8	-77	22	123-86-4	C6H12O2	116.2

Figure A 2 Details of the pre-screening. This step of was for screening for beneficial physical properties density, log P, melting point, and flash point with the respective thresholds. In case that the properties fit into the pre-determined ranges, the respective value is highlighted in green. Solvents that have favorable properties regarding all parameters are highlighted in blue. The data was previously published<sup>148</sup> and is reprinted with permission of Sustainable Energy & Fuels.

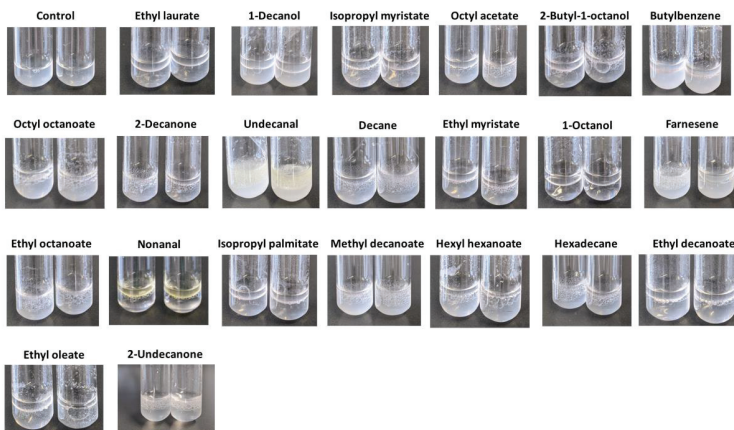


Figure A 3 Images of the cultivation broth of the growth assay. The production host was cultivated in airtight tubes with 33 vol% of the respective solvent. The qualitative comparison of the images was included in the weighted decision matrix during the solvent screening. The data was previously published<sup>148</sup> and is reprinted with permission of Sustainable Energy & Fuels.

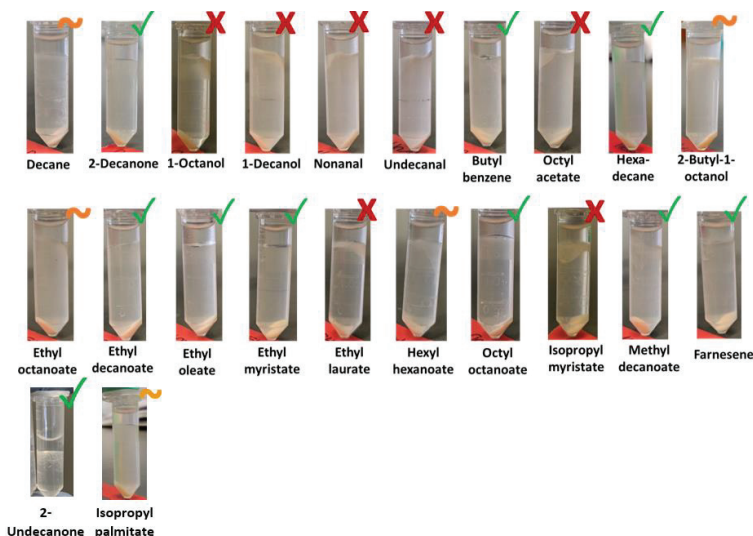


Figure A 4 Images of interphases after *in situ* extraction of methyl ketones. The images were used for qualitative assessment of interphase formation to estimate phase separation. The results were included in the weighted decision matrix during the solvent screening, where a green tick ✓ gave five points, a ~ gave three points, and a red X gave 1 point. The data was previously published<sup>148</sup> and is reprinted with permission of Sustainable Energy & Fuels.

Table A 2 Strains used in this study for the defined inoculum of the fuel tank simulation. The method was adapted from Ackermann *et al.*<sup>192</sup> for methyl ketones. The table was previously published<sup>148</sup> and is reprinted with permission of Sustainable Energy & Fuels.

Strain	Database number	Source
<i>Acinetobacter beijernikii</i>	DSM 22901	DSMZ
<i>Acinetobacter venetianus</i>	DSM 23050	DSMZ
<i>Burkholderia cepacia</i>	DSM 7288	DSMZ
<i>Micrococcus luteus</i>	-	Leuchtle <i>et al.</i> <sup>191</sup>
<i>Micrococcus yunnanensis</i>	DSM 21948	DSMZ
<i>Pseudomonas fluorescens</i>	-	Leuchtle <i>et al.</i> <sup>191</sup>
<i>Pseudomonas poae</i>	-	Leuchtle <i>et al.</i> <sup>191</sup>
<i>Candida cylindracea</i>	DSM 2031	DSMZ
<i>Debaryomyces hansenii</i>	DSM 70244	DSMZ
<i>Debaryomyces polymorphus</i>	DSM 70816	DSMZ
<i>Pichia membranifaciens</i>	DSM 21959	DSMZ
<i>Raffaelea</i> sp.	-	Leuchtle <i>et al.</i> <sup>191</sup>
<i>Rhodotorula mucilaginosa</i>	DSM 18184	DSMZ
<i>Ustilago maydis</i>	-	Leuchtle <i>et al.</i> <sup>191</sup>
<i>Yarrowia deformans</i>	CBS 2071	DSMZ
<i>Yarrowia lipolytica</i>	-	Leuchtle <i>et al.</i> <sup>191</sup>
<i>Paecilomyces lilacinus</i>	DSM 846	DSMZ
<i>Penicillium chrysogenum</i>	DSM 21171	DSMZ
<i>Penicillium citrinum</i>	-	Leuchtle <i>et al.</i> <sup>191</sup>
<i>Micrococcus luteus</i>	-	Leuchtle <i>et al.</i> <sup>191</sup>

Table A 3 Composition of the chemically defined medium (CDM) according to Otto *et al.*<sup>332</sup> and Poolman and Konings.<sup>381</sup> The table was previously published<sup>329</sup> and is reprinted with permission of Green Chemistry.

Substance		Concentration
Glucose	$C_6H_{12}O_6$	10 or 40 g·L <sup>-1</sup>
Dipotassium phosphate	$K_2HPO_4$	2.5 g·L <sup>-1</sup>
Monopotassium phosphate	$KH_2PO_4$	3 g·L <sup>-1</sup>
Triammonium citrate	$C_6H_{17}N_3O_7$	0.6 g·L <sup>-1</sup>
Sodium acetate	$C_2H_3NaO_2$	1 g·L <sup>-1</sup>
Cysteine hydrochloride	$C_3H_8ClNO_2S$	0.25 g·L <sup>-1</sup>
Salt-free, vitamin-free casein hydrolysate		5 g·L <sup>-1</sup>
100x Vitamin solution		10 mL·L <sup>-1</sup>
100x Metal solution		10 mL·L <sup>-1</sup>
100x Nucleic acid solution		10 mL·L <sup>-1</sup>
<b>100x Vitamin solution for CDM</b>		
Substance		Concentration [mg·L <sup>-1</sup> ]
Pyridoxine hydrochloride	$C_8H_{12}ClNO_3$	200
Nicotinic acid	$C_6H_5NO_2$	100
Thiamin hydrochloride	$C_{12}H_{18}Cl_2N_4OS$	100
Riboflavin	$C_{17}H_{20}N_4O_6$	100
Calcium D-pantothenate	$C_{18}H_{32}CaN_2O_{10}$	100
Sodium p-aminobenzoate	$C_7H_6NNaO_2$	1,000
D-biotin	$C_{10}H_{16}N_2O_3S$	1,000
Folic acid	$C_{19}H_{19}N_7O_6$	100
Vitamin B12	$C_{63}H_{88}CoN_{14}O_{14}P$	100
Orotic acid	$C_5H_4N_2O_4$	500
2-Deoxythymidine	$C_{10}H_{14}N_2O_5$	500
Inosine	$C_{10}H_{12}N_4O_5$	500
DL-6,8-Thioctic acid	$C_8H_{14}O_2S_2$	250
Pyridoxamine hydrochloride	$C_8H_{13}ClN_2O_2$	500
<b>100x Metal solution for CDM</b>		

Substance		Concentration [mg·L <sup>-1</sup> ]
Magnesium chloride hexahydrate	MgCl <sub>2</sub> · 6H <sub>2</sub> O	20
Calcium chloride dihydrate	CaCl <sub>2</sub> · 2H <sub>2</sub> O	5
Iron chloride tetrahydrate	FeCl <sub>2</sub> · 4H <sub>2</sub> O	0.5
Zinc sulfate heptahydrate	ZnSO <sub>4</sub> · 7H <sub>2</sub> O	0.5
Cobalt chloride hexahydrate	CoCl · 6H <sub>2</sub> O	0.25

**100x Nucleic acid solution for CDM**

Substance		per 10 mL 0.1 M NaOH [g]
Adenine	C <sub>5</sub> H <sub>5</sub> N <sub>5</sub>	10
Uracil	C <sub>4</sub> H <sub>4</sub> N <sub>2</sub> O <sub>2</sub>	10
Xanthine	C <sub>5</sub> H <sub>4</sub> N <sub>4</sub> O <sub>2</sub>	10
Guanine	C <sub>5</sub> H <sub>5</sub> N <sub>5</sub> O	10

**Amino acid addition to CDM  
according to Poolmann and  
Konings<sup>381</sup>**

Substance		Concentration [mg·L <sup>-1</sup> ]
L-Alanine	C <sub>3</sub> H <sub>7</sub> NO <sub>2</sub>	240
L-Arginine	C <sub>6</sub> H <sub>14</sub> N <sub>4</sub> O <sub>2</sub>	125
L-Asparagine	C <sub>4</sub> H <sub>8</sub> N <sub>2</sub> O <sub>3</sub>	350
L-Glutamine	C <sub>5</sub> H <sub>10</sub> N <sub>2</sub> O <sub>3</sub>	390
Glycine	C <sub>2</sub> H <sub>5</sub> NO <sub>2</sub>	175
L-Histidine	C <sub>6</sub> H <sub>9</sub> N <sub>3</sub> O <sub>2</sub>	150
L-Isoleucine	C <sub>6</sub> H <sub>13</sub> NO <sub>2</sub>	210
L-Leucine	C <sub>6</sub> H <sub>13</sub> NO <sub>2</sub>	475
L-Lysine	C <sub>6</sub> H <sub>14</sub> N <sub>2</sub> O <sub>2</sub>	440
L-Methionine	C <sub>5</sub> H <sub>11</sub> NO <sub>2</sub> S	125
L-Phenylalanine	C <sub>9</sub> H <sub>11</sub> NO <sub>2</sub>	275
L-Proline	C <sub>5</sub> H <sub>9</sub> NO <sub>2</sub>	675
L-Serine	C <sub>3</sub> H <sub>7</sub> NO <sub>3</sub>	340
L-Threonine	C <sub>4</sub> H <sub>9</sub> NO <sub>3</sub>	225
L-Tryptophan	C <sub>11</sub> H <sub>12</sub> N <sub>2</sub> O <sub>2</sub>	50

Substance		Concentration [mg·L <sup>-1</sup> ]
L-Tyrosine	C <sub>9</sub> H <sub>11</sub> NO <sub>3</sub>	200
L-Valine	C <sub>5</sub> H <sub>11</sub> NO <sub>2</sub>	325

Table A 4 Composition of the CDMPC medium. Price *et al.*<sup>333</sup> developed a chemically defined medium for prolonged cultivation (CDMPC) of *L. lactis*. The amino acid, metal, vitamin, and alkaline solutions were prepared as stock solutions. After the addition of all components and stock solutions, the medium was sterilized via filtration. Detailed instructions for the preparation are provided by the authors. The table was previously published<sup>329</sup> and is reprinted with permission of Green Chemistry.

Substance		Concentration
Glucose	$C_6H_{12}O_6$	10 or 40 g·L <sup>-1</sup>
Potassium phosphate	$KH_2PO_4$	2.75 g·L <sup>-1</sup>
Sodium chloride	$NaCl$	2.90 g·L <sup>-1</sup>
Sodium phosphate	$NaH_2PO_4$	2.85 g·L <sup>-1</sup>
10x Amino acid solution		100 mL·L <sup>-1</sup>
100x Metal solution		10 mL·L <sup>-1</sup>
100x Vitamin solution		10 mL·L <sup>-1</sup>
100x Alkaline solution		10 mL·L <sup>-1</sup>

#### 10x Amino acid solution for CDMPC

Substance		Concentration [g·L <sup>-1</sup> ]
L-Alanine	$C_3H_7NO_2$	1.30
L-Arginine	$C_6H_{14}N_4O_2$	2.44
L-Asparagine	$C_4H_8N_2O_3$	0.80
L-Aspartic acid	$C_4H_7NO_4$	1.37
L-Cysteine hydrochloride monohydrate	$C_3H_7NO_2S \cdot HCl \cdot H_2O$	0.61
L-Glutamic acid	$C_5H_9NO_4$	0.97
L-Glutamine	$C_5H_{10}N_2O_3$	0.96
Glycine	$C_2H_5NO_2$	0.29
L-Histidine	$C_6H_9N_3O_2$	0.24
L-Isoleucine	$C_6H_{13}NO_2$	0.82
L-Leucine	$C_6H_{13}NO_2$	1.17
L-Lysine monohydrochloride	$C_6H_{14}N_2O_2 \cdot HCl$	1.87

Substance		Concentration [g·L <sup>-1</sup> ]
L-Methionine	$C_5H_{11}NO_2S$	0.38
L-Phenylalanine	$C_9H_{11}NO_2$	0.64
L-Proline	$C_5H_9NO_2$	4.12



Substance		Concentration [g·L <sup>-1</sup> ]
L-Serine	C <sub>3</sub> H <sub>7</sub> NO <sub>3</sub>	1.72
L-Threonine	C <sub>4</sub> H <sub>9</sub> NO <sub>3</sub>	0.68
L-Tryptophan	C <sub>11</sub> H <sub>12</sub> N <sub>2</sub> O <sub>2</sub>	0.36
L-Valine	C <sub>5</sub> H <sub>11</sub> NO <sub>2</sub>	0.86

**100x Metal solution for CDMPC**

Substance		Concentration [mg·L <sup>-1</sup> ]
Ammonium molybdate tetrahydrate	(NH <sub>4</sub> ) <sub>6</sub> Mo <sub>7</sub> O <sub>24</sub> · 4H <sub>2</sub> O	30
Calcium chloride dihydrate	CaCl <sub>2</sub> · 2H <sub>2</sub> O	300
Cobalt sulfate heptahydrate	CoSO <sub>4</sub> · 7H <sub>2</sub> O	30
Copper sulfate pentahydrate	CuSO <sub>4</sub> · 5H <sub>2</sub> O	30
Iron chloride tetrahydrate	FeCl <sub>2</sub> · 4H <sub>2</sub> O	400
Magnesium chloride hexahydrate	MgCl <sub>2</sub> · 6H <sub>2</sub> O	20,000
Manganese chloride tetrahydrate	MnCl <sub>2</sub> · 4H <sub>2</sub> O	400
Zinc sulfate heptahydrate	ZnSO <sub>4</sub> · 7H <sub>2</sub> O	30

**100x Vitamin solution for CDMPC**

Substance		Concentration [mg·L <sup>-1</sup> ]
α-Lipoic acid	C <sub>8</sub> H <sub>14</sub> O <sub>2</sub> S <sub>2</sub>	200
D-Pantothenic acid hemicalcium salt	C <sub>9</sub> H <sub>16</sub> NO <sub>5</sub> · 0.5 Ca	50
Nicotinic acid	C <sub>6</sub> H <sub>5</sub> NO <sub>2</sub>	100
Pyridoxal hydrochloride	C <sub>8</sub> H <sub>9</sub> NO <sub>3</sub> · HCl	100
Pyridoxine hydrochloride	C <sub>8</sub> H <sub>11</sub> NO <sub>3</sub> · HCl	100
Thiamine hydrochloride	C <sub>12</sub> H <sub>17</sub> CIN <sub>4</sub> OS · HCl	100

**100x Alkaline solution for CDMPC**

Substance		Concentration [mg·L <sup>-1</sup> ]
Biotin	C <sub>10</sub> H <sub>16</sub> N <sub>2</sub> O <sub>3</sub> S	10
Substance		Concentration [mg·L <sup>-1</sup> ]
L-Tyrosine	C <sub>9</sub> H <sub>11</sub> NO <sub>3</sub>	5,000

Table A 5 Composition of the resting cell buffer. The phosphate buffer, trace elements, and magnesium solution were prepared as individual stock solutions in 100x concentration. The glucose solution was prepared as a 500 g·L<sup>-1</sup> stock solution. All stock solutions were autoclaved except for the trace element solution that was sterile filtered. For the preparation of the washing buffer, used for the washing step during resting cell experiments, glucose was omitted. The table was previously published<sup>329</sup> and is reprinted with permission of Green Chemistry.

Phosphate buffer		Concentration [g·L <sup>-1</sup> ]
Dipotassium phosphate	K <sub>2</sub> HPO <sub>4</sub>	3.88
Monosodium phosphate	NaH <sub>2</sub> PO <sub>4</sub>	1.63
Magnesium sulfate	MgSO <sub>4</sub>	0.25
Trace elements		Concentration [mg·L <sup>-1</sup> ]
EDTA	C <sub>10</sub> H <sub>16</sub> N <sub>2</sub> O <sub>8</sub>	10
Magnesium chloride hexahydrate	MgCl <sub>2</sub> · 6H <sub>2</sub> O	100
Zinc sulfate heptahydrate	ZnSO <sub>4</sub> · 7H <sub>2</sub> O	2.0
Calcium chloride dihydrate	CaCl <sub>2</sub> · 2H <sub>2</sub> O	1.0
Iron sulfate heptahydrate	FeSO <sub>4</sub> · 7H <sub>2</sub> O	5.0
Sodium molybdate dihydrate	Na <sub>2</sub> MoO <sub>4</sub> · 2H <sub>2</sub> O	0.2
Copper sulfate pentahydrate	CuSO <sub>4</sub> · 5H <sub>2</sub> O	0.2
Cobalt chloride hexahydrate	CoCl <sub>2</sub> · 6H <sub>2</sub> O	0.4
Manganese chloride dihydrate	MnCl <sub>2</sub> · 2H <sub>2</sub> O	1.0

Table A 6 Acetoin concentrations and current densities in supernatants. Overview of the acetoin concentration in the respective media and applied current densities for electrochemical conversion of acetoin to 2-butanone. HS = Hestrin Schramm; LB = lysogeny broth; YEP = yeast extract peptone. The table was previously published<sup>329</sup> and is reprinted with permission of Green Chemistry.

Medium	Concentration [g·L <sup>-1</sup> ]	Current density [mA·cm <sup>-2</sup> ]
M17	6	10
HS	7	10
LB	8	10
YEP	14	25
M17	16	25
Resting cell buffer	19	25

Table A 7 Deleted genes in the mutant strain *P. taiwanensis* VLB120  $\Delta 6$  pProd for the genome-scale model. The BiGG database was used to identify the corresponding gene ID in the *iJN1463* model. The table was previously published<sup>284</sup> and is reprinted with permission of the Journal of Industrial Microbiology and Biotechnology.

Name	Description	Gene ID in <i>iJN1463</i>
<i>tesB</i>	codes for fatty-acid-CoA thioesterases	PP_4762
<i>pha</i>	codes for poly 3 hydroxyalkanoate polymerase	PP_5003, PP_5005
<i>FadA</i>	codes for acetyl-CoA C-acetyltransferase	PP_2051
<i>FadA2</i>	Isoenzymes	PP_3754, PP_4636
<i>FadE</i>	codes for acyl-CoA dehydrogenase	PP_1893
<i>FadE2</i>	Isoenzymes	PP_0368, PP_2216, PP_2048, PP_2039

Table A 8 Score explanation for establishing the weighted decision matrix. The growth assay had a weighting of 40%, the sum of health and safety score had a weighting of 30%, the partition coefficient had a weighting of 10%, and the interphase formation had a weighting of 20%. The data was previously published<sup>148</sup> and is reprinted with permission of Sustainable Energy & Fuels.

Score	Growth assay	Sum of health and safety score	Partition coefficient	Interphase formation
1	no turbidity	>7	$\leq 33$	strong interphase
2	-	6	34 to 43	-
3	medium turbidity + color change	5	44 to 53	slight interphase
4	medium turbidity	4	53 to 61	-
5	turbidity like control	<4	62 to 135	no interphase

Table A 9 Results of the weighted decision matrix. Solvents are given in declining order regarding their score. The data was previously published<sup>148</sup> and is reprinted with permission of Sustainable Energy & Fuels.

Solvent	Score
Octyl octanoate	4.8
Farnesene	4.7
Methyl decanoate	4.7
2-Undecanone	4.6
Hexadecane	4.6
Ethyl decanoate	4.6
2-Butyl-1-octanol	4.4
Ethyl octanoate	4.3
Isopropyl palmitate	4.3
Hexyl hexanoate	4.2
Isopropyl myristate	4.1
Octyl acetate	4.1
2-Decanon	3.9
1-Decanol	3.9
Butylbenzene	3.6
Ethyl myristate	3.4
Decane	3.3
Ethyl oleate	3.3
Ethyl laurate	2.9
Undecanal	2.9
Nonanal	2.8
1-Octanol	2.4

Table A 10 Influence of the oxygen transfer rate (OTR) on acetoin formation. Variation of filling volume in 500 mL shake flasks was applied to vary the oxygen transfer for cultivations of *L. lactis* VJ017 and investigate the influence on product formation. <sup>a</sup>The oxygen transfer rate (OTR) was calculated according to Meier *et al.*<sup>334</sup> The data associated with this table was obtained from Fabian Speen's Master Thesis under supervision by Carolin Grütering.<sup>331</sup> The table was previously published<sup>329</sup> and is reprinted with permission of Green Chemistry.

Filling volume [mL]	Glucose concentration [mg·L <sup>-1</sup> ]	OTR [mmol·L <sup>-1</sup> ·h <sup>-1</sup> ] <sup>a</sup>	Acetoin titer [g·L <sup>-1</sup> ]	Acetoin yield [g <sub>acetoin</sub> ·g <sub>glucose</sub> <sup>-1</sup> ]	Specific acetoin yield [g <sub>acetoin</sub> ·g <sub>CDW</sub> <sup>-1</sup> ]
50	40	28.6	13.8	0.35	2.26
25	40	47.8	16.5	0.41	2.97
25	10	47.8	4.8	0.48	1.85

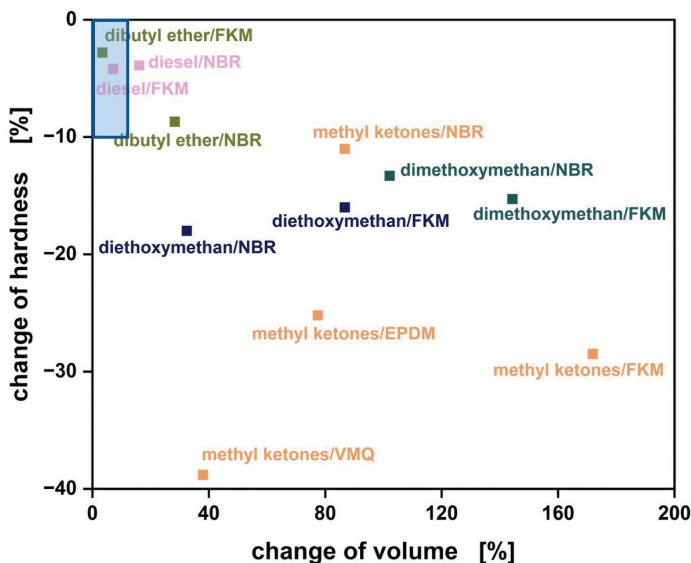


Figure A 5 Change of volume and hardness for different bio-hybrid fuels and reference elastomer sealing materials. Light blue area shows the tolerance area for dynamic seals. FKM = fluorine kautschuk material; NBR = nitrile butadiene rubber; EPDM = ethylene propylene diene monomer rubber; VMQ = vinyl methyl silicone. The data associated with this figure was obtained in cooperation with Marius Hofmeister. The figure was previously published<sup>148</sup> and is reprinted with permission of Sustainable Energy & Fuels.

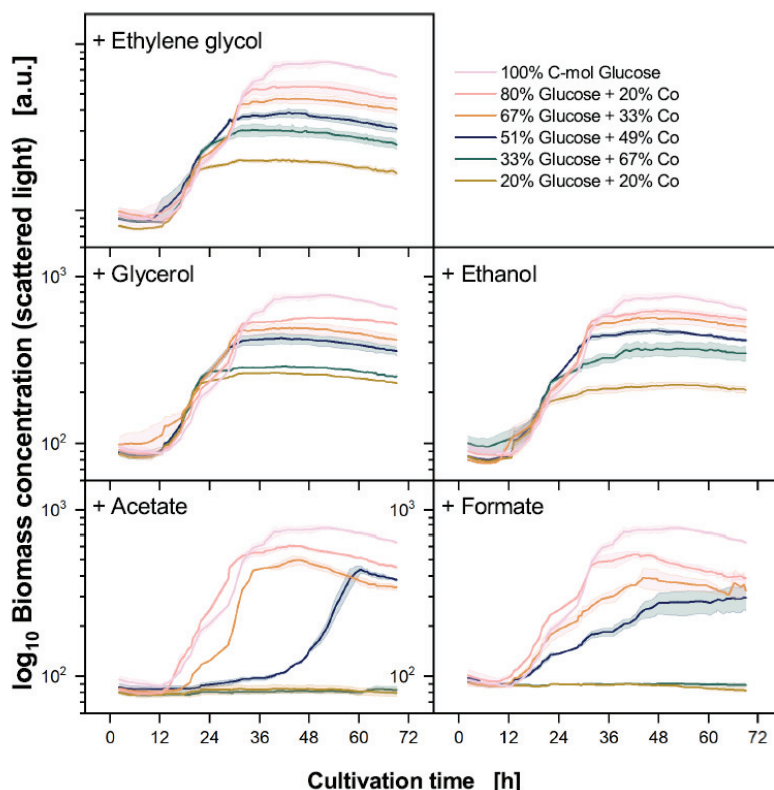


Figure A 6 Biomass growth of *P. taiwanensis* VLB120  $\Delta 6$  pProd in microtiter plates with glucose and the five different co-fed substrates ethylene glycol, glycerol, ethanol, acetate, and formate in BioLector cultivations. In every cultivation, the same total amount of C-mole of substrate was applied. Growth curves result from the average of three different growth experiments. The error is calculated from the standard deviation of these three biological replicates. The figure, originally created by Leon Poduschnick under supervision by Carolin Grütering and Anita Ziegler, was previously published,<sup>284</sup> and is reprinted with permission of the Journal of Industrial Microbiology and Biotechnology.

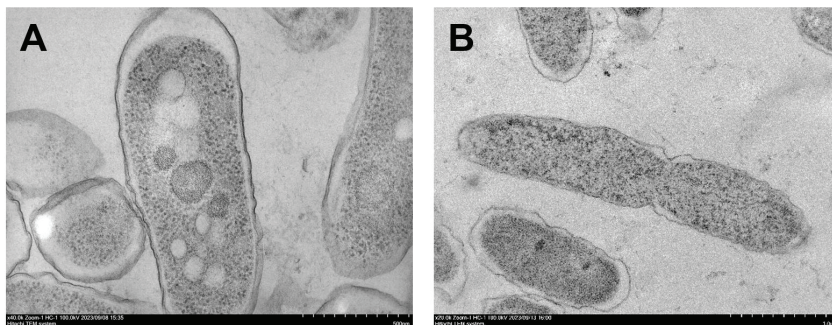


Figure A 7 Transmission electron microscopy of *P. taiwanensis* VLB120 wild type (A) and *P. taiwanensis* VLB120  $\Delta 6$  pProd (B) in stationary phase 30 hours after inoculation. The cells were obtained from a cultivation in 500 mL shake flasks with 50 mL MSM  $10 \text{ g} \cdot \text{L}^{-1}$  glucose. Methyl ketone production in (B) was induced with 2 mM IPTG and 1 mM arabinose at the time point of inoculation. 2 mL of each culture was transferred to a sterile Eppendorf tube, centrifuged for 1 minute at 13,000 rpm, and stored on ice. MSM = mineral salt media. Following steps were executed by Dr. rer. nat. Miriam Buhl from the Institute of Pathology at the University Hospital Aachen. The samples were frozen by high pressure-freezing in Leica EM ice and embedded in Epon with a freeze substitution. Images were taken with a TEM HT7800 by Hitachi (Hitachi Ltd. Corporation, Chiyoda, Japan) at 100 kV. IPTG = isopropyl  $\beta$ -D-1-thiogalactopyranoside.

---

# References

---





## References

1. M. Bonaiuti, Bioeconomics, in *Degrowth: a vocabulary for a new era*, ed. G. D. D'Alisa, Federico; Kallis, Giorgos, Taylor&Francis Group, London, 1 edn., 2014, pp. 56-60.
2. D. J. Soeder, Fossil Fuels and Climate Change, in *Fracking and the Environment: A scientific assessment of the environmental risks from hydraulic fracturing and fossil fuels*, ed. D. J. Soeder, Springer International Publishing, Cham, 1 edn., 2021, pp. 155-185.
3. N. Amaroli and V. Balzani, The Legacy of Fossil Fuels, *Chemistry – An Asian Journal*, 2011, **6**, 768-784. <https://doi.org/10.1002/asia.201000797>
4. M. Höök and X. Tang, Depletion of fossil fuels and anthropogenic climate change - A review, *Energy Policy*, 2013, **52**, 797-809. <https://doi.org/10.1016/j.enpol.2012.10.046>
5. F. Johnsson, J. Kjärstad and J. Rootzén, The threat to climate change mitigation posed by the abundance of fossil fuels, *Climate Policy*, 2019, **19**, 258-274. [10.1080/14693062.2018.1483885](https://doi.org/10.1080/14693062.2018.1483885)
6. S. Fawzy, A. I. Osman, J. Doran and D. W. Rooney, Strategies for mitigation of climate change: a review, *Environmental Chemistry Letters*, 2020, **18**, 2069-2094. [10.1007/s10311-020-01059-w](https://doi.org/10.1007/s10311-020-01059-w)
7. B. B. Osborne, B. T. Bestelmeyer, C. M. Currier, P. M. Homyak, H. L. Throop, K. Young and S. C. Reed, The consequences of climate change for dryland biogeochemistry, *New Phytologist*, 2022, **236**, 15-20. <https://doi.org/10.1111/nph.18312>
8. H. Desing, D. Brunner, F. Takacs, S. Nahrath, K. Frankenberger and R. Hirschier, A circular economy within the planetary boundaries: Towards a resource-based, systemic approach, *Resources, Conservation and Recycling*, 2020, **155**, 104673. <https://doi.org/10.1016/j.resconrec.2019.104673>
9. M. Sureth, M. Kalkuhl, O. Edenhofer and J. Rockström, A Welfare Economic Approach to Planetary Boundaries, *Jahrbücher für Nationalökonomie und Statistik*, 2023, **243**, 477-542. [doi:10.1515/jbnst-2022-0022](https://doi.org/10.1515/jbnst-2022-0022)
10. A. P. M. Velenturf, P. Purnell, L. E. Macaskie, W. M. Mayes and D. J. Sapsford, A New Perspective on a Global Circular Economy, in *Resource Recovery from Wastes: Towards a Circular Economy*, eds. L. E. Macaskie, D. J. Sapsford and W. M. Mayes, The Royal Society of Chemistry, 1 edn., 2019, pp. 1-22.
11. Ellen MacArthur Foundation, The butterfly diagram: visualising the circular economy, <https://www.ellenmacarthurfoundation.org/circular-economy-diagram>, (accessed January 09, 2024).
12. European Commission, *Closing the loop – An EU action plan for the circular economy*, Brussels, 2015.
13. Ellen MacArthur Foundation, The Business Opportunity of a Circular Economy, in *An Introduction to Circular Economy*, eds. L. Liu and S. Ramakrishna, Springer Singapore, Singapore, 1 edn., 2021, pp. 397-417.
14. K. McCormick and N. Kautto, The Bioeconomy in Europe: An Overview, *Sustainability*, 2013, **5**, 2589-2608.
15. D. D'Amato and J. Korhonen, Integrating the green economy, circular economy and bioeconomy in a strategic sustainability framework, *Ecological Economics*, 2021, **188**, 107143. <https://doi.org/10.1016/j.ecolecon.2021.107143>
16. S. Maina, V. Kachrimanidou and A. Koutinas, A roadmap towards a circular and sustainable bioeconomy through waste valorization, *Current Opinion in Green and Sustainable Chemistry*, 2017, **8**, 18-23. <https://doi.org/10.1016/j.cogsc.2017.07.007>
17. P. Stegmann, M. Londo and M. Junginger, The circular bioeconomy: Its elements and role in European bioeconomy clusters, *Resources, Conservation & Recycling: X*, 2020, **6**, 100029. <https://doi.org/10.1016/j.rcrx.2019.100029>
18. I. Bavuso, G. Furlan, E. E. Intagliata and J. Steding, Circular Economy in the Roman Period and the Early Middle Ages – Methods of Analysis for a Future Agenda, *Open Archaeology*, 2023, **9**, 20220301. [doi:10.1515/opar-2022-0301](https://doi.org/10.1515/opar-2022-0301)
19. P. K. Hajoary, V. Ramani and C. Nuur, New for Some, Old for Others: Circular Economy Practices in Ancient Time, *Circular Economy and Sustainability*, 2023.
20. J. Philp, Biotechnologies to Bridge the Schism in the Bioeconomy, *Energies*, 2021, **14**, 8393.
21. J. Meyers, J. B. Mensah, F. J. Holzhäuser, A. Omari, C. C. Blesken, T. Tiso, S. Palkovits, L. M. Blank, S. Pischinger and R. Palkovits, Electrochemical conversion of a bio-derivable hydroxy acid to a drop-in oxygenate diesel fuel, *Energy & Environmental Science*, 2019, **12**, 2406-2411. [10.1039/c9ee01485c](https://doi.org/10.1039/c9ee01485c)
22. T. Schwanemann, E. A. Urban, C. Eberlein, J. Gärgens, D. Rago, N. Krink, P. I. Nikel, H. J. Heipieper, B. Wynands and N. Wierckx, Production of (hydroxy)benzoate-derived polyketides by engineered *Pseudomonas* with *in situ* extraction, *Bioresource Technology*, 2023, **388**, 129741. <https://doi.org/10.1016/j.biortech.2023.129741>
23. S. Hinderer, L. Brändle and A. Kuckertz, Transition to a Sustainable Bioeconomy, *Sustainability*, 2021, **13**, 8232.
24. S. A. Neves and A. C. Marques, Drivers and barriers in the transition from a linear economy to a circular economy, *Journal of Cleaner Production*, 2022, **341**, 130865. <https://doi.org/10.1016/j.jclepro.2022.130865>
25. S. F. Pfau, J. E. Hagens, B. Dankbaar and A. J. M. Smits, Visions of Sustainability in Bioeconomy Research, *Sustainability*, 2014, **6**, 1222-1249.
26. European Commission, *New perspectives on the knowledge-based bio-economy*, Brussels, 2005.

27. C. Venter and D. Cohen, The Century of Biology, *New Perspectives Quarterly*, 2004, **21**, 73-77. <https://doi.org/10.1111/j.1540-5842.2004.00701.x>
28. W. Soetaert and E. Vandamme, The impact of industrial biotechnology, *Biotechnology Journal*, 2006, **1**, 756-769. <https://doi.org/10.1002/biot.200600066>
29. T. Angelin Swetha, K. Mohanarasu, M. Sudhakar, R. Raja, K. Ponnuchamy, G. Muthusamy and A. Arun, A comprehensive review on techniques used in conversion of biomass into bioeconomy, *Sustainable Energy Technologies and Assessments*, 2022, **53**, 102682. <https://doi.org/10.1016/j.seta.2022.102682>
30. M. Kircher, Bioeconomy of Microorganisms, in *The bioeconomy system*, eds. D. Thrän and U. Moesenfechtel, Springer Berlin Heidelberg, Berlin, Heidelberg, 1 edn., 2022, pp. 85-103.
31. H. W. Ma and A. P. Zeng, The connectivity structure, giant strong component and centrality of metabolic networks, *Bioinformatics*, 2003, **19**, 1423-1430. [10.1093/bioinformatics/btg177](https://doi.org/10.1093/bioinformatics/btg177)
32. S. Sudarsan, S. Dethlefsen, L. M. Blank, M. Siemann-Herzberg and A. Schmid, The Functional Structure of Central Carbon Metabolism in *Pseudomonas putida* KT2440, 2014, **80**, 5292-5303. [doi:10.1128/AEM.01643-14](https://doi.org/10.1128/AEM.01643-14)
33. T. Friedlander, A. E. Mayo, T. Tlustý and U. Alon, Evolution of Bow-Tie Architectures in Biology, *PLOS Computational Biology*, 2015, **11**, e1004055. [10.1371/journal.pcbi.1004055](https://doi.org/10.1371/journal.pcbi.1004055)
34. T. Tiso, B. Winter, R. Wei, J. Hee, J. de Witt, N. Wierckx, P. Quicker, U. T. Bornscheuer, A. Bardow, J. Nogales and L. M. Blank, The metabolic potential of plastics as biotechnological carbon sources – Review and targets for the future, *Metabolic Engineering*, 2022, **71**, 77-98. <https://doi.org/10.1016/j.ymben.2021.12.006>
35. J. D. Carballeira, M. A. Quezada, P. Hoyos, Y. Simeó, M. J. Hernaiz, A. R. Alcantara and J. V. Sinisterra, Microbial cells as catalysts for stereoselective red–ox reactions, *Biotechnology Advances*, 2009, **27**, 686-714. <https://doi.org/10.1016/j.biotechadv.2009.05.001>
36. S. Wenda, S. Illner, A. Mell and U. Kragl, Industrial biotechnology - the future of green chemistry?, *Green Chemistry*, 2011, **13**, 3007-3047. [10.1039/C1GC15579B](https://doi.org/10.1039/C1GC15579B)
37. A. Flores, X. Wang and D. R. Nielsen, Recent trends in integrated bioprocesses: aiding and expanding microbial biofuel/biochemical production, *Curr Opin Biotechnol*, 2019, **57**, 82-87. [10.1016/j.copbio.2019.02.007](https://doi.org/10.1016/j.copbio.2019.02.007)
38. N. A. C. Jackson, K. E. Kester, D. Casimiro, S. Gurunathan and F. DeRosa, The promise of mRNA vaccines: a biotech and industrial perspective, *npj Vaccines*, 2020, **5**, 11. [10.1038/s41541-020-0159-8](https://doi.org/10.1038/s41541-020-0159-8)
39. T. Uslu, Advantages, risks and legal perspectives of GMOs in 2020s, *Plant Biotechnology Reports*, 2021, **15**, 741-751. [10.1007/s11816-021-00714-0](https://doi.org/10.1007/s11816-021-00714-0)
40. A. Holzinger, K. Keilblinger, P. Holub, K. Zatloukal and H. Müller, AI for life: Trends in artificial intelligence for biotechnology, *New Biotechnology*, 2023, **74**, 16-24. <https://doi.org/10.1016/j.nbt.2023.02.001>
41. L. M. Helleckes, J. Hemmerich, W. Wiechert, E. von Lieres and A. Grünberger, Machine learning in bioprocess development: from promise to practice, *Trends in Biotechnology*, 2023, **41**, 817-835. [10.1016/j.tibtech.2022.10.010](https://doi.org/10.1016/j.tibtech.2022.10.010)
42. Y. Lokko, M. Heijde, K. Schebesta, P. Scholtès, M. Van Montagu and M. Giacca, Biotechnology and the bioeconomy - Towards inclusive and sustainable industrial development, *New Biotechnology*, 2018, **40**, 5-10. <https://doi.org/10.1016/j.nbt.2017.06.005>
43. C. L. Gargalo, I. Udugama, K. Pontius, P. C. Lopez, R. F. Nielsen, A. Hasanzadeh, S. S. Mansouri, C. Bayer, H. Junicke and K. V. Gernaey, Towards smart biomanufacturing: a perspective on recent developments in industrial measurement and monitoring technologies for bio-based production processes, *Journal of Industrial Microbiology and Biotechnology*, 2020, **47**, 947-964. [10.1007/s10295-020-02308-1](https://doi.org/10.1007/s10295-020-02308-1)
44. I. Knezevic, M. A. Liu, K. Peden, T. Zhou and H.-N. Kang, Development of mRNA Vaccines: Scientific and Regulatory Issues, *Vaccines*, 2021, **9**, 81.
45. H. Chmiel, J. Friedle, T. Schroeder, S. Schuldt, T. Winkelkemper and G. Schembecker, Aufarbeitung (Downstream Processing), in *Bioproszesstechnik*, ed. H. Chmiel, Spektrum Akademischer Verlag, Heidelberg, 3 edn., 2011, pp. 295-372.
46. N. Danielson, S. McKay, P. Bloom, J. Dunn, N. Jakel, T. Bauer, J. Hannon, M. C. Jewett and B. Shanks, Industrial Biotechnology - An Industry at an Inflection Point, *Industrial Biotechnology*, 2020, **16**, 321-332. [10.1089/ind.2020.29230.nda](https://doi.org/10.1089/ind.2020.29230.nda)
47. P. Saling, Assessing Industrial Biotechnology Products with LCA and Eco-Efficiency, in *Sustainability and Life Cycle Assessment in Industrial Biotechnology*, eds. M. Fröhling and M. Hiete, Springer International Publishing, Cham, 1 edn., 2020, pp. 325-357.
48. D. Bachmann, U. Pal, J. A. Bockwoldt, L. Schaffert, R. Roentgen, J. Büchs, J. Kalinowski, L. M. Blank and T. Tiso, C-, N-, S-, and P-Substrate Spectra in and the Impact of Abiotic Factors on Assessing the Biotechnological Potential of *Paracoccus pantotrophus*, *Applied Microbiology*, 2023, **3**, 175-198.
49. K. Wefelmeier, S. Schmitz, A. M. Haut, J. Otten, T. Jülich and L. M. Blank, Engineering the methylotrophic yeast *Ogataea polymorpha* for lactate production from methanol, *Frontiers in Bioengineering and Biotechnology*, 2023, **11**, 1223726. [10.3389/fbioe.2023.1223726](https://doi.org/10.3389/fbioe.2023.1223726)
50. Z. Gong, J. Nielsen and Y. J. Zhou, Engineering Robustness of Microbial Cell Factories, *Biotechnology Journal*, 2017, **12**, 1700014. <https://doi.org/10.1002/biot.201700014>
51. C. Navarrete, I. H. Jacobsen, J. L. Martínez and A. Procentese, Cell Factories for Industrial Production Processes: Current Issues and Emerging Solutions, *Processes*, 2020, **8**, 768.
52. J. Michels, The Use of Biomass for the Production of Fuel and Chemicals, in *Bioeconomy for Beginners*, ed. J. Pietzsch, Springer Berlin Heidelberg, Berlin, Heidelberg, 1 edn., 2020, pp. 77-103.

53. M. A. Fahim, T. A. Alsahhaf and A. Elkilani, Refinery Feedstocks and Products, in *Fundamentals of Petroleum Refining*, eds. M. A. Fahim, T. A. Alsahhaf and A. Elkilani, Elsevier, Amsterdam, 1 edn., 2010, pp. 11-31.
54. R. U. Ayres, Petroleum and Petrochemicals, in *The History and Future of Technology: Can Technology Save Humanity from Extinction?*, ed. R. U. Ayres, Springer International Publishing, Cham, 1 edn., 2021, pp. 199-221.
55. N. Singh, R. R. Singhania, P. S. Nigam, C.-D. Dong, A. K. Patel and M. Puri, Global status of lignocellulosic biorefinery: Challenges and perspectives, *Bioresource Technology*, 2022, **344**, 126415. <https://doi.org/10.1016/j.biortech.2021.126415>
56. M. Gavrilescu and Y. Chisti, Biotechnology - a sustainable alternative for chemical industry, *Biotechnology Advances*, 2005, **23**, 471-499. <https://doi.org/10.1016/j.biotechadv.2005.03.004>
57. J. Amoah, P. Kahar, C. Ogino and A. Kondo, Bioenergy and Biorefinery: Feedstock, Biotechnological Conversion, and Products, *Biotechnology Journal*, 2019, **14**, 1800494. <https://doi.org/10.1002/biot.201800494>
58. Y.-H. P. Zhang, Reviving the carbohydrate economy via multi-product lignocellulose biorefineries, *Journal of Industrial Microbiology and Biotechnology*, 2008, **35**, 367-375. <https://doi.org/10.1007/s10295-007-0293-6>
59. S. Octave and D. Thomas, Biorefinery: Toward an industrial metabolism, *Biochimie*, 2009, **91**, 659-664. <https://doi.org/10.1016/j.biochi.2009.03.015>
60. S. Banerjee, S. Mudliar, R. Sen, B. Giri, D. Satpute, T. Chakrabarti and R. A. Pandey, Commercializing lignocellulosic bioethanol: technology bottlenecks and possible remedies, *Biofuels, Bioproducts and Biorefining*, 2010, **4**, 77-93. <https://doi.org/10.1002/bbb.188>
61. M. Abreu, L. Silva, B. Ribeiro, A. Ferreira, L. Alves, S. M. Paixão, L. Gouveia, P. Moura, F. Carvalho, L. C. Duarte, A. L. Fernando, A. Reis and F. Girio, Low Indirect Land Use Change (ILUC) Energy Crops to Bioenergy and Biofuels: A Review, *Energies*, 2022, **15**, 4348.
62. A. Arevalo-Gallegos, Z. Ahmad, M. Asgher, R. Parra-Saldivar and H. M. N. Iqbal, Lignocellulose: A sustainable material to produce value-added products with a zero waste approach - A review, *International Journal of Biological Macromolecules*, 2017, **99**, 308-318. <https://doi.org/10.1016/j.ijbiomac.2017.02.097>
63. F. Adom, J. B. Dunn, J. Han and N. Sather, Life-Cycle Fossil Energy Consumption and Greenhouse Gas Emissions of Bioderived Chemicals and Their Conventional Counterparts, *Environmental Science & Technology*, 2014, **48**, 14624-14631. <https://doi.org/10.1021/es503766e>
64. Z. Strassberger, S. Tanase and G. Rothenberg, The pros and cons of lignin valorisation in an integrated biorefinery, *RSC Advances*, 2014, **4**, 25310-25318. <https://doi.org/10.1039/C4RA04747H>
65. B. E. Dale and R. G. Ong, Energy, wealth, and human development: Why and how biomass pretreatment research must improve, *Biotechnology Progress*, 2012, **28**, 893-898. <https://doi.org/10.1002/btpr.1575>
66. S. H. Hazeena, R. Sindhu, A. Pandey and P. Binod, Lignocellulosic bio-refinery approach for microbial 2,3-Butanediol production, *Bioresource Technology*, 2020, **302**, 122873. <https://doi.org/10.1016/j.biortech.2020.122873>
67. D. Sidiras, D. Politi, G. Giakoumakis and I. Salapa, Simulation and optimization of organosolv based lignocellulosic biomass refinery: A review, *Bioresource Technology*, 2022, **343**, 126158. <https://doi.org/10.1016/j.biortech.2021.126158>
68. A. J. Ragauskas, C. K. Williams, B. H. Davison, G. Britovsek, J. Cairney, C. A. Eckert, W. J. Frederick, J. P. Hallett, D. J. Leak, C. L. Liotta, J. R. Mielenz, R. Murphy, R. Temple and T. Tschaplinski, The Path Forward for Biofuels and Biomaterials, *Science*, 2006, **311**, 484-489. [doi:10.1126/science.1114736](https://doi.org/10.1126/science.1114736)
69. G.-Q. Chen, New challenges and opportunities for industrial biotechnology, *Microbial Cell Factories*, 2012, **11**, 111. <https://doi.org/10.1186/1475-2859-11-111>
70. M. S. Singhvi and D. V. Gokhale, Lignocellulosic biomass: Hurdles and challenges in its valorization, *Applied Microbiology and Biotechnology*, 2019, **103**, 9305-9320. <https://doi.org/10.1007/s00253-019-10212-7>
71. J. Keasling, H. Garcia Martin, T. S. Lee, A. Mukhopadhyay, S. W. Singer and E. Sundstrom, Microbial production of advanced biofuels, *Nature Reviews Microbiology*, 2021, **19**, 701-715. <https://doi.org/10.1038/s41579-021-00577-w>
72. IEA, *Net Zero by 2050*, IEA, 2021.
73. E. Çabukoglu, G. Georges, L. Küng, G. Pareschi and K. Boulouchos, Battery electric propulsion: An option for heavy-duty vehicles? Results from a Swiss case-study, *Transportation Research Part C: Emerging Technologies*, 2018, **88**, 107-123. <https://doi.org/10.1016/j.trc.2018.01.013>
74. H. Kim, K. Y. Koo and T.-H. Joong, A study on the necessity of integrated evaluation of alternative marine fuels, *Journal of International Maritime Safety, Environmental Affairs, and Shipping*, 2020, **4**, 26-31. <https://doi.org/10.1080/25725084.2020.1779426>
75. S. Osella, J. Kargul, M. Izzo and B. Trzaskowski, Architecture and Function of Biohybrid Solar Cell and Solar-to-Fuel Nanodevices, in *Theory and Simulation in Physics for Materials Applications: Cutting-Edge Techniques in Theoretical and Computational Materials Science*, eds. E. V. Levchenko, Y. J. Dappe and G. Ori, Springer International Publishing, Cham, 1 edn., 2020, pp. 227-274.
76. A. Ramirez, S. M. Sarathy and J. Gascon, CO<sub>2</sub> Derived E-Fuels: Research Trends, Misconceptions, and Future Directions, *Trends in Chemistry*, 2020, **2**, 785-795. <https://doi.org/10.1016/j.trechm.2020.07.005>
77. L. Goswami, R. Kayalvizhi, P. K. Dikshit, K. C. Sherpa, S. Roy, A. Kushwaha, B. S. Kim, R. Banerjee, S. Jacob and R. C. Rajak, A critical review on prospects of bio-refinery products from second and third generation biomasses, *Chemical Engineering Journal*, 2022, **448**, 137677. <https://doi.org/10.1016/j.cej.2022.137677>

78. E. B. Goh, E. E. Baidoo, J. D. Keasling and H. R. Beller, Engineering of bacterial methyl ketone synthesis for biofuels, *Applied and Environmental Microbiology*, 2012, **78**, 70-80. 10.1128/AEM.06785-11
79. R. M. Lennen and B. F. Pfleger, Microbial production of fatty acid-derived fuels and chemicals, *Current Opinion in Biotechnology*, 2013, **24**, 1044-1053. 10.1016/j.copbio.2013.02.028
80. C. A. Rabinovitch-Deere, J. W. K. Oliver, G. M. Rodriguez and S. Atsumi, Synthetic Biology and Metabolic Engineering Approaches To Produce Biofuels, *Chemical Reviews*, 2013, **113**, 4611-4632. 10.1021/cr300361t
81. K. W. George, J. Alonso-Gutierrez, J. D. Keasling and T. S. Lee, Isoprenoid Drugs, Biofuels, and Chemicals - Artemisinin, Farnesene, and Beyond, in *Biotechnology of Isoprenoids*, eds. J. Schrader and J. Bohlmann, Springer International Publishing, Cham, 1 edn., 2015, pp. 355-389.
82. C. Bayse and F. O'Gara, Role of Membrane Structure During Stress Signalling and Adaptation in *Pseudomonas*, in *Pseudomonas*, eds. J. L. Ramos and A. Filloux, 1 edn., 2007, pp. 193-224.
83. Y. Hu, Z. Zhu, J. Nielsen and V. Siewers, Engineering *Saccharomyces cerevisiae* cells for production of fatty acid-derived biofuels and chemicals, *Open Biology*, 2019, **9**, 190049. doi:10.1098/rsob.190049
84. A. M. Ruffing and C. A. Trahan, Biofuel toxicity and mechanisms of biofuel tolerance in three model cyanobacteria, *Algal Research*, 2014, **5**, 121-132. <https://doi.org/10.1016/j.algal.2014.07.006>
85. J. Sheng and X. Feng, Metabolic engineering of yeast to produce fatty acid-derived biofuels: bottlenecks and solutions, *Frontiers in Microbiology*, 2015, **6**, 554. 10.3389/fmicb.2015.00554
86. M. J. Dunlop, Engineering microbes for tolerance to next-generation biofuels, *Biotechnology for Biofuels*, 2011, **4**, 32. 10.1186/1754-6834-4-32
87. R. A. Fernandes, A. K. Jha and P. Kumar, Recent advances in Wacker oxidation: from conventional to modern variants and applications, *Catalysis Science & Technology*, 2020, **10**, 7448-7470. 10.1039/D0CY01820A
88. N. W. Kimps, B. W. Bissinger, C. S. Apperson, D. E. Sonenshine and R. M. Roe, First report of the repellency of 2-tridecanone against ticks, *Medical and Veterinary Entomology*, 2011, **25**, 202-208. <https://doi.org/10.1111/j.1365-2915.2010.00918.x>
89. E. B. Goh, E. E. K. Baidoo, H. Burd, T. S. Lee, J. D. Keasling and H. R. Beller, Substantial improvements in methyl ketone production in *E. coli* and insights on the pathway from *in vitro* studies, *Metab Eng*, 2014, **26**, 67-76. 10.1016/j.ymben.2014.09.003
90. F. E. Liew, R. Nogle, T. Abdalla, B. J. Rasor, C. Canter, R. O. Jensen, L. Wang, J. Strutz, P. Chirania, S. De Tissera, A. P. Mueller, Z. Ruan, A. Gao, L. Tran, N. L. Engle, J. C. Bromley, J. Daniell, R. Conrado, T. J. Tschaplinski, R. J. Giannone, R. L. Hettich, A. S. Karim, S. D. Simpson, S. D. Brown, C. Leang, M. C. Jewett and M. Kopke, Carbon-negative production of acetone and isopropanol by gas fermentation at industrial pilot scale, *Nature Biotechnology*, 2022, **40**, 335-344. 10.1038/s41587-021-01195-w
91. K. W. Harrison and B. G. Harvey, High cetane renewable diesel fuels prepared from bio-based methyl ketones and diols, *Sustainable Energy & Fuels*, 2018, **2**, 367-371. 10.1039/C7SE00415J
92. G. Yu, T. T. H. Nguyen, Y. Guo, I. Schauvinhold, M. E. Aldridge, N. Bhuiyan, I. Ben-Israel, Y. Iijima, E. Fridman, J. P. Noel and E. Pichersky, Enzymatic Functions of Wild Tomato Methylketone Synthases 1 and 2, *Plant Physiology*, 2010, **154**, 67-77. 10.1104/pp.110.157073
93. F. W. Forney and A. J. Markovetz, The biology of methyl ketones, *Journal of Lipid Research*, 1971, **12**, 383-395. [https://doi.org/10.1016/S0022-2275\(20\)39487-6](https://doi.org/10.1016/S0022-2275(20)39487-6)
94. Z. Zhu, Y. J. Zhou, A. Krivoruchko, M. Grininger, Z. K. Zhao and J. Nielsen, Expanding the product portfolio of fungal type I fatty acid synthases, *Nature Chemical Biology*, 2017, **13**, 360-362. 10.1038/nchembio.2301
95. E. K. R. Hanco, C. M. Denby, I. N. V. Sanchez, W. Lin, K. J. Ramirez, C. A. Singer, G. T. Beckham and J. D. Keasling, Engineering beta-oxidation in *Yarrowia lipolytica* for methyl ketone production, *Metabolic Engineering*, 2018, **48**, 52-62. 10.1016/j.ymben.2018.05.018
96. J. Dong, Y. Chen, V. T. Benites, E. E. K. Baidoo, C. J. Petzold, H. R. Beller, A. Eudes, H. V. Scheller, P. D. Adams, A. Mukhopadhyay, B. A. Simmons and S. W. Singer, Methyl ketone production by *Pseudomonas putida* is enhanced by plant-derived amino acids, *Biotechnology and Bioengineering*, 2019, **116**, 1909-1922. 10.1002/bit.26995
97. S. C. Nies, T. B. Alter, S. Nötling, S. Thiery, A. N. T. Phan, N. Drummen, J. D. Keasling, L. M. Blank and B. E. Ebert, High titer methyl ketone production with tailored *Pseudomonas taiwanensis* VLB120, *Metabolic Engineering*, 2020, **62**, 84-94. 10.1016/j.ymben.2020.08.003
98. Q. Yan and B. F. Pfleger, Revisiting metabolic engineering strategies for microbial synthesis of oleochemicals, *Metabolic Engineering*, 2020, **58**, 35-46. 10.1016/j.ymben.2019.04.009
99. Q. Yan, T. R. Simmons, W. T. Cordell, N. J. Hernandez Lozada, C. J. Breckner, X. Chen, M. A. Jindra and B. F. Pfleger, Metabolic engineering of beta-oxidation to leverage thioesterases for production of 2-heptanone, 2-nonanone and 2-undecanone, *Metabolic Engineering*, 2020, **61**, 335-343. 10.1016/j.ymben.2020.05.008
100. M. Partipilo, E. J. Ewins, J. Frallicciardi, T. Robinson, B. Poolman and D. J. Slotboom, Minimal Pathway for the Regeneration of Redox Cofactors, *JACS Au*, 2021, **1**, 2280-2293. 10.1021/jacsau.1c00406
101. L. M. Blank, G. Ionidis, B. E. Ebert, B. Bühler and A. Schmid, Metabolic response of *Pseudomonas putida* during redox biocatalysis in the presence of a second octanol phase, *The FEBS Journal*, 2008, **275**, 5173-5190. <https://doi.org/10.1111/j.1742-4658.2008.06648.x>
102. P. I. Nikel, D. Pérez-Pantoja and V. de Lorenzo, Pyridine nucleotide transhydrogenases enable redox balance of *Pseudomonas putida* during biodegradation of aromatic compounds, *Environmental Microbiology*, 2016, **18**, 3565-3582. <https://doi.org/10.1111/1462-2920.13434>

103. K. A. Kohler, C. Ruckert, S. Schatschneider, F. J. Vorholter, R. Szczepanowski, L. M. Blank, K. Niehaus, A. Goesmann, A. Puhler, J. Kalinowski and A. Schmid, Complete genome sequence of *Pseudomonas* sp. strain VLB120 a solvent tolerant, styrene degrading bacterium, isolated from forest soil, *Journal of Biotechnology*, 2013, **168**, 729-730. 10.1016/j.jbiotec.2013.10.016
104. T. Schwanemann, M. Otto, N. Wierckx and B. Wynands, *Pseudomonas* as Versatile Aromatics Cell Factory, *Biotechnology Journal*, 2020, **15**, 1900569. <https://doi.org/10.1002/biot.201900569>
105. P. Demling, A. Ankenbauer, B. Klein, S. Noack, T. Tiso, R. Takors and L. M. Blank, *Pseudomonas putida* KT2440 endures temporary oxygen limitations, *Biotechnology and Bioengineering*, 2021, **118**, 4735-4750. <https://doi.org/10.1002/bit.27938>
106. D. Hoell, T. Mensing, R. Roggenbuck, M. Sakuth, E. Sperlich, T. Urban, W. Neier and G. Strehlke, 2-Butanone, in *Ullmann's Encyclopedia of Industrial Chemistry*, Wiley-VCH, 2009.
107. C. Hemken, U. Burke, K.-Y. Lam, D. F. Davidson, R. K. Hanson, K. A. Heufer and K. Kohse-Höinghaus, Toward a better understanding of 2-butanone oxidation: Detailed species measurements and kinetic modeling, *Combustion and Flame*, 2017, **184**, 195-207. <https://doi.org/10.1016/j.combustflame.2017.06.007>
108. H. Yoneda, D. J. Tantillo and S. Atsumi, Biological Production of 2-Butanone in *Escherichia coli*, *ChemSusChem*, 2014, **7**, 92-95. <https://doi.org/10.1002/cssc.201300853>
109. Z. Chen, H. Sun, J. Huang, Y. Wu and D. Liu, Metabolic Engineering of *Klebsiella pneumoniae* for the Production of 2-Butanone from Glucose, *PLOS ONE*, 2015, **10**, e0140508. 10.1371/journal.pone.0140508
110. M. Tokic, N. Hadadi, M. Ataman, D. Neves, B. E. Ebert, L. M. Blank, L. Miskovic and V. Hatzimanikatis, Discovery and Evaluation of Biosynthetic Pathways for the Production of Five Methyl Ethyl Ketone Precursors, *ACS Synthetic Biology*, 2018, **7**, 1858-1873. 10.1021/acssynbio.8b00049
111. C. R. Mehrer, J. M. Rand, M. R. Incha, T. B. Cook, B. Demir, A. H. Motagamwala, D. Kim, J. A. Dumesic and B. F. Pfleger, Growth-coupled bioconversion of levulinic acid to butanone, *Metabolic Engineering*, 2019, **55**, 92-101. <https://doi.org/10.1016/j.ymben.2019.06.003>
112. T. Harhues, L. Portheine, C. Plath, J. Viell, R. Keller, J. Büchs and M. Wessling, Direct Electrosynthesis of 2-Butanone from Fermentation Supernatant, *ACS Sustainable Chemistry & Engineering*, 2022, **10**, 6483-6492. 10.1021/acssuschemeng.2c01971
113. Z. Xiao and J. R. Lu, Strategies for enhancing fermentative production of acetoin: A review, *Biotechnology Advances*, 2014, **32**, 492-503. <https://doi.org/10.1016/j.biotechadv.2014.01.002>
114. S. Maina, A. A. Prabhu, N. Vivek, A. Vlysidis, A. Koutinas and V. Kumar, Prospects on bio-based 2,3-butanediol and acetoin production: Recent progress and advances, *Biotechnology Advances*, 2022, **54**, 107783. <https://doi.org/10.1016/j.biotechadv.2021.107783>
115. S. J. Bae, S. Kim and J. S. Hahn, Efficient production of acetoin in *Saccharomyces cerevisiae* by disruption of 2,3-butanediol dehydrogenase and expression of NADH oxidase, *Scientific Reports*, 2016, **6**, 27667. 10.1038/srep27667
116. V. Kandasamy, J. Liu, S. H. Dantoft, C. Solem and P. R. Jensen, Synthesis of (3R)-acetoin and 2,3-butanediol isomers by metabolically engineered *Lactococcus lactis*, *Scientific Reports*, 2016, **6**, 36769. 10.1038/srep36769
117. J. Arnau, F. Jørgensen, M. Madsen Søren, A. Vrang and H. Israelsen, Cloning of the *Lactococcus lactis adhE* Gene, Encoding a Multifunctional Alcohol Dehydrogenase, by Complementation of a Fermentative Mutant of *Escherichia coli*, *Journal of Bacteriology*, 1998, **180**, 3049-3055. 10.1128/jb.180.12.3049-3055.1998
118. S. M. de Smit, T. D. van Mameren, Y. Xie, D. P. B. T. B. Strik and J. H. Bitter, Trace metals from microbial growth media form *in situ* electro-catalysts, *Electrochimica Acta*, 2023, **462**, 142722. <https://doi.org/10.1016/j.electacta.2023.142722>
119. U. A. Salas-Villalobos, R. V. Gómez-Acata, J. Castillo-Reyna and O. Aguilar, *In situ* product recovery as a strategy for bioprocess integration and depletion of inhibitory products, *Journal of Chemical Technology & Biotechnology*, 2021, **96**, 2735-2743. <https://doi.org/10.1002/jctb.6797>
120. A. Freeman, J. M. Woodley and M. D. Lilly, *In Situ* Product Removal as a Tool for Bioprocessing, *BioTechnology*, 1993, **11**, 1007-1012. 10.1038/nbt0993-1007
121. N. Qureshi, M. A. Cotta and B. C. Saha, Bioconversion of barley straw and corn stover to butanol (a biofuel) in integrated fermentation and simultaneous product recovery bioreactors, *Food and Bioprocess Processing*, 2014, **92**, 298-308. <https://doi.org/10.1016/j.fbp.2013.11.005>
122. K. Schügerl and J. Hubbuch, Integrated bioprocesses, *Current Opinion in Microbiology*, 2005, **8**, 294-300. <https://doi.org/10.1016/j.mib.2005.01.002>
123. V. Outram, C. A. Lalander, J. G. M. Lee, E. T. Davies and A. P. Harvey, Applied *in situ* product recovery in ABE fermentation, *Biotechnol Prog*, 2017, **33**, 563-579. 10.1002/btpr.2446
124. P. Chaichol and N. Weeranoppanant, Advances in *in situ* and in-line liquid-liquid extraction for bioprocess intensification, *Reaction Chemistry & Engineering*, 2023, **8**, 2387-2402. 10.1039/D3RE00266G
125. C. Xue, J. Zhao, C. Lu, S.-T. Yang, F. Bai and I. C. Tang, High-titer n-butanol production by *clostridium acetobutylicum* JB200 in fed-batch fermentation with intermittent gas stripping, *Biotechnology and Bioengineering*, 2012, **109**, 2746-2756. <https://doi.org/10.1002/bit.24563>
126. E. Rochón, G. Cortizo, M. I. Cabot, M. T. García Cubero, M. Coca, M. D. Ferrari and C. Lareo, Bioprocess intensification for isopropanol, butanol and ethanol (IBE) production by fermentation from sugarcane and sweet sorghum juices through a gas stripping-pervaporation recovery process, *Fuel*, 2020, **281**, 118593. <https://doi.org/10.1016/j.fuel.2020.118593>



127. W. Yuan, M. Wiehn, Y. Wang, H. W. Kim, B. E. Rittmann and D. R. Nielsen, Solid-phase extraction of long-chain fatty acids from aqueous solution, *Separation and Purification Technology*, 2013, **106**, 1-7. <https://doi.org/10.1016/j.seppur.2012.12.025>
128. H. D. Lee, M. Y. Lee, Y. S. Hwang, Y. H. Cho, H. W. Kim and H. B. Park, Separation and Purification of Lactic Acid from Fermentation Broth Using Membrane-Integrated Separation Processes, *Industrial & Engineering Chemistry Research*, 2017, **56**, 8301-8310. 10.1021/acs.iecr.7b02011
129. W. Van Hecke, P. Vandezande, M. Dubreuil, M. Uytendaele, H. Beckers and H. De Wever, Biobutanol production from C5/C6 carbohydrates integrated with pervaporation: experimental results and conceptual plant design, *Journal of Industrial Microbiology and Biotechnology*, 2016, **43**, 25-36. 10.1007/s10295-015-1717-3
130. J. M. Woodley and N. J. Titchener-Hooker, The use of windows of operation as a bioprocess design tool, *Bioprocess Engineering*, 1996, **14**, 263-268. 10.1007/BF00369924
131. Y. H. Zhou and N. J. Titchener-Hooker, Visualizing integrated bioprocess designs through "windows of operation", *Biotechnology and Bioengineering*, 1999, **65**, 550-557. [https://doi.org/10.1002/\(SICI\)1097-0290\(19991205\)65:5<550::AID-BIT8>3.0.CO;2-0](https://doi.org/10.1002/(SICI)1097-0290(19991205)65:5<550::AID-BIT8>3.0.CO;2-0)
132. C. Xue, Z.-X. Wang, G.-Q. Du, L.-H. Fan, Y. Mu, J.-G. Ren and F.-W. Bai, Integration of ethanol removal using carbon nanotube (CNT)-mixed membrane and ethanol fermentation by self-flocculating yeast for antifouling ethanol recovery, *Process Biochemistry*, 2016, **51**, 1140-1146. <https://doi.org/10.1016/j.procbio.2016.05.030>
133. G. M. Teke and R. W. M. Pott, Design and evaluation of a continuous semipartition bioreactor for *in situ* liquid-liquid extractive fermentation, *Biotechnology and Bioengineering*, 2021, **118**, 58-71. <https://doi.org/10.1002/bit.27550>
134. A. Pérez de los Ríos, F. J. Hernández-Fernández, P. A. Zapata Henríquez, F. Missoun, J. Hernández-Fernández, V. Ortiz-Martínez, M. J. Salar-García, L. J. Lozano Blanco and C. Godínez, Keys for Bioethanol Production Processes by Fermentation and Ionic Liquid Extraction, *ACS Sustainable Chemistry & Engineering*, 2017, **5**, 6986-6993. 10.1021/acssuschemeng.7b01170
135. M. A. Eiteman and J. L. Gainer, *In situ* extraction versus the use of an external column in fermentation, *Applied Microbiology and Biotechnology*, 1989, **30**, 614-618. 10.1007/BF00255368
136. A. R. Lara, E. Galindo, O. T. Ramírez and L. A. Palomares, Living with heterogeneities in bioreactors, *Molecular Biotechnology*, 2006, **34**, 355-381. 10.1385/MB:34:3:355
137. J. Dafae and A. Daugulis, *In situ* product removal in fermentation systems: Improved process performance and rational extractant selection, *Biotechnology Letters*, 2014, **36**, 443-460. 10.1007/s10529-013-1380-6
138. P. Demling, M. von Campenhausen, C. Grütering, T. Tiso, A. Jupke and L. M. Blank, Selection of a recyclable *in situ* liquid-liquid extraction solvent for foam-free synthesis of rhamnolipids in a two-phase fermentation, *Green Chemistry*, 2020, **22**, 8495-8510. 10.1039/d0gc02885a
139. S. Dorobantu Loredana, K. C. Yeung Anthony, M. Foght Julia and R. Gray Murray, Stabilization of Oil-Water Emulsions by Hydrophobic Bacteria, *Applied and Environmental Microbiology*, 2004, **70**, 6333-6336. 10.1128/AEM.70.10.6333-6336.2004
140. B. P. Binks, Particles as surfactants - similarities and differences, *Current Opinion in Colloid & Interface Science*, 2002, **7**, 21-41. [https://doi.org/10.1016/S1359-0294\(02\)00008-0](https://doi.org/10.1016/S1359-0294(02)00008-0)
141. M. H. Ly, M. Naïtali-Bouchez, T. Meylheuc, M.-N. Bellon-Fontaine, T. M. Le, J.-M. Belin and Y. Waché, Importance of bacterial surface properties to control the stability of emulsions, *International Journal of Food Microbiology*, 2006, **112**, 26-34. <https://doi.org/10.1016/j.ijfoodmicro.2006.05.022>
142. A. S. Heeres, C. S. F. Picone, L. A. M. van der Wielen, R. L. Cunha and M. C. Cuellar, Microbial advanced biofuels production: overcoming emulsification challenges for large-scale operation, *Trends in Biotechnology*, 2014, **32**, 221-229. 10.1016/j.tibtech.2014.02.002
143. H. T. Chen and S. Middleman, Drop size distribution in agitated liquid-liquid systems, *AIChE Journal*, 1967, **13**, 989-995. <https://doi.org/10.1002/aic.690130529>
144. R. Verma, L. Mehan, R. Kumar, A. Kumar and A. Srivastava, Computational fluid dynamic analysis of hydrodynamic shear stress generated by different impeller combinations in stirred bioreactor, *Biochemical Engineering Journal*, 2019, **151**, 107312. <https://doi.org/10.1016/j.bej.2019.107312>
145. M. von Campenhausen, P. Demling, P. Bongartz, A. Scheele, T. Tiso, M. Wessling, L. M. Blank and A. Jupke, Novel multiphase loop reactor with improved aeration prevents excessive foaming in Rhamnolipid production by *Pseudomonas putida*, *Discover Chemical Engineering*, 2023, **3**, 2. 10.1007/s43938-023-00018-5
146. B. Weber, M. von Campenhausen, T. Maßmann, A. Bednarz and A. Jupke, CFD based compartment-model for a multiphase loop-reactor, *Chemical Engineering Science: X*, 2019, **2**, 100010. <https://doi.org/10.1016/j.cesx.2019.100010>
147. A. Bednarz, A. Jupke, M. Schmidt and B. Weber, Multi-phase loop reactor and method of operation, WO2017149099A1, 2017.
148. C. Grütering, C. Honecker, M. Hofmeister, M. Neumann, L. Raßpe-Lange, M. Du, B. Lehrheuer, M. von Campenhausen, F. Schuster, M. Surger, B. E. Ebert, A. Jupke, T. Tiso, K. Leonhard, K. Schmitz, S. Pischinger and L. M. Blank, Methyl ketones: a comprehensive study of a novel biofuel, *Sustainable Energy & Fuels*, 2024, **8**, 2059-2072. 10.1039/D4SE00035H
149. G. P. Prpich and A. J. Daugulis, Solvent selection for enhanced bioproduction of 3-methylcatechol in a two-phase partitioning bioreactor, *Biotechnol Bioeng*, 2007, **97**, 536-543. 10.1002/bit.21257

150. M. Anvari, H. Pahlavanzadeh, E. Vasheghani-Farahani and G. Khayati, *In situ* recovery of 2,3-butanediol from fermentation by liquid–liquid extraction, *Journal of Industrial Microbiology & Biotechnology*, 2009, **36**, 873–873. 10.1007/s10295-009-0586-z
151. A. K. Sánchez-Castañeda, M. Moussa, L. Ngansop, I. C. Trelea and V. Athès, Organic phase screening for in-stream reactive extraction of bio-based 3-hydroxypropionic acid: biocompatibility and extraction performances, *Journal of Chemical Technology & Biotechnology*, 2020, **95**, 1046–1056. <https://doi.org/10.1002/jctb.6284>
152. L. J. Bruce and A. J. Daugulis, Solvent Selection Strategies for Extractive Biocatalysis, *Biotechnology Progress*, 1991, **7**, 116–124. <https://doi.org/10.1021/bp00008a006>
153. P. De Brabander, E. Uitterhaegen, E. Verhoeven, C. Vander Cruysen, K. De Winter and W. Soetaert, *In Situ* Product Recovery of Bio-Based Industrial Platform Chemicals: A Guideline to Solvent Selection, *Fermentation*, 2021, **7**, 26. 10.3390/fermentation7010026
154. A. F. Arroyo-Avira, S. Carreño-Guzmán, J. Lorenzo-Llanes, N. F. Gajardo-Parra, R. Santiago, C. Held, J. Palomar and R. I. Canales, *In Situ* Product Recovery of  $\beta$ -Ionone from a Fermentation Broth: Computational Solvent Selection and Process Design of Its Extraction and Purification, *ACS Sustainable Chemistry & Engineering*, 2023, **11**, 9065–9076. 10.1021/acssuschemeng.3c01739
155. A. Inoue and K. Horikoshi, Estimation of solvent-tolerance of bacteria by the solvent parameter log *P*, *Journal of Fermentation and Bioengineering*, 1991, **71**, 194–196. [https://doi.org/10.1016/0922-338X\(91\)90109-T](https://doi.org/10.1016/0922-338X(91)90109-T)
156. Y. N. Sardesai and S. Bhosle, Industrial Potential of Organic Solvent Tolerant Bacteria, *Biotechnology Progress*, 2004, **20**, 655–660. <https://doi.org/10.1021/bp0200595>
157. H. J. Heipieper, F. J. Weber, J. Sikkema, H. Keweloh and J. A. M. de Bont, Mechanisms of resistance of whole cells to toxic organic solvents, *Trends in Biotechnology*, 1994, **12**, 409–415. [https://doi.org/10.1016/0167-7799\(94\)90029-9](https://doi.org/10.1016/0167-7799(94)90029-9)
158. D. J. W. Blum and R. E. Speece, Quantitative structure-activity relationships for chemical toxicity to environmental bacteria, *Ecotoxicology and Environmental Safety*, 1991, **22**, 198–224. [https://doi.org/10.1016/0147-6513\(91\)90059-X](https://doi.org/10.1016/0147-6513(91)90059-X)
159. J. L. Ramos, E. Duque, M.-T. Gallegos, P. Godoy, M. I. Ramos-González, A. Rojas, W. Terán and A. Segura, Mechanisms of Solvent Tolerance in Gram-Negative Bacteria, *Annual Review of Microbiology*, 2002, **56**, 743–768. 10.1146/annurev.micro.56.012302.161038
160. S. P.-d. I. Cuesta, L. Knopper, L. A. M. van der Wielen and M. C. Cuellar, Techno-economic assessment of the use of solvents in the scale-up of microbial sesquiterpene production for fuels and fine chemicals, *Biofuels, Bioproducts and Biorefining*, 2019, **13**, 140–152. 10.1002/bbb.1949
161. A. G. Santos, T. L. de Albuquerque, B. D. Ribeiro and M. A. Z. Coelho, *In situ* product recovery techniques aiming to obtain biotechnological products: A glance to current knowledge, *Biotechnology and Applied Biochemistry*, 2021, **68**, 1044–1057. <https://doi.org/10.1002/bab.2024>
162. M. Froning, C. Grütering, L. M. Blank and H. Hayen, Determination of double bond positions in methyl ketones by gas chromatography–mass spectrometry using dimethyl disulfide derivatives, *Rapid Communications in Mass Spectrometry*, 2023, **37**, e9457. <https://doi.org/10.1002/rcm.9457>
163. D. Hanahan, Studies on transformation of *Escherichia coli* with plasmids, *Journal of Molecular Biology*, 1983, **166**, 557–580. [https://doi.org/10.1016/S0022-2836\(83\)80284-8](https://doi.org/10.1016/S0022-2836(83)80284-8)
164. S. Hartmans, J. P. Smits, M. J. van der Werf, F. Volkering and J. A. de Bont, Metabolism of Styrene Oxide and 2-Phenylethanol in the Styrene-Degrading *Xanthobacter* Strain 124X, *Applied and Environmental Microbiology*, 1989, **55**, 2850–2855. 10.1128/aem.55.11.2850-2855.1989
165. R. Breit, Optimizing methyl ketone production in *Pseudomonas taiwanensis* VLB120 for the production of advanced oleochemicals, Institute of Applied Microbiology, RWTH Aachen, 2023.
166. N. J. Hernandez Lozada, R. Y. Lai, T. R. Simmons, K. A. Thomas, R. Chowdhury, C. D. Maranas and B. F. Pfeleger, Highly Active C<sub>8</sub>-Acyl-ACP Thioesterase Variant Isolated by a Synthetic Selection Strategy, *ACS Synthetic Biology*, 2018, **7**, 2205–2215. 10.1021/acssynbio.8b00215
167. K.-H. Choi, A. Kumar and H. P. Schweizer, A 10-min method for preparation of highly electrocompetent *Pseudomonas aeruginosa* cells: Application for DNA fragment transfer between chromosomes and plasmid transformation, *Journal of Microbiological Methods*, 2006, **64**, 391–397. <https://doi.org/10.1016/j.mimet.2005.06.001>
168. M. Kunze, C. Lattermann, S. Diederichs, W. Kroutil and J. Buchs, Minireactor-based high-throughput temperature profiling for the optimization of microbial and enzymatic processes, *Journal of Biological Engineering*, 2014, **8**, 22. 10.1186/1754-1611-8-22
169. National Institutes of Health, PubChem, <https://pubchem.ncbi.nlm.nih.gov/>, (accessed September 17, 2023).
170. Deutsche Gesetzliche Unfallversicherung, GESTIS-Stoffdatenbank, <http://www.dguv.de/ifa/stoffdatenbank/>, (accessed September 28, 2023).
171. L. E. Hüsken, M. Oomes, K. Schroën, J. Tramper, J. A. M. de Bont and R. Beekink, Membrane-facilitated bioproduction of 3-methylcatechol in an octanol/water two-phase system, *Journal of Biotechnology*, 2002, **96**, 281–289. [https://doi.org/10.1016/S0168-1656\(02\)00045-7](https://doi.org/10.1016/S0168-1656(02)00045-7)
172. A. Biselli, A.-L. Willenbrink, M. Leipnitz and A. Jupke, Development, evaluation, and optimisation of downstream process concepts for rhamnolipids and 3-(3-hydroxyalkanyloxy)alkanoic acids, *Separation and Purification Technology*, 2020, **250**, 117031. 10.1016/j.seppur.2020.117031



173. *Messung der kinematischen Viskosität mit dem Ubbelohde-Viskosimeter*, Report DIN 51562-1, Beuth Verlag GmbH, Berlin, 1976.
174. M. Hofmeister, A. Frische, M. Grunewald, M. A. Reddemann, C. Grütering, L. M. Blank, R. Kneer and K. Schmitz, Tribological properties of PTFE sealing materials with regard to bio-hybrid fuels, 21. International Sealing Conference, Stuttgart, Germany, October 12-13, 2022.
175. M. Hofmeister, J. Laker, M. Fischer, S. Pischinger and K. Schmitz, Neue Herausforderungen an Dichtungswerkstoffe im Hinblick auf bio-hybride Kraftstoffe, *Mobility*, 2022, **7**, 44-48.
176. *Elastomere oder thermoplastische Elastomere*, Report DIN ISO 1817, Beuth Verlag GmbH, Berlin, 2016.
177. *Elastomere - Standard - Referenz - Elastomere (SRES) zur Charakterisierung des Verhaltens von Flüssigkeiten auf Elastomere*, Report DIN ISO 13226, Beuth Verlag GmbH, Berlin, 2021.
178. *Elastomere oder thermoplastische Elastomere*, Report DIN ISO 48, Beuth Verlag GmbH, Berlin, 2016.
179. *Dieselmotoren – Bestimmung der Schmierfähigkeit unter Verwendung eines Schwingungsverschleiß-Prüfgerätes (HFRR)*, Report DIN EN ISO 12156, Beuth Verlag GmbH, Berlin, 2019.
180. A. Klamt, F. Eckert and W. Arlt, COSMO-RS: An Alternative to Simulation for Calculating Thermodynamic Properties of Liquid Mixtures, *Annual Review of Chemical and Biomolecular Engineering*, 2010, **1**, 101-122. [10.1146/annurev-chembioeng-073009-100903](https://doi.org/10.1146/annurev-chembioeng-073009-100903)
181. J. Reinisch and A. Klamt, Predicting Flash Points of Pure Compounds and Mixtures with COSMO-RS, *Industrial & Engineering Chemistry Research*, 2015, **54**, 12974-12980. [10.1021/acs.iecr.5b03083](https://doi.org/10.1021/acs.iecr.5b03083)
182. J. P. Perdew, Density-functional approximation for the correlation energy of the inhomogeneous electron gas, *Physical Review B*, 1986, **33**, 8822-8824. [10.1103/PhysRevB.33.8822](https://doi.org/10.1103/PhysRevB.33.8822)
183. A. D. Becke, Density-functional exchange-energy approximation with correct asymptotic behavior, *Physical Review A*, 1988, **38**, 3098-3100. [10.1103/PhysRevA.38.3098](https://doi.org/10.1103/PhysRevA.38.3098)
184. A. Schäfer, C. Huber and R. Ahlrichs, Fully optimized contracted Gaussian basis sets of triple zeta valence quality for atoms Li to Kr, *The Journal of Chemical Physics*, 1994, **100**, 5829-5835. [10.1063/1.467146](https://doi.org/10.1063/1.467146)
185. P. Seidenspinner, *AFIDA 2805 Advanced Fuel Ignition Delay Analyzer Research Versions*, ASG Analytik-Service AG, Neusaess, Germany, 2023.
186. D02 Committee, *Standard test method for determination of indicated cetane number (ICN) of diesel fuel oils using a constant volume combustion chamber reference fuels calibration method*, Report ASTM D8183-22, 2022.
187. A. Janssen, M. Muether, S. Pischinger, A. Kolbeck and M. Lamping, *Tailor-made fuels: the potential of oxygen content in fuels for advanced diesel combustion systems*, Report 2009-01-2765, SAE technical paper series, 2009.
188. B. Heuser, F. Kremer, S. Pischinger, J. Julis and W. Leitner, *Optimization of diesel combustion and emissions with newly derived biogenic alcohols*, Report 0148-7191, SAE International, 2013.
189. B. Heuser, M. Jakob, T. Laible, F. Kremer and S. Pischinger, *C<sub>8</sub>-Oxygenates for Clean Diesel Combustion*, Report 2014-01-1253, 2014.
190. C. Honecker, B. Lehrheuer, S. Pischinger and K. A. Heufer, Molecularly-controlled high swirl combustion system for ethanol 1-octanol dual fuel combustion, *Fuel*, 2023, **345**, 128184. <https://doi.org/10.1016/j.fuel.2023.128184>
191. B. Leuchtle, L. Epping, W. Xie, S. J. Eiden, W. Koch, D. Diarra, K. Lucka, M. Zimmermann and L. M. Blank, Defined inoculum for the investigation of microbial contaminations of liquid fuels, *International Biodeterioration & Biodegradation*, 2018, **132**, 84-93. <https://doi.org/10.1016/j.ibiod.2017.05.017>
192. P. Ackermann, K. E. Braun, P. Burkardt, S. Heger, A. König, P. Morsch, B. Lehrheuer, M. Surger, S. Volker, L. M. Blank, M. Du, K. A. Heufer, M. Ross-Nickoll, J. Viell, N. von der Assen, A. Mitsos, S. Pischinger and M. Dahmen, Designed to Be Green, Economic, and Efficient: A Ketone-Ester-Alcohol-Alkane Blend for Future Spark-Ignition Engines, *ChemSusChem*, 2021, **14**, 5254-5264. [10.1002/cssc.202101704](https://doi.org/10.1002/cssc.202101704)
193. S. Heger, J. Brendt, H. Hollert, M. Roß-Nickoll and M. Du, Green toxicological investigation for biofuel candidates, *Science of The Total Environment*, 2021, **764**, 142902. <https://doi.org/10.1016/j.scitotenv.2020.142902>
194. N. I. Vollmer, J. L. S. P. Driessen, C. K. Yamakawa, K. V. Gernaey, S. I. Mussatto and G. Sin, Model development for the optimization of operational conditions of the pretreatment of wheat straw, *Chemical Engineering Journal*, 2022, **430**, 133106. <https://doi.org/10.1016/j.cej.2021.133106>
195. Z. Liu, A. M. Feist, G. Dragone and S. I. Mussatto, Lipid and carotenoid production from wheat straw hydrolysates by different oleaginous yeasts, *Journal of Cleaner Production*, 2020, **249**, 119308. <https://doi.org/10.1016/j.jclepro.2019.119308>
196. L. F. Ballesteros, J. A. Teixeira and S. I. Mussatto, Selection of the Solvent and Extraction Conditions for Maximum Recovery of Antioxidant Phenolic Compounds from Coffee Silverskin, *Food and Bioprocess Technology*, 2014, **7**, 1322-1332. [10.1007/s11947-013-1115-7](https://doi.org/10.1007/s11947-013-1115-7)
197. J. Nogales, J. Mueller, S. Gudmundsson, F. J. Canalejo, E. Duque, J. Monk, A. M. Feist, J. L. Ramos, W. Niu and B. O. Palsson, High-quality genome-scale metabolic modelling of *Pseudomonas putida* highlights its broad metabolic capabilities, *Environmental Microbiology*, 2020, **22**, 255-269. <https://doi.org/10.1111/1462-2920.14843>
198. J. Nogales, S. Gudmundsson, E. Duque, J. L. Ramos and B. O. Palsson, Expanding the computable reactome in *Pseudomonas putida* reveals metabolic cycles providing robustness, *bioRxiv*, 2017, 139121. [10.1101/139121](https://doi.org/10.1101/139121)

199. A. L. Ziegler, C. Grütering, L. Poduschnick, A. Mitsos and L. M. Blank, Open-source dataset: Co-feeding enhances the yield of methyl ketones, [https://git.rwth-aachen.de/avt-svt/public/methylketones\\_cofeeding](https://git.rwth-aachen.de/avt-svt/public/methylketones_cofeeding), 2023.
200. B. E. Ebert, F. Kurth, M. Grund, L. M. Blank and A. Schmid, Response of *Pseudomonas putida* KT2440 to increased NADH and ATP demand, *Applied and Environmental Microbiology*, 2011, **77**, 6597-6605. 10.1128/AEM.05588-11
201. A. Ebrahim, J. A. Lerman, B. O. Palsson and D. R. Hyde, COBRApy: COntstraints-Based Reconstruction and Analysis for Python, *BMC Systems Biology*, 2013, **7**, 74. 10.1186/1752-0509-7-74
202. A. Varma and B. O. Palsson, Stoichiometric flux balance models quantitatively predict growth and metabolic by-product secretion in wild-type *Escherichia coli* W3110, *Applied and Environmental Microbiology*, 1994, **60**, 3724-3731. doi:10.1128/aem.60.10.3724-3731.1994
203. R. Takors, Systembiologie in der Bioverfahrenstechnik, in *Bioprozesstechnik*, eds. H. Chmiel, R. Takors and D. Weuster-Botz, Springer Berlin Heidelberg, Berlin, Heidelberg, 3 edn., 2018, pp. 545-569.
204. C. Dellomonaco, J. M. Clomburg, E. N. Miller and R. Gonzalez, Engineered reversal of the beta-oxidation cycle for the synthesis of fuels and chemicals, *Nature*, 2011, **476**, 355-359. 10.1038/nature10333
205. Statista, Distribution of carbon dioxide emissions worldwide in 2021, by sector, <https://www.statista.com/statistics/1129656/global-share-of-co2-emissions-from-fossil-fuel-and-cement/>, (accessed July 05, 2023).
206. K. Maniatis, D. Chiaramonti and E. van den Heuvel, Post COVID-19 Recovery and 2050 Climate Change Targets: Changing the Emphasis from Promotion of Renewables to Mandated Curtailment of Fossil Fuels in the EU Policies, *Energies*, 2021, **14**, 1347.
207. M. Contestabile, G. J. Offer, R. Slade, F. Jaeger and M. Thoenes, Battery electric vehicles, hydrogen fuel cells and biofuels. Which will be the winner?, *Energy & Environmental Science*, 2011, **4**, 3754-3772. 10.1039/C1EE01804C
208. P. Burkardt, M. Fleischmann, T. Wegmann, M. Braun, J. Knöll, L. Schumacher, F. vom Lehn, B. Lehrheuer, M. Meinke, H. Pitsch, R. Kneer, W. Schröder and S. Pischinger, On the Use of Active Pre-chambers and Bio-hybrid Fuels in Internal Combustion Engines, in *Engines and Fuels for Future Transport*, eds. G. Kalghatgi, A. K. Agarwal, F. Leach and K. Senecal, Springer Singapore, Singapore, 1 edn., 2022, pp. 205-231.
209. K. Lokesh, L. Ladu and L. Summerton, Bridging the Gaps for a 'Circular' Bioeconomy: Selection Criteria, Bio-Based Value Chain and Stakeholder Mapping, *Sustainability*, 2018, **10**, 1695.
210. M. A. Masri, D. Garbe, N. Mehlmer and T. B. Brück, A sustainable, high-performance process for the economic production of waste-free microbial oils that can replace plant-based equivalents, *Energy & Environmental Science*, 2019, **12**, 2717-2732. 10.1039/c9ee00210c
211. T. N. Do, C. You and J. Kim, A CO<sub>2</sub> utilization framework for liquid fuels and chemical production: techno-economic and environmental analysis, *Energy & Environmental Science*, 2022, **15**, 169-184. 10.1039/D1EE01444G
212. L. R. Lynd, G. T. Beckham, A. M. Guss, L. N. Jayakody, E. M. Karp, C. Maranas, R. L. McCormick, D. Amador-Noguez, Y. J. Bomble, B. H. Davison, C. Foster, M. E. Himmel, E. K. Holwerda, M. S. Laser, C. Y. Ng, D. G. Olson, Y. Román-Leshkov, C. T. Trinh, G. A. Tuskan, V. Upadhyay, D. R. Vardon, L. Wang and C. E. Wyman, Toward low-cost biological and hybrid biological/catalytic conversion of cellulosic biomass to fuels, *Energy & Environmental Science*, 2022, **15**, 938-990. 10.1039/D1EE02540F
213. M. Antar, D. Lyu, M. Nazari, A. Shah, X. Zhou and D. L. Smith, Biomass for a sustainable bioeconomy: An overview of world biomass production and utilization, *Renewable and Sustainable Energy Reviews*, 2021, **139**, 110691. <https://doi.org/10.1016/j.rser.2020.110691>
214. G. Antranikian and W. R. Streit, Microorganisms harbor keys to a circular bioeconomy making them useful tools in fighting plastic pollution and rising CO<sub>2</sub> levels, *Extremophiles*, 2022, **26**, 10. 10.1007/s00792-022-01261-4
215. D. Dahiya, H. Sharma, A. K. Rai and P. S. Nigam, Application of biological systems and processes employing microbes and algae to Reduce, Recycle, Reuse (3Rs) for the sustainability of circular bioeconomy, *AIMS Microbiology*, 2022, **8**, 83-102. 10.3934/microbiol.2022008
216. J. Wesseler, G. Kleter, M. Meulenbroek and K. P. Purnhagen, EU regulation of genetically modified microorganisms in light of new policy developments: Possible implications for EU bioeconomy investments, *Applied Economic Perspectives and Policy*, 2023, **45**, 839-859. <https://doi.org/10.1002/aep.13259>
217. S. C. Nies, R. Dinger, Y. Chen, G. G. Wordofa, M. Kristensen, K. Schneider, J. Büchs, C. J. Petzold, J. D. Keasling, L. M. Blank and B. E. Ebert, The metabolic response of *Pseudomonas taiwanensis* to NADH dehydrogenase deficiency, *Applied and Environmental Microbiology*, 2019, **86**, e03038-03019. 10.1101/624536
218. J. Volmer, A. Schmid and B. Buhler, The application of constitutively solvent-tolerant *P. taiwanensis* VLB120ΔCΔttgV for stereospecific epoxidation of toxic styrene alleviates carrier solvent use, *Biotechnology Journal*, 2017, **12**, 1600558. 10.1002/biot.201600558
219. M. R. Pursell, M. A. Mendes-Tatsis and D. C. Stuckey, Effect of fermentation broth and biosurfactants on mass transfer during liquid-liquid extraction, *Biotechnology and Bioengineering*, 2004, **85**, 155-165. <https://doi.org/10.1002/bit.10840>

220. H. Gonzalez-Penas, T. A. Lu-Chau, M. T. Moreira and J. M. Lema, Solvent screening methodology for *in situ* ABE extractive fermentation, *Applied Microbiology and Biotechnology*, 2014, **98**, 5915-5924. 10.1007/s00253-014-5634-6
221. K. Khosravi-Darani and E. Vasheghani-Farahani, Application of Supercritical Fluid Extraction in Biotechnology, *Critical Reviews in Biotechnology*, 2005, **25**, 231-242. 10.1080/07388550500354841
222. C. Brandenbusch, S. Glonke, J. Collins, R. Hoffrogge, K. Grunwald, B. Bühler, A. Schmid and G. Sadowski, Process boundaries of irreversible scCO<sub>2</sub>-assisted phase separation in biphasic whole-cell biocatalysis, *Biotechnology and Bioengineering*, 2015, **112**, 2316-2323. <https://doi.org/10.1002/bit.25655>
223. S. Glonke, G. Sadowski and C. Brandenbusch, Applied catastrophic phase inversion: a continuous non-centrifugal phase separation step in biphasic whole-cell biocatalysis, *Journal of Industrial Microbiology and Biotechnology*, 2016, **43**, 1527-1535. 10.1007/s10295-016-1837-4
224. J. T. Boock, A. J. E. Freedman, G. A. Tompsett, S. K. Muse, A. J. Allen, L. A. Jackson, B. Castro-Dominguez, M. T. Timko, K. L. J. Prather and J. R. Thompson, Engineered microbial biofuel production and recovery under supercritical carbon dioxide, *Nature Communications*, 2019, **10**, 587. 10.1038/s41467-019-08486-6
225. L. Janssen, G. Sadowski and C. Brandenbusch, Continuous phase separation of stable emulsions from biphasic whole-cell biocatalysis by catastrophic phase inversion, *Biotechnology Journal*, 2023, **18**, e2200489. <https://doi.org/10.1002/biot.202200489>
226. A. Bednarz, Development of a systematic evaluation of process alternatives for separation of bio-based diamines, Aachener Verfahrenstechnik, RWTH Aachen, 2019.
227. H. J. Heipieper and J. A. de Bont, Adaptation of *Pseudomonas putida* S12 to ethanol and toluene at the level of fatty acid composition of membranes, *Applied and Environmental Microbiology*, 1994, **60**, 4440-4444. doi:10.1128/aem.60.12.4440-4444.1994
228. J. Volmer, C. Neumann, B. Bühler and A. Schmid, Engineering of *Pseudomonas taiwanensis* VLB120 for constitutive solvent tolerance and increased specific styrene epoxidation activity, *Applied and Environmental Microbiology*, 2014, **80**, 6539-6548. 10.1128/AEM.01940-14
229. B. Wynands, M. Otto, N. Runge, S. Preckel, T. Polen, L. M. Blank and N. Wierckx, Streamlined *Pseudomonas taiwanensis* VLB120 Chassis Strains with Improved Bioprocess Features, *ACS Synthetic Biology*, 2019, **8**, 2036-2050. 10.1021/acssynbio.9b00108
230. H. Kusumawardhani, R. Hosseini and J. H. de Winde, Solvent Tolerance in Bacteria: Fulfilling the Promise of the Biotech Era?, *Trends in Biotechnology*, 2018, **36**, 1025-1039. 10.1016/j.tibtech.2018.04.007
231. P. Bernal, A. Segura and J.-L. Ramos, Compensatory role of the cis-trans-isomerase and cardiolipin synthase in the membrane fluidity of *Pseudomonas putida* DOT-T1E, *Environmental Microbiology*, 2007, **9**, 1658-1664. <https://doi.org/10.1111/j.1462-2920.2007.01283.x>
232. D. Prat, J. Hayler and A. Wells, A survey of solvent selection guides, *Green Chemistry*, 2014, **16**, 4546-4551. 10.1039/c4gc01149j
233. D. Prat, A. Wells, J. Hayler, H. Sneddon, C. R. McElroy, S. Abou-Shehadeh and P. J. Dunn, CHEM21 selection guide of classical- and less classical-solvents, *Green Chemistry*, 2016, **18**, 288-296. 10.1039/c5gc01008j
234. H. J. Heipieper, G. Neumann, S. Cornelissen and F. Meinhardt, Solvent-tolerant bacteria for biotransformations in two-phase fermentation systems, *Applied Microbiology and Biotechnology*, 2007, **74**, 961-973. 10.1007/s00253-006-0833-4
235. M. F. Hassan, M. Z. M. Saman, S. Sharif and B. Omar, Sustainability evaluation of alternative part configurations in product design: weighted decision matrix and artificial neural network approach, *Clean Technologies and Environmental Policy*, 2016, **18**, 63-79. 10.1007/s10098-015-0990-1
236. Q. Chen, D. B. Janssen and B. Witholt, Growth on octane alters the membrane lipid fatty acids of *Pseudomonas oleovorans* due to the induction of alkB and synthesis of octanol, *Journal of Bacteriology*, 1995, **177**, 6894-6901. 10.1128/jb.177.23.6894-6901.1995
237. F. Schuster, Solvent screening for microbial biofuel production with *Pseudomonas taiwanensis* VLB120, Institute of Applied Microbiology, RWTH Aachen, 2021.
238. S. Pedraza-de la Cuesta, L. Keijzers, L. A. M. van der Wielen and M. C. Cuellar, Integration of Gas Enhanced Oil Recovery in Multiphase Fermentations for the Microbial Production of Fuels and Chemicals, *Biotechnology Journal*, 2018, **13**, e1700478. 10.1002/biot.201700478
239. M. Matsumoto, K. Mochiduki and K. Kondo, Toxicity of ionic liquids and organic solvents to lactic acid-producing bacteria, *Journal of Bioscience and Bioengineering*, 2004, **98**, 344-347. [https://doi.org/10.1016/S1389-1723\(04\)00293-2](https://doi.org/10.1016/S1389-1723(04)00293-2)
240. R. Bar, Effect of interphase mixing on a water-organic solvent two-liquid phase microbial system: ethanol fermentation, *Journal of Chemical Technology & Biotechnology*, 1988, **43**, 49-62. <https://doi.org/10.1002/jctb.280430106>
241. E. B. Goh, Y. Chen, C. J. Petzold, J. D. Keasling and H. R. Beller, Improving methyl ketone production in *Escherichia coli* by heterologous expression of NADH-dependent FabG, *Biotechnology and Bioengineering*, 2018, **115**, 1161-1172. 10.1002/bit.26558
242. M. A. Hazrat, M. G. Rasul, M. Mofijur, M. M. K. Khan, F. Djavandroodi, A. K. Azad, M. M. K. Bhuiya and A. S. Silitonga, A Mini Review on the Cold Flow Properties of Biodiesel and its Blends, *Frontiers in Energy Research*, 2020, **8**, 598651. 10.3389/fenrg.2020.598651

243. A. Nicolau, C. V. Lutckmeier, D. Samios, M. Gutterres and C. M. S. Piatnick, The relation between lubricity and electrical properties of low sulfur diesel and diesel/biodiesel blends, *Fuel*, 2014, **117**, 26-32. <https://doi.org/10.1016/j.fuel.2013.09.026>
244. B. Graziano, F. Kremer, S. Pischinger, K. A. Heufer and H. Rohs, On the Potential of Oxygenated Fuels as an Additional Degree of Freedom in the Mixture Formation in Direct Injection Diesel Engines, *SAE International journal of fuels and lubricants*, 2015, **8**, 62-79.
245. M. Zübel, O. P. Bhardwaj, B. Heuser, B. Holderbaum, S. Doerr and J. Nuottimäki, Advanced fuel formulation approach using blends of paraffinic and oxygenated biofuels: analysis of emission reduction potential in a high efficiency diesel combustion system, *SAE International journal of fuels and lubricants*, 2016, **9**, 481-492.
246. M. J. Surger and L. M. Blank, Assessment of microbial activity by CO<sub>2</sub> production during heating oil storage, *Engineering in Life Sciences*, 2022, **22**, 508-518. <https://doi.org/10.1002/elsc.202100144>
247. M. Gürü, U. Karakaya, D. Altıparmak and A. Alicılar, Improvement of Diesel fuel properties by using additives, *Energy Conversion and Management*, 2002, **43**, 1021-1025. [https://doi.org/10.1016/S0196-8904\(01\)00094-2](https://doi.org/10.1016/S0196-8904(01)00094-2)
248. P. Suppajariyawat, A. F. B. d. Andrade, M. Elie, M. Baron and J. Gonzalez-Rodriguez, The Use Of Chemical Composition And Additives To Classify Petrol And Diesel Using Gas Chromatography–Mass Spectrometry And Chemometric Analysis: A Uk Study, *Open Chemistry*, 2019, **17**, 183-197. doi:10.1515/chem-2019-0021
249. A. Völker, A. Kirschner, U. T. Bornscheuer and J. Altenbuchner, Functional expression, purification, and characterization of the recombinant Baeyer-Villiger monooxygenase MekA from *Pseudomonas veronii* MEK700, *Applied Microbiology and Biotechnology*, 2008, **77**, 1251-1260. 10.1007/s00253-007-1264-6
250. N. Graf and J. Altenbuchner, Functional characterization and application of a tightly regulated MekR/P<sup>mekA</sup> expression system in *Escherichia coli* and *Pseudomonas putida*, *Applied Microbiology and Biotechnology*, 2013, **97**, 8239-8251. 10.1007/s00253-013-5030-7
251. J. Frey, S. Kaßner and B. Schink, Two Marine *Desulfotomaculum* spp. of Different Origin are Capable of Utilizing Acetone and Higher Ketones, *Current Microbiology*, 2021, **78**, 1763-1770. 10.1007/s00284-021-02441-9
252. F. E. Khalid, Z. S. Lim, S. Sabri, C. Gomez-Fuentes, A. Zulkharnain and S. A. Ahmad, Bioremediation of Diesel Contaminated Marine Water by Bacteria: A Review and Bibliometric Analysis, *Journal of Marine Science and Engineering*, 2021, **9**, 155.
253. L. N. Komariah, S. Arita, M. Rendana, C. Ramayanti, N. L. Suriani and D. Erisna, Microbial contamination of diesel-biodiesel blends in storage tank; an analysis of colony morphology, *Heliyon*, 2022, **8**, e09264. <https://doi.org/10.1016/j.heliyon.2022.e09264>
254. C. Eickhoff, W. Hobbs, J. Weakland, A. Buchan, K. Lee, M. Tran and H. C. Bailey, Toxicity of gasoline, diesel and weathered diesel related petroleum hydrocarbons to freshwater and marine organisms, Salts Sea Ecosystem Conference, April 21, 2020.
255. L. M. Blank, T. Naranic, J. Mampel, T. Tiso and K. O'Connor, Biotechnological upcycling of plastic waste and other non-conventional feedstocks in a circular economy, *Current Opinion in Biotechnology*, 2020, **62**, 212-219. <https://doi.org/10.1016/j.copbio.2019.11.011>
256. E. Çelik, N. Ozbay, N. Oktar and P. Çalık, Use of Biodiesel Byproduct Crude Glycerol as the Carbon Source for Fermentation Processes by Recombinant *Pichia pastoris*, *Industrial & Engineering Chemistry Research*, 2008, **47**, 2985-2990. 10.1021/ie071613o
257. S. I. Mussatto, C. K. Yamakawa, L. van der Maas and G. Dragone, New trends in bioprocesses for lignocellulosic biomass and CO<sub>2</sub> utilization, *Renewable and Sustainable Energy Reviews*, 2021, **152**, 111620. <https://doi.org/10.1016/j.rser.2021.111620>
258. J. E. G. van Dam, B. de Klerk-Engels, P. C. Struik and R. Rabbinge, Securing renewable resource supplies for changing market demands in a bio-based economy, *Industrial Crops and Products*, 2005, **21**, 129-144. <https://doi.org/10.1016/j.indcrop.2004.02.003>
259. A. Tyczewski, T. Twardowski and E. Woźniak-Gientka, Agricultural biotechnology for sustainable food security, *Trends in Biotechnology*, 2023, **41**, 331-341. 10.1016/j.tibtech.2022.12.013
260. F. Saâdaoui, S. Ben Jabeur and J. W. Goodell, Causality of geopolitical risk on food prices: Considering the Russo–Ukrainian conflict, *Finance Research Letters*, 2022, **49**, 103103. <https://doi.org/10.1016/j.frl.2022.103103>
261. G. Wu, Q. Yan, J. A. Jones, Y. J. Tang, S. S. Fong and M. A. G. Koffas, Metabolic Burden: Cornerstones in Synthetic Biology and Metabolic Engineering Applications, *Trends in Biotechnology*, 2016, **34**, 652-664. <https://doi.org/10.1016/j.tibtech.2016.02.010>
262. Y. Liu, Y. Cao, G. Du and L. Liu, Systems and synthetic metabolic engineering: Challenges and prospects, in *Systems and Synthetic Metabolic Engineering*, eds. L. Liu, G. Du and Y. Liu, Academic Press, 1 edn., 2020, pp. 237-264.
263. T. N. K. Zu, S. Liu, E. S. Gerlach, W. Mojadedi and C. J. Sund, Co-feeding glucose with either gluconate or galacturonate during clostridial fermentations provides metabolic fine-tuning capabilities, *Scientific Reports*, 2021, **11**, 29. 10.1038/s41598-020-76761-4
264. B. G. Ergün, J. Berrios, B. Binay and P. Pickers, Recombinant protein production in *Pichia pastoris*: from transcriptionally redesigned strains to bioprocess optimization and metabolic modelling, *FEMS Yeast Research*, 2021, **21**, foab057. 10.1093/femsyr/foab057

265. L. Ullmann, A. N. T. Phan, D. K. P. Kaplan and L. M. Blank, Ustilaginaceae Biocatalyst for Co-Metabolism of CO<sub>2</sub>-Derived Substrates toward Carbon-Neutral Itaconate Production, *Journal of Fungi*, 2021, **7**, 98. 10.3390/jof7020098
266. J. O. Park, N. Liu, K. M. Holinski, D. F. Emerson, K. Qiao, B. M. Woolston, J. Xu, Z. Lazar, M. A. Islam, C. Vidoudez, P. R. Girguis and G. Stephanopoulos, Synergistic substrate cofeeding stimulates reductive metabolism, *Nature Metabolism*, 2019, **1**, 643-651. 10.1038/s42255-019-0077-0
267. C. Li, K. L. Lesnik and H. Liu, Microbial Conversion of Waste Glycerol from Biodiesel Production into Value-Added Products, *Energies*, 2013, **6**, 4739-4768.
268. F. R. Bengelsdorf and P. Dürre, Gas fermentation for commodity chemicals and fuels, *Microbial Biotechnology*, 2017, **10**, 1167-1170. <https://doi.org/10.1111/1751-7915.12763>
269. C. A. R. Cotton, N. J. Claassens, S. Benito-Vaquero and A. Bar-Even, Renewable methanol and formate as microbial feedstocks, *Current Opinion in Biotechnology*, 2020, **62**, 168-180. <https://doi.org/10.1016/j.copbio.2019.10.002>
270. C. D. Pinales-Márquez, R. M. Rodríguez-Jasso, R. G. Araújo, A. Loreda-Treviño, D. Nabarlaz, B. Gullón and H. A. Ruiz, Circular bioeconomy and integrated biorefinery in the production of xylooligosaccharides from lignocellulosic biomass: A review, *Industrial Crops and Products*, 2021, **162**, 113274. <https://doi.org/10.1016/j.indcrop.2021.113274>
271. H. Y. Leong, C.-K. Chang, K. S. Khoo, K. W. Chew, S. R. Chia, J. W. Lim, J.-S. Chang and P. L. Show, Waste biorefinery towards a sustainable circular bioeconomy: a solution to global issues, *Biotechnology for Biofuels*, 2021, **14**, 87. 10.1186/s13068-021-01939-5
272. M. Broda, D. J. Yelle and K. Serwańska, Bioethanol Production from Lignocellulosic Biomass: Challenges and Solutions, *Molecules*, 2022, **27**, 8717.
273. A. Kang and T. S. Lee, Converting Sugars to Biofuels: Ethanol and Beyond, *Bioengineering*, 2015, **2**, 184-203. 10.3390/bioengineering2040184
274. S. S. Hassan, G. A. Williams and A. K. Jaiswal, Moving towards the second generation of lignocellulosic biorefineries in the EU: Drivers, challenges, and opportunities, *Renewable and Sustainable Energy Reviews*, 2019, **101**, 590-599. <https://doi.org/10.1016/j.rser.2018.11.041>
275. X. Kang, R. Lin, R. O'Shea, C. Deng, L. Li, Y. Sun and J. D. Murphy, A perspective on decarbonizing whiskey using renewable gaseous biofuel in a circular bioeconomy process, *Journal of Cleaner Production*, 2020, **255**, 120211. <https://doi.org/10.1016/j.jclepro.2020.120211>
276. Y. Xu, X. Duan, Y. Wu, T. Fu, W. Hou, S. Xue and Z. Yi, The efficiency and stability of soil organic carbon sequestration by perennial energy crops cultivation on marginal land depended on root traits, *Soil and Tillage Research*, 2024, **235**, 105909. <https://doi.org/10.1016/j.still.2023.105909>
277. D. Kim, Physico-Chemical Conversion of Lignocellulose: Inhibitor Effects and Detoxification Strategies: A Mini Review, *Molecules*, 2018, **23**, 309.
278. R. Roy, M. S. Rahman and D. E. Raynie, Recent advances of greener pretreatment technologies of lignocellulose, *Current Research in Green and Sustainable Chemistry*, 2020, **3**, 100035. <https://doi.org/10.1016/j.crgsc.2020.100035>
279. L. J. Jönsson, B. Alriksson and N.-O. Nilvebrant, Bioconversion of lignocellulose: inhibitors and detoxification, *Biotechnology for Biofuels*, 2013, **6**, 16. 10.1186/1754-6834-6-16
280. L.-T. Wang, C.-J. Tai, Y.-C. Wu, Y.-B. Chen, F.-L. Lee and S.-L. Wang, *Pseudomonas taiwanensis* sp. nov., isolated from soil, *International Journal of Systematic and Evolutionary Microbiology*, 2010, **60**, 2094-2098. <https://doi.org/10.1099/ijs.0.014779-0>
281. K. A. Kohler, L. M. Blank, O. Frick and A. Schmid, D-Xylose assimilation via the Weimberg pathway by solvent-tolerant *Pseudomonas taiwanensis* VLB120, *Environmental Microbiology*, 2015, **17**, 156-170. 10.1111/1462-2920.12537
282. I. Bator, A. Wittgens, F. Rosenau, T. Tiso and L. M. Blank, Comparison of Three Xylose Pathways in *Pseudomonas putida* KT2440 for the Synthesis of Valuable Products, *Frontiers in Bioengineering and Biotechnology*, 2020, **7**, 480. 10.3389/fbioe.2019.00480
283. G. G. Wordofa and M. Kristensen, Tolerance and metabolic response of *Pseudomonas taiwanensis* VLB120 towards biomass hydrolysate-derived inhibitors, *Biotechnology for Biofuels*, 2018, **11**, 199. 10.1186/s13068-018-1192-y
284. A. L. Ziegler, C. Grütering, L. Poduschnick, A. Mitsos and L. M. Blank, Co-feeding enhances the yield of methyl ketones, *Journal of Industrial Microbiology and Biotechnology*, 2023, **50**, kuad029.
285. W. J. Li, L. N. Jayakody, M. A. Franden, M. Wehrmann, T. Daun, B. Hauer, L. M. Blank, G. T. Beckham, J. Klebensberger and N. Wierckx, Laboratory evolution reveals the metabolic and regulatory basis of ethylene glycol metabolism by *Pseudomonas putida* KT2440, *Environmental Microbiology*, 2019, **21**, 3669-3682. 10.1111/1462-2920.14703
286. T. Tiso, T. Narancic, R. Wei, E. Pollet, N. Beagan, K. Schröder, A. Honak, M. Jiang, S. T. Kenny, N. Wierckx, R. Perrin, L. Avérus, W. Zimmermann, K. O'Connor and L. M. Blank, Towards bio-upcycling of polyethylene terephthalate, *Metabolic Engineering*, 2021, **66**, 167-178. <https://doi.org/10.1016/j.ymben.2021.03.011>
287. J. Yang, J. H. Son, H. Kim, S. Cho, J.-g. Na, Y. J. Yeon and J. Lee, Mevalonate production from ethanol by direct conversion through acetyl-CoA using recombinant *Pseudomonas putida*, a novel biocatalyst for terpenoid production, *Microbial Cell Factories*, 2019, **18**, 168. 10.1186/s12934-019-1213-y



288. I. Poblete-Castro, C. Wittmann and P. I. Nikel, Biochemistry, genetics and biotechnology of glycerol utilization in *Pseudomonas* species, *Microbial Biotechnology*, 2020, **13**, 32-53. <https://doi.org/10.1111/1751-7915.13400>
289. S. Zobel, J. Kuepper, B. Ebert, N. Wierckx and L. M. Blank, Metabolic response of *Pseudomonas putida* to increased NADH regeneration rates, *Engineering in Life Sciences*, 2017, **17**, 47-57. 10.1002/elsc.201600072
290. I. Bator, T. Karmański, T. Tiso and L. M. Blank, Killing Two Birds With One Stone – Strain Engineering Facilitates the Development of a Unique Rhamnolipid Production Process, *Frontiers in Bioengineering and Biotechnology*, 2020, **8**, 899. 10.3389/fbioe.2020.00899
291. L. Poduschnick, Developing co-feeding strategies for the improved biofuel production in *Pseudomonas taiwanensis* VLB120 using *in silico* and experimental approaches, Institute of Applied Microbiology, RWTH Aachen, 2022.
292. S. García-Condado, R. López-Lozano, L. Panarello, I. Cerrani, L. Nisini, A. Zucchini, M. Van der Velde and B. Baruth, Assessing lignocellulosic biomass production from crop residues in the European Union: Modelling, analysis of the current scenario and drivers of interannual variability, *GCB Bioenergy*, 2019, **11**, 809-831. <https://doi.org/10.1111/gcbb.12604>
293. A. Brosowski, R. Bill and D. Thrän, Temporal and spatial availability of cereal straw in Germany - Case study: Biomethane for the transport sector, *Energy, Sustainability and Society*, 2020, **10**, 42. 10.1186/s13705-020-00274-1
294. S. I. Mussatto, G. Dragone and I. C. Roberto, Influence of the toxic compounds present in brewer's spent grain hemicellulosic hydrolysate on xylose-to-xylitol bioconversion by *Candida guilliermondii*, *Process Biochemistry*, 2005, **40**, 3801-3806. <https://doi.org/10.1016/j.procbio.2005.06.024>
295. F. Rojo, Carbon catabolite repression in *Pseudomonas*: optimizing metabolic versatility and interactions with the environment, *FEMS Microbiology Reviews*, 2010, **34**, 658-684. 10.1111/j.1574-6976.2010.00218.x
296. L. Molina, R. La Rosa, J. Nogales and F. Rojo, Influence of the Crc global regulator on substrate uptake rates and the distribution of metabolic fluxes in *Pseudomonas putida* KT2440 growing in a complete medium, *Environmental Microbiology*, 2019, **21**, 4446-4459. <https://doi.org/10.1111/1462-2920.14812>
297. T. Anderlei and J. Büchs, Device for sterile online measurement of the oxygen transfer rate in shaking flasks, *Biochemical Engineering Journal*, 2001, **7**, 157-162. [https://doi.org/10.1016/S1369-703X\(00\)00116-9](https://doi.org/10.1016/S1369-703X(00)00116-9)
298. H. Kawaguchi, T. Hasunuma, C. Ogino and A. Kondo, Bioprocessing of bio-based chemicals produced from lignocellulosic feedstocks, *Current Opinion in Biotechnology*, 2016, **42**, 30-39. <https://doi.org/10.1016/j.copbio.2016.02.031>
299. G. Sperotto, L. G. Stasiak, J. P. M. G. Godoi, N. C. Gabiatti and S. S. De Souza, A review of culture media for bacterial cellulose production: complex, chemically defined and minimal media modulations, *Cellulose*, 2021, **28**, 2649-2673. 10.1007/s10570-021-03754-5
300. J. R. Almeida, T. Modig, A. Petersson, B. Hahn-Hägerdal, G. Lidén and M. F. Gorwa-Grauslund, Increased tolerance and conversion of inhibitors in lignocellulosic hydrolysates by *Saccharomyces cerevisiae*, *Journal of Chemical Technology & Biotechnology*, 2007, **82**, 340-349. <https://doi.org/10.1002/jctb.1676>
301. C. Weng, R. Tang, X. Peng and Y. Han, Co-conversion of lignocellulose-derived glucose, xylose, and aromatics to polyhydroxybutyrate by metabolically engineered *Cupriavidus necator*, *Bioresource Technology*, 2023, **374**, 128762. <https://doi.org/10.1016/j.biortech.2023.128762>
302. F. A. Hasmann, V. C. Santos, D. B. Gurpilhares, A. Pessoa-Junior and I. C. Roberto, Aqueous two-phase extraction using thermoseparating copolymer: a new system for phenolic compounds removal from hemicellulosic hydrolysate, *Journal of Chemical Technology & Biotechnology*, 2008, **83**, 167-173. <https://doi.org/10.1002/jctb.1779>
303. G.-T. Jeong, S.-K. Kim and D.-H. Park, Detoxification of hydrolysate by reactive-extraction for generating biofuels, *Biotechnology and Bioprocess Engineering*, 2013, **18**, 88-93. 10.1007/s12257-012-0417-3
304. C. Syldatk, H. Chmiel, C. Brandenbusch, B. Bühler, G. Sadowski, A. Schmid, M. A. Mirata, J. Schrader and D. Bryniok, Mikrobielle Prozesse, in *Bioprozesstechnik*, ed. H. Chmiel, Spektrum Akademischer Verlag, Heidelberg, 3 edn., 2011, pp. 477-505.
305. J. Li, R. Zhao, Y. Xu, X. Wu, S. R. Bean and D. Wang, Fuel ethanol production from starchy grain and other crops: An overview on feedstocks, affecting factors, and technical advances, *Renewable Energy*, 2022, **188**, 223-239. <https://doi.org/10.1016/j.renene.2022.02.038>
306. R. B. Cabulong, W.-K. Lee, A. B. Bañares, K. R. M. Ramos, G. M. Nisola, K. N. G. Valdehuesa and W.-J. Chung, Engineering *Escherichia coli* for glycolic acid production from D-xylose through the Dahms pathway and glyoxylate bypass, *Applied Microbiology and Biotechnology*, 2018, **102**, 2179-2189. 10.1007/s00253-018-8744-8
307. M. P. Almario, L. H. Reyes and K. C. Kao, Evolutionary engineering of *Saccharomyces cerevisiae* for enhanced tolerance to hydrolysates of lignocellulosic biomass, *Biotechnology and Bioengineering*, 2013, **110**, 2616-2623. <https://doi.org/10.1002/bit.24938>
308. Z. Cui, M. Zheng, M. Ding, W. Dai, Z. Wang and T. Chen, Efficient production of acetoin from lactate by engineered *Escherichia coli* whole-cell biocatalyst, *Applied Microbiology and Biotechnology*, 2023, **107**, 3911-3924. 10.1007/s00253-023-12560-x
309. T. Werpy and G. Petersen, *Results of Screening for Potential Candidates from Sugars and Synthesis Gas*, Report PNNL-14808, United States, 2004.

310. P. R. Jensen and K. Hammer, Minimal Requirements for Exponential Growth of *Lactococcus lactis*, *Applied and Environmental Microbiology*, 1993, **59**, 4363–4366. doi:10.1128/aem.59.12.4363-4366.1993
311. A. A.-L. Song, L. L. A. In, S. H. E. Lim and R. A. Rahim, A review on *Lactococcus lactis*: from food to factory, *Microbial Cell Factories*, 2017, **16**, 55. 10.1186/s12934-017-0669-x
312. E. Morello, L. G. Bermúdez-Humarán, D. Llull, V. Solé, N. Miraglio, P. Langella and I. Poquet, *Lactococcus lactis*, an efficient cell factory for recombinant protein production and secretion, *Journal of Molecular Microbiology and Biotechnology*, 2008, **14**, 48–58. 10.1159/000106082
313. M. M. Baizer, T. Nonaka, K. Park, Y. Saito and K. Nobe, Electrochemical conversion of 2,3-butanediol to 2-butanone in undivided flow cells: a paired synthesis, *Journal of Applied Electrochemistry*, 1984, **14**, 197–208. 10.1007/BF00618738
314. J. R. Ochoa-Gómez, F. Fernández-Carretero, F. Río-Pérez, A. García-Luis, T. Roncal and E. J. García-Suárez, Electrosynthesis of 2,3-butanediol and methyl ethyl ketone from acetoin in flow cells, *Green Chemistry*, 2019, **21**, 164–177. 10.1039/C8GC03028F
315. Z. Liu, W. Huo, H. Ma and K. Qiao, Development and Commercial Application of Methyl-ethyl-ketone Production Technology, *Chinese Journal of Chemical Engineering*, 2006, **14**, 676–684. [https://doi.org/10.1016/S1004-9541\(06\)60134-1](https://doi.org/10.1016/S1004-9541(06)60134-1)
316. U. Burke, J. Beeckmann, W. A. Kopp, Y. Uygun, H. Olivier, K. Leonhard, H. Pitsch and K. A. Heufer, A comprehensive experimental and kinetic modeling study of butanone, *Combustion and Flame*, 2016, **168**, 296–309. <https://doi.org/10.1016/j.combustflame.2016.03.001>
317. F. Hoppe, U. Burke, M. Thewes, A. Heufer, F. Kremer and S. Pischinger, Tailor-Made Fuels from Biomass: Potentials of 2-butanone and 2-methylfuran in direct injection spark ignition engines, *Fuel*, 2016, **167**, 106–117. <https://doi.org/10.1016/j.fuel.2015.11.039>
318. K. Min, S. Kim, T. Yum, Y. Kim, B.-I. Sang and Y. Um, Conversion of levulinic acid to 2-butanone by acetoacetate decarboxylase from *Clostridium acetobutylicum*, *Applied Microbiology and Biotechnology*, 2013, **97**, 5627–5634. 10.1007/s00253-013-4879-9
319. A. Multer, N. McGraw, K. Hohn and P. Vadlani, Production of Methyl Ethyl Ketone from Biomass Using a Hybrid Biochemical/Catalytic Approach, *Industrial & Engineering Chemistry Research*, 2013, **52**, 56–60. 10.1021/ie3007598
320. B. Heyman, H. Tulke, S. P. Putri, E. Fukusaki and J. Büchs, Online monitoring of the respiratory quotient reveals metabolic phases during microaerobic 2,3-butanediol production with *Bacillus licheniformis*, *Engineering in Life Sciences*, 2020, **20**, 133–144. 10.1002/elsc.201900121
321. Y.-j. Lang, L. Bai, Y.-n. Ren, L.-h. Zhang and S. Nagata, Production of ectoine through a combined process that uses both growing and resting cells of *Halomonas salina* DSM 5928T, *Extremophiles*, 2011, **15**, 303–310. 10.1007/s00792-011-0360-9
322. M. K. Julsing, D. Kuhn, A. Schmid and B. Bühler, Resting cells of recombinant *E. coli* show high epoxidation yields on energy source and high sensitivity to product inhibition, *Biotechnology and Bioengineering*, 2012, **109**, 1109–1119. <https://doi.org/10.1002/bit.24404>
323. P. Hols, M. Kleerebezem, A. N. Schanck, T. Ferain, J. Hugenholtz, J. Delcour and W. M. de Vos, Conversion of *Lactococcus lactis* from homolactic to homoalanine fermentation through metabolic engineering, *Nature Biotechnology*, 1999, **17**, 588–592. 10.1038/9902
324. J. Palmfeldt, M. Paese, B. Hahn-Hägerdal and E. W. J. v. Niel, The Pool of ADP and ATP Regulates Anaerobic Product Formation in Resting Cells of *Lactococcus lactis*, *Applied and Environmental Microbiology*, 2004, **70**, 5477–5484. doi:10.1128/AEM.70.9.5477-5484.2004
325. N. Salonen, K. Salonen, M. Leisola and A. Nyssölä, d-Tagatose production in the presence of borate by resting *Lactococcus lactis* cells harboring *Bifidobacterium longum* L-arabinose isomerase, *Bioprocess and Biosystems Engineering*, 2013, **36**, 489–497. 10.1007/s00449-012-0805-2
326. J. L. Cotter, M. S. Chinn and A. M. Grunden, Ethanol and acetate production by *Clostridium ljungdahlii* and *Clostridium autoethanogenum* using resting cells, *Bioprocess and Biosystems Engineering*, 2009, **32**, 369–380. 10.1007/s00449-008-0256-y
327. M. G. Acedos, V. E. Santos and F. García-Ochoa, Resting cells isobutanol production by *Shimwellia blattae* (p4241bPSO): Influence of growth culture conditions, *Biotechnology Progress*, 2018, **34**, 1073–1080. <https://doi.org/10.1002/btpr.2705>
328. V. Ripoll, M. Ladero and V. E. Santos, Kinetic modelling of 2,3-butanediol production by *Raoultella terrigena* CECT 4519 resting cells: Effect of fluid dynamics conditions and initial glycerol concentration, *Biochemical Engineering Journal*, 2021, **176**, 108185. <https://doi.org/10.1016/j.bej.2021.108185>
329. C. Grütering, T. Harhues, F. Speen, R. Keller, M. Zimmermann, P. R. Jensen, M. Wessling and L. M. Blank, Acetoin production by resting cells of *Lactococcus lactis* for direct electrochemical synthesis of 2-butanone, *Green Chemistry*, 2023, **25**, 9218–9225. 10.1039/D3GC02513F
330. B. Cesselin, C. Henry, A. Gruss, K. Gloux and P. Gaudu, Mechanisms of Acetoin Toxicity and Adaptive Responses in an Acetoin-Producing Species, *Lactococcus lactis*, *Applied and Environmental Microbiology*, 2021, **87**, e01079–01021. doi:10.1128/AEM.01079-21
331. F. Speen, Process optimization of microbial acetoin production for advanced biofuels, Institute of Applied Microbiology, RWTH Aachen, 2023.
332. R. Otto, B. ten Brink, H. Veldkamp and W. N. Konings, The relation between growth rate and electrochemical proton gradient of *Streptococcus cremoris*, *FEMS Microbiology Letters*, 1983, **16**, 69–74. 10.1111/j.1574-6968.1983.tb00261.x

333. C. E. Price, F. Branco dos Santos, A. Hesseling, J. J. Uusitalo, H. Bachmann, V. Benavente, A. Goel, J. Berkhout, F. J. Bruggeman, S.-J. Marrink, M. Montalban-Lopez, A. de Jong, J. Kok, D. Molenaar, B. Poolman, B. Teusink and O. P. Kuipers, Adaption to glucose limitation is modulated by the pleotropic regulator CcpA, independent of selection pressure strength, *BMC Evolutionary Biology*, 2019, **19**, 15. [10.1186/s12862-018-1331-x](https://doi.org/10.1186/s12862-018-1331-x)
334. K. Meier, W. Klöckner, B. Bonhage, E. Antonov, L. Regestein and J. Büchs, Correlation for the maximum oxygen transfer capacity in shake flasks for a wide range of operating conditions and for different culture media, *Biochemical Engineering Journal*, 2016, **109**, 228-235. <https://doi.org/10.1016/j.bej.2016.01.014>
335. J. L. Snoep, M. J. T. d. Mattos, M. J. Starrenburg and J. Hugenholtz, Isolation, characterization, and physiological role of the pyruvate dehydrogenase complex and alpha-acetolactate synthase of *Lactococcus lactis* subsp. *lactis* bv. *diacetylactis*, *Journal of Bacteriology*, 1992, **174**, 4838-4841. [doi:10.1128/jb.174.14.4838-4841.1992](https://doi.org/10.1128/jb.174.14.4838-4841.1992)
336. F. A. Zuljan, G. D. Repizo, S. H. Alarcon and C. Magni,  $\alpha$ -Acetolactate synthase of *Lactococcus lactis* contributes to pH homeostasis in acid stress conditions, *International Journal of Food Microbiology*, 2014, **188**, 99-107. <https://doi.org/10.1016/j.ijfoodmicro.2014.07.017>
337. F. Suo, J. Liu, J. Chen, X. Li, C. Solem and P. R. Jensen, Efficient Production of Pyruvate Using Metabolically Engineered *Lactococcus lactis*, *Frontiers in Bioengineering and Biotechnology*, 2020, **8**, 611701. [10.3389/fbioe.2020.611701](https://doi.org/10.3389/fbioe.2020.611701)
338. B. J. Koebmann, C. Solem, M. B. Pedersen, D. Nilsson and P. R. Jensen, Expression of Genes Encoding F<sub>1</sub>-ATPase Results in Uncoupling of Glycolysis from Biomass Production in *Lactococcus lactis*, *Applied and Environmental Microbiology*, 2002, **68**, 4274-4282. [doi:10.1128/AEM.68.9.4274-4282.2002](https://doi.org/10.1128/AEM.68.9.4274-4282.2002)
339. Y. Nakashimada, K. Kanai and N. Nishio, Optimization of dilution rate, pH and oxygen supply on optical purity of 2, 3-butanediol produced by *Paenibacillus polymyxa* in chemostat culture, *Biotechnology letters*, 1998, **20**, 1133-1138. [10.1023/A:1005324403186](https://doi.org/10.1023/A:1005324403186)
340. H. G. Mengers, N. Guntermann, W. Graf von Westarp, A. Jupke, J. Klankermayer, L. M. Blank, W. Leitner and D. Rother, Three Sides of the Same Coin: Combining Microbial, Enzymatic, and Organometallic Catalysis for Integrated Conversion of Renewable Carbon Sources, *Chemie Ingenieur Technik*, 2023, **95**, 485-490. <https://doi.org/10.1002/cite.202200169>
341. M. Naidoo, S. L. Tai and S. T. L. Harrison, Energy requirements for the *in-situ* recovery of biobutanol via gas stripping, *Biochemical Engineering Journal*, 2018, **139**, 74-84. <https://doi.org/10.1016/j.bej.2018.07.022>
342. P. E. Plaza, M. Coca, S. L. Yagüe, G. Gutiérrez, E. Rochón and M. T. García-Cubero, Bioprocess intensification for acetone-butanol-ethanol fermentation from brewer's spent grain: Fed-batch strategies coupled with *in-situ* gas stripping, *Biomass and Bioenergy*, 2022, **156**, 106327. <https://doi.org/10.1016/j.biombioe.2021.106327>
343. M. Covarrubias-Cervantes, I. Mokbel, D. Champion, J. Jose and A. Volley, Saturated vapour pressure of aroma compounds at various temperatures, *Food Chemistry*, 2004, **85**, 221-229. <https://doi.org/10.1016/j.foodchem.2003.07.004>
344. V. L. U. Khuat, V. T. T. Bui, H. T. D. Tran, N. X. Truong, T. C. Nguyen, P. H. H. Mai, T. L. A. Dang, H. M. Dinh, H. T. A. Pham and T. T. H. Nguyen, Characterization of *Solanum melongena* Thioesterases Related to Tomato Methylketone Synthase 2, *Genes*, 2019, **10**, 549.
345. C. M. D. Swarbrick, J. D. Nanson, E. I. Patterson and J. K. Forwood, Structure, function, and regulation of thioesterases, *Progress in Lipid Research*, 2020, **79**, 101036. [10.1016/j.plipres.2020.101036](https://doi.org/10.1016/j.plipres.2020.101036)
346. N. J. Hernández Lozada, T. R. Simmons, K. Xu, M. A. Jindra and B. F. Pfeiffer, Production of 1-octanol in *Escherichia coli* by a high flux thioesterase route, *Metabolic Engineering*, 2020, **61**, 352-359. <https://doi.org/10.1016/j.ymben.2020.07.004>
347. J. M. Borrero-de Acuña, A. Bielecka, S. Häussler, M. Schobert, M. Jahn, C. Wittmann, D. Jahn and I. Poblete-Castro, Production of medium chain length polyhydroxyalkanoate in metabolic flux optimized *Pseudomonas putida*, *Microbial Cell Factories*, 2014, **13**, 88. [10.1186/1475-2859-13-88](https://doi.org/10.1186/1475-2859-13-88)
348. Z. Xu, C. Pan, X. Li, N. Hao, T. Zhang, M. J. Gaffrey, Y. Pu, J. R. Cort, A. J. Ragauskas, W.-J. Qian and B. Yang, Enhancement of polyhydroxyalkanoate production by co-feeding lignin derivatives with glycerol in *Pseudomonas putida* KT2440, *Biotechnology for Biofuels*, 2021, **14**, 11. [10.1186/s13068-020-01861-2](https://doi.org/10.1186/s13068-020-01861-2)
349. C. B. Huang, Y. Alimova, T. M. Myers and J. L. Ebersole, Short- and medium-chain fatty acids exhibit antimicrobial activity for oral microorganisms, *Archives of Oral Biology*, 2011, **56**, 650-654. <https://doi.org/10.1016/j.archoralbio.2011.01.011>
350. L. A. Royce, P. Liu, M. J. Stebbins, B. C. Hanson and L. R. Jarboe, The damaging effects of short chain fatty acids on *Escherichia coli* membranes, *Applied Microbiology and Biotechnology*, 2013, **97**, 8317-8327. [10.1007/s00253-013-5113-5](https://doi.org/10.1007/s00253-013-5113-5)
351. M. Asadpoor, G.-N. Ithakisiou, P. A. J. Henricks, R. Pieters, G. Folkerts and S. Braber, Non-Digestible Oligosaccharides and Short Chain Fatty Acids as Therapeutic Targets against Enterotoxin-Producing Bacteria and Their Toxins, *Toxins*, 2021, **13**, 175.
352. Y.-M. Zhang and C. O. Rock, Transcriptional regulation in bacterial membrane lipid synthesis, *Journal of Lipid Research*, 2009, **50**, S115-S119. [10.1194/jlr.R800046-JLR200](https://doi.org/10.1194/jlr.R800046-JLR200)
353. T. Harayama and H. Riezman, Understanding the diversity of membrane lipid composition, *Nature Reviews Molecular Cell Biology*, 2018, **19**, 281-296. [10.1038/nrm.2017.138](https://doi.org/10.1038/nrm.2017.138)
354. B. Sonnleitner and H. Chmiel, Wachstum: Kinetik und Prozessführung, in *Bioproszesstechnik*, ed. H. Chmiel, Spektrum Akademischer Verlag, Heidelberg, 3 edn., 2011, pp. 99-149.



355. A. Barberán, H. C. Velazquez, S. Jones and N. Fierer, Hiding in Plain Sight: Mining Bacterial Species Records for Phenotypic Trait Information, *mSphere*, 2017, **2**, e00237-00217. doi:10.1128/msphere.00237-17
356. K. Sangkharak, A. Choonut, T. Rakkan and P. Prasertsan, The Degradation of Phenanthrene, Pyrene, and Fluoranthene and Its Conversion into Medium-Chain-Length Polyhydroxyalkanoate by Novel Polycyclic Aromatic Hydrocarbon-Degrading Bacteria, *Current Microbiology*, 2020, **77**, 897-909. 10.1007/s00284-020-01883-x
357. P. G. Ward, G. d. Roo and K. E. O'Connor, Accumulation of Polyhydroxyalkanoate from Styrene and Phenylacetic Acid by *Pseudomonas putida* CA-3, *Applied and Environmental Microbiology*, 2005, **71**, 2046-2052. doi:10.1128/AEM.71.4.2046-2052.2005
358. I. Poblete-Castro, D. Binger, R. Oehlert and M. Rohde, Comparison of mcl-Poly(3-hydroxyalkanoates) synthesis by different *Pseudomonas putida* strains from crude glycerol: citrate accumulates at high titer under PHA-producing conditions, *BMC Biotechnology*, 2014, **14**, 962. 10.1186/s12896-014-0110-z
359. J. Blazeck and H. S. Alper, Promoter engineering: Recent advances in controlling transcription at the most fundamental level, *Biotechnology Journal*, 2013, **8**, 46-58. https://doi.org/10.1002/biot.201200120
360. S. Kóbbing, L. M. Blank and N. Wierckx, Characterization of Context-Dependent Effects on Synthetic Promoters, *Frontiers in Bioengineering and Biotechnology*, 2020, **8**, 551. 10.3389/fbioe.2020.00551
361. M. Dragosits and D. Mattanovich, Adaptive laboratory evolution – principles and applications for biotechnology, *Microbial Cell Factories*, 2013, **12**, 64. 10.1186/1475-2859-12-64
362. S. Oide, W. Gunji, Y. Moteki, S. Yamamoto, M. Suda, T. Jojima, H. Yukawa and M. Inui, Thermal and Solvent Cross-Tolerance Conferred to *Corynebacterium glutamicum* by Adaptive Laboratory Evolution, *Applied and Environmental Microbiology*, 2015, **81**, 2284-2298. doi:10.1128/AEM.03973-14
363. I. I. Moiseev, Biotechnology is storming the heights of petrochemistry, *Kinetics and Catalysis*, 2016, **57**, 405-421. 10.1134/S0023158416040078
364. L. Landeweerd, M. Surette and C. van Driel, From petrochemistry to biotech: a European perspective on the bio-based economy, *Interface Focus*, 2011, **1**, 189-195. doi:10.1098/rsfs.2010.0014
365. T. J. Tse, D. J. Wiens and M. J. T. Reaney, Production of Bioethanol - A Review of Factors Affecting Ethanol Yield, *Fermentation*, 2021, **7**, 268.
366. B. Sharma, C. Larroche and C.-G. Dussap, Comprehensive assessment of 2G bioethanol production, *Bioresource Technology*, 2020, **313**, 123630. https://doi.org/10.1016/j.biortech.2020.123630
367. D. D. McClure, Z. Zheng, G. Hu and J. M. Kavanagh, Towards *in situ* product recovery for bubble column bioreactors, *Chemical Engineering Journal*, 2020, **393**, 124745. https://doi.org/10.1016/j.cej.2020.124745
368. T. A. Grein, D. Loewe, H. Dieken, T. Weidner, D. Salzig and P. Czermak, Aeration and Shear Stress Are Critical Process Parameters for the Production of Oncolytic Measles Virus, *Frontiers in Bioengineering and Biotechnology*, 2019, **7**, 78. 10.3389/fbioe.2019.00078
369. C. B. Elias, R. B. Desai, M. S. Patole, J. B. Joshi and R. A. Mashelkar, Turbulent shear stress - Effect on mammalian cell culture and measurement using laser Doppler anemometer, *Chemical Engineering Science*, 1995, **50**, 2431-2440. https://doi.org/10.1016/0009-2509(95)00084-1
370. O. Rosales-Calderon and V. Arantes, A review on commercial-scale high-value products that can be produced alongside cellulosic ethanol, *Biotechnology for Biofuels*, 2019, **12**, 240. 10.1186/s13068-019-1529-1
371. S. T. Chambers, B. Peddie and A. Pithie, Ethanol disinfection of plastic-adherent microorganisms, *Journal of Hospital Infection*, 2006, **63**, 193-196. https://doi.org/10.1016/j.jhin.2006.01.009
372. E. Cámara, L. Olsson, J. Zimec, A. Zeleznik, C. Geijer and Y. Nygård, Data mining of *Saccharomyces cerevisiae* mutants engineered for increased tolerance towards inhibitors in lignocellulosic hydrolysates, *Biotechnology Advances*, 2022, **57**, 107947. https://doi.org/10.1016/j.biotechadv.2022.107947
373. C. Sun, X. Meng, F. Sun, J. Zhang, M. Tu, J.-S. Chang, A. Reungsang, A. Xia and A. J. Ragauskas, Advances and perspectives on mass transfer and enzymatic hydrolysis in the enzyme-mediated lignocellulosic biorefinery: A review, *Biotechnology Advances*, 2023, **62**, 108059. https://doi.org/10.1016/j.biotechadv.2022.108059
374. B. Dettwiler, I. J. Dunn, E. Heinzel and J. E. Prenosil, A simulation model for the continuous production of acetoin and butanediol using *Bacillus subtilis* with integrated pervaporation separation, *Biotechnology and Bioengineering*, 1993, **41**, 791-800. https://doi.org/10.1002/bit.260410805
375. S. Wydra, Value Chains for Industrial Biotechnology in the Bioeconomy-Innovation System Analysis, *Sustainability*, 2019, **11**, 2435.
376. A. H. Tullo, *LanzaTech and Twelve to make polypropylene*, American Chemical Society, Chemical & Engineering News, 2021.
377. M. Dallendörfer, S. Dieken, M. Henseleit, F. Siekmann and S. Venghaus, Investigating citizens' perceptions of the bioeconomy in Germany – High support but little understanding, *Sustainable Production and Consumption*, 2022, **30**, 16-30. https://doi.org/10.1016/j.spc.2021.11.009
378. J. Macht, J. L. Klink-Lehmann and J. Simons, German citizens' perception of the transition towards a sustainable bioeconomy: A glimpse into the Rheinische Revier, *Sustainable Production and Consumption*, 2022, **31**, 175-189. https://doi.org/10.1016/j.spc.2022.02.010
379. K. Sanderson, *COP28 climate summit signals the end of fossil fuels - but is it enough?*, Nature, 2023.
380. A. Grundwald, Bioeconomy: Key to Unlimited Economic and Consumption Growth?, in *Bioeconomy for Beginners*, ed. J. Pietzsch, Springer Berlin Heidelberg, Berlin, Heidelberg, 1 edn., 2020, pp. 203-209.

381. B. Poolman and W. N. Konings, Relation of growth of *Streptococcus lactis* and *Streptococcus cremoris* to amino acid transport, *Journal of Bacteriology*, 1988, **170**, 700-707. doi:10.1128/jb.170.2.700-707.1988



---

# Curriculum Vitae

---



## Curriculum Vitae

Carolin Grütering  
Vaalser Straße 314  
52074 Aachen  
Phone +49 152 07196588  
E-mail carolin.gruetering@rwth-aachen.de

Born on April 27, 1994, in Marl, Germany

### Education

- 08/2020 – 05/2024 **Institute for Applied Microbiology, Aachen**  
Ph.D. candidate “Producing methyl ketones in integrated bioprocesses”
- 04/2017 – 04/2020 **RWTH Aachen, Aachen**  
Master studies “Molecular and Applied Biotechnology”, major in Bioprocess Engineering; final grade 1.0 with extinction
- 10/2013 – 04/2017 **RWTH Aachen, Aachen**  
Bachelor studies “Molecular and Applied Biotechnology”; final grade 1.3 with extinction
- 08/2004 – 06/2013 **Gymnasium im Loekamp, Marl**  
German Abitur; final grade 1.0

### Professional Profile

- 01/2022 – 05/2022 **Technical University of Denmark, Copenhagen**  
External research stay; research group Biomass Conversion and Bioprocess Technology
- 09/2019 – 03/2020 **Institute for Applied Microbiology, Aachen**  
Master thesis “Bioprocess Intensification for Rhamnolipid Production by Implementing Liquid-Liquid Extraction in an Innovative Multiphase Loop Reactor”; grade 1.0
- 02/2018 – 07/2018 **Instituto Superior Técnico, Lisbon**  
Erasmus+ scholarship; studies in Biological Engineering
- 03/2017 – 07/2017 **Evonik Industries AG, Marl**  
Internship at the department for bioprocess engineering

09/2016 – 12/2016 **RWTH Aachen, Aachen**

Bachelor thesis „Directed evolution of a *Yersinia mollaretii* phytase with increased activity at higher pH using Site Saturation Mutagenesis”; grade 1.0

10/2015 – 01/2016 **Institute for Biotechnology, Aachen**

Work as a research assistant in the field of “Directed Evolution”

### Engagement and Awards

05/2023

**11<sup>th</sup> International Conference Fuel Science, Aachen**

Best presentation award

06/2021

**MSE Master Award, Aachen**

Award for Master thesis

10/2018 – 10/2019 **RWTH-Bildungsfonds, Aachen**

Deutschlandstipendium scholarship

01/2017, 01/2021

**Dean’s List of RWTH, Aachen**

Dean’s List award of faculty 1

09/2015

**iGEM Competition, Boston**

Gold medal and award for “Best Manufacturing Project”

### Peer reviewed publications

C. Grütering, C. Honecker, M. Hofmeister, M. Neumann, L. Raßpe-Lange, M. Du, B. Lehrheuer, M. von Campenhausen, F. Schuster, M. Surger, B. E. Ebert, A. Jupke, T. Tiso, K. Leonhard, K. Schmitz, S. Pischinger, L. M. Blank. Methyl ketones: a comprehensive study of a novel biofuel. *Sustainable Energy & Fuels*. 2024, 8(9), 2059-2072.

A. L. Ziegler<sup>§</sup>, C. Grütering<sup>§</sup>, L. Poduschnick, A. Mitsos, L. M. Blank. Co-feeding enhances the yield of methyl ketones. *Journal of Industrial Microbiology and Biotechnology*, 2023, 50(1).

<sup>§</sup>equally contributing authors

C. Grütering, T. Harhues, F. Speen, R. Keller, M. Zimmermann, P. R. Jensen, M. Wessling, L. M. Blank. Acetoin production by resting cells of *Lactococcus lactis* for direct electrochemical synthesis of 2-butanone. *Green Chemistry*, 2023, 25(22), 9218-9225.

M. Hofmeister, A. Frische, M. Grunewald, M. Reddemann, C. Grütering, L. M. Blank, R. Kneer, K. Schmitz. Dichtungsmaterialuntersuchung mit Bio-Hybrid-Kraftstoffen. Dichten. Kleben. Polymer. Jahrbuch 2024. 2023. 68-78.

M. Froning, C. Grütering, L. M. Blank, H. Hayen. Determination of double bond positions in methyl ketones by gas chromatography–mass spectrometry using dimethyl disulfide derivatives. Rapid Communications in Mass Spectrometry, 2022, 37(6), e9457.

M. Hofmeister, A. Frische, M. Grunewald, M. Reddemann, C. Grütering, L. M. Blank, R. Kneer, K. Schmitz. Tribological properties of PTFE sealing materials with regard to bio-hybrid fuels. 21<sup>st</sup> International Sealing Conference. 2022. 89-104.

P. Demling, M. von Campenhausen, C. Grütering, T. Tiso, A. Jupke, L. M. Blank. Selection of a recyclable *in situ* liquid-liquid extraction solvent for foam-free synthesis of rhamnolipids in a two phase fermentation. Green Chemistry, 2020, 22(23), 8495-8510.

G. Körfer, C. Novoa, J. Kern, E. Balla, C. Grütering, M. D. Davari, R. Martinez, L. Vojcic, U. Schwaneberg. Directed evolution of an acid *Yersinia mollaretii* phytase for broadened activity at neutral pH. Applied Microbiology and Biotechnology. 2018, 102(22), 9607-9620.

### **Oral presentations**

C. Grütering, T. Tiso, M. Neumann, C. Honecker, A. Jupke, S. Pischinger, L. M. Blank. A bioprocess for *in situ* recovery of methyl ketones. Himmelfahrtstagung on Bioprocess Engineering 2023. Weimar, Germany. May 2023.

C. Grütering, T. Tiso, M. Neumann, C. Honecker, A. Jupke, S. Pischinger, L. M. Blank. Microbial production of methyl ketone blends an integrated bioprocess for sustainable drop-in fuels. 45<sup>th</sup> Symposium on Biomaterials, Fuels and Chemicals. Portland, USA. May 2023.

C. Grütering, T. Tiso, C. Honecker, M. Neumann, A. Jupke, S. Pischinger, L. M. Blank. Bioprocessing Drop in Fuels: Methyl Ketones From Tailored Microorganisms in an Integrated Bioprocess. Fuel Science – From Production to Propulsion 11<sup>th</sup> International Conference. Aachen, Germany. May 2023.



C. Grütering, T. Tiso, M. Neumann, A. Jupke, S. Pischinger, L. M. Blank. Microbial production of methyl ketones in the novel bioreactor multiphase-loop reactor MLPR - integrated *in situ* extraction for simple product recovery. Recent Advances in Fermentation Technology RAFT14. Orlando, USA. November 2022.

### Poster presentations

C. Grütering, T. Tiso, L. M. Blank. *In situ* extraction of oleochemicals produced by *Pseudomonas taiwanensis* VLB120. 3<sup>rd</sup> Pseudomonas Grassroots Meeting. Munich, Germany. November 2023.

C. Honecker, C. Grütering, M. Neumann, A. Jupke, L. M. Blank, S. Pischinger. Engine Testing of a Blend of Renewable Methyl Ketones as Drop-in Fuel for Diesel Engines. Fuel Science - From Production to Propulsion 11<sup>th</sup> International Conference. Aachen, Germany. May 2023.

C. Grütering, M. Neumann, L. Raßpe-Lange, S. Pischinger, K. Schmitz, K. Leonhard, A. Jupke, T. Tiso, L. M. Blank. Process design for microbial production of methyl ketones as advanced biofuel blends. Fuel Science – From Production to Propulsion 10<sup>th</sup> International Conference. Aachen, Germany. May 2022.

C. Grütering, F. Schuster, M. von Campenhausen, T. Tiso, A. Jupke, L. M. Blank. Process design for microbial production of methyl ketones as advanced biofuel blends. Fuel Science – From Production to Propulsion 9<sup>th</sup> International Conference. Aachen, Germany. June 2021.

C. Grütering, P. Demling, M. von Campenhausen, T. Tiso, A. Jupke, L. M. Blank. Bioprocess Intensification of Surfactant Production by Implementing Liquid-Liquid Extraction for *in situ* Product Removal. BioProcessingDays 2020. Recklinghausen, Germany. February 2020.

+ co-authorship of two successful grant proposals